ANALYSIS OF THE DYNAMICS AND STABILITY OF FIXED BED REACTORS

A thesis submitted for the degree of

Doctor of Philosophy

in

The University of Leeds

by

Hussam M. Naim, B.Sc., M.Sc. (Alexandria)

under the direction of

C. McGreavy, B.Sc. (Leeds),
M.Eng., D.Eng. (Yale), C.Eng.,
M.I.Ch.E., F.B.C.S.

o=0-o

Department of Chemical Engineering,
Houldsworth School of Applied Science,
The University of Leeds,
Leeds, LS2 9JT.

MAY, 1974

ABSTRACT

Various problems regarding the behaviour of fixed bed catalytic reactors involving highly exothermic reactions have been studied in relation to optimal design and control.

Steady and unsteady state mathematical models of various degrees of complexity have been used from those considering axial and radial diffusion to the simple one dimensional representation neglecting both mechanisms. Since these models would be used repeatedly, they must be relatively simply solved by a computer in a reasonable time and without loss of detail necessary to take full advantage of control or optimization processes.

Orthogonal collocation has proved a very efficient method of solution for solution of the radial diffusion and axial diffusion models. It has been shown that in the former case, an optimal distribution of the collocation points in the radial direction requires the minimum number of points. Double collocation, under certain conditions, is an efficient integration procedure both for steady and unsteady state models. In the case of the axial diffusion model, some orthogonal polynomials converge faster than others depending on the profiles to be approximated.

It has been recognised that further reduction in computing time is usually coupled with a reduction in model dimensionality. A model reduction technique has been used to lump the radial profiles in the unsteady state radial diffusion model. This lumped model has the ability to regenerate the radial profiles from simple algebraic expressions with reasonable accuracy compared with the distributed parameter system.

Studies on the transient behaviour of the reactor have indicated that the major dynamic factor is the solid heat capacitance and that the inlet temperature and concentration may be manipulated to effectively control the reactor in a multi-variable mode. Consideration has also been given to the response of the reactor to sinusoidal and damped

sinusoidal perturbations at the inlet. It has been found that for certain frequencies severe hot spots may be formed over a part of the radial profiles before a safe quasi-stationary state is reached. A detailed examination of this behaviour has shown that the differences in the speeds of propagation of the concentration and temperature waves along the reactor were significant factors in determining the resulting behaviour.

A steady state axial diffusion model in which the radial variation in temperature is approximated by a parabolic radial temperature profile has been considered. The limitations of this approximation have been identified and treated by the model reduction technique. Thus the model developed gives adequate representation of axial and radial dispersion processes. Axial dispersion becomes important if the axial temperature and concentration gradients increase beyond a certain value. This value may be calculated from the axial profiles of the one dimensional model which neglects axial diffusion.

Consideration has been given to a dynamic model based on the above and the collocation and the reduction technique used to solve the model. The solution time is reduced to reasonable levels making it suitable for detailed studies. Including the axial dispersion in the dynamic model did not alter the qualitative behaviour of the reactor.

The exceptional cases are those related to parametric sensitivity or temperature runaway studies. Instability arising from parametric sensitivity or multiple states in either the radial or axial diffusion models has been considered. The criteria developed indicate that if instability is to occur in the reactor, it is likely to originate from the solid phase regardless of the mechanisms considered in the fluid. Thus, conditions of catalyst particle stability are essential in establishing local stability of the reactor.

ACKNOWLEDGMENTS

I am particularly indebted to my supervisor, Professor C. McGreavy, for his constant encouragement and advice throughout the period of this research.

I would also like to thank Professor G.G. Haselden, for permitting me to carry out this work in the Department of Chemical Engineering.

No words can express my feeling to my father, Professor M. Naim, whose financial support made this research possible, a debt which can never be repaid.

I am also grateful to my friends and colleagues in the Department for their interest, in particular to Dr. C. Adderley and Dr. M.A. Soliman for their help and co-operation. Thanks are also due to Mrs. J. Murray of the Houldsworth School Library and Mr. L. Bailey for his assistance with some of the computation. This manuscript was typed by Miss S. Toon of the Ceramics Department, to whom I am grateful for the excellence of the final product.

Last, and by no means least, I wish to thank my wife, Mehry, for her constant help and encouragement throughout the many anxious periods of this research.

CONTENTS

LIST OF FIGURES

LIST OF TABLES

CHAPTER 1

INTRODUCTION AND RESEARCH OBJECTIVES

In recent years an increasing amount of effort has been expended in attempting to simulate chemical processes. Simulation has been made possible by the wider availability of electronic computers and the work has been stimulated by the ever-increasing cost of experimental work, which is time consuming and often gives no real insight into the behaviour of the process being examined. This is particularly true of the complex systems when strong interaction occurs between some of the physical and/or chemical phenomena. Such interaction makes optimization of the process virtually impossible using experimental data only, and satisfactory control strategies must be developed largely by trial and error.

Mathematical modelling, however, is relatively inexpensive and it is possible to perform many simulations in a relatively short time. Moreover, it is necessary to examine at least some of the underlying effects in the process, and this enables a greater understanding of the system to be developed. In general, the more complex the process, the more benefits are potentially available from a successful mathematical model.

It is unlikely that many processes can be completely and accurately modelled without any experimental work being required. Whenever a simple mathematical model is available, however, it is possible to use calculations from the model to determine the best way of tackling the experimental programme so that the maximum benefit can be obtained from the minimum amount of practical work.

If a mathematical model of a process can be developed which is capable of solution in a very short time, then it may be possible to

incorporate it into a control strategy designed to improve the profitability of the system as well as using it as a basis for some optimization procedure at the design stage. In general, the initial models of processes are unsuited to this type of use, since they are primarily designed to provide information about the way the system works and to examine the dominant processes involved. Once this has been done, it may be possible to use the results to simplify the model to a stage where it can be solved rapidly enough to meet the requirements necessary for on-line control or optimization. Such model reduction has been attempted in a limited way and on steady state processes only. Since these reduced models are primarily designed to be put to practical use, it is essential that they are based on realistic and reliable mechanistic models of the process if they are to have the requisite flexibility. The wider use of reduced models will, therefore, tend to increase the number of complex models which are necessary, rather than reduce the demand for them.

In the past, chemical reaction engineering has posed considerable problems in both design and operation and has received a corresponding amount of attention in the development of mathematical modelling techniques. In particular, heterogeneous systems such as the packed bed catalytic reactor has received much of the attention since they often form the basis of new manufacturing processes.

The packed tubular reactor is particularly useful for carrying out exothermic or endothermic catalytic reactions, and has been in widespread use for many years. The reactor normally consists of a number of small diameter tubes, the external surfaces of which are cooled or heated by a flowing or boiling liquid. In the case of endothermic reactions, the heat is necessary to keep the reaction going at an acceptable rate, and hence to keep down the size of reactor required for a given production

rate, whereas for exothermic reactions the heat removal is necessary either to minimize the production of unwanted by-products, or to prevent overheating, which may cause damage to the reactor or catalyst. This overheating is commonly referred to as "temperature runaway" and can lead to hazardous conditions.

One of the major problems with tubular reactors has been the difficulty of predicting the performance of the reactor from mechanistic models, since these are necessarily complex, and the system is very sensitive to changes in some of the parameters involved. In particular, the addition or removal of heat through the tube walls may set up severe thermal gradients in the radial direction and since the chemical rate terms are normally a highly nonlinear function of temperature, their values may vary by an order of magnitude across the tube radius. This makes it very difficult to work in terms of radial mean values of the state variables, and initially at least, a two dimensional model of the reactor is necessary. The heterogeneous nature of the system may also cause difficulties, since there are resistances to heat and mass transfer, both around and within the catalyst pellets and these will generally have to be included in any realistic model of a reactor.

Although much information exists on the steady state behaviour of the reactor, it is insufficient to predict its performance since the state of the reactor variables, when subjected to any kind of change, depends on its previous history as well as its environmental conditions. Sometimes a small perturbation in reactor parameters can lead to a very high temperature inside it with consequential burn out of the catalyst or even an explosion. It is also possible for the reactor variables to exist in two different states for the same set of operational parameters or for a small change in one of them and usually one state is an order of magnitude larger. Such multiple states, or in the former case temperature runaway, can lead to the undesirable effects mentioned above. Failure to

allow for adequate heat removal is perhaps the greatest source of dangerous conditions which arise industrially. Thus studying the conditions under which the reactor can be considered stable (i.e. a small change in the parameters can only bring about a small change in reactor state variables) is vital for the safety of industrial processes and has to be considered in design or deciding on a control strategy for a reactor. Moreover, in any detailed study required for reactor design or control, information on the transient behaviour of the reactor should preferably be available as well.

A mathematical model of the complexity needed to describe the effects which have been mentioned is clearly unsatisfactory for use in either optimization or control and may well require too much computation even for routine design problems. Consequently, there are many difficulties to be overcome before the full capability of on-line control becomes feasible for reactors of this type. The conventional approach of using empirical 'black box' models is in many ways an unsatisfactory approach. Particularly since there may be internal constraints on the operating conditions, such as a maximum temperature, and also because many of the effects in the system arise from the distributed parameter nature of the problem and may not be capable of analysis using a simple lumped parameter approximation.

To try to discover the exact nature of the problems involved in perfectly general terms is likely to be an impossibly difficult task because of the large number of degrees of freedom. A more profitable approach is to conduct a series of case studies which, hopefully, will indicate some general properties. The work reported here covers some aspects of such a study and relates to the catalytic oxidation of benzene to maleic anhydride in a tubular fixed bed reactor. This reaction, which contains consecutive and parallel reaction steps is highly exothermic and

is normally carried out in the presence of a large excess of air. A suitable objective of the control strategy would be to maximise the profitability of the whole process, but this could often involve a sub-optimal problem, such as optimizing the production rate or yield of maleic anhydride from the reaction itself.

The requirements of a mathematical model to be used in design and control, of such complex problems, are somewhat different. The design model must have general application over a wide range of conditions. The control model, however, must be capable of very rapid solution but may only need to be applied over a narrower range of conditions, but with frequent up-dating of the parameters. However, in both cases, the models have to give an accurate representation of the important state variables in the reactor. Preferably the control model should be obtained from the design model using suitable model reduction techniques.

Much of the basic groundwork for the formulation of design model and the identification of the transport phenomena which occur in the heterogeneous reactor has been done by Cresswell[14] and Thornton[46] and the application of the model reduction technique on the steady state model has been tried successfully by Turner.[78] Although there is much information on the steady state behaviour of the heterogeneous reactor, no parallel studies have been carried out on the dynamic behaviour of fixed bed reactors, except on simplified one dimensional models, which are of limited use. This is because increasing complexity of the reactor model usually results in an increase in computing time, which in turn makes such detailed studies difficult.

One of the aims of this research is to introduce more efficient numerical methods to solve the reactor models and to develop dynamic models to take into consideration the radial and/or axial transport of

heat and mass. Another objective is to extend the application of the model reduction technique to the transient models of the reactor and identification of some of the dynamic characteristics of the complex system. The degree of sophistication required, with particular reference to the flexibility of using these models as a basis for optimal design and control, is also outlined. The reactor instability problem which may exist as a result of some of the parameter values and/or to the dynamic behaviour of the reactor is also considered.

Such a general approach to the examination of the general problem of the highly exothermic heterogeneous reactor contributes to the control and/or design policies. Since it pays particular attention to the accuracy of representation, the need for small computation times, and understanding of the interaction of the physical and chemical processes taking place in the reactor. In short, it identifies the essential structure of the problem and the influence this has on exploiting the capability of the system to the maximum extent within the practical constraints.

CHAPTER 2

PREVIOUS WORK AND BASIS OF THE PROPOSED MODELS

2.1 General literature

In recent years a wealth of literature has been published on heterogeneous catalysis and its relevance to reactor design. Among the books covering general aspects of the subject are those by Thomas and Thomas[1], Satterfield and Sherwood[2], Aris[3] and Petersen[4], Denbigh and Turner[5] and Perlmutter[6]. Several review articles have also been published, the more recent ones being those by Froment[7,8], Hlavacek[9] and Ray[10].

The methods of obtaining data for the models are not discussed in detail within this thesis, since there have been several excellent reviews published[11,12,39]. All the data required in the proposed models (other than kinetic and thermodynamic data) can be found or estimated using information in the books or papers by Satterfield and Sherwood[2], Hougen[11], Beek[39], Carberry[12] and Paris and Stevens.[13]

Since the majority of published work has been concerned only with specific aspects of reactor modelling or catalysis, it is convenient to discuss the main body of the work under headings which reveal the structure of the problem and the significance of relevant contributions and which are related to the present research.

2.2 Catalyst pellet studies

Recent work on the performance of single catalyst pellets has been concerned with non-isothermal systems, particularly where the rates of reaction are different from those which would be expected from purely kinetic considerations. The importance of such studies stems primarily from two considerations. Firstly the presence of the catalyst particles

in the reactor causes considerable distortion for the flow patterns in the reactor. Secondly, the catalyst pellets are usually porous to increase the surface on which the reaction can take place, and the reactants therefore have to diffuse inside these pores to react and the products then diffuse back again. These processes are normally classified as transport resistances and the most general models of catalyst particles have been developed to include the following effects:-(14)

1. Mass transfer resistance within the pores. This is expressed by means of an effective pore diffusion coefficient.

2. Mass transfer resistance, at the exterior pellet surface between the solid and the gas phase, expressed as a film mass transfer coefficient.

3. Heat transfer resistance within the pellet expressed by means of an effective thermal conductivity coefficient.

4. Heat transfer resistance across the boundary layer surrounding the pellet, expressed as a film heat transfer coefficient.

The pellet model which takes into consideration the above four items, as well as the reaction rate and the heat generated by the exothermic reaction, is given in Appendix (A1.1). This model gives rise to a simultaneous set of non-linear two point boundary value differential equations, the solution of which can only be obtained by numerical methods. Besides requiring large amounts of computation time, the numerical method used to solve this system is by no means simple to apply. Nor should it be forgotten that the pellet model when incorporated in a reactor model has to be solved at each point inside the reactor to provide the temperature and concentration at the pellet surface. Due to the heat and mass resistances mentioned above it is to be expected that the temperature and concentration would have different values from those in the fluid. A measure of these differences has been formulated in terms of the

effectiveness factor η = $\frac{\text{actual reaction rate at pellet conditions}}{\text{reaction rate evaluated at fluid conditions}}$

and the selectivity ψ = $\frac{\text{rate of reactants consumption}}{\text{rate of products production}}$

Once they are known, they can be used in the fluid equations. It is apparent that a considerable amount of computation would be necessary, and most of the work done has been therefore concentrated on two fronts. An immediate problem is to find more efficient numerical methods than the finite difference method[14]; in this respect the recent development of orthogonal collocation method[15,16] for solving the differential equations have proved to be very efficient as will be shown in Chapter Three. The other alternative is to make assumptions which would simplify the model. Obviously the two procedures are related, and a significant part of this thesis is concerned with this problem.

Much of the early work appears to deal with simplified models. The effect of transport phenomena on the performance of the catalyst pellets was initially studied to help the experimentalist in his efforts to measure the true kinetic rates so that the kinetic constants might be calculated. It is clearly desirable to measure rates undisturbed by transport effects and where diffusion can be ignored as in the case of nonporous catalysts. However, in the case of a porous catalyst, it has been demonstrated that[46,18] diffusion is an important factor in catalyst performance. The influence of diffusion (effect (1) above) on the performance of an isothermal catalyst was first examined by Thiele[19] and Zeldowitsch.[20] The studies were extended by Wheeler[21] and by Weisz and Prater[22] who suggested a criterion for avoiding the region where diffusion changed the rate of reaction by more than 5%. Weisz[23,24] also examined non-first order reactions and developed a criterion for

predicting an upper bound on the Thiele modulus, below which the effectiveness factor would vary from unity by less than a specified amount. These criteria were shown by Schneider and Mikchka[25] to be inappropriate for reactions subject to product inhibition, such as those obeying a Langmuir-Hinshelwood type of rate expression. However, Hudgins[26] showed that a similar criterion could be developed which is valid for any type of kinetic expression and any order reaction. The criterion reduces to the Weisz-Prater form for a first order reaction. A model of the catalyst pellet which has a non-uniform pore structure was proposed by Mingle and Smith.[27] The pellet was considered to have a system of micropores branching from macropores, and the authors succeeded in evaluating effectiveness factor for a single irreversible first order reaction. This type of model is particularly useful for a catalyst made by compacting powder into pellets. The treatment of Mingle and Smith was extended by Carberry to include reversible[29] and consecutive[28] reaction schemes.

Non-isothermal systems have been studied by a number of authors and in many cases effectiveness factors much larger than unity have been reported.[12,30,31] Wheeler[32] and Prater[33] considered pellets subject to effects (1) and (3) and demonstrated the possible existence of severe thermal gradients. The latter showed that for given surface conditions, the concentration and temperature within the catalyst pellet are linearly related and that this relationship is independent of pellet geometry and of the form of the kinetic rate expression.

The effect of reaction order in exothermic systems was examined by Tinkler and Metzner[34] who showed that, in general, second order reactions are much less sensitive to temperature than are first order. Østergaard[35] studied the effect of fluid temperature on the apparent reaction rate, and demonstrated that the apparent activation energy can be

very sensitive to small changes in temperature when the reactions are exothermic. The exothermic case was also studied by Carberry[12] including, for the first time, the interphase resistances (effects (2) and (4)). However, the vast majority of published work has been concerned with systems where the interphase resistances (2) and (4) may be ignored. This is unfortunate, since in most practical cases, the interphase heat transfer resistance is considerable and often controls the behaviour of the system. On the other hand, the resistance to mass transfer is relatively small and can often be ignored without loss of accuracy. Inclusion of a heat and mass transfer resistances (effects (2) and (4)) between the phases means that for most of the published work, it is necessary to find the appropriate surface conditions by an iterative procedure. This clearly adds considerably to the computational effort required to solve the pellet models which do not already include these resistances. In the case of complex reactions such as used in this research, ignoring the interphase transport resistances can only be construed as an attempt at mathematical or model simplifications and must be regarded with suspicion for non-isothermal systems.

Several methods of simplification have been proposed, besides those mentioned above. Schilson and Amundson[37,38] considered the pellet under non-isothermal conditions, approximating the heat generation function by one or two straight line segments. The method was found to be fairly good for the system they considered but is unsuitable for extension to complex reactions where interphase transport resistances are present. Beek[39] considered a system where interphase heat transport resistance is included. The model can be solved very rapidly, but is based on the assumption that the reaction rate varies linearly with temperature, and this severely restricts the range of application over which the model is valid. Peterson[40,4,41] used the relationship developed by Prater[33] as the

basis of an approximation method which is asymptotically valid under conditions of diffusion control where the reactant concentration falls to zero in the outer layers of the catalyst pellet. This method was extended by McGreavy and Cresswell[74,31,14] to the case where interphase transport resistances are important. Hatfield and Aris[43] have also used this approach in a general parametric study of the catalyst pellet. Gunn[44] assumed that the temperature profile within the pellet could be represented by a straight line and Tinkler and Pigford[45] allowed for small, but significant, temperature rise by using a perturbation series technique. Both these methods are only useful over a narrow range of conditions.

Numerical computations performed by Cresswell[14] have shown that, over the whole range of practical operating conditions (when the fluid is a gas) the catalyst pellet is essentially isothermal, the temperature rise between fluid and pellet centre being concentrated almost entirely in the interphase region. This result was anticipated by Beek[39] and also suggested from the results of Hutchings and Carberry.[36] Cresswell[14] proceeded to assume isothermality within the pellet, thus allowing an analytic solution of the mass transport equation for a first order reaction. Later Thornton[46] extended the isothermal pellet assumption to include the complex reactions with parallel and consecutive reactions as well as in the case of non-first order reactions with the use of a pseudo-first order rate expression. His model is shown in Appendix (A1.2) and is used in this thesis. Thornton[46] has shown that the isothermal model gives an accurate estimate of the steady state and over a wide range of parameter values. This conclusion is also confirmed by Hlavacek and Kubicek.[47,48] The consequences of these simplifications are very significant, resulting in the pellet model being reduced to a single nonlinear algebraic equation in temperature to be solved, instead of the original system of differential equations.

While considerable effort has gone into attempts to simplify the description of the single catalyst pellet, a few attempts have been made to relax some of the assumptions on which even the more complex models are based. In particular, the shape of the pellets has received some attention. Most studies reported in the literature have been concerned with spherical pellets, but Aris[49] showed that by using the volume/surface ratio as a characteristic dimension, the asymptotes of charts (i.e. kinetic control and pore diffusion control) coincided for various shapes. Extensive calculations have been performed by Gunn[50] for finite and hollow cylinders, and by Luss and Amundson[51] for finite cylinders and parallel-pipeds. Their results have been summarized and compared by Rester and Aris.[52] Attempts to simulate the effects of particle shape away from the asymptotes have been made by Rester et al.[53]

Whereas all previous papers had assumed symmetry in the fluid conditions, Copelowitz and Aris[54] considered the behaviour of a pellet situated in steep gradients in the axial direction. Solution of the relevant equations is not straightforward and introduction of interphase transport resistances would increase the difficulty. Moreover, steep axial gradients commonly imply steep radial gradients (in the fluid) and in this case not even axial symmetry can be assumed in the fluid phase. It therefore seems unlikely in the near future that such models will be used in reactor design.

Comparatively little experimental work has been carried out on single catalyst pellets, and the results are somewhat contradictory. This is not surprising since the experimental difficulties are great, particularly in the measurement of intraparticle temperature profiles. Cunningham et al.[55] demonstrated the existence of large temperature difference between the fluid and pellet centre, and found experimental values of the η as high as 25. Miller and Deans[56] also reported large temperature rises and η greater than unity. Probably the most

reliable work on radial temperature gradients was reported by Irving and Butt[57] who carried out measurements on several pellets using extremely fine thermocouples (0.001 in. diameter). Very large temperature rises across the boundary layer were measured, with relatively small ones occurring within the pellet. This work showed the same features as that of Fulton and Crosser[58] who demonstrated the importance of film resistances by using catalyst pellets of various sizes. They also reported the work of Ramaswami[59] who is alleged to have obtained fluid film temperature rise of up to 420°C.

Little attention has been given to the transient behaviour of the catalyst pellet and most of the research done in this area has been concerned with stability studies. McGuire and Lapidus[60] used a transient single pellet model within a transient model of the reactor. They ignored the interphase transport resistances which were shown to be of importance in any realistic model by Feick and Qion.[62] Wei[61] also examined the transient problem and showed that the maximum temperature achieved may be considerably greater than the steady state maximum which is predicted by the Prater[33] relationship.

The equations describing the dynamic behaviour of the catalyst pellet and which include all transport resistances are given in Appendix (A1.2.2). This model has been studied by Thornton[46] for the highly exothermic reactions in which adsorption effects are unimportant as in the partial oxidation of hydrocarbons. He showed that the heat capacitance is much larger than the mass capacitance and therefore the rate of change of concentration within the pellet is much faster than that of temperature. This result, which has been confirmed computationally, means that the changing temperature drives the concentration profile, which may be considered to be at a pseudo-steady state. In systems where strong surface adsorption occurs, Nussey[105]

has shown that its effect may be accounted for by modification of the diffusion coefficient in the mass balance equation. Thus when Henry's law applies to the adsorption equilibrium, the parameter, DP_A in equation (A1.1) becomes:

$$\frac{(DP_A + K'D_s)}{(1 + K')}$$

where K' is an adsorption equilibrium constant and D_s is a surface diffusion coefficient. The reaction rate term is similarly modified so that A_{oi} becomes $\frac{A_{oi}}{(1 + K)}$.

Thus the form of the unsteady state pellet equations under these circumstances is unchanged, although the numerical values of the coefficients are different from those used in the steady state. Some workers[10,106] have inferred from the results of Kabel et al.[107] that strong adsorption will cause the adsorption time constant of the catalyst pellet to become greater than the thermal time constant. Kabel et al.[107] studied the effect of temperature disturbances on the dehydration of ethanol over an ion exchange resin catalyst in an isothermal reactor. The interpretation of their results is, however, open to question for several reasons. No attempt appears to have been made to establish the lack of importance of the heat transfer effects within the system. Also, because the system was designed to operate isothermally, the perturbations were applied to both the reactor inlet and the coolant so that the effect was distributed throughout the system. Perhaps the most important point about this work is that virtually all of the concentration disturbances occurred during the temperature perturbations and not subsequent to them and to infer from this that the concentration changes are driving the response is open to question. There is no evidence that this is the case with the highly exothermic reactions of interest here. Indeed the experimental results of Kehoe and Butt[64] and Horak and

Jiracek[108] show that the mass capacitance of the catalyst pellet is much less than the thermal capacitance so that the concentration changes within the pellet occur faster than the temperature changes. In these circumstances the concentration profiles within the pellet may be treated as if they pass through a series of pseudo-steady states which are determined by the changing temperature profiles.

Applying the assumption of pellet isothermality, Thornton[46] demonstrated that the catalyst pellet also remains essentially isothermal in the transient state. Although a slight temperature gradient within the pellet has been noticed at the beginning of a transient response, it is rapidly flattened indicating isothermality. Kehoe and Butt[64] measured the temperature profiles in the pellet when subjected to fluid perturbations. They found that pellet isothermality might be obtained through the transient period for a relatively high thermal conductivity. Hughes and Koh[65] have demonstrated experimentally that a small intra-particle temperature rise during the transient response of the catalyst particle is possible. However, most of this rise occurred near the surface with the bulk of the profile in the pellet being flat. They also found that the film heat transfer resistances are far more important, and during the transient response the intraparticle temperature gradient has very little effect on the effectiveness factor. These conclusions have also been confirmed by Thornton.[46] In this respect the approx-imation of isothermality of the pellet is as good in the unsteady state as it is in the steady state. Treating the pellet as isothermal and considering the mass transport equation to be at a pseudo-steady state and therefore can be solved analytically. The dynamic model for the catalyst pellet then becomes a single first order differential equation as shown in Appendix (A1.2.2). The advantages of this formulation are clearly evident, the model gives an accurate estimate of the reaction rate limitation imposed by the catalyst pellet and may be solved rapidly enough to be included in a dynamic model of the reactor.

2.3 The tubular reactor

In the fixed bed reactors, which are of interest here, the reactor normally consists of a cylindrical tube packed with catalyst particles with the gaseous reactants passing through the length of the tube. The reaction is assumed to take place only on, or within the catalyst pellets. If the pellet conditions (i.e. its temperature and species concentration) are considered as that of the fluid, the packing is taken purely from the point of fluid dynamics and its effect on the fluid flow. This type of treatment is categorized as a quasi-homogeneous reactor. On the other hand if the differences in solid and fluid conditions are allowed in addition to the fluid dynamical effects, the rates of reaction are modified by an effectiveness and selectivity factors which are obtained by the solution of the catalyst pellet model, the term heterogeneous reactors is then used. Many of the chemical reactions which occur in packed bed reactors are associated with large heats of reaction and it is often necessary to take into consideration the limitations imposed by the solid phase[7,46,14,62] i.e. they should be treated as heterogeneous reactors. In order to retain control of the reactor and to prevent irreversible damage to the catalyst, external cooling around the tube is usually utilized. In such a situation radial temperature gradients exist perpendicular to the direction of reactant flow, and as a consequence, concentration gradients. Also, due to axial temperature and concentration gradients as well as the turbulent effects of the packing, an axial diffusion of heat and mass opposing the fluid flow may occur. Therefore, to describe the spatial distribution of heat and mass inside the heterogeneous reactor, the mathematical model required should take into account the effects of the axial and radial gradients.

The packed bed reactor is essentially discrete in character and an exact model would need to describe the fluid on a microscopic scale,

taking into consideration the spatial distribution of individual catalyst pellets. A rigorous analysis on this scale which would take account of the discontinuous nature of the bed, is impossible at the present time, and is not really warranted. In practice the fluid must follow the random passages in the bed, whereas the chemical reaction occurs only within the catalyst pellets. The problem is therefore best tackled as if the properties of the bed were averaged out to give a pseudo-homogeneous structure. The transport of heat and mass within the bed may then be described in terms of differential equations, using effective transport paramaters. Such reactor models are of a continuum nature and although the bed properties are space averaged, the equations describing the heat and mass transfer within the catalyst pellets are solved for the actual size of the pellet being used. This means that the rates of reaction and heat production per unit volume may be calculated at any point in the reactor as if a catalyst pellet and its associated average voidage were acting at that point.

In contrast to the continuum models which have been described above, Deans and Lapidus[66] proposed a mixing cell model in which the reactor is treated as a two-dimensional network of stirred tanks. Each cell has the dimensions of one catalyst pellet and its associated bed voidage. Such models have been used by several other workers[60,67] and although they have certain mathematical advantages, the computing time was found to be excessive. This is because to get accurate representation a large number of these cells must be employed and it ~~is~~ then corresponds to the finite difference representation for solving the continuum model.[68] For this reason the continuum representation of a reactor is used in this research.

When heat is removed through the walls of a tubular reactor, radial temperature gradients are set up and these cause radial concentration

profiles to develop. The system can therefore only be described in detail by a model which is at least two-dimensional. The first models proposed were concerned with homogeneous or quasi-homogeneous systems.[70,69] Beek[71] gives an excellent review of the design of reactors based on quasi-homogeneous models, and also discusses some of the transport effects which occur in the models. Nickley and Letts[72] extended the model to include multiple reactions with arbitrary rate terms. An attempt was made to discover the size of yield losses due to radial mixing and failure to withdraw the reactant stream at the points where local yields are at their maximum. A two-dimensional transient model of the homogeneous reactor was solved analytically by Amundson,[73] but since the rate of reaction was assumed to be independent of the concentration and linearly dependent upon temperature, the solution can be considered to be of mathematical interest only. McGreavy and Cresswell[74,14] and Thornton[46] proposed a heterogeneous model taking into consideration the radial transport of heat and mass. The equations describing the behaviour of the system were of a quasi-homogeneous form, but the rate terms were modified at each point in the bed to take account of the influence on the reaction rate of the resistances to heat and mass transfer in and around the catalyst pellets. The results were shown to be significantly different from those predicted by models taking account of pure kinetic rates only. In particular, it was shown that in many cases, where the quasi-homogeneous model predicts temperature runaway, the heterogeneous model predicts stable profiles. Such a model generally consists of a set of nonlinear partial differential equations which describe the distribution of heat and mass in the reactor. These equations are coupled with the catalyst pellet equations and because of their nonlinear nature they have to be solved numerically. The most generally applicable method is the Crank-Nicholson finite difference

representation. Although the finite difference method is reliable, it is not an efficient method for solving the reactor model of such complexity and takes large computing times. If, in addition, transient models are considered, the computing time increases enormously[62] making these methods of solution unsuitable for design or control of reactors, or even for a detailed study related to reactor problems. For these reasons, two main approaches have been developed to tackle these difficulties. The first approach is to use a more efficient solution method such as the alternating direction explicit method[62] or the relatively new collocation methods[63,75,76] (see Chapter Three in this thesis). The second approach is to reduce the complexity of the original problem by, for example, reducing its dimensionality. Since it is the axial concentration and temperature profiles which are of principal importance, it is possible to eliminate the radial and axial diffusion derivatives. However, it has been shown[46,77] that this kind of simplification of the reactor model is unappropriate in many cases. Thornton[46] developed a one-dimensional model based on the assumption of a paraholic radial temperature profile which results in a modified wall Nusselt number. Although such a model takes a small amount of computational effort, it has limitations regarding the accuracy of profile representation.[77] Such a model has been used extensively in transient studies by Adderley[109] who identified its limitations and tried to increase the model accuracy. Turner[78] used a semi-empirical method of model reduction to approximate the radial profiles. His method has been shown to be adequate in the steady state models. An attempt to extend the method to the dynamic case can be seen in Chapter Four.

In the above models the radial diffusion of heat and mass has only been considered and most workers tend to neglect the axial diffusion of heat and mass as unimportant. This tendency has been widely accepted, because neglecting the axial diffusion terms simplifies the equations

considerably and thus many criteria and conditions have been put forward to justify neglecting it.

Generally the mixing in the axial direction which is due to the turbulence and the presence of packing, is accounted for by superposing an effective mechanism upon the overall transport by plug flow.[7] The flux due to this is described by an expression analogous to Fick's law for mass transfer and Fourier's law for heat transfer. The respective proportionality constants are effective diffusivities and conductivities. Because of the assumptions involved in their derivation, they implicitly contain the effect of a radial velocity profile and the short circuiting effects due to packing. The principal experimental results concerning the effective diffusivity and conductivity in the axial direction[131,132, 133,134,159,160] show that the Peclet number based on the particle diameter for heat and mass lies between 1 and 2. The addition of a mixing term in the equations describing the heat and mass transport in the reactor transfer a first order ordinary differential equation, i.e. plug flow model, to a second order ordinary differential equation of the boundary value type. The form of these boundaries has given rise to extensive discussion.[161,92,93,162,163,120] However, the generally acceptable forms are those of the derivative type based on the Fick and Fourier laws. This type of unsymmetrical nonlinear boundary value problem poses a number of difficulties in methods of solution.

Carberry and Wendel[79] developed a nonisothermal steady state model based on the parabolic radial temperature profile assumption and neglected the interphase resistances between the fluid and solid. They solved the system by implicit finite difference procedure and concluded that the axial diffusion can be considered unimportant if the bed length exceeds 50 particle diameters. It was also reported that the axial diffusion can be neglected for high flow velocities[79,80], a case usually

attained in industrial practice. On the other hand Liu and Amundson[125] studied the effect of axial diffusion in an adiabatic reactor and concluded that its effect cannot be ignored when dealing with multiple states. They solved the equations by the implicit finite difference method and reported a computation time of about 2 hrs. for a transient run. Lee[127] utilized the quadratic conversion of the quasilinearization technique and reduced the computing time. In the case of isothermal reactions[164,165,166], where the number of equations can be reduced to one, it can be integrated backwards with the aim of satisfying the boundary condition at the reactor inlet. However, apart from the numerical instability problems, in the case of adiabatic or nonisothermal cases which are of industrial importance and where the number of equations is more than one,. the method of solution becomes infeasible, and may require optimisation methods to promote convergence. As an alternative method of solution, collocation procedures have shown to be more suitable and can deal with such unsymmetrical problems.[120,80]

Considering the axial and radial diffusion, the problem becomes even more complex. Deans and Lapidus[66] and later McGuire and Lapidus[60] used the concept of mixing cell arrays in formulating such a comprehensive model. However the computing times were prohibitive. Ranzi et al.[130] used an integral transformation method and indicated that under certain conditions axial diffusion may affect the temperature and concentration profiles in the reactor. The most comprehensive dynamic model has been solved by Feick and Quon.[62] They included the axial and radial diffusion terms and the particle inter and intra particle transports and employed the alternative direction explicit finite difference method. The computing time was again excessive to the extent that no detailed studies have been carried out.

It is clear that the problems imposed by considering the axial

diffusion are considerable and the criteria and conditions for neglecting it have not been definitively established.[120] The collocation method together with the model reduction technique will be employed in Chapters Six and Seven to solve such comprehensive models including axial and radial diffusion, and extensive investigations of the basic assumptions made.

It is worth examining some of the other assumptions implicit in the formulation of reactor models. In all the models, axial symmetry of the concentration and temperature profiles is assumed. In single tube reactors this is usually the case, since the coolant conditions do not vary around the tube circumference. In the larger industrial units where the coolant may flow perpendicular to the tube axis, temperature gradients may, under some circumstances, occur in the coolant flow direction.[109] There will also, of course, be variations in the coolant velocity around the tubes. The difficulties of describing these variations are very great and to obtain an accurate description, the temperatures and heat transfer coefficients around all the tubes would have to be measured or estimated. Even if sufficient data existed to estimate these variations to any degree of reliability the results would certainly not be reproducible in other systems or even in the same system.

Similar reasoning may be applied to conditions inside the tube so that it is generally assumed that within the bed every point on the surface of each catalyst particle is in contact with gas of uniform concentration and temperature and is also equally accessible for the purposes of heat and mass transport. This further implies that the rates of reaction and heat generation at each point in the bed may be calculated as if a catalyst particle is acting at that point.

For the purposes of the work described in this thesis the catalyst pellets are assumed spherical and of uniform size and activity. Other

pellet shapes may be considered without much difficulty by defining an appropriate characteristic radius.[4] The effect of varying the pellet size throughout the bed, in an attempt to optimise the reactor performance, has been investigated by Brusset et al.[104] Calderbank and co-workers[102] and Stewart and Sorensen[76] have modelled reactors in which the packing is diluted with inert spheres, and Shadman-Yazdi and Peterson[103] have considered the effect of varying the catalyst activity within individual pellets in order to obtain better yields in cases where the product can be consumed. Catalysts are usually subject to deactivation with time and more importantly with temperature. Little is known, however, about the exact mechanism of catalyst deactivation except that a rapid increase in temperature will usually enhance it. In most studies of the dynamic behaviour of reactors the perturbations last for a relatively short period compared with the time needed to cause significant deactivation. Over longer periods deactivation may need to be considered and studies have been made of long term performance where it is the principal factor.[111,83] When temperature runaway occurs, deactivation can take place so that the kinetic model is no longer applicable. Since one of the purposes of reactor modelling is to identify regions of operation where such undesirable behaviour occurs, inclusion of catalyst deactivation effects in the models used here is not really necessary.

A common assumption employed in reactor modelling is that all of the physical and chemical parameters in the system are independent of position, concentration and temperature. Clearly this is not the case in practice, but usually the increase in computational efforts required to solve a model which includes such variations (even when they are known) is not justified by the increase in accuracy which is obtained.[46] This is especially true in, for example, the case of heat transfer coefficients which can usually only be estimated to about 10% accuracy in any case. Perhaps the most doubtful of assumption is that of plug flow of the gas

through the reactor which is related to the assumption of uniform bed voidage. The voidage of a packed bed is not uniform, being greatest near the tube wall.[81] Since the gas will tend to take the path of least resistance through the bed, its velocity profile will therefore be deformed. This in turn will also cause a variation in the values of the mass and heat transport parameters. Thornton[46] has shown that the performance of a reactor can be significantly affected by small variations in value of the voidage. Valstar[82] found similar disagreement between the predictions of a reactor model which contain a velocity profile expression and one in which plug flow was assumed. More recently Stanek and Szekely[112] have suggested that significant gas flow maldistribution may occur not only due to local variations in bed voidage but also because of the variation in properties caused by the radial temperature gradients. These results appear to some extent to conflict with those of Hoiberg et al.[77] who found that the steady state and transient response predicted by a plug flow model was no different from that predicted by a model which included an arbitrarily specified velocity profile with a large peak near the tube wall. They concluded that in their system, at least, the radial heat and mass transfer occurred rapidly enough to counteract the effects of the higher local velocities. Clearly then, more investigation of this problem is required. As Valstar[82] and Hoiberg et al.[77] have shown, inclusion of a velocity profile in the reactor model is not difficult. However, the validity and applicability of both the model and its predictions is uncertain. The distribution of voidage within the bed, and therefore the form of the velocity profile, is very system-dependent.[81] Since one of the aims of this work is to contribute towards a general picture of reactor behaviour, there seems to be little alternative to

using the assumption of plug flow, at least until more is known about the fluid dynamics of packed beds.

As a result of these concepts and assumptions the reactor models, in general, becomes a set of simulations, non-linear ordinary or partial differential equations describing the spatial variation of temperature and concentration within the bed. One equation consists of a heat balance over the reactor and the others are mass balances on each reactant. These equations are coupled with the catalyst pellet model. In the solution of the reactor equations at each point in the bed, where the gas concentration and temperature are calculated, the catalyst pellet model must also be solved to obtain the reaction rate and heat generation rate.

2.4 Reactor stability

If a small change in reactor inlet conditions can bring about large changes either within the reactor bed or at the exit, then the reactor is said to be unstable. This instability may be due to parametric sensitivity, in which case removing the perturbation causes the system to tend to return to its original state. The other cause for instability is the existence of multiple steady states in the reactor whereby the original state cannot be restored by merely removing the inlet perturbation.[46] Multiplicity may occur in the catalyst pellets or may be present in the reactor without packing. The existence of possible multiple steady state for the catalyst pellet creates considerable difficulties in the reactor design and operation, since the performance of the reactor is uncertain unless the history of each pellet is known. The reactor is also likely to be unstable in the transient case, since the pellets tend to change from one state to another under these conditions. Even more important, however, is the fact that the reaction rate at one steady state is often several orders of magnitude greater than at another. Nevertheless instability due to parametric sensitivity or multiplicity

can lead to several undesirable results, such as bad selectivity, catalyst deactivation or reactor burn out. Therefore the primary motive for identifying the regions of potential instability is that operating conditions of the reactor can be kept away from these regions, thus avoiding the associated undesirable effects.

The vast majority of published literature on the catalyst pellet stability or multiplicity has been concerned with systems where the inter- and intra-phase resistances were not taken into consideration. Since these investigations cannot be extended to allow for the phase resistances[10,46] they are of academic interest only. Use can be made, however, of stability criteria for catalyst pellets with no intraphase resistances[47,115] when applied to nonporous pellets or catalytic wires.

For models developed which include all transport resistances there appear to be three possible steady states of which the middle one is metastable. However as high as five steady states have been reported.[43,85] These results lie outside the practical range of operating conditions and occur only over a very narrow range of parameters.

For unpacked reactors or even quasi-homogeneous systems when radial or axial diffusion of heat and mass are included in the reactor model, the possibility[87] of three steady states for the same inlet conditions exists. This kind of multiplicity and its relation to the system stability has been discussed by Perlmutter[6] and reviewed by Ray.[10] If axial diffusion is considered in the reactor model, multiplicity may arise, as Froment has pointed out.[8] However, the magnitude of the back mixing which could produce multiple steady states is greater than that usually encountered in industrial fixed bed reactors.[92,93] Instability may also occur due to recycling in the reactor system[88,89,90] or to using counter current cooling fluids.[91] Recently the effects of the cooling medium on the stability of the packed bed reactors has been investigated by Adderley.[109]

In an attempt to relate the pellet multiple steady states with the general stability problem of the fixed bed reactor, McGreavy and Thornton[94] and Thornton[46] developed a method in which the region of multiple steady states of the pellet may be plotted on a phase diagram, then the reactor trajectories can be plotted on the same diagram to indicate whether they pass through a region of multiplicity or not. However it has been shown that in fact parametric sensitivity near regions of multiplicity[46,109] could pose more serious problems.

Most of the studies stated above have been concerned with the simple reaction of the type A ⟶ B. Extension of the available methods or criteria to the complex reactions of the type under study is either invalid or gross assumptions have to be made, which in turn gives very conservative estimates on the stability or multiplicity of the reactor. This point is discussed in more detail in Chapter 8 of this thesis.

2.5 Concluding comments

The widespread use of high speed computers has enabled increasingly sophisticated models of chemical reactors to be solved and some of the assumptions usually made to be relaxed and tested. Studies concerning asymmetrical heat and mass profiles within the catalyst pellet[95,96,97] or catalyst pellets exists in non-uniform fluid concentration and temperature[98,99,100] have been carried out. This kind of study is impossible to verify by the present state of experimental techniques and appears to be of little practical value. Attempts to control the hot spot formation in the reactor have been suggested, for example, by using larger catalyst pellets near the hot spot,[104] since this will tend to slow the reaction down. Dilution of the bed with inert spheres is also possible,[102,76] or even considering the effects of varying the catalyst activity within individual pellets has been studied by Petersen et al.[103] The cooling

jacket may also be divided into several sections each at a different temperature.[101] However, such a strategy may add to the mechanical problems considerably.

Although the trend has been towards increasingly complex models, it seems likely that in the future, the emphasis will be on the development of models of reducing complexity or on more efficient solution methods, while retaining the detailed description which is associated with the more complex models. Such efficient models can thus be used in design and improvements of practical systems with minimum expense. Also as basis of control algorithms using state and parameter estimators.

CHAPTER 3

SOLUTION OF THE RADIAL DIFFUSION MODEL WITH COLLOCATION METHOD

3.1 Introduction

Many catalytic systems of industrial importance involve transport effects in and around the catalyst particles of the reactor bed, and this can cause appreciable variations in the reaction rate predicted. Therefore it is desirable that heterogeneous models distinguishing between solid and fluid should be employed. Moreover, in many industrial systems the catalytic reactions are highly exothermic and a cooling medium is needed at the outer walls of the reactor tubes to remove the excess heat generated. This will induce radial variations in temperature and consequently in concentration. Thus, a two dimensional model is needed to describe the radial temperature and concentration profiles at various axial positions.

McGreavy and co-workers[14,46] have proposed a suitable heterogeneous model. Although the equations describing the system are essentially in a quasi-homogeneous form, the rate terms are modified at each point in the bed to take account of the influence on the reaction rate arising from the resistances to heat and mass transfer in and around the catalyst pellets. Their proposed model will be used in the following work. The treatment which follows will deal with a reaction scheme of the following form:

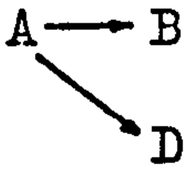

where B is the desired product and it is typical of a wide range of reaction schemes found industrially. The set of partial differential equations which represents the above scheme is given below (equations 3.1 to 3.5). These are coupled and nonlinear equations and can only be solved numerically. Unfortunately, quite often in such a

complicated system, large computation times have to be used in the solution, and this cannot really be justified.

In the present study, orthogonal collocation as an alternative numerical procedure to the finite difference method will be investigated. This method has been exploited by Villadsen and Stewart[113] for boundary value problems and showed that collocating at the zeros of an orthogonal polynomial gives better convergence properties. McGowin and Perlmutter[114] used arbitrary chosen collocation points and obtained slower convergence. Ferguson and Finlayson[16] used it to solve the transient heat and mass transfer equations for a catalyst particle and Legendre polynomials were recommended for Neumann type boundary conditions. The equations for the homogeneous reactor have been solved by Finlayson[15] who showed that as the wall Nusselt number increases more collocation points are needed to approximate the radial profiles. In all these investigations the orthogonal collocation method has been used to reduce the equations to a system of ordinary differential equations which subsequently are integrated by Runge Kutta methods. Villadsen and Sorensen[117] integrated the resulting ordinary differential equations by the collocation method as well, and called the method double collocation. They used the linear heat transfer equation to illustrate the procedure and claimed that this method is more efficient than integrating by the fourth order Runge Kutta method. Stewart and Sorensen[76] outlined the use of orthogonal collocation in solving the distributed parameter system typical of fixed bed catalytic reactors and have shown that it is a feasible procedure.

In this chapter the double collocation method will be applied on the nonlinear problem under study. The minimum number of collocation points required to approximate the radial profiles and its relation with the location of the collocation points will be investigated. An assessment in terms of accuracy of representation and computing times between

the finite difference, the single collocation and the double collocation methods is also given.

3.2 Formulation of the Equations

The heat and mass balances on an element of fluid volume in the catalytic tubular reactor and for the reaction scheme, subject to the assumptions given in Appendix (A4), can be represented in dimensionless form as follows:[46]

$$\frac{1}{r}\frac{\partial}{\partial r}\left(r\frac{\partial CA}{\partial r}\right) - G_1\frac{\partial CA}{\partial z} - G_1 G_2 \eta (\phi_1^2 + \phi_3^2)CA = 0 \qquad (3.1)$$

$$\frac{1}{r}\frac{\partial}{\partial r}\left(r\frac{\partial CB}{\partial r}\right) - G_1\delta\frac{\partial CB}{\partial z} + G_1 G_2 \eta \gamma (\phi_1^2 + \phi_3^2)CA = 0 \qquad (3.2)$$

$$\frac{1}{r}\frac{\partial}{\partial r}\left(r\frac{\partial T}{\partial r}\right) - G_3\frac{\partial T}{\partial z} + G_3 G_4 (T_P - T) = 0 \qquad (3.3)$$

The boundary conditions being

$$\frac{\partial CA}{\partial r} = \frac{\partial CB}{\partial r} = \frac{\partial T}{\partial r} = 0 \quad \text{at } r = 0,\ z \geqq 0 \qquad (3.4)$$

$$\left.\begin{aligned} \frac{\partial CA}{\partial r} &= \frac{\partial CB}{\partial r} = 0 \\ \frac{\partial T}{\partial r} &= N_{uw}(T_c - T) \end{aligned}\right\} \quad \text{at } r = 1,\quad z \geqq 0 \qquad (3.5)$$

Let the inlet conditions be

$CA = CA(r)$, $CB = CB(r)$ and $T = T(r)$ at $z = 0$, $0 \leq r \leq 1$

The dimensionless groups introduced are defined as follows:

$$CA = \frac{C_{FA}}{C_0} \qquad CB = \frac{C_{FB}}{C_0}$$

$$r = \frac{x}{R} \qquad z = \frac{l}{L}$$

$$G_1 = \frac{R^2 u}{DF_A L} = \frac{R^2 PeM}{2bL} \qquad G_2 = \frac{(1-e)LDP_A}{b^2 u e}$$

$$G_3 = \frac{R^2 \rho cp\ u}{KF\ L} = \frac{R^2 Pe_H}{2bL} \qquad G_4 = \frac{(1-e)\ 3hL}{b \rho cp\ ue}$$

$$\delta = \frac{DF_A}{DF_B} \qquad N_{uw} = \frac{RU}{eKF}$$

$$T_c = \frac{TC\ Rg}{E_1} \qquad T = \frac{TF\ Rg}{E_1}$$

$$Pe_M = \frac{2bu}{DF_A} \qquad Pe_H = \frac{2b \rho cp\ u}{KF}$$

$$\phi_i^2 = \theta_i^2 \exp(-\frac{E_i}{E_1 T}) \qquad \theta_i^2 = \frac{b^2 A_{oi}}{DP_A} \qquad i = 1,2,3$$

The radial heat and mass transfer coefficients are related to the velocity in such a way that Pe_M and Pe_H remain constant[168], with a value of approximately 10. Moreover, it may also be assumed that the radial diffusivities are equal for each component in the fluid phase, making $\delta = 1.0$. This occurs because dispersion is caused mainly as a result of the turbulent motion of the fluid.

The effectiveness factor, η, selectivity, ψ, and pellet temperature Tp are obtained by solving the isothermal pellet equation (details are given in Appendix (A1.2.1)). It can be represented in dimensionless form as follows[46]:

$$B_O(Sh_A(CA - C_{PAS})(\frac{K_1(1 + H_2)}{K_1 + K_3} + \frac{K_3 H_3}{K_1 + K_3}) - Sh_B H_2(C_{PBS} - CB)) - Tp + T = 0.00 \qquad (3.6)$$

The dimensionless groups and the equations giving the concentrations C_{PAS} and C_{PBS} at the pellet surface can be seen in Appendix (A1.2.1).

3.3 Methods of Solution

3.3.1 Finite difference:

The equations given by (3.1 to 3.5) can be solved by a Crank-Nicholson finite difference formulation. The dimensionality of the system imposes limitations on the numerical solution in terms of computing time and storage requirements. Also the nonlinearity of the problem restricts the integration steps to low values. For more details involved in the steps required for solution, see reference (46).

This method has the advantage of giving a solution which can be used as a basis for comparison of other approximation methods.

3.3.2 Single collocation:

Obviously, any method which can reduce the dimensionality of the above system of equations and retain the accuracy of the numerical solution must be welcomed. Orthogonal collocation is but one technique in a class of methods known as weighted residual methods, which have the ability to reduce the dimensionality of the system, thus leading to shorter computing time, less storage and acceptable accuracy of the solution. In this section the orthogonal collocation method will be employed to approximate the radial differential operations only. Details of its application can be found in Appendix (A1.4).

The radial heat and mass profiles can be approximated by the following trial solutions:

$$T(r,z) = T(1,z) + (1 - r^2) \sum_{i=0}^{N-1} a_i P_i(r^2) \qquad (3.7)$$

$$CA(r,z) = CA(1,z) + (1 - r^2) \sum_{i=0}^{N-1} a_i P_i(r^2) \qquad (3.8)$$

$$CB(r,z) = CB(1,z) + (1 - r^2) \sum_{i=0}^{N-1} a_i P_i(r^2) \qquad (3.9)$$

where the a_i are arbitrary coefficients determined in such a way as to

minimize the errors between the above approximate solution and the exact one over the domain. $P_i(r^2)$ are members of a suitable family of even power orthogonal polynomials. The approximate solution can be substituted into the differential operators, thus enabling the equations to be solved directly for the ordinate instead of for the coefficients a_i (see Appendix (A1.4)).

Substituting for the radial differential operators in the system given by equations (3.1 to 3.5), a 3(N+1) ordinary differential equation results. The number of equations can be reduced to 3N equations by eliminating those accounting for the boundary conditions. This is done by substituting into the resulted ordinary differential equations and thus the final form may be represented as follows:

$$\left.\frac{dCA}{dz}\right|_J = \frac{1}{G_1} \sum_{i=1}^{N} Q_{J,i}\, CA_i - \left(G_2 \zeta\, (\phi_1^2 + \phi_3^2) CA\right)\Big|_J \qquad (3.10)$$

$$\left.\frac{dC_B}{dz}\right|_J = \frac{1}{G_1 \delta} \sum_{i=1}^{N} Q_{J,i}\, CB_i - \left(G_2 \zeta \psi\, (\phi_1^2 + \phi_3^2) CA\right)\Big|_J \qquad (3.11)$$

$$\left.\frac{dT}{dz}\right|_J = \frac{1}{G_3} \sum_{i=1}^{N} W_{J,i}\, T_i + \frac{1}{G_3} V_J + G_4(T_p - T)\Big|_J \qquad (3.12)$$

$$J = 1, 2, \ldots . N$$

with initial conditions

$$CA(z) = CA_J(0), \quad CB(z) = CB_J(0) \text{ and } T(z) = T_J(0) \text{ at } z = 0.0,\ 0 < r < 1$$

where $$\sum_{i=1}^{N} Q_{J,i} = \sum_{i=1}^{N} \left(B_{J,i} - \frac{B_{J,N+1}\, A_{N+1,i}}{A_{N+1,N+1}}\right)$$

$$\sum_{i=1}^{N} W_{J,i} = \sum_{i=1}^{N} \left(B_{J,i} - \frac{B_{J,N+1}\, A_{N+1,i}}{N_{uw} + A_{N+1,N+1}}\right)$$

$$V_J = \frac{B_{J,N+1}\, N_{uw}\, T_c}{N_{uw} + A_{N+1,N+1}}$$

The A_{Ji} and B_{Ji} are the collocation coefficients for the first and second order differential operators respectively and N is the number of interior zeros of the orthogonal polynomial used. Explicit forms for A and B may be found in Appendix (A1), tables (A1.1and A1.2).

3.3.3 Remarks on the solution steps:

The system of equations (3.10 to 3.12) is an initial value problem and may be solved by any suitable explicit integration procedure. In this study the fourth order Runge Kutta Merson has been used. The pellet equations are solved at the collocation points radially (i.e. at J = 1,2... N) and at every axial step. To obtain the state variablesvalues anywhere along the radial direction, a quadrature formula is used based on the trial solutions given by (3.7 to 3.9). To do this we first estimate the values of the parameters a_i at the collocation points where the values of the state variables were obtained (see Appendix (A1.4.1)). Having estimated a_i, the radial profiles can be generated at any point $0 \leq r \leq 1$. This method has been used during the integration and the state variables values obtained at r = 0.0 by extrapolation and is therefore subject to some error, depending on the order of the orthogonal polynomial used. It should be mentioned here that reducing the number of equations to be integrated from 3(N+1) to 3N does not reduce the accuracy of solution, when working to 4 significant figures.

3.3.4 Double collocation:

The above system given by (3.10 to 3.12) can in fact be solved by any integration method, either explicitly by Runge Kutta methods or implicitly using a finite difference procedure or collocation method. It is useful to attempt to apply the double collocation, i.e. in each of the two independent variables, r and z. The attraction of double collocation is particularly evident when transient behaviour of the system is being

studied. Here, a three dimensional partial differential equation can, in principle, be reduced to a system of first order ordinary differential equations without loss of accuracy.

Thus the system given by (3.10 to 3.12) may be reduced to a system of nonlinear algebraic equations. The details of the reduction method are given in Appendix (A1.5). In compact form they can be represented by the following:

$$\sum_{J=1}^{N}\sum_{K=2}^{M+2}\sum_{i=1}^{M+1}\left(\Delta z(B_{J,i}\ CA_{K,i}) - G_1(AA_{K,i}\ CA_{i,J})\right) - \sum_{J=1}^{N}\sum_{K=2}^{M+2} RA\Big|_{K,J} = 0.0 \qquad (3.13)$$

$$\sum_{J=1}^{N}\sum_{K=2}^{M+2}\sum_{i=1}^{M+1}\left(\Delta z(B_{J,i}\ CB_{K,i}) - G_1(AA_{K,i}\ CB_{i,J})\right) - \sum_{J=1}^{N}\sum_{K=2}^{M+2} RB\Big|_{K,J} = 0.0 \qquad (3.14)$$

$$\sum_{J=1}^{N}\sum_{K=2}^{M+2}\sum_{i=1}^{M+1}\left(\Delta z(B_{J,i}\ T_{K,i}) - G_3(AA_{K,i}\ T_{i,J})\right) + \sum_{J=1}^{N}\sum_{K=2}^{M+2} RT\Big|_{K,J} = 0.0 \qquad (3.15)$$

the boundary conditions are:

$$\sum_{J=1}^{N}\sum_{K=2}^{M+2}\sum_{i=1}^{M+1} A_{N+1,i}\ CA_{K,i} = 0.0$$

$$\sum_{J=1}^{N}\sum_{K=2}^{M+2}\sum_{i=1}^{M+1} A_{N+1,i}\ CB_{K,i} = 0.0 \qquad \text{at } r = 1 \qquad (3.16)$$

$$\sum_{J=1}^{N}\sum_{K=2}^{M+2}\sum_{i=1}^{M+1} A_{N+1,i}\ T_{K,i} = \sum_{J=1}^{N}\sum_{K=2}^{M+2} Nuw(T_e - T_{K,N+1})$$

the initial conditions being:

$$\sum_{J=1}^{N} CA_{1J} = CA(r_J),\quad \sum_{J=1}^{N} CB_{1J} = CB(r_J) \text{ and } \sum_{J=1}^{N} T_{1J} = T(r_J) \text{ at } z = 0.0$$

$$0 \leqq r \leqq 1 \qquad (3.17)$$

where $RA_{K,J} = \Delta z\ G_1 G_2\ (\phi_1^2 + \phi_3^2) CA\big|_{K,J}$

$RB_{K,J} = -\Delta z\ G_1 G_2\ (\phi_1^2 + \phi_3^2) CA\big|_{K,J}$

$RT_{K,J} = -\Delta z\ G_3 G_4\ (T_p - T)\big|_{K,J}$

M = number of interior zeros to approximate the axial profile during the integration step and M+1 = 0.0 and M+2 = 1.

z = axial integration step

AA = The collocation coefficients used to apprcximate the axial first order differential operator. Explicit forms are given in Table (A1.3).

The system of algebraic equations given above can be rearranged into matrix form as described in Appendix (A1.5). In general terms it takes the following form:

$$[Q][Y] = [V] - [R]$$

where M = a square matrix containing the coefficients B^s and AA^s

Y = a column vector containing the state variables to be determined

V = a column vector containing the boundary values at r = 1 and the initial values for an integration step

R = a column vector containing the nonlinear reaction terms.

Two methods can be used to solve the above matrix system. A Newton Raphson method will provide quadratic convergence of the non-linear system, if it does converge. Alternatively a matrix inversion method can be employed as in linear systems. Both methods are iterative and no difficulties concerning convergence have been met in all the cases studied. The details of the computational procedure are given in Appendix (A1.6).

3.4 Discussion

It is useful here to examine the conditions under which an accurate solution can be obtained in an acceptable computation time. Two factors are particularly relevant, namely, the properties of the orthogonal polynomials employed and the number of collocation points which can be used to approximate a differential operator to a certain accuracy.

Jacobi and Legendre orthogonal polynomials have been investigated. These chosen types cover a wide range of the general properties of orthogonal polynomials which may be relevant to reactor problems. The general form of these polynomials[121] can be represented by $P_i^{\alpha,\beta}(x)$, where the members of these polynomials are orthogonal with respect to the weighting function $W^{\alpha,\beta}(x)$. Thus, if $W^{\alpha,\beta}(x) = (1-x)^{\alpha}x^{\beta}$, varying the values of α and/or β gives rise to different kinds of polynomials, as illustrated in Appendix (A1.3). For example putting $\alpha = \beta = 0$ gives Legendre polynomials, while Jacobi polynomials may be obtained by putting $\alpha = 1$ and $\beta = 0$. In effect the values of α and β determine the distribution of the polynomials zeros in the approximation interval. When α and β take on large values, the zeros are usually clustered in the middle of the interval. Changing only α or β, the zeros are shifted to one end only, while using low values of both α and β in the range between $-\frac{1}{2}$ to 1 a more uniform distribution may be obtained. Legendre polynomials have zeros well distributed, with some concentration near to the two ends of the interval. Jacobi polynomials emphasize the middle of the approximation interval. It has been observed that[121] Legendre polynomials give the smallest approximation errors at both ends, although large errors may occur within the approximation interval. On the other hand Jacobi polynomials give the minimum errors in the middle regions.

The general behaviour of the different orthogonal polynomials and the relation between the zerosdistribution and the approximation power

depends to a great extent on the problem to be approximated. In the reactor problem under study, the type of boundary conditions, the behaviour and magnitude of change of the nonlinear function to be approximated and the location where the maximum accuracy in the integration interval is required may demand certain conditions not given by the above properties. In actual practice, this can be interpreted in terms of convergence rate and accuracy which sometimes means fewer collocation points and therefore shorter computing times.

Listed in Tables 3.1 and 3.2 are the members of the set which require the smallest computational time yet give answers within the error tolerance specified. Comparison was made between the finite difference, the single collocation and the double collocation procedures and the data used in this simulation is given in Table 3.3.

Table 3.1 for the case $N_{uw} = 2.0$ and Table 3.2 for $N_{uw} = 5.0$ indicate that the single collocation method with N = 3 (N is the number of interior collocation points in the radial direction) for any type of polynomial is from 4 to 7 times faster than the finite difference solution when working for 3 to 4 significant figures accuracy. The corresponding axial temperature and concentration profiles are shown in figures 3.1 and 3.2, and the respective radial profiles can be seen in figures 3.3 and 3.4, which demonstrate that in such severe situations, when a radial temperature difference of 40% using N_{uw} = 2.0 or more than 45% in the case $N_{uw} = 5.0$, a 3 point collocation in the radial direction is sufficient to give 4 significant figures accuracy in temperature and 3 figures accuracy in concentration. On the other hand, with N = 2, the approximation of such severe radial profiles was inadequate. However, the Legendre polynomials still approximate the profiles more closely than Jacobi polynomials.

Table 3.1: Comparison between single, double collocation and finite difference methods for Nuw = 2.0

Method of integration r z	N	M	Approx. computing time in seconds	Average no. of iterations per step	Absolute errors at z = 0.6 and r = 0.0		
					T 0.07735	CA 0.02166	CB 0.29742
Legendre-Runge Kutta	2+	80	150	2	0.0001	0.001	0.001
	2+	50	120	2	"	"	"
	3	80	190	2	0.00001	0.0002	0.00023
	3	50	160	2	"	"	"
Legendre - Legendre	2+	80	130(180)	1-2(2-4)	0.0001	0.003	0.001
	2+	50	120(200)	1-3(3-5)	"	"	"
	3	80	160(250)	2-3(3-5)	0.00001	0.00013	0.0002
	3+	50	150(260)	2-3(4-7)	"	"	"
Jacobi-Runge Kutta	3	80	170	2	0.00001	0.0001	0.0005
	4	80	240	2	"	"	0.0001
Jacobi - Legendre	3	80	170(300)	1-3(3-5)	0.0004	0.001	0.002
Finite difference	15	150	750	3-5	0.0001	0.01	0.005
(Crank Nicholson)	20	200	960	2-5	0.00001	0.0001	0.00001

1. N = number of interior collocation points in the radial direction r.
2. M = number of axial integration steps.
3. Values between brackets are solutions obtained without linearization.
4. For the given E_1 an error of 0.001 in dimensionless temperature equal 19°C.

+ using the square values of the zeros.

Table 3.2: Comparison between single, double collocation and finite difference methods for Nuw = 5.0

Method of integration r z	N	M	Approx. computing time in seconds	Average no. of iterations per step	Absolute errors at z = 0.5 and r = 0.0		
					T 0.06726	CA 0.06382	CB 0.34613
Legendre-Runge Kutta	3	80	190	2	0.00001	0.0001	0.0001
	4	80	240	2	"	"	"
Legendre - Legendre	3+	80	160	1-2(3-6)	"	"	"
Jacobi - Legendre	3	80	180	1-2(3-6)	0.0001	0.001	0.003
Finite difference	15	150	770	3-5	0.001	0.01	0.006
	20	200	1040	2-5	0.00001	0.0001	0.0001

A_{01}	3.62×10^{9} sec^{-1}	θ_1	2.09×10^{5}
A_{02}	7.99×10^{5} sec^{-1}	θ_2	3.10×10^{3}
A_{03}	1.60×10^{5} sec^{-1}	θ_3	1.39×10^{3}
E_1	32 kcal/g.mole	B_o	5.01×10^{-5}
E_2	21 kcal/g.mole	H_2	0.695
E_3	18 kcal/g.mole	H_3	1.695
$(-\Delta H_1)$	367 kcal/g.mole	E_{2/E_1}	0.656
$(-\Delta H_2)$	255 kcal/g.mole	E_{3/E_1}	0.563
$(-\Delta H_3)$	622 kcal/g.mole	Sh_A, Sh_B	500
Dp_A, Dp_B	3.66×10^{-3} cm^2/sec	Nu	1.0
DF_A, DF_B	6.88 cm^2/sec	N_{uw}	2.0
k_{c_A}, k_{c_B}	4.36 cm/sec	N_{uw}^*	1.33
h	1.2×10^{-3} $cal/cm^2 sec°K$	γ_1	24.51
b	0.21 cm	γ_3	13.79
L	125 cm	β_1	0.667
Kp	5.04×10^{-4} $cal/cm/sec°K$	β_2	0.46
KF	1.7×10^{-3} $cal/cm/sec°K$	β_3	1.13
u	164 cm/sec	G_1	0.84
R	2.1 cm	G_2	0.095
U	6.7×10^{-4} $cal/cm^2/sec°K$	G_3	0.84
e	0.4	G_4	76.85
C_p	0.25 $cal/g/°K$	N_{uw}	2.0
ρ	9.9×10^{-4} g/cm^3	CA (inlet)	1.0
C_o	3.05×10^{-7} $g.moles/cm^3$	CB (inlet)	0.0
TF(inlet)	660 °K	T (inlet)	0.0408
TC	660 °K	T_c	0.0408
Pe_H, Pe_M	10	G_5	0.64 secs.
Pe_{Ha}, Pe_{Ma}	600	G_6	0.64 secs.
$C_p^* \rho^*$	0.0177 $cal/cm^3/°K$	G_5'	0.76 secs.
		G_6'	0.76 secs.
		K_T	1.55 secs.

Table 3.3: A typical set of data used in the solution of the reactor models (unless otherwise specified in figures)

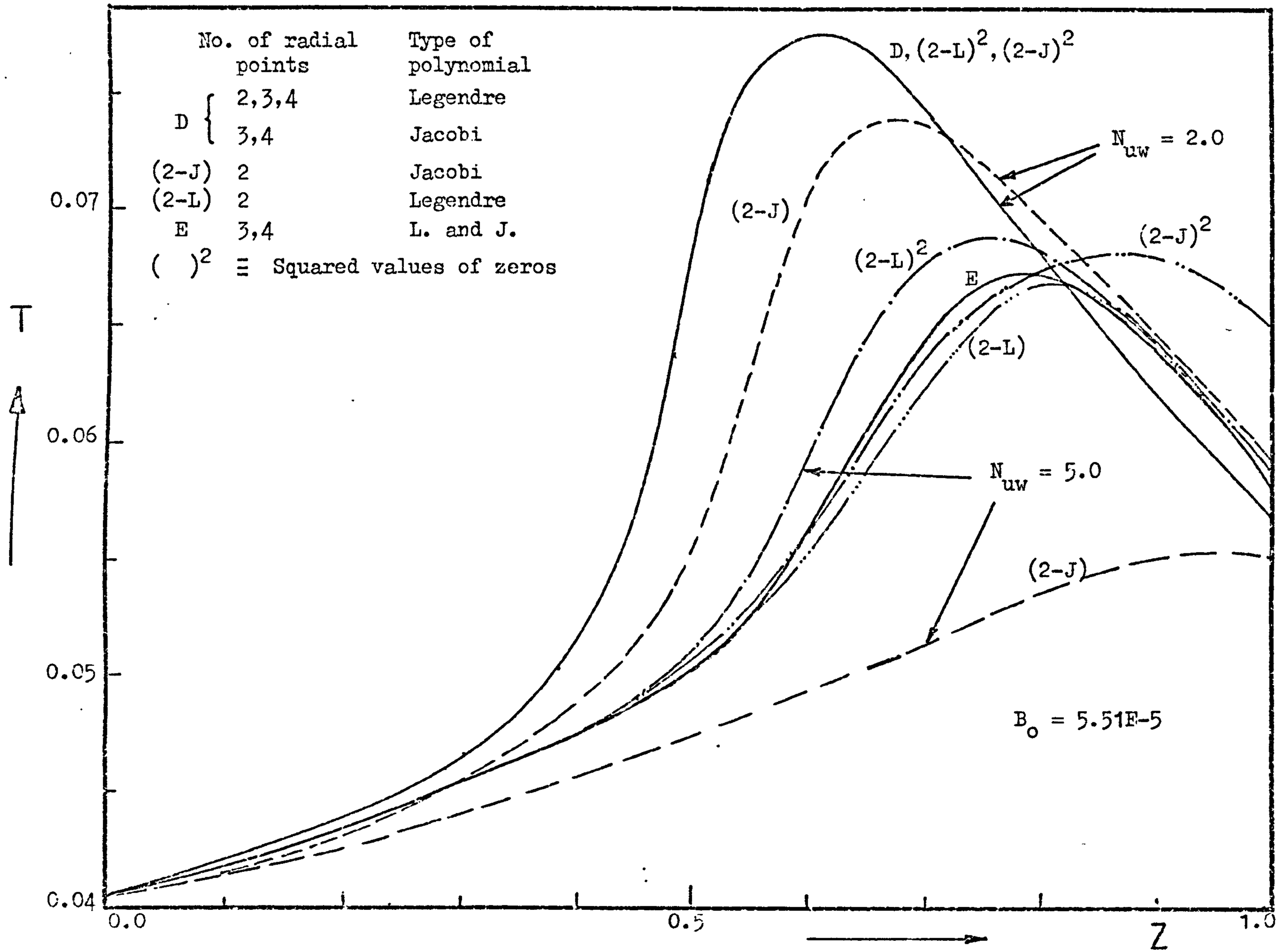

Figure 3.1: Effect of number and position of radial collocation points on accuracy of approximating axial temperature profiles at r = 0.0. Data as given in Table 3.3.

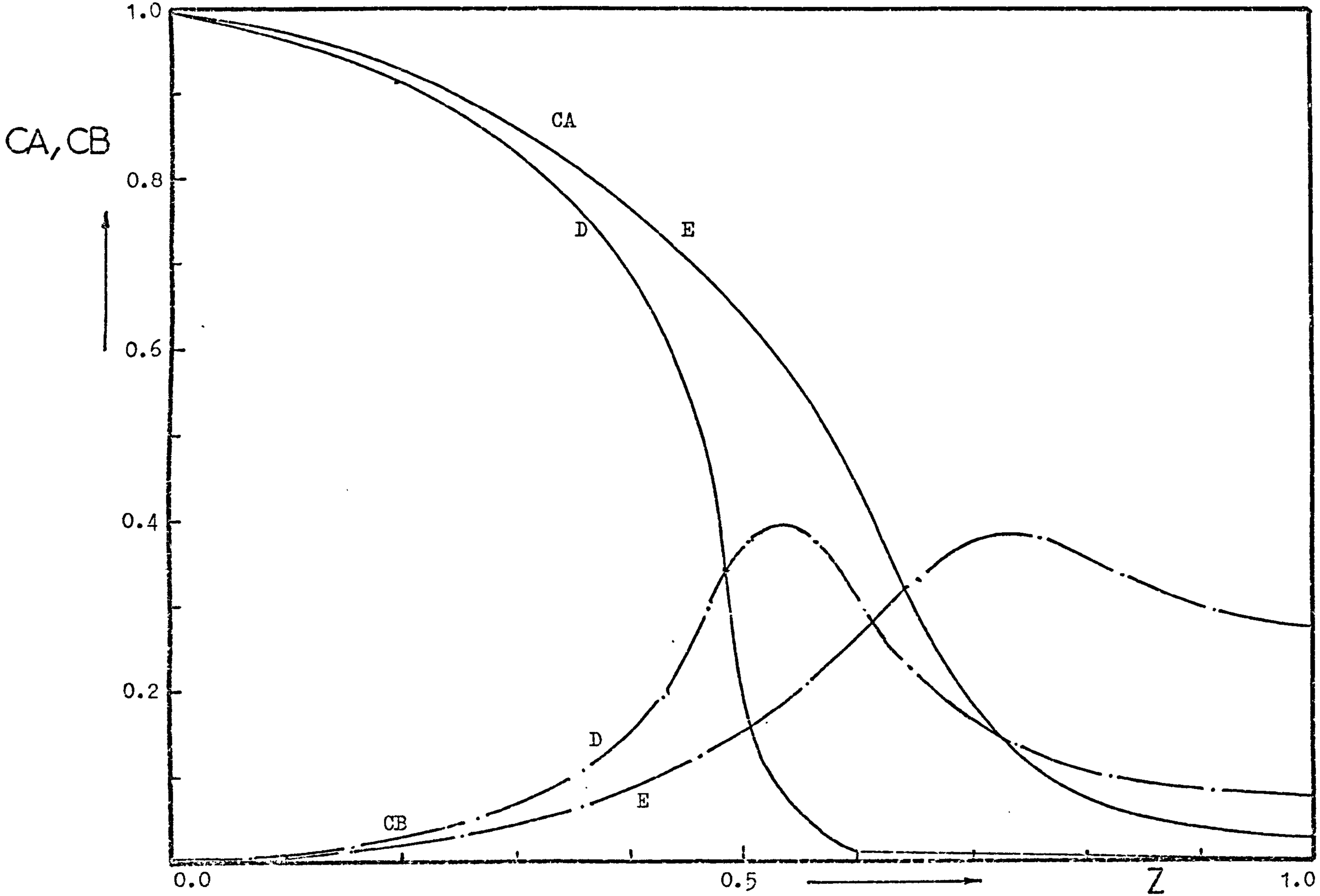

Figure 3.2: Axial concentration profiles corresponding to case D and E in Figure 3.1.

It is imperative here to indicate that the importance of decreasing the number of N from 3 to 2 reduces the computing time by about 30% as shown from Tables 3.1 and 3.2. This reduction is mainly due to the smaller number of the pellet equations which have to be evaluated, and also to the size of the matrix which has to be inverted. Nevertheless, the reason that Legendre polynomials (w = 1) with N = 2 give better approximation may be due to the fact that the zeros are situated nearer to r = 1, and thus emphasizing this region, as can be seen from figure 3.3. In the case of Jacobi polynomials, with w = $(1 - r)^2$, the zeros are shifted nearer to the middle of the interval r = 0.0 and r = 1. However, since the temperature and concentration at r = 0.0 are obtained by extrapolating those at the collocation points, the nearer these are to the centre, the more accurate the extrapolated values would be. Therefore a situation arises which indicates that there may be an optimal distribution of the collocation points to give the best approximation for the function. This optimal distribution becomes less important as N increases as can be seen from figure 3.3 for N = 2, 3, and 4 for Legendre and Jacobi polynomials. In this respect it may be seen that any polynomial gives the same accuracy. Squaring the zeros of Legendre and Jacobi for N = 2 and 3, a new distribution of the collocation points may be obtained by which the axial profiles can be recomputed and compared to those obtained above as shown in figure 3.1. It is obvious that in the case of N_{uw} = 2 and using N = 2, the new locations of the collocation points shown in figure 3.3 give an accuracy comparable to N = 3. However, increasing N_{uw} to 5 where the radial difference in temperature is more than 45% at z = 0.8 (see figure 3.3), the approximation does not improve, although the new distribution of the collocation points still

gives a better approximation, and in the case of Legendre zeros an upper bound on temperature has been obtained at r = 0.0. In other cases, where temperature increases of about 30% across the radial direction and for Nuw = 2 or 5, the new distribution of the collocation points for N = 2 using the squares of Legendre zeros gives 3 significant figures accuracy in temperature and 2 figures accuracy in concentration at the axial positions (i.e. r = 0.0). Such accuracy needs 3 collocation points with the original distribution of the Legendre zeros.

From figure 3.3 the zeros of the Legendre polynomials and their squared values are located on the radial temperature profile. It can be observed that the positions for N = 2 depend to some extent on the behaviour of the function to be approximated. The new locations of the squared zeros are located such that they take into consideration the full variations which occur. This is more apparent for Legendre than Jacobi squared values. Moreover the new Legendre squared zeros for N = 2 enable the extrapolated values to be obtained with more accuracy.

It has been noticed that, in all the cases studied, the convergence rate of the new distribution of the collocation points has improved for N = 2 and 3 and for both Legendre and Jacobi squared zeros. This observation contradicts the basic property of collocating at the orthogonal polynomial zeros, namely that the best distribution of the collocation points is at the zeros of the orthogonal polynomials. However, this property applies strictly to linear problems and should be looked at with reservation when dealing with nonlinear problems. Moreover, it seems that the rate of convergence for low values of N

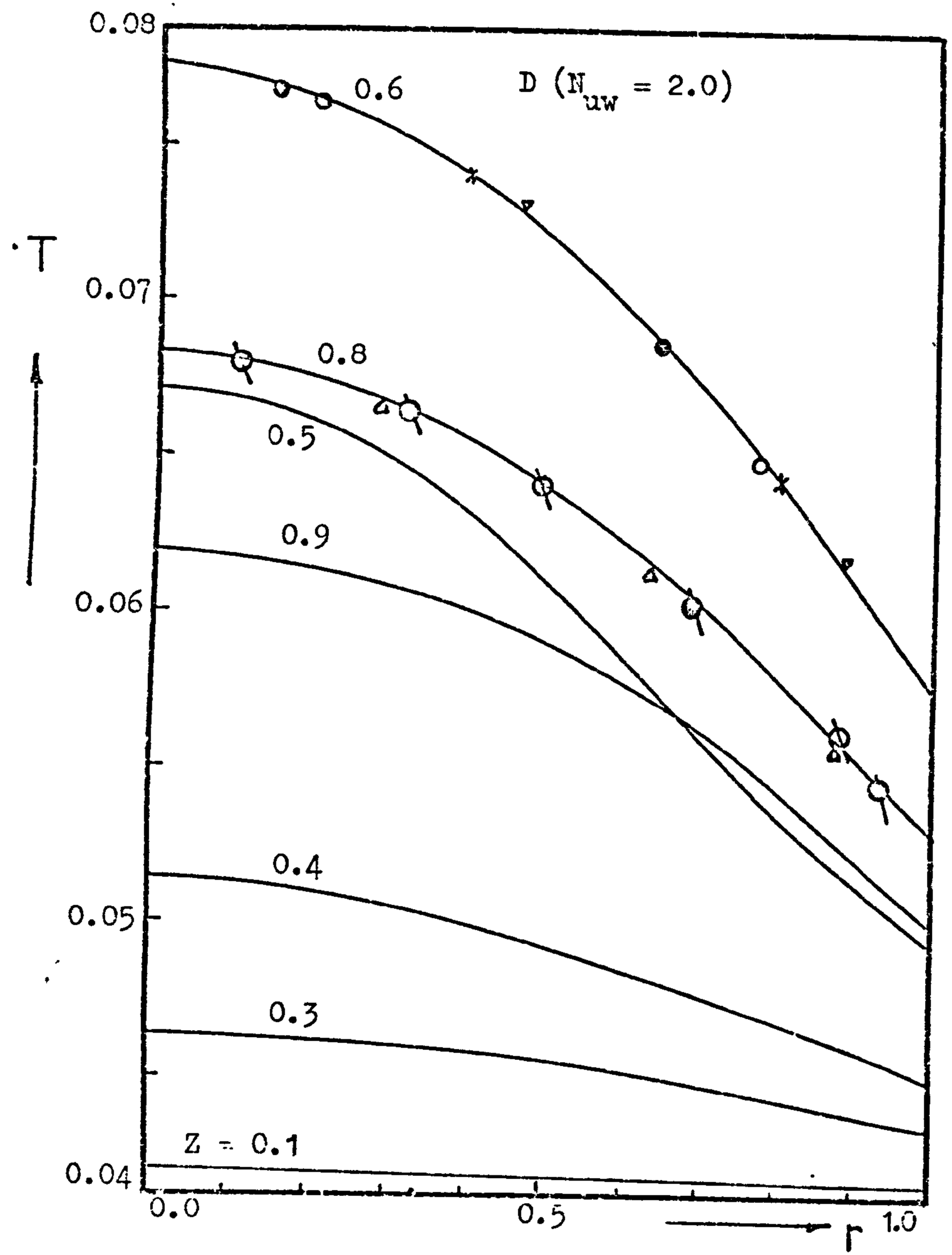

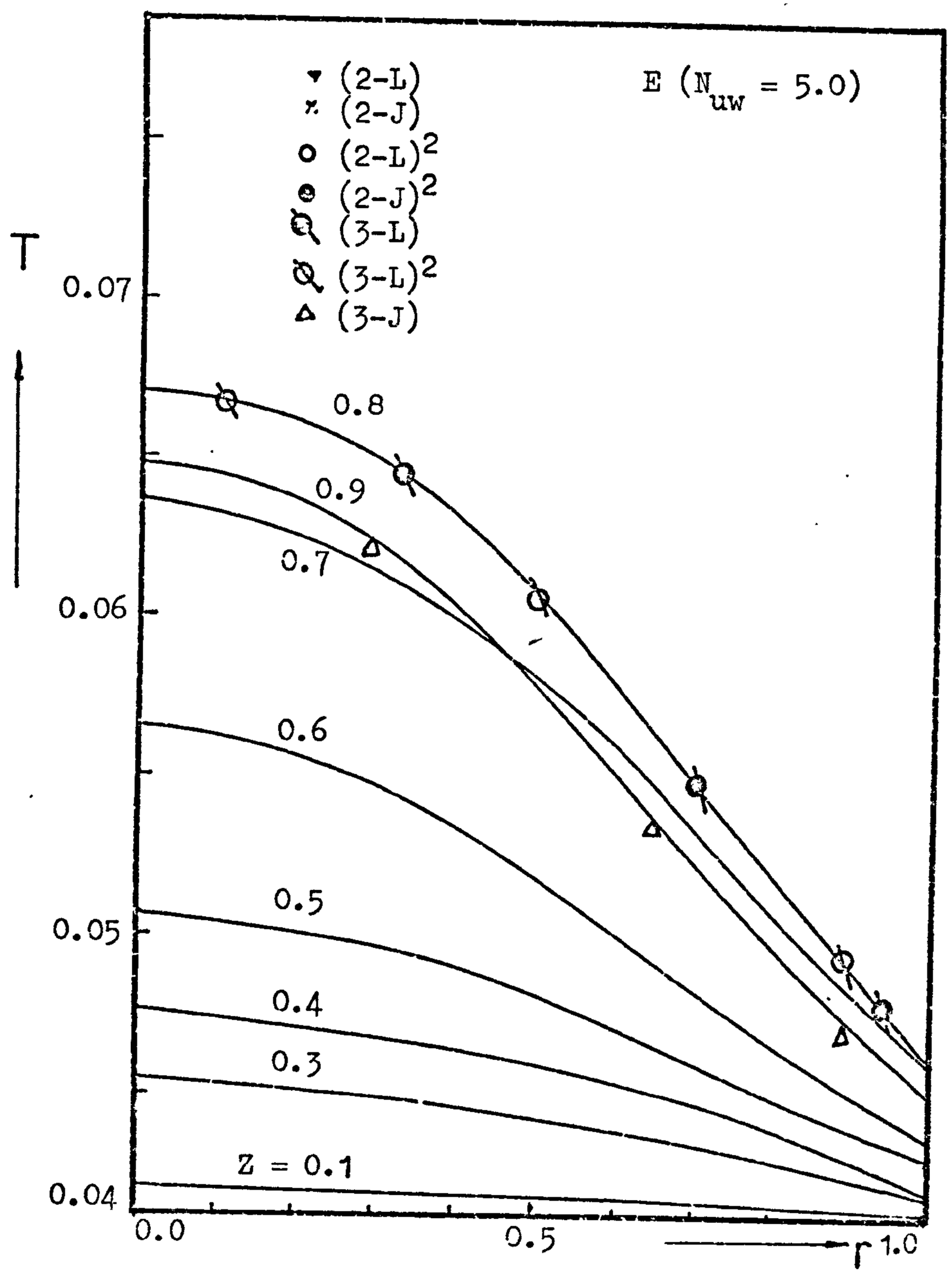

Figure 3.3: Location of various collocation points on the radial temperature profiles corresponding to case D and E in Figure 3.1.

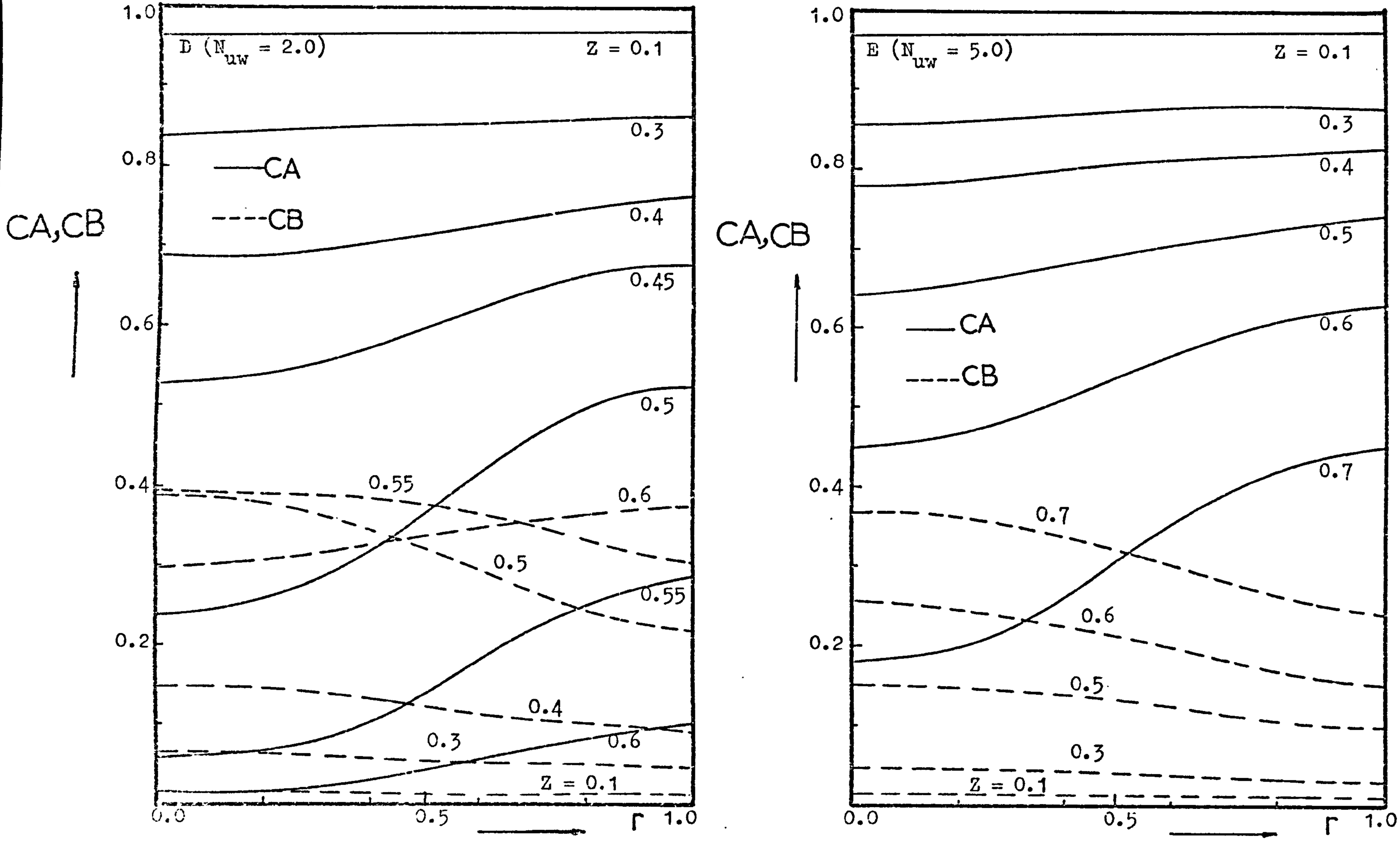

Figure 3.4: Radial concentration profiles corresponding to case D and E in Figure 3.1.

is independent of the orthogonal polynomials properties and that for $N \geq 4$, the convergence rate becomes better for the collocation points situated at the orthogonal polynomial zeros. For high values of N any orthogonal polynomial can be used, and thus the argument about the best locations for the collocation points is not so important.

The above results therefore indicate that a reduction in the number of collocation points can be attained if the location of the collocation points are chosen in such a way as to take into consideration the behaviour of the function to be approximated. From the above results N may be reduced by one for the same accuracy of approximation or an increase in accuracy for the same N can be obtained.

When the collocation method is also used as an integration procedure instead of Runge Kutta method, the term double collocation is used. It has to be remembered that although one kind of orthogonal polynomials may be used in the radial and axial directions, the difference is that the first are even polynomials (due to the radial symmetry), while in the axial direction and due to the unsymmetry of the axial profiles, the zeros of the polynomials and their coefficients are slightly different (see Appendix (A1.4.2)). 80 axial integration steps were sufficient when either Runge Kutta Merson or the collocation procedures were employed. In fact even with steep gradients such as those shown for temperature and concentration profiles in figures 3.1 and 3.2, 50 axial steps can be used without affecting the accuracy of integration. It has been indicated that the optimum value of M (the number of interior collocation points in axial direction) is between 2 and 3. This optimum number is based primarily on consideration of the size of the matrices involved, the number of axial

steps and therefore on computing time. Legendre polynomials were found to give the most accurate results when used as an integration method. This could be expected, since Legendre polynomials give the minimum errors at the ends of the integration interval, and thus the inherited errors from any previous step should be kept to a minimum throughout the integration.

From Tables 3.1 and 3.2, using Runge Kutta Merson or Legendre orthogonal polynomials with M = 2, together with Newton Raphson method to enhance convergence as an integration method, indicates that for a given accuracy no appreciable reduction in computing time results using the latter. This contradicts the results of Villadsen and Sorensen who claimed that using Legendre polynomials, instead of the fourth order Runge Kutta method, reduces the computing times by a factor of 4 to 10 for linear problems. The argument for their resultant improvements has been based on using M = 2 in the axial direction where the fifth term in the truncated Taylor series expansion is almost correct, while it is truncated in the fourth order Runge Kutta. Thus the attainable accuracy as well as the convergence rate might be expected to improve using the collocation method with fewer axial steps. However, in our case two factors must be taken into consideration. Due to the nonlinearity of the problem, use is made of Newton Raphson method, which in turn involves a matrix inversion. The second factor which to a great extend depends on the first, is that due to the iterative nature of the solution method in each integration step, more than one matrix inversion is usually necessary. This is not the case with Runge Kutta. So it seems that the time taken in matrix inversion over-rides the advantages to be found in the linear problem. It is possible to solve the system without Newton Raphson and

in this case, no matrix inversion is involved, although the solution procedure is still iterative. As can be seen from Tables 3.1 and 3.2, the values in the brackets indicate that the number of iterations increases and as a result the computing time is even greater.

Thus the decision to use either procedure depends on three factors:

1. The relative computing time involved in function evaluation at each collocation point (in our case the pellet equations) as compared to the time taken in matrix inversion, the size of which is determined by N and M.

2. The magnitude of changes taking place in the integration process which can be translated to the number of iterations per step.

3. Whether the solution is repeated several times as in the case of optimization, or optimal control algorithms.

Using the procedure without Newton Raphson, making the double collocation faster than Runge Kutta Merson, if the number of iterations per step does not exceed 2. In the case of Runge Kutta Merson, 5 function evaluations are needed per step and it has been observed that it takes 2 iterations for convergence. In the case of the double collocation, 4 function evaluations are needed, so it is apparent that the latter could be faster in nonlinear problems as is the case here.

The conditions stated above are found in the transient state where the changes during a time step are usually small, and this makes the double collocation a more suitable method of solution. In addition, its ability to reduce a system of three dimensions, as in the transient state, to one dimension is certainly a significant factor and cannot be ignored. This method will therefore be used in the next chapter and examined further.

3.5 Conclusions

The system of nonlinear partial differential equations describing the physical and chemical processes in the reactor at steady state, has been solved by collocation. Comparisons in terms of accuracy of solution and computing time have been made between the implicit finite difference representation (Crank Nicholson), the single and double collocation procedures.

It has been shown that the single collocation method (collocating in the radial direction and integrating with Runge Kutta Merson), with $N \leqq 3$ is from 4 to 7 times faster than the finite difference method with $N \leqq 20$ for a comparable accuracy. A radial temperature gradient of more than 45% needs 4 collocation points while less than 40%, 3 collocation points can be used. If for such steep gradients less radial collocation points were used, the approximation seems to underestimate the parameters at the boundary. However it has been shown that a better approximation with fewer collocation points can be obtained if the distribution of the locations of the collocations is such that they emphasize certain regions where the function value is needed with great accuracy. In this respect reduction of N by one point has been obtained for comparable accuracy, faster convergence and reduction of computing times by about 30%.

The comparison between the single collocation and the double collocation procedures revealed that for nonlinear problems, where linearization procedures are used, no appreciable reduction in computing times is possible, unlike the linear problems.

Without linearization, the solution converges with slower rates. However, in certain cases where the changes taking place are small, and where not more than 2 iterations per step are required for the solution to converge, the double collocation, without linearization, can be appreciably faster than single collocation. Such conditions can be found in the study of transient problems.

Finally the collocation solution (for $N \leq 3$) for the radial diffusion model solved in this chapter takes from 3 to 4 times longer computing time than the corresponding plug flow model without radial diffusion.

CHAPTER 4

DYNAMIC MODEL WITH RADIAL DIFFUSION

4.1 Introduction

The particular attraction of mathematical modelling of fixed bed catalytic reactors has been the possibility of using these models as a basis for the design and control of reactors, and more importantly also for investigating the dynamic behaviour in regions of potential instability.

While dynamic models can, in principle, include as much detail as required to describe the behaviour adequately, the time taken to solve them is usually excessive. Thus it is desirable to develop either a more rapid method of computing the solution, such as the collocation method already described, or to simplify the models used. At this point, it is worth considering the general characteristics upon which selection of the appropriate model might depend. Clearly, it is not profitable to employ a model which is more elaborate than is necessary to satisfy the minimum requirements of accuracy and description in any given situation. Two considerations are relevant here; the first is the discrepancy between solutions obtained from different models of the system. If the results do not differ significantly over the practical range of operating conditions, then the simpler model should be used, provided that the necessary parameters can be satisfactorily measured or predicted. The second consideration is the need to relate the parameters of the model to physically identifiable processes. This is usually possible in complex models, but in the case of simpler models, the parameters may not be so readily identifiable.

For highly exothermic reactions, particularly where radial temperature gradient exists, a two dimensional model is needed to satisfy the constraints of accuracy, general reliability and description of the

physical phenomena. In dynamic modelling the situation becomes even more demanding as the resulting three dimensional model results in such prohibitive computing times[62,109] that no detailed examination of the reactor performance is possible. Most of the above workers used some form of finite difference methods of solution. However, it has been shown in the previous chapter that a substantial reduction in computing time can be achieved by using the more efficient methods such as collocation.[76]

Transient one dimensional models may be derived, but this is a result of grossly simplifying assumptions for the problem being considered, for example a parabolic radial temperature profile.[46,109] In such cases the estimated radial profiles tend to be inaccurate. Thus, although the dynamic models based on the one dimensional approach take considerably less computation time, they are inadequate in representing such systems and limit their use to qualitative predictions only. Consequently, any method which would both reduce the dimensionality of the model, yet retain some knowledge of that eliminated dimension certainly would be welcomed.

Model reduction techniques have been applied by McGreavy and Turner[135] to steady state models with reasonable success. Basically the technique, which will be the basis of that used here, is to eliminate one dimension, in this case the radial direction, and then reconstruct the solution in that eliminated dimension in a simple algebraic form. This can considerably reduce the computing time. In other words, instead of solving the system of equations as in the collocation method, by evaluating the parameters a_i to satisfy a trial function of the form

$$Y(r,z) = \sum_{i=0}^{N-1} a_i P_i (r^2),$$

in model reduction an attempt is made to formulate the parameters a_i

in terms of the physical parameters of the system and/or to a general form of $P_i(r^2)$, not necessarily orthogonal polynomials, to satisfy the radial boundary conditions. In some measure this takes account of the problem by choosing the appropriate polynomial and collocation points.

In this chapter the model reduction technique will be applied to the heterogeneous two dimensional dynamic model based on that given in Chapter Three. An assessment of the reduced model in terms of accuracy of representation and computing time in comparison with the collocation procedure solution will be carried out. Its advantages and disadvantages over the one dimensional dynamic model with the assumption of radial parabolic temperature profile will be examined.

Consideration is also given to the identification of some of the dynamic characteristics of the reactor which may be of particular concern in formulating control strategies.

4.2 Formulation and solution of equations

Using the same nomenclature as that used for the steady state model of the reactor (see Chapter Three), the equations representing the heat and mass balances for the system may be written in dimensionless form as follows:

$$G_5 \frac{\partial CA}{\partial \tau} = \frac{1}{r}\frac{\partial}{\partial r}\left(r\frac{\partial CA}{\partial r}\right) - G_1\frac{\partial CA}{\partial z} - G_1G_2\eta(\phi_1^2 + \phi_3^2)CA \qquad (4.1)$$

$$G_5 \frac{\partial CB}{\partial \tau} = \frac{1}{r}\frac{\partial}{\partial r}\left(r\frac{\partial CB}{\partial r}\right) - G_1\delta\frac{\partial CB}{\partial z} + G_1G_2\eta\gamma(\phi_1^2 + \phi_3^2)CA \qquad (4.2)$$

$$G_6\frac{\partial T}{\partial \tau} = \frac{1}{r}\frac{\partial}{\partial r}\left(r\frac{\partial T}{\partial r}\right) - G_3\frac{\partial T}{\partial z} + G_3G_4\,(T_p - T) \qquad (4.3)$$

with boundary conditions

$$\frac{\partial CA}{\partial r} = \frac{\partial CB}{\partial r} = \frac{\partial T}{\partial r} = 0 \quad \text{at } r = 0,\ z \geqq 0, \tau \geqq 0 \qquad (4.4)$$

$$\left.\begin{aligned} \frac{\partial CA}{\partial r} &= \frac{\partial CB}{\partial r} = 0 \\ \frac{\partial T}{\partial r} &= N_{uw}\,(T_c - T) \end{aligned}\right\} \quad \text{at } r = 1,\ z \geqq 0, \tau \geqq 0 \qquad (4.5)$$

the initial conditions being

$CA = CA(r,\tau)$, $CB = CB(r,\tau)$ and $T = T(r,\tau)$ at $z = 0$, $0 \leqq r \leqq 1$ and $\tau \geqq 0$

The additional dimensionless quantities are

$$G_5 = G_1 \frac{L}{u} \text{ sec.} \quad \text{and} \quad G_6 = G_3 \frac{L}{u} \text{ sec.}$$

The pellet temperature T_p, the effectiveness factor η and the selectivity ψ can be estimated by solving the dynamic pellet equation

$$\frac{2}{3} \frac{K_T}{Nu} \frac{dT_p}{d\tau} = T - T_p + B_o \left[(sh_A (CA - C_{pAS}) \left(\frac{K_1(1 + H_2)}{K_1 + K_3} + \frac{K_3 \quad H_3}{K_1 + K_3} \right) - sh_B H_2 (C_{pBS} - CB) \right] \qquad (4.6)$$

This equation represents a heat balance on the pellet which is assumed to be isothermal. This assumption has been shown to be valid in the dynamic case.[46] For details and equations giving the concentrations C_{pAS} and C_{pBS} see Appendix (A1.2.2). The double collocation method applied in Chapter Three is employed here to reduce the partial differential equations to a system of first order ordinary differential equations. The Runge Kutta Merson integration method can then be used to integrate both the fluid and pellet in the time domain.

In a dynamic system where coupled transient effects are occurring, as is the case here, it is necessary to consider only those phenomena where the relative rates of change are of the same order of magnitude. If this is not the case, then the faster changes will enable one of the variables to reach a pseudo steady state, and the response will depend only on the transient event having the longest time constant. It is clear in the present case that the time constants of the fluid are small compared with that of the solid phase, since $G_5 = G_6 = 0.639$ sec. as against that of the solid $K_T = 1.55$ sec. This means that by putting the

time derivatives equal to zero, the fluid equations are reduced to algebraic system of nonlinear equations. The dynamic effect, therefore, comes only from the transient pellet equations. The system has been solved using this approximation which is in fact valid, as demonstrated elsewhere.(46,109)

The solution procedure, in general, is similar to that described in the case of steady state, except that the inlet variables are updated at the beginning of every time step. For details of the solution steps followed, see Appendix (A2.1).

Preliminary computation indicates that the changes in fluid conditions over the period of a time step are small. In this case, the system of algebraic equations describing the fluid may be solved without employing the Newton-Raphson iteration. This approach has confirmed that the convergence of the system is quite satisfactory. The average number of iterations per axial step has been found to be 1 or 2 over wide ranges of conditions. However, in the case of temperature runaway or similar severe cases, the number of iterations increases to 3 or 4. Such severe conditions usually occur over short time durations, making the advantage of solving the system without Newton-Raphson attractive, since it obviously requires shorter computation time and less storage.

In the following section a lumped dynamic model will be developed and assessed against the distributed parameter model described above.

4.3 The dynamic lumped model

In a one dimensional representation all the state variables are radial mean values. The reaction rates are also radial mean values and this is likely to raise problems of evaluation, since for nonlinear functions the radial mean value is not the same as the value at the radial mean conditions. Methods of tackling this difficulty have been

mostly confined to assuming radial parabolic temperature profiles[46,109] from which the mean rate is evaluated and an effective wall Nusselt number is derived as $N_{uw}^{*} = \frac{N_{uw}}{1 + 0.5\ N_{uw}}$. However it has been shown[46] that the discrepancy between the one and two dimensional models is mainly due to the deviation of the radial temperature profile from the assumed parabolic representation with the result that either the reaction rate is underestimated, or the heat removal is being overestimated, or both. Since the two cases produce similar effects, it appears that the model can be improved by adjusting both of them in a suitable way.

4.3.1 Formulation of equations

The distributed system of equations given by (4.1 to 4.5) can be lumped to eliminate the radial operator terms and so defining the state variables as mean values (for details of reduction procedure see Appendix (A2.2)). Multiplying the above system of equations by 2rdr, integrating with respect to r over the radius[78] and then substituting for the boundary conditions, we get:

$$G_5 \frac{\partial CA_m}{\partial \tilde{t}} = -G_1 \frac{\partial CA_m}{\partial z} - D_{CA}\left(\zeta(\phi_1^{*2} k_1 + \phi_3^{*2} k_3)CA\right)_m \qquad (4.7)$$

$$G_5 \frac{\partial CB_m}{\partial \tilde{t}} = -G_1 \delta \frac{\partial CB_m}{\partial z} + D_{CB}\left(\zeta \gamma (\phi_1^{*2} k_1 + \phi_3^{*2} k_3)CA\right)_m \qquad (4.8)$$

$$G_6 \frac{\partial T_m}{\partial \tilde{t}} = -G_3 \frac{\partial T_m}{\partial z} - 2\ Nu'(T_m - 1) + D_T G_3 G_4 (T_p - T)_m \qquad (4.9)$$

The initial condition being

$CA_m = CA(\tilde{t}, z)$, $CB_m = CB(\tilde{t}, z)$ and $T_m = T(\tilde{t}, z)$ at $z = 0$ and $\tilde{t} \geqq 0$

The dimensional quantities which have been introduced are defined as follows:

$$T = \frac{TF}{TC}, \quad CA = \frac{C_{FA}}{C_o}, \quad CB = \frac{C_{FB}}{C_o}$$

$$\phi_i^{*2} = \frac{(1-e)R^2 A_{oi} \exp(-\gamma_i)}{e\, DF_A}, \qquad \gamma_i = \frac{E_i}{R_g T C} \quad \text{where } i = 1, 2 \text{ and } 3$$

$$K_i^*(T_m) = \eta(m) \exp(\gamma_i) \exp(-\frac{\gamma_i}{T_m}), \qquad k_i = \exp\left(\frac{\gamma_i (T(m) - 1)}{T(m)}\right)$$

The parameters involving argument m are evaluated at the mean conditions and the pseudo parameters are defined as follows:

1. The modified wall Nusselt number $Nu' = N_{uw}\left(\frac{T(r=1) - 1}{T(r=m) - 1}\right)$

2. The distribution factor $D = \frac{\text{the mean rate } R(T, CA, CB)_m}{\text{the rate at the mean state conditions } R(T_m, CA_m, CB_m)}$

It should be noted that accuracy of the reduced model given by (4.7 to 4.9) depends on adequate formulation of the pseudo parameters. They are radially dependent and therefore, knowledge of the radial temperature and concentration profiles is necessary.

4.3.2 The general form of the radial profiles

The algebraic expressions for estimating the radial temperature and concentration profiles are given below.[78] In the case of temperature, a correction function is added to the parabolic representation to account for the distortion of the profiles from the parabolic forms resulting from chemical reaction. The equations take the form:=

$$(T(r) - 1) = (1 + 0.5\, N_{uw}(1 - r^2))(w_5\,(1 - 3r^2 + 2r^3) + 1))$$

$$\left(\left(\frac{N_{uw}}{1.2\, N_{uw} + 4}\right)^2 (1 - 3r^2 + 2r^3) + 1)(T(1) - 1)\right) \qquad (4.10)$$

$$CA(r) = \Delta CA_T\,(3r^2 - 2r^3 - 0.7) + CA(m) \qquad (4.11)$$

$$CB(r) = \Delta CB\,(3r^2 - 2r^3 - 0.7) + CB(m) \qquad (4.12)$$

where $w_5 = \frac{10}{3}(\beta_1 \Delta CA_1 + \beta_3\, \Delta CA_3 + \beta_2\, \psi(m)\, \Delta CA_T)$

β_1, β_2 and β_3 are the thermicity factors for different reaction steps, in dimensionless form $\beta_i = \dfrac{(-\Delta H_i)\, C_o \dot{DF}_A}{KF\ T\ C}$ $\quad i = 1, 2$ and 3

ΔCA_T and ΔCB are pseudo parameters which will be defined later.

4.3.3 The form of the modified Nusselt number

Based on the corrected form of the radial temperature profile expression given above, the modified Nusselt number may be formulated as follows (see Appendix (A2.2)).

$$\text{If} \quad Nu' = N_{uw} \left(\frac{T(1) - 1}{T(m) - 1}\right)$$

where the mean temperature is defined by

$$(T(m) - 1) = 2 \int_0^1 (T(r) - 1) r\, d\, r$$

Substituting for $(T(r) - 1)$ from equation (4.10) and carrying out the integration, an expression for Nu' can be derived as

$$Nu' = \frac{N_{uw}}{(1 + 0.25\ N_{uw}) + P(N_{uw}) + Q(w5, N_{uw})} \qquad (4.13)$$

where $P(N_{uw}) = \left(\dfrac{N_{uw}}{1.2\ N_{uw} + 4}\right)^2 (0.3 + 0.11\ N_{uw})$

$$Q(w5, N_{uw}) = w5\left((0.3 + 0.11\ N_{uw}) + \left(\frac{N_{uw}}{1.2\ N_{uw} + 4}\right)^2 (0.17 + 0.47\ N_{uw})\right)$$

For a particular reactor, the wall Nusselt number N_{uw} is constant, so that $P(N_{uw})$ is constant and $Q(w5, N_{uw})$ is a direct linear function of w5. The terms P and Q are considered as corrections to the effective Nusselt number N_{uw}^* derived from the assumption of a parabolic temperature profile.

4.3.4 The form of the distribution factor

The distribution factor as defined earlier can be considered a correction factor for the radial fluid temperature and concentration

profiles in the one dimensional model which assumes it to be equal unity. It is possible to generate the radial reaction rate profile from the radial temperature and concentration profiles, from which the radial mean reaction rate can be determined by direct numerical integration using Simpson's rule.[78] However in generating the reaction rate at each radial node it is necessary to solve the pellet equations so that the reduced model could be said to be degenerating back to a two dimensional system. Therefore the number of radial points used in the radial integration should be kept to a minimum when evaluating the radial mean reaction rate (R(m)).

Using the simplest form of Simpson's integration rule, i.e.

$$R(m) = \tfrac{2}{3} R(\tfrac{1}{2}) + \tfrac{1}{3} R(1)$$

and the general form of the distribution factor can be written as

$$D = \frac{2R(\frac{1}{2}) + R(1)}{3R(m)}$$

where R(m) is defined as follows:

for species A given by equation (4.7)

$$R(m) = \left(\gamma (\phi_1^{*2} k_1 + \phi_3^{*2} k_3) CA \right)\Big|_m$$

for species B given by equation (4.8)

$$R(m) = \left(\gamma \psi (\phi_1^{*2} k_1 + \phi_3^{*2} k_3) CA \right)\Big|_m$$

and for temperature Tm given by equation (4.9)

$$R(m) = (T_p - T)\Big|_m$$

4.3.5 The pseudo parameter ΔCA_T

The functional form of ΔCA_T should reflect the inter-dependance of concentration and temperature profiles through the reaction rate expressions. A measure of the radial concentration difference may be used, namely $\Delta CA_T = CA(1) - CA(0)$. The value of ΔCA_T is not directly

available in terms of the reduced model, but is required in order to estimate the distribution factors, Nu' and to generate the radial temperature and concentration profiles. An empirical derivation has been carried out,[78] based mainly on relating ΔCA_T to the mean system states such as CA_m, Tm and the reaction rate constant $K^*(m)$. The resulting asymptotic value for ΔCA can be written as

$$\Delta CA_{ai} = \left[\frac{N_{uw} \, (K_i^*(m) - 1)}{1.18 \, K_i^*(m) \, (N_{uw} + 0.25) + 7.2 \, N_{uw} + 1/\phi_i^{*2}} \right]^2 \qquad (4.14)$$

where i = 1, 2, 3 for each reaction step.

For the general case where $K_i^*(m) \neq 1$, ΔCA_{ai} does not fulfil the inlet conditions for the concentration (i.e. $\Delta CA_{ai}|_{z=0} = 0$). In that event, the functional ΔCA_{ai} approaches its asymptotic form from the inlet $\Delta CA_{ai}|_{z=0} = 0$ in a manner which may be described by a development function of the following form:

$\Delta CA_i = \Delta CA_{ai}(1 - \exp(-\mathcal{F}_i))$ where ΔCA_{ai} is the asymptotic value and $\mathcal{F}$ is a pseudo parameter which is axially dependent function having in general an inverse relationship to ΔCA_{ai}. A convenient form is given by:

$$\mathcal{F}_i = \left[\frac{2(K_i^*(t_{mo}) - 1) + 1/\phi_i^{*2}}{K_i^*(t_{mo}) - 1} \right]^2 (1 - CA_m) \qquad (4.15)$$

This form becomes zero at z = 0 for $CA_m = 1$. The principal dependent variable of this function $\mathcal{F}_i$ is the radial mean conversion $(1 - CA_m)$. While this function takes care of the general temperature inlet conditions, in the case of concentration disturbances, where $CA_m \neq 1$, the developing function will not be zero initially. Depending on such disturbances, the development function will therefore pass through a maximum or minimum which will result in large errors being introduced. To remove this problem, a modified function of the following form can be used.

$$\xi_i = \left[\frac{2K_i^*(t_{mo}) - 1) + 1/\phi_i^{*2}}{K_i^*(T_{mo}) - 1} \right]^2 (CAI - CA_m) \qquad (4.16)$$

where CAI = a constant, always equal to the inlet mean concentration CA_m.

Finally the overall ΔCA_T for the complex reaction can be written as:

$$\Delta CA_T = \Delta CA_1 + \Delta CA_3$$

and $$\Delta CB = -\gamma(m)\ \Delta CA_T$$

4.3.6 Method of solution

This hyperbolic system of equations given by (4.7 to 4.9) can profitably be solved by the method of characteristics described in appendix (A2.3), using the Runge Kutta Merson procedure. The steps of the solution are as follows:

1. Assume values of CA_m, CB_m and T_m at the first (or next) axial position where they are unknown.

2. Using the values of step 1, evaluate CA, CB and T from the radial expressions at r = 0.5 and r = 1.0.

3. Integrate the transient equations for the catalyst pellet to evaluate Tp_m, ζ_m and ψ_m and also the values at r = 0.5 and r = 1.0 for this axial position and at the current time step.

4. Using the values of step 3, i.e. Tp, ζ and ψ at r = 0.5 and 1.0, evaluate the distribution factors for the fluid variables, and the values ζ_m and ψ_m to evaluate Nu'.

5. Integrate the fluid equations to evaluate the mean state variables at that position.

6. Compare the evaluated state variables with those used in step 1. If agreement is satisfactory continue to step 7, otherwise repeat from step 2 using the new predicted values of CA_m, CB_m and T_m.

7. Repeat from step 1 for $z \leqq 1$.

8. Repeat the whole computation for the next time step and continue as long as necessary.

For the purpose of this algorithm, Tp, γ and ψ are needed between each time step. Changes in Tp can be considered linear over the time step and the fluid equations are effectively subjected to a ramp change in Tp. Numerical calculations of the distribution factors have shown that the values of γ and ψ required may be estimated by using noniterative steady state equations, for the pellet. This approximation has been found more accurate in estimating intermediate values for γ and ψ than considering the changes to be linear, especially in regions of temperature runaway or multiplicity.

4.4 Comparison of the models and improvement of the lumped model

4.4.1 General comments

Previous numerical evidence[46,109] indicates that the capacitance of the fluid to absorb heat and mass is usually negligible in comparison to that of the catalyst pellets and therefore can be considered at a pseudo steady state. While this assumption has been found adequate in cases of one and two dimensional dynamic models, it is not necessarily valid in this lumped model because of its semi empirical structure. Preliminary computed results of the lumped model may be seen in Figure 4.1 where the temperature profiles are compared at three times for a step decrease in inlet temperature, for $G_5 = G_6 = 0$ and $G_5 = G_6 = 0.639$. The difference between the curves is negligible in comparison with the magnitude of the changes which are occurring. Treating the reactor fluid as being at a pseudo steady state enables great savings in computational effort to be made, particularly when step changes in concentration occur at the inlet, since it would then be necessary to take very small steps in the time direction to follow the disturbance through the reactor.

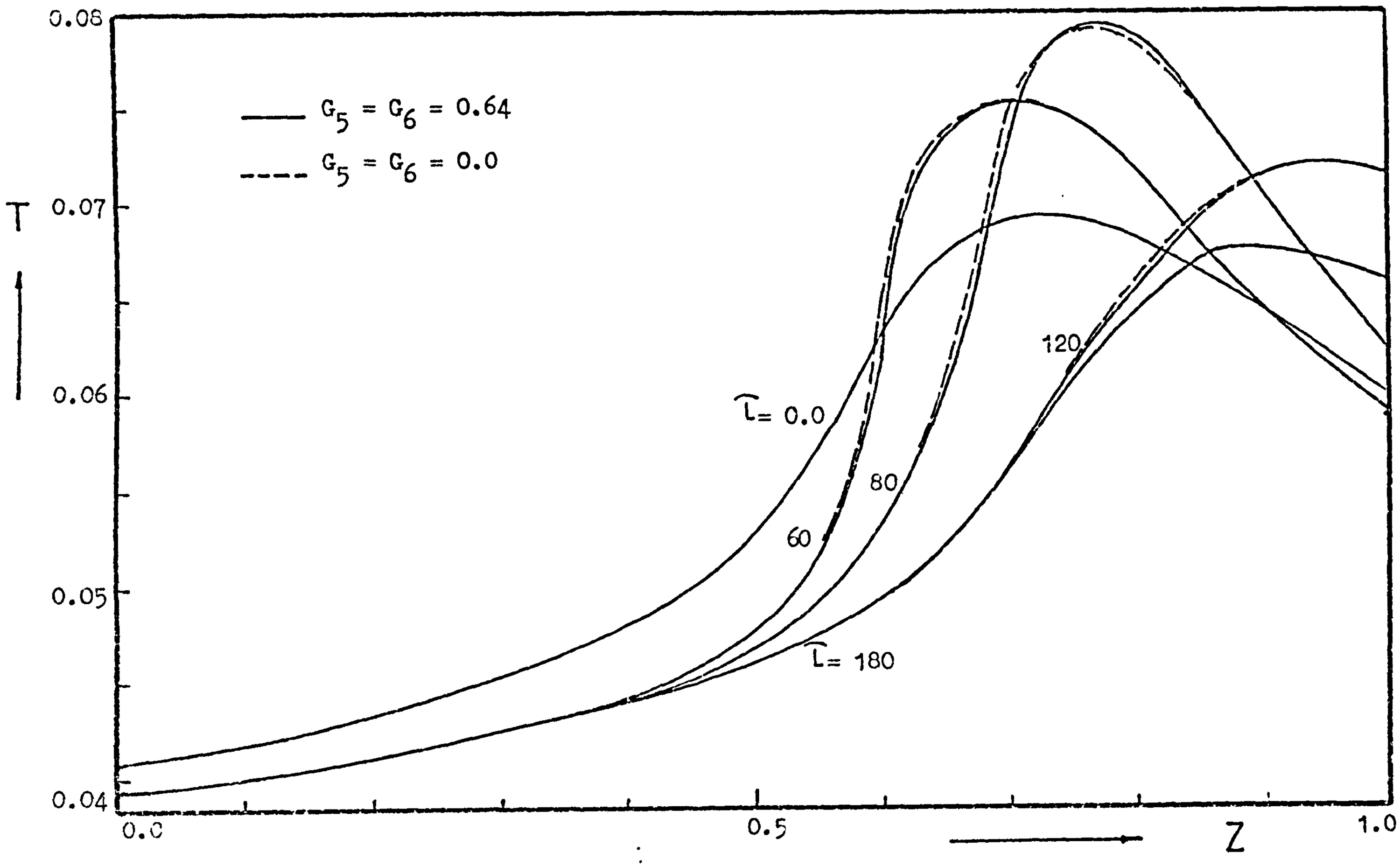

Figure 4.1: The effect of G_5 and G_6 on the centreline temperature profiles following a step decrease of 0.0013 in dimensionless inlet temperature. Data as given in Table 3.3. For the given E_1 this change represents approximately 21°C.

In the case of $G_5 = G_6 \neq 0$, time steps of 0.05 to 0.1 have been found necessary, to ensure convergence, while in the case of $G_5 = G_6 = 0.0$ a time step of 1.0 second has been found adequate in all cases studied here. In all cases 80 axial steps have proved satisfactory.

Comparison between the two dimensional dynamic model (3 point collocation) and the lumped model is shown in Figure 4.2 for a step decrease in inlet temperature. It can be seen that the discrepancy is negligible. Furthermore the ability of the lumped model to generate the radial temperature and concentration profiles may be seen from Figure 4.3 and Figure 4.4.

It is worthwhile mentioning here that, at each axial step, the pellet dynamic equations are evaluated at three radial points in the lumped model compared with only one evaluation in the one dimensional model. The direct solution of the two dimensional model using three point collocation also requires the solution of the pellet equations three times. Indeed, the lumped model gives accuracy comparable with the three point collocation, but it takes about $\frac{2}{3}$ the computation time. This is because the increase in the number of fluid field equations, as a result of radial discretization, increases the computational effort. In fact, it takes the same time as a two point collocation solution. Comparing the computational times of the one dimensional model, the lumped and the two dimensional model (three collocation points), they are of the order 1:3:4 respectively.

It has been observed that most of the computation time is taken up with pellet parameter evaluations. Thus, any gain to be made from this point onwards should be directed to reduce the number of pellet equations evaluations.

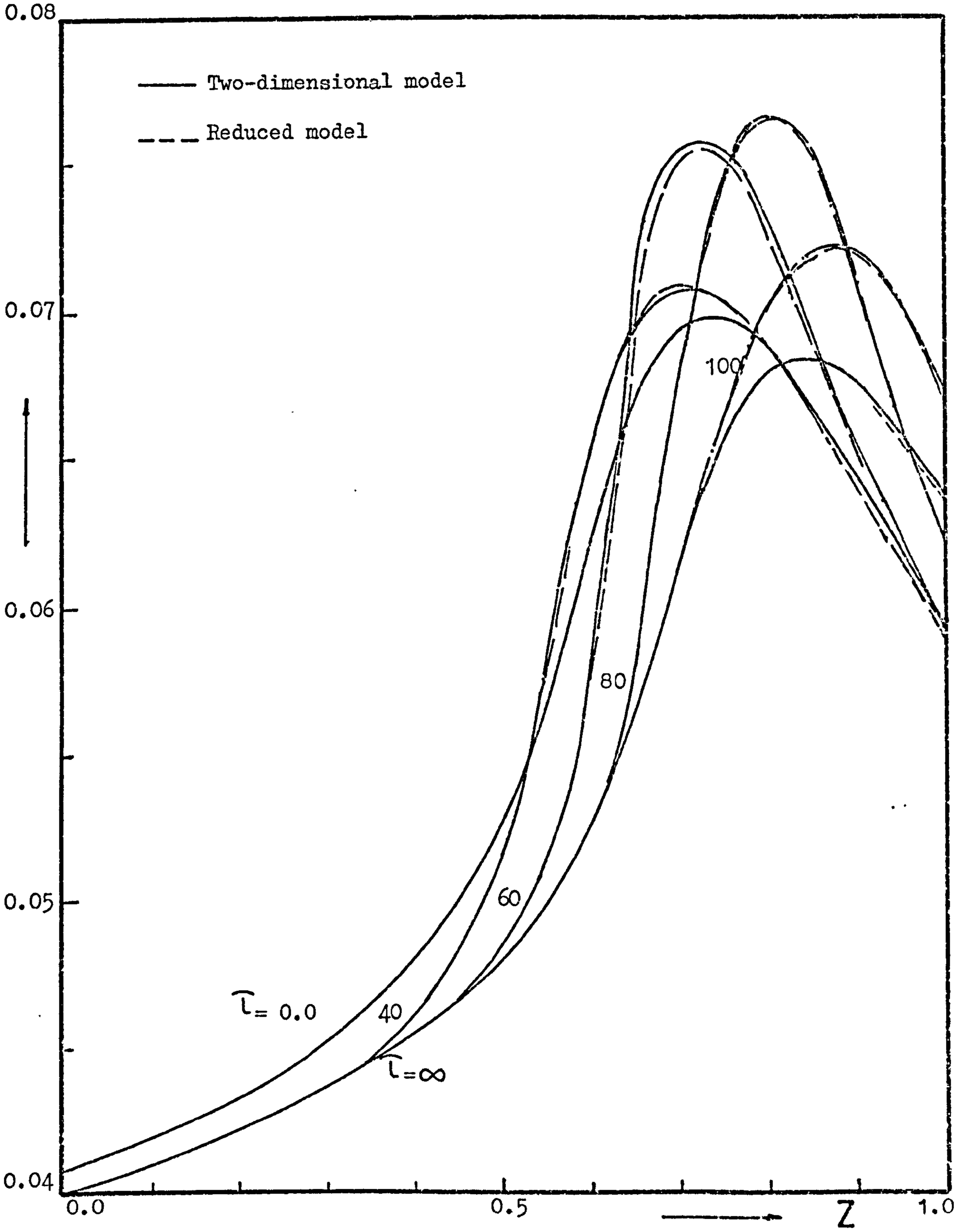

Figure 4.2: Comparison of temperature profiles at r = 0.0 predicted by the two-dimensional and reduced models following a step decrease in dimensionless inlet temperature of 0.0008. Data as given in Table 3.3. For the given E_1 this change represents approximately 13°C.

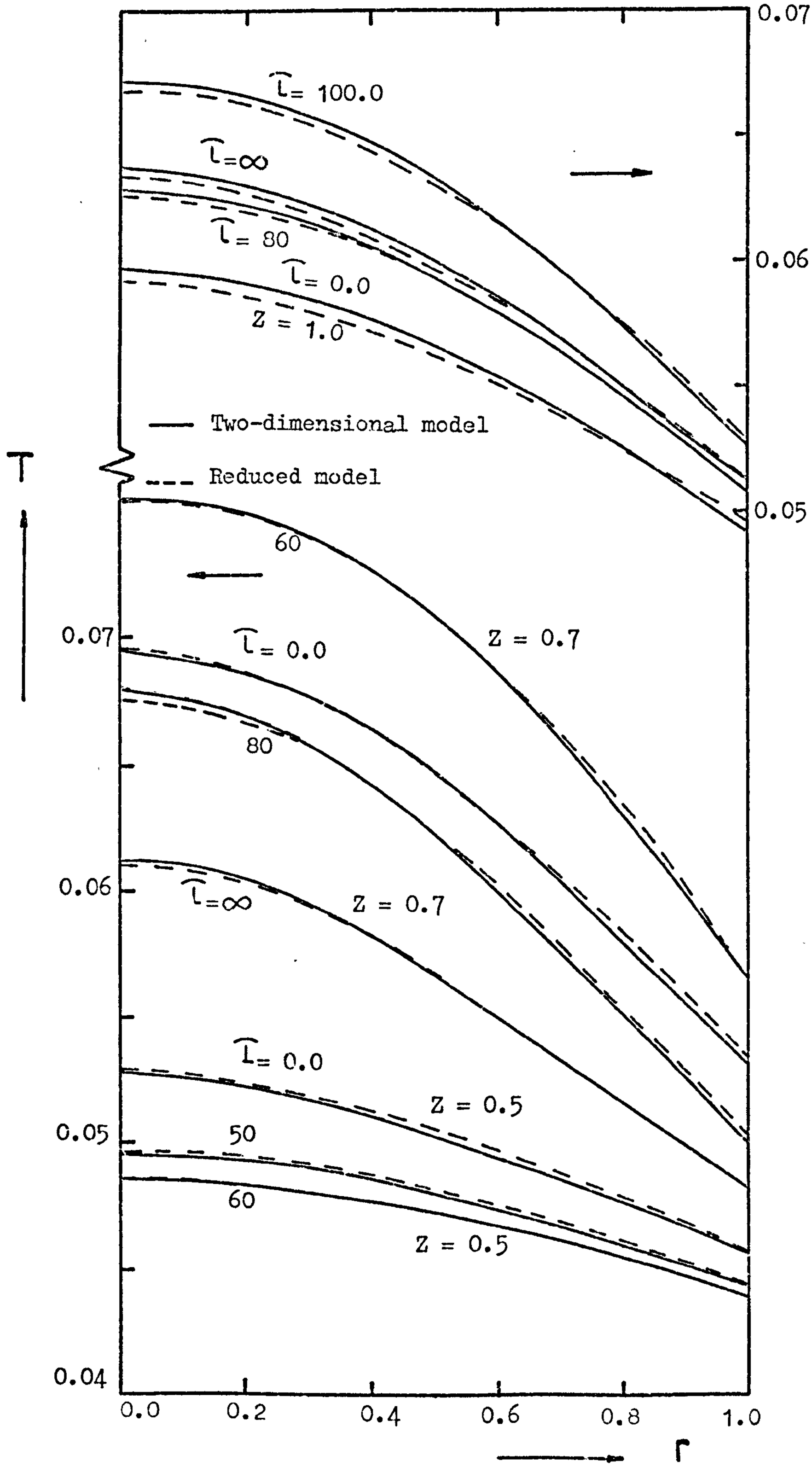

Figure 4.3: Radial temperature profiles corresponding to Figure 4.2.

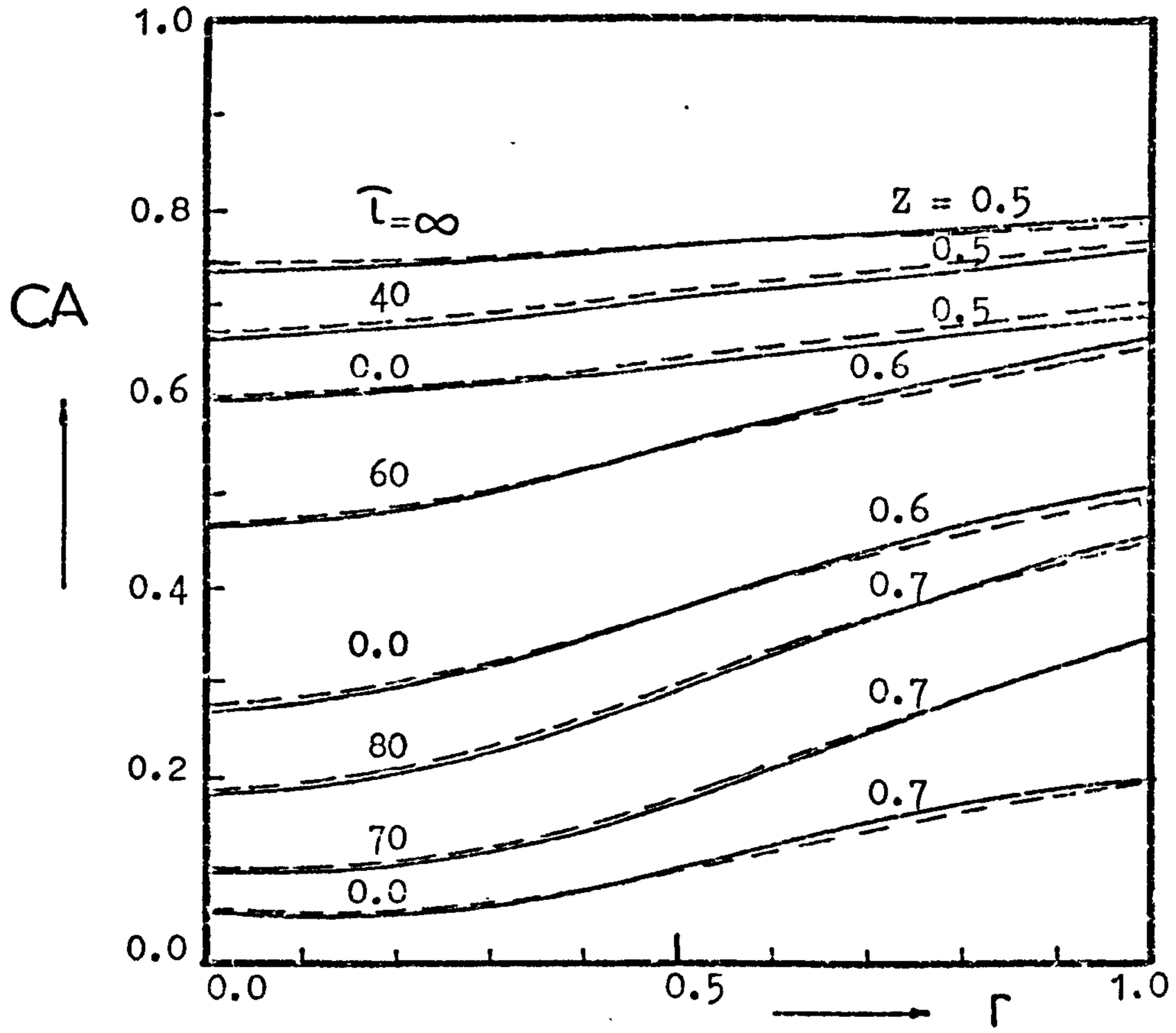

Figure 4.4: Radial concentration profiles of species A and B corresponding to Figure 4.2.

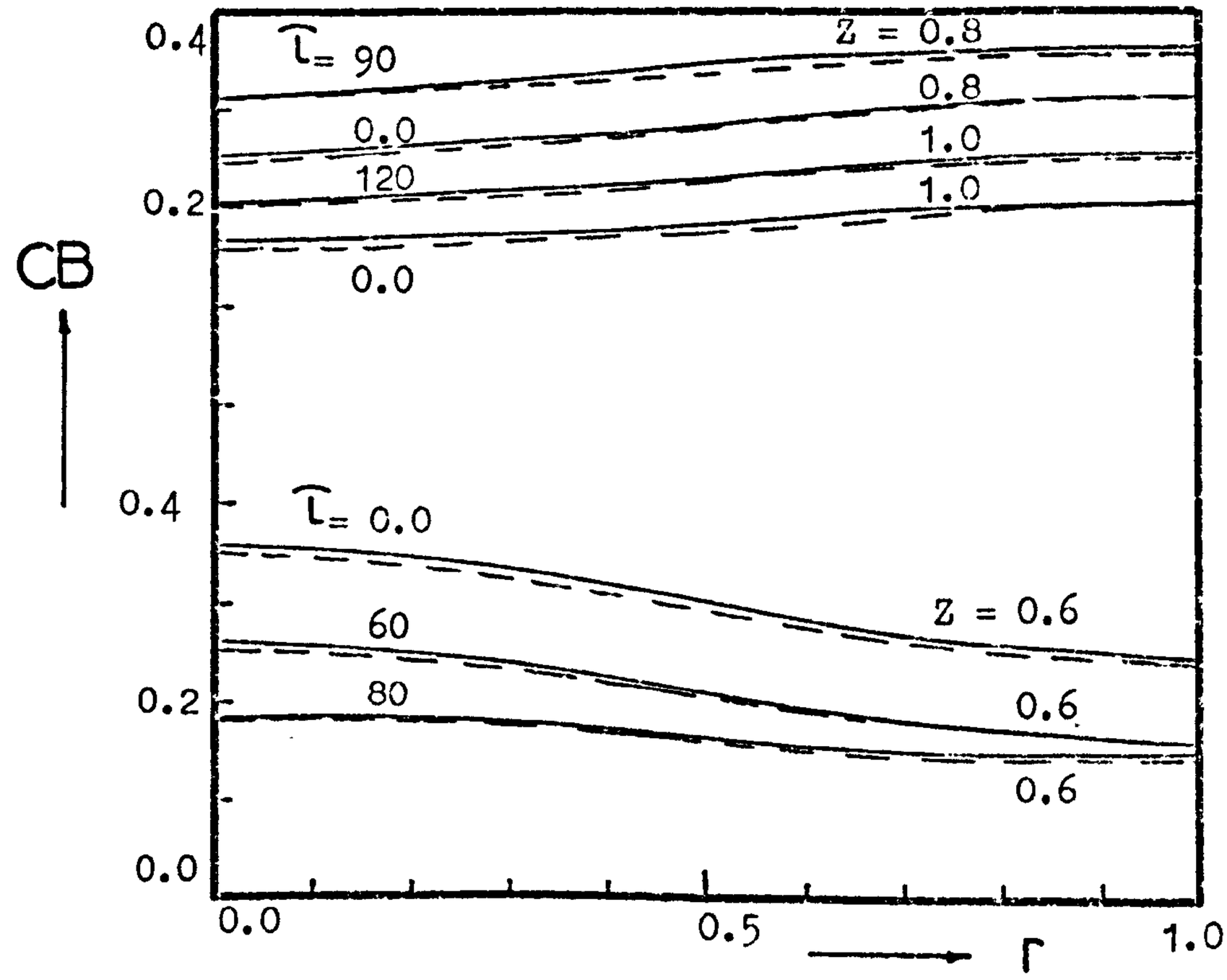

4.4.2 Improvement of the lumped model

As noted above, the evaluation of the distribution factors in the lumped model requires the evaluation of the pellet equations at two radial points (at r = 0.5 and r = 1.0) other than at the mean state values. If the pellet temperature can be estimated without solving the pellet equations, a significant gain can be made in computation time.

4.4.3 A first approximation for the distribution factor

From extensive numerical calculations, it has been observed that near the wall, the difference between the fluid and solid temperatures is almost constant, except in regions where parametric sensitivity or multiplicity prevail. At these conditions the nonlinear behaviour dominates, especially at r = 0.5 where the pellet temperature gradient increases more rapidly than that of the fluid temperature. At r = 1, the difference between the fluid and pellet temperatures is almost constant over a wide range of parameter values and in most cases can be fitted without any difficulty. The solid temperature at the wall can be estimated by the following expression:

$$(Tp(1) - 1) = \frac{N_{uw}}{Nu'} (Tp(m) - 1) \qquad (4.17)$$

This expression is similar to that used to evaluate the fluid temperature at the wall. While this expression satisfies the conditions of nearly constant temperature difference, it also implicitly takes into account the various pellet parameters and their effect in the value of Tp(m) used. Figure 4.5 shows the transient response for a step decrease in temperature with this modification. It can be seen that the errors due to this approximation are negligible compared with the original model. The error estimate for the most severe conditions of this model was tested has not exceeded 1%. Moreover, a 30% reduction in computation time has been achieved.

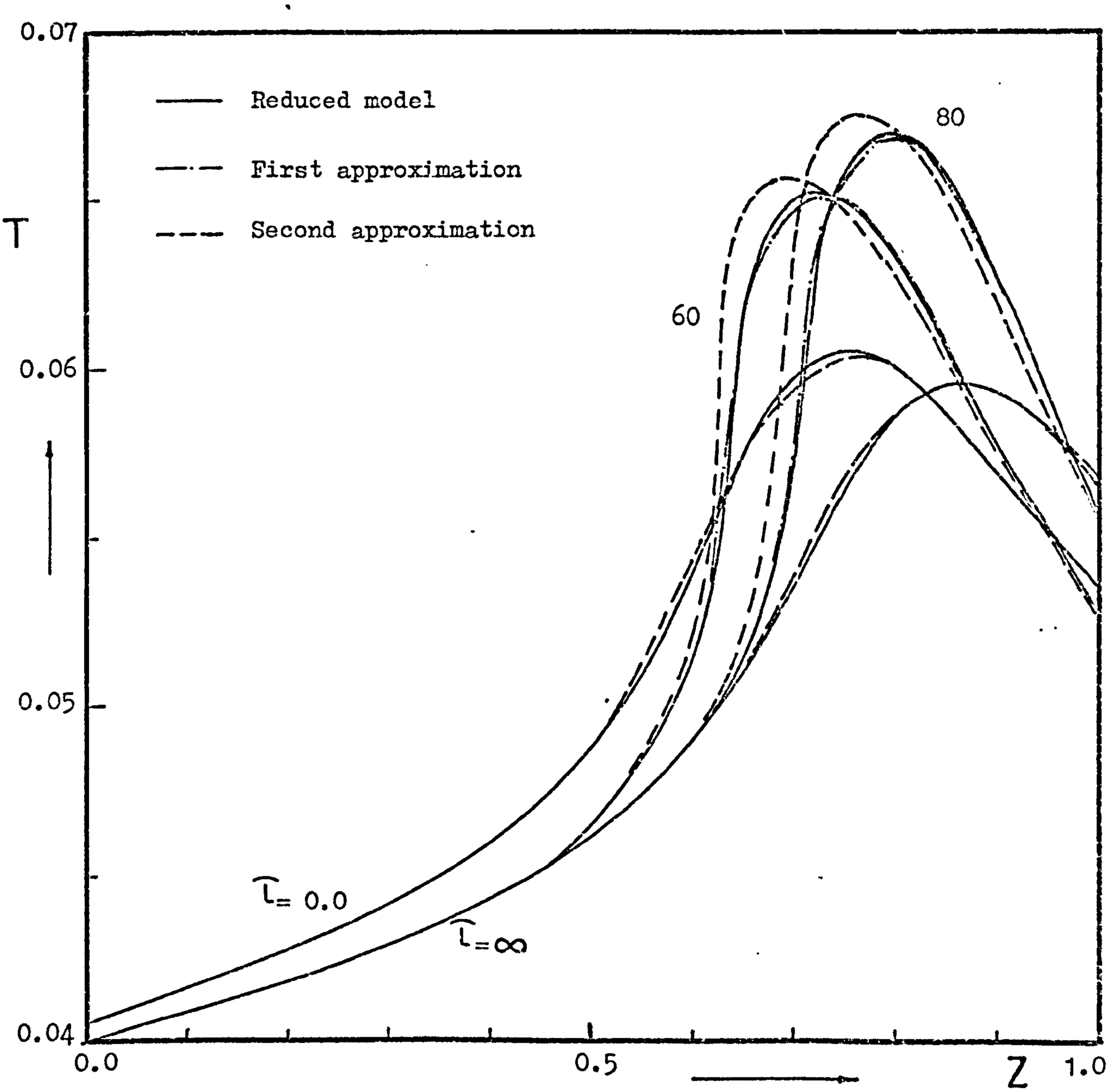

Figure 4.5: Comparison of radial mean temperature profiles predicted by the reduced model using the first and second approximations of distribution factors following a step decrease of 0.0008 in dimensionless inlet temperature. Data as given in Table 3.3.

4.4.4 A second approximation for the distribution factor

The problem of approximating the pellet temperature at r = 0.5 is difficult to predict since the nonlinear relation between the fluid and solid temperature dominates at the radial positions where the fluid temperature is already high (i.e. high reaction rates). Nevertheless, as a first approximation and following the same argument stated above and using a similar algebraic expression as that used in the case of the fluid temperature estimate, it is possible to evaluate the radial solid temperature and add a correction function to account for the deviation which occurs as the fluid temperature increases. Thus,

$$(Tp(r)-1) = (1 + 0.5\ N_{uw}(1-r^2))\ (w5(1-3r^2+2r^3)+1)\left(\left(\frac{N_{uw}}{1.2\ N_{uw}+4}\right)^2\right.$$

$$\left.(1-3r^2+2r^3+1)\right)(Tp(1)-1) + AF(T,Tp,z) \qquad (4.18)$$

where F(T,Tp,z) is an axially dependent function which depends on Tp(m), while A is radially dependent. The simplest form for this correction function is:

$$AF(T,Tp,z) = B(1-r^2)(Tp(m) - T(m)) \qquad (4.19)$$

From numerical experimentation, it has been observed that B is a constant over a wide range of fluid temperature and has a value of 0.04.

Figure 4.5 shows also the dynamic behaviour of the reactor to a step decrease in inlet temperature with this approximation. It can be seen that even with this gross approximation, the errors in predicting the axial fluid temperature profiles are not serious. From several test runs with these approximations and for variation in inlet fluid temperature and concentration, errors amounting to 5% have been noticed compared with 1%, using only the first approximation given by equation (4.17). However, in cases of temperature runaway, using the completely lumped model, errors

of 15% may be obtained. Nevertheless, the ability of this model to detect these cases is always adequate, since these are the regions which are always avoided in practice. The time of computation is about the same as that of the one dimensional model with radial temperature parabolic approximation. The ability of the lumped model to estimate the radial profiles, as well as the mean state variables, with minimum error makes this completely reduced model adequate and reliable even for optimisation and control studies.

4.5 Discussion of results

Despite the fact that the postulated models represent moderately complex cases in identifying the chemical and physical behaviour, typical of the class of highly exothermic heterogeneous reactors, it is still not possible to give a perfectly general solution which will cover all possible types of behaviour. Even by confining attention to the practical ranges for the dimensionless groups characterizing the differential equations, it is only feasible to attempt to investigate the kind of response for a particular problem and to try to find some pattern, or special features, which will characterize the system. This is the kind of information which is useful in deciding on the control strategy to be used (i.e. what variables will be manipulated, measured and controlled). Furthermore any unusual behaviour will be invaluable when deciding how near to the limit of stability the reactor can work. In short, the simulation should provide a basis for knowing what effects to take into account when designing a reactor. The lumped model developed above will be used in some of the present computations and will be compared with the two dimensional model (using a 3 point collocation in the radial direction) to further establish its validity. In the following discussion, most attention will be paid to the longitudinal axial profiles (i.e. at r = 0)

because at this position these are the major variables which limit the long term behaviour of the system and the safety and satisfactory operation of the reactor. Table 3.3 in Chapter Three gives the values of the data and the corresponding values of the dimensionless groups used in the simulation discussed here.

The reactor response to a step decrease in inlet temperature is shown in Figure 4.2. In the period immediately following the initial drop in inlet temperature, the most important effect is the resulting fall in temperature of the solid in the inlet region caused by the cooling effect of the gases entering the reactor. This results in less of the reactant being consumed until it reaches the section of the bed which has not yet been cooled. A situation thus arises where an increasing concentration is reaching parts of the bed which are already hot, so that the temperature begins to rise rapidly. As the cooled regions in the reactor inlet gradually move into the bed, the balance between reaction and heat removal is adjusted until the final steady state is reached. This type of response is an excellent demonstration of the distributed parameter effect and of how an apparently safe action, i.e. reduction of the inlet temperature, may give rise to severe hot spots. Although it is ultimately the reaction rate dependency on temperature and concentration which gives the fixed bed its characteristic behaviour, it is the travelling heat and mass waves down the bed and their interaction which is responsible for this unexpected behaviour.

To generalise the above behaviour, the response will be termed the cold wave effect. In front of this wave the concentration is always higher than it should be at any axial position in the reactor. This results in a high concentration wave reaching an already hot part of the bed which leads to the formation of accentuated hot spots. At the back of this cold wave the concentration is also higher than originally, due to the cooling down of the solid. This results in feeding more reactant

than that supplied by the cold wave alone.

Studying a step decrease in inlet concentration, the temperature and concentration profiles are shown in Figure 4.6. As a cold wave is developed, it can be observed that a monotonic decrease in temperature results. Although the concentration in front of the cold wave is still higher than it could have been without the cold wave, the difference is that at the rear of the cold wave, the concentration is lower than originally. In effect, no supply of reactant is added to that produced by the cold wave. Moreover, because the concentration wave moves at about the same velocity as the fluid, the level of concentration everywhere in the reactor is immediately lowered. This action would still weaken the concentration wave in front of the cold wave. As a result, the temperature decreases monotonically. However, if the cold wave is so extensive, as when applying a step decrease in temperature and concentration at the same time, the cold temperature wave could supply more reactant than originally and a situation may arise where temperature increases before settling down, as in the case of a step decrease in temperature alone. Of course, this situation may arise if the step decrease in concentration and temperature does not affect the reaction rate with equal magnitude, i.e. it depends on the reaction rate expression. This point will be discussed later.

Opposing the cold wave, there is the hot wave which can be demonstrated by observing the temperature and concentration profiles for a ramp increase in the inlet fluid temperature. This is seen in Figure 4.7. First, it causes a new peak to begin to form nearer the inlet than the old peak, while the latter begins to decay and moves towards the reactor outlet. The response of the reactor to a ramp increase in temperature is basically what would be expected from intuitive consideration. As this hot wave moves down the bed, and as a result of the reaction, a low concentration wave always occurs in front of the hot wave. This low

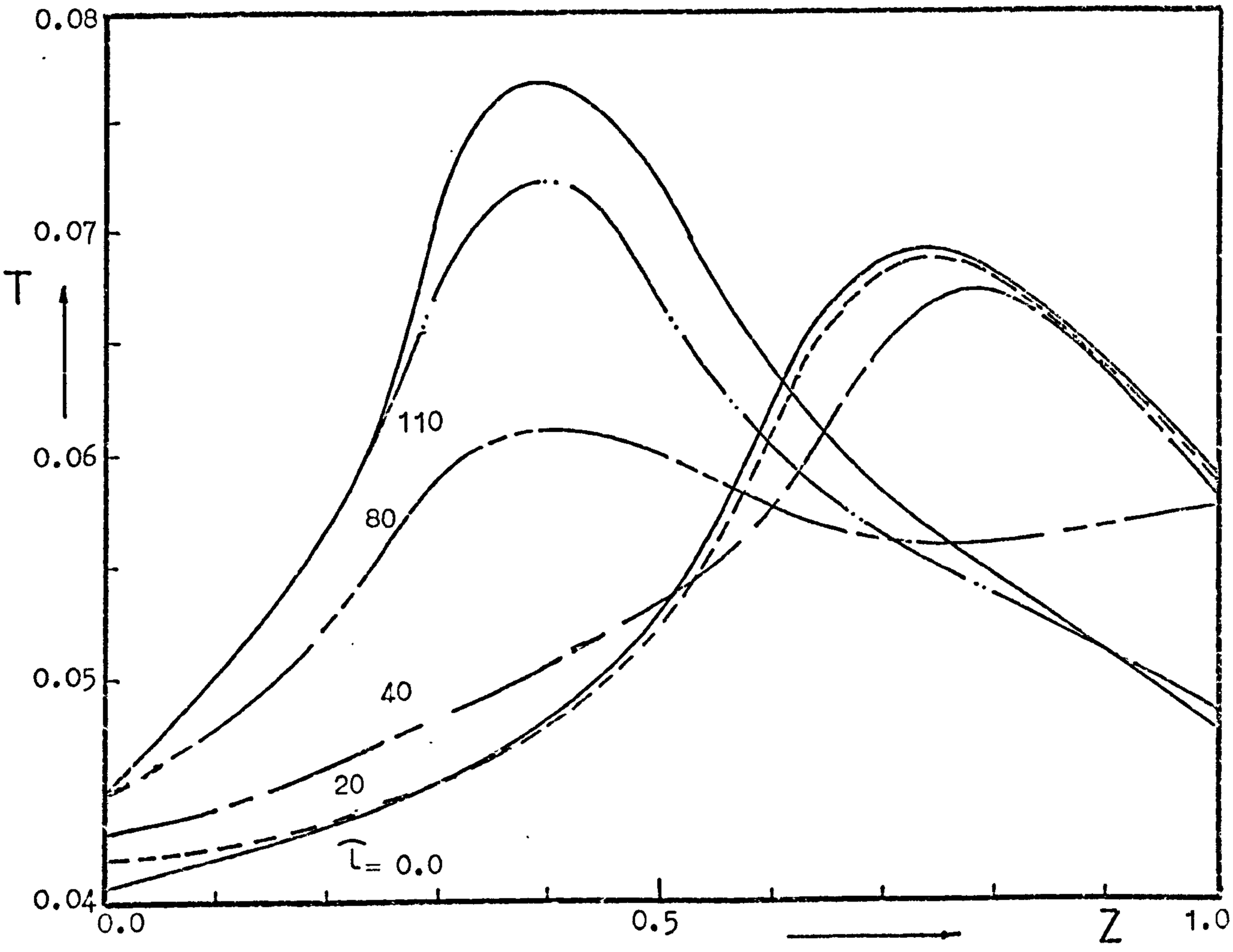

Figure 4.7: The centreline temperature profiles following a ramp increase of 0.00005 per second. Data as given in Table 3.3.

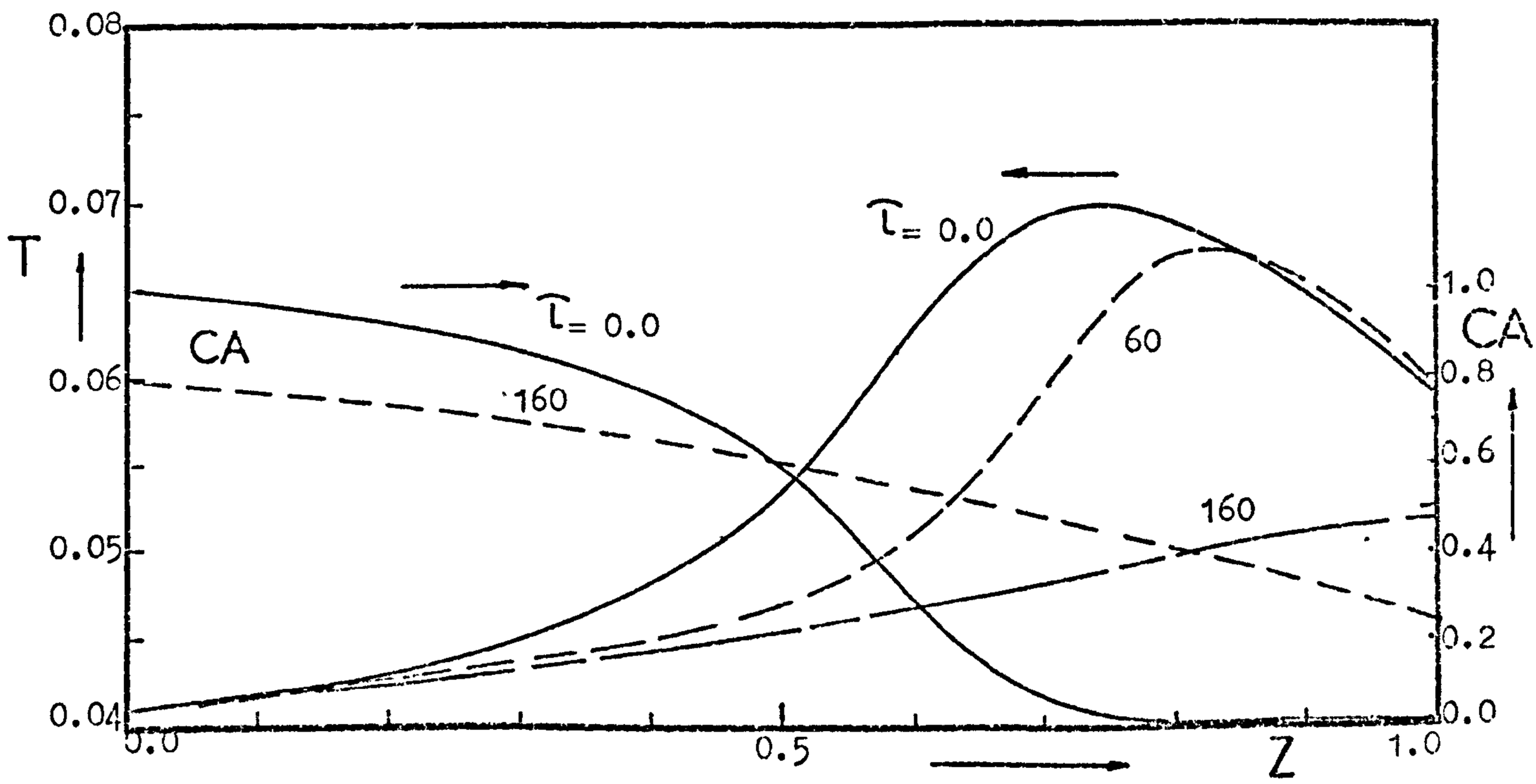

Figure 4.6: The centreline temperature and concentration profiles following a step decrease of 0.2 in dimensionless inlet concentration CA. Data as given in Table 3.3.

concentration wave lowers the temperature level in the rest of the reactor. At the back of the hot wave, the concentration is always higher than in front. This higher concentration wave keeps the temperature at a relatively high level as the heat wave passes through. In the case of a ramp increase in concentration, as can be seen from Figure 4.8, the same mechanism as for the hot wave applies here. The only difference is that the hot wave originated at the inlet by the increase in concentration, rather than by temperature. The hot and cold wave propagations always occur when the reactor is subjected to inlet temperature or concentration perturbations. The intensity of the effect of these waves for a specific set of parameters is a function of the magnitudes of the perturbation, the form of the reaction rate, and the initial steady state profiles (i.e. the levels of the temperature and concentration in the spatial co-ordinates of the reactor).

In practice the flow rate might be subjected to fluctuations. Indeed, in severe cases these perturbations may arise as a result of electrical or mechanical failure in a pumping system. Perturbations in the system linear fluid velocity should also be studied as a factor which might be of importance in reactor control. The film transfer coefficients h and K_{CA}, as well as the effective thermal conductivity KF and the overall wall heat transfer coefficient U, are dependent on the fluid velocity and increase as the fluid velocity increases. Any perturbations in velocity must also be applied to these coefficients. Figure 4.9 shows the axial concentration and temperature profiles for a 6% (10 cm/sec) ramp increase in the inlet fluid linear velocity. It can be seen that as the fluid velocity increases, the film coefficients h and K_{CA} and KF and U also increase, allowing more heat to be dissipated from the catalyst pellets and eventually transferred through the reactor wall more easily. As a result of lowering the pellet temperature because of these cooling effects, the reaction rate is lowered. Thus, we arrive

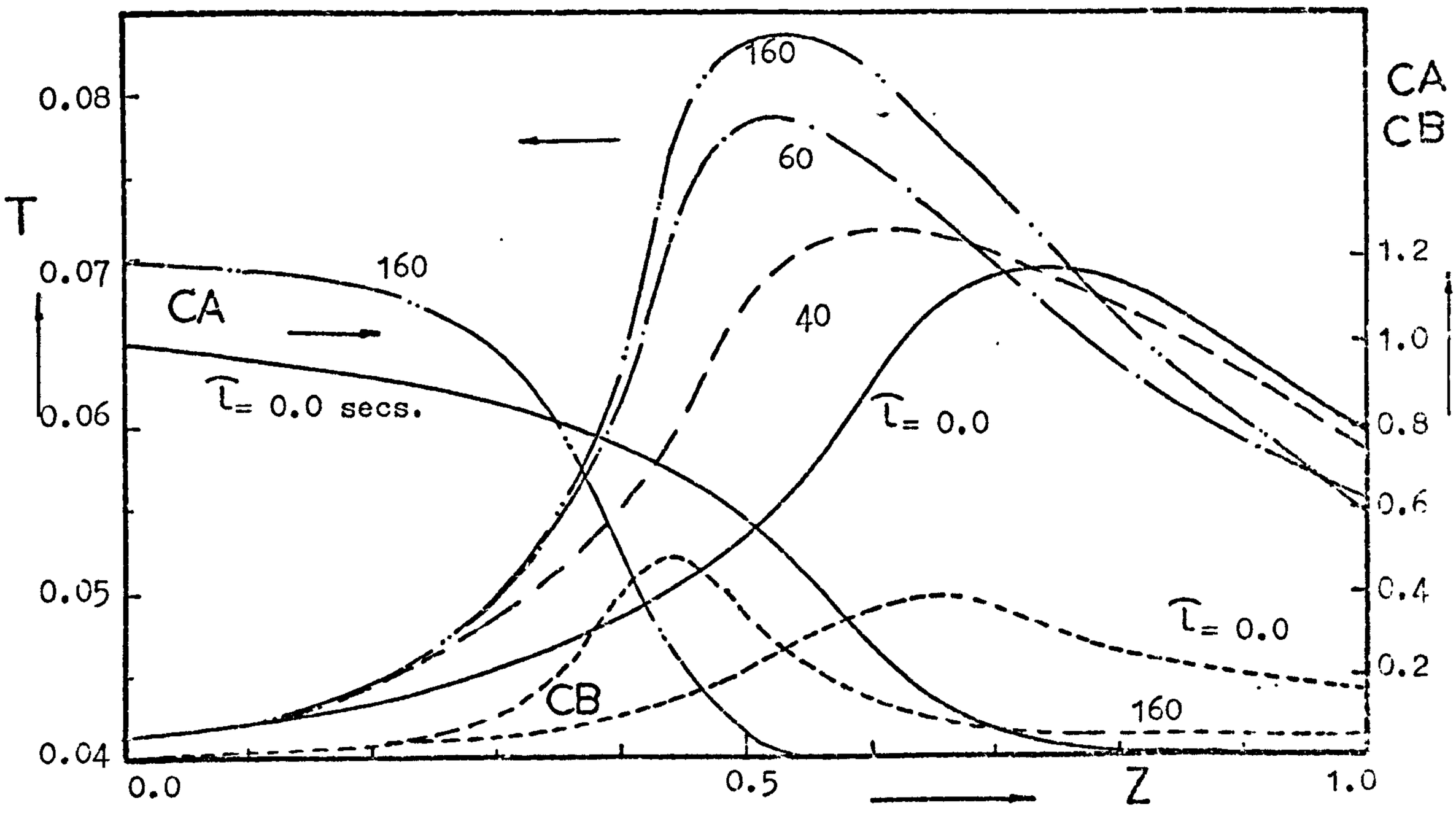

Figure 4.8: Axial temperature and concentration profiles at r = 0.0 following a ramp increase of 0.01 per second in dimensionless inlet concentration CA. Data as given in Table 3.3.

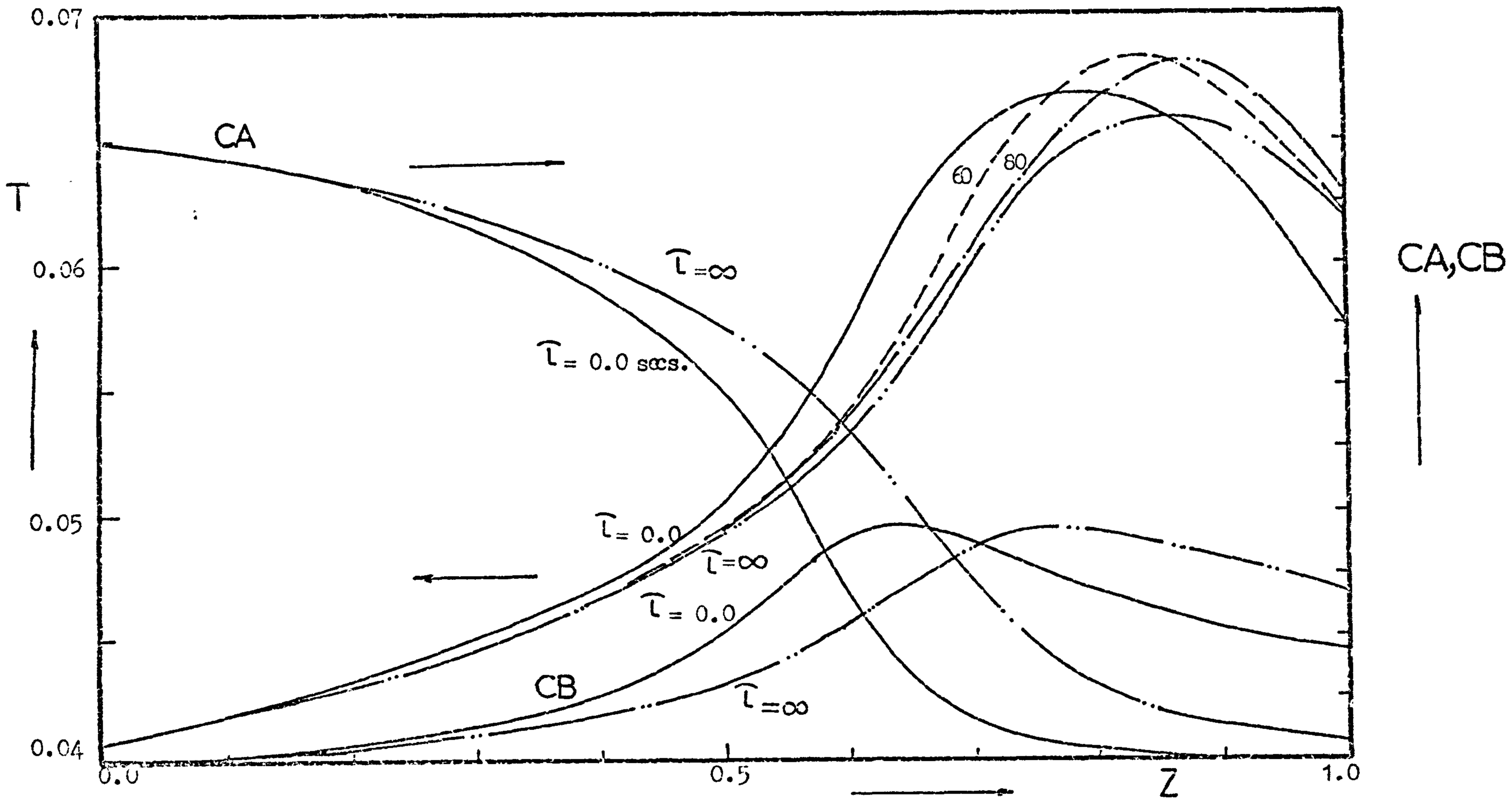

Figure 4.9: Temperature and concentration profiles at r = 0.0 following a ramp increase in inlet fluid velocity of 1 cm per second over a period of 10 seconds. Data as given in Table 3.3.

at a situation where a cold wave starts to develop and produce higher temperature peaks before the final lower steady state is established. This general behaviour is similar to that encountered with a ramp decrease in temperature. Increasing the fluid velocity leads to a final lower temperature profile, contrary to an increase in concentration, and it seems that the reactor behaviour is relatively sensitive to small perturbations in flow rates.

The response of the reactor to a ramp decrease in fluid linear velocity of 6% (10 cm/sec) can be seen from Figure 4.10 for a monotonic increase in temperature, with the formation of hot waves which move down the reactor. These hot waves are caused because the film transfer coefficients and KF and U decrease and as a consequence increase the pellet temperature and the reaction rate.

It is obvious from the previous study that the heat effects in the packed bed are the most important factor in reactor dynamics. It has been shown that the slow moving heat waves, which may vary in intensity, can interact with the fast moving concentration waves and a situation may arise which cannot even be detected from the input or output variables. Thus, studying the factors which affect and determine the velocity of propagation of heat waves may prove of importance. Knowing the relative velocity of propagation of concentration and heat waves and their intensity, it may be possible to act in opposition, thus weakening the reaction at certain specific axial positions. The concentration waves in this study propagate at approximately the velocity of the fluid. It is possible to take into account the absorbing capacity of the catalyst pellets. However, it has been shown (see Appendix (A1.2.2)) that the pellet capacitance for mass is much smaller than that for heat and can be neglected. On the other hand the major factor which determines the heat wave propagation velocity is the thermal capacity of the solid and its ratio to that of the fluid,

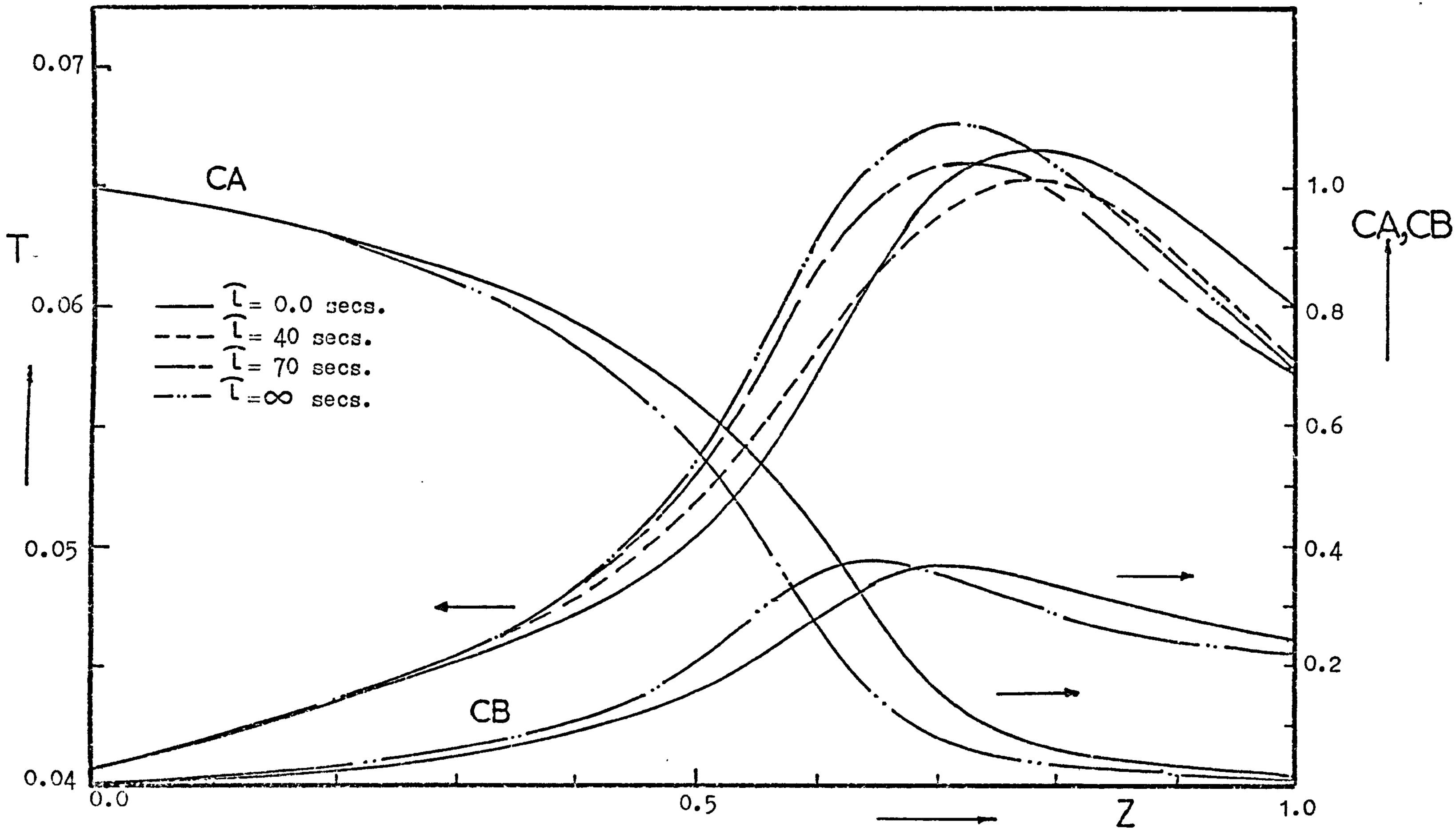

Figure 4.10: Temperature and concentration profiles at r = 0.0 following a ramp decrease in inlet fluid velocity of 1 cm per second (over a period of 10 seconds). Data as given in Table 3.3.

i.e. $e(\rho Cp)_{fluid}/(1 - e)(\rho^* Cp^*)_{solid}$. This ratio for the values of parameters used here is 0.0011, which indicates that the capacity of the solid to absorb heat is nearly 1000times that of the fluid. Increasing the solid thermal capacitance will thus slow down the heat wave velocity. Figure 4.11 shows the reactor axial temperature profiles at different axial positions for a step decrease in inlet temperature, for a solid thermal capacitance of 1.55 and 3.0 seconds. Changing the thermal capacitance of the solid amounts to changing the specific heat of the solid, or its density ρ^*. Not only does the moving heat wave slow down, but because the heating up of the solid takes more time, packing of high thermal capacity may stabilize the reactor against any small perturbations in operational parameter values, if these perturbations are of small time duration.

From the structure of the rate equations, which in general are of Arrhenius form, the effects of concentration and temperature on the reaction rates vary in magnitude depending on the temperature and concentration levels in the reactor. In fact, it is these differences which characterize the dynamic behaviour of the reactor. For example the cold wave action which results from a step decrease in inlet fluid temperature can cause severe hot spots in the later sections of the bed. The reason for this has been shown to be the result of mass accumulation by convective flow which reaches these high temperature zones before the cold wave. If this mass accumulation can be reduced by changing the inlet concentration, it will prevent the hot spot formation and give enough time for the cold wave to move far enough to eliminate these high temperature zones. In this case, with knowledge of the relative speeds of concentration and temperature waves and the manner in which they interact with the reaction rate, it is possible to manipulate the temperature and concentration to act so as to enhance or reduce the reaction rate at specific positions in the reactor.

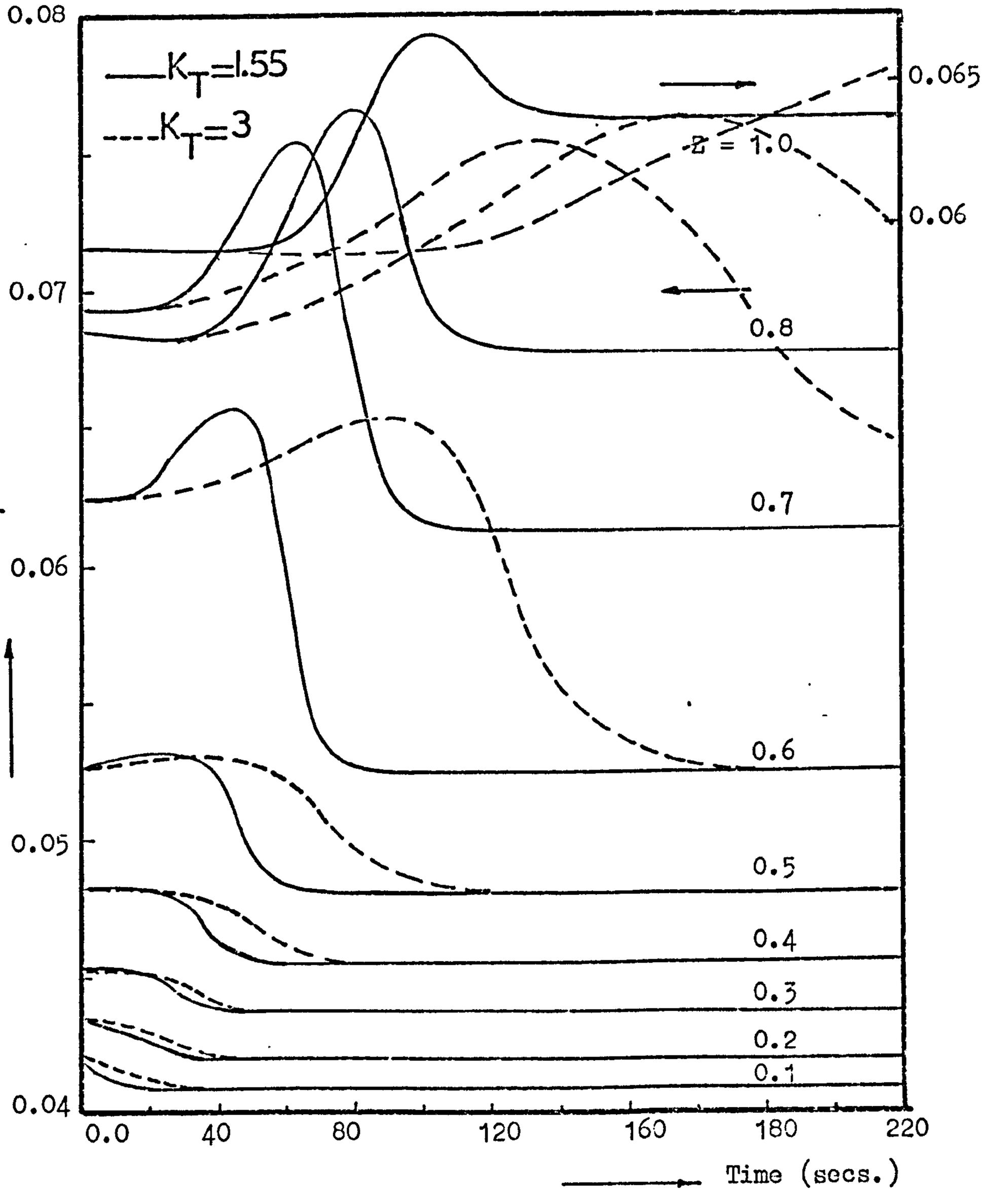

Figure 4.11: The effect of solid heat capacitance on reactor response, showing centreline temperature profiles following a step decrease of 0.0008 in dimensionless inlet temperature. Data as given in Table 3.3.

Figure 4.12 shows the responses of the temperature profiles at different axial positions for a step decrease in temperature. The inlet concentration is kept at the steady state value for 40 seconds. This time lag is to allow the cold wave to move down the bed where the reaction rate is not very large and also to keep the solid hot enough in the first part of the bed. As the cold wave reaches z = 0.5, it can be observed that the hot spot is starting to develop at z = 0.6, as a result of mass accumulation from the early parts of the bed. The inlet concentration is then reduced from 1.0 to 0.8 for a period of 40 seconds. This step decrease in concentration depletes the reactor of species A at those parts of the bed where the reaction rate is very sensitive to small increase in CA. It can be seen that this action has completely eliminated the hot spot. In fact the decrease in concentration was large enough to cause excessive reduction in the rate of reaction. However, under the same conditions as above, but with the concentration reduced from 1.0 to 0.9 only, Figure 4.13 indicates that this step decrease in concentration has not been enough to overcome the accumulation of mass formed in the latter parts of the bed. As a result, a hot spot has been formed. These figures emphasize the fact that knowledge of the effects of different concentration and temperature levels on the specific reaction rate must be available. This information can be obtained by solving the pellet equations at various concentration and temperature values to estimate bounds on temperature, and would define allowable concentrations at certain parts of the bed to prevent overheating or overcooling. It is not the concern here to give these optimum conditions, but rather to demonstrate the importance of studying the relative velocity of propagation of heat and mass waves and their interaction on the reaction rate for a specific system.

Despite the fact that step changes are not common in practice, they

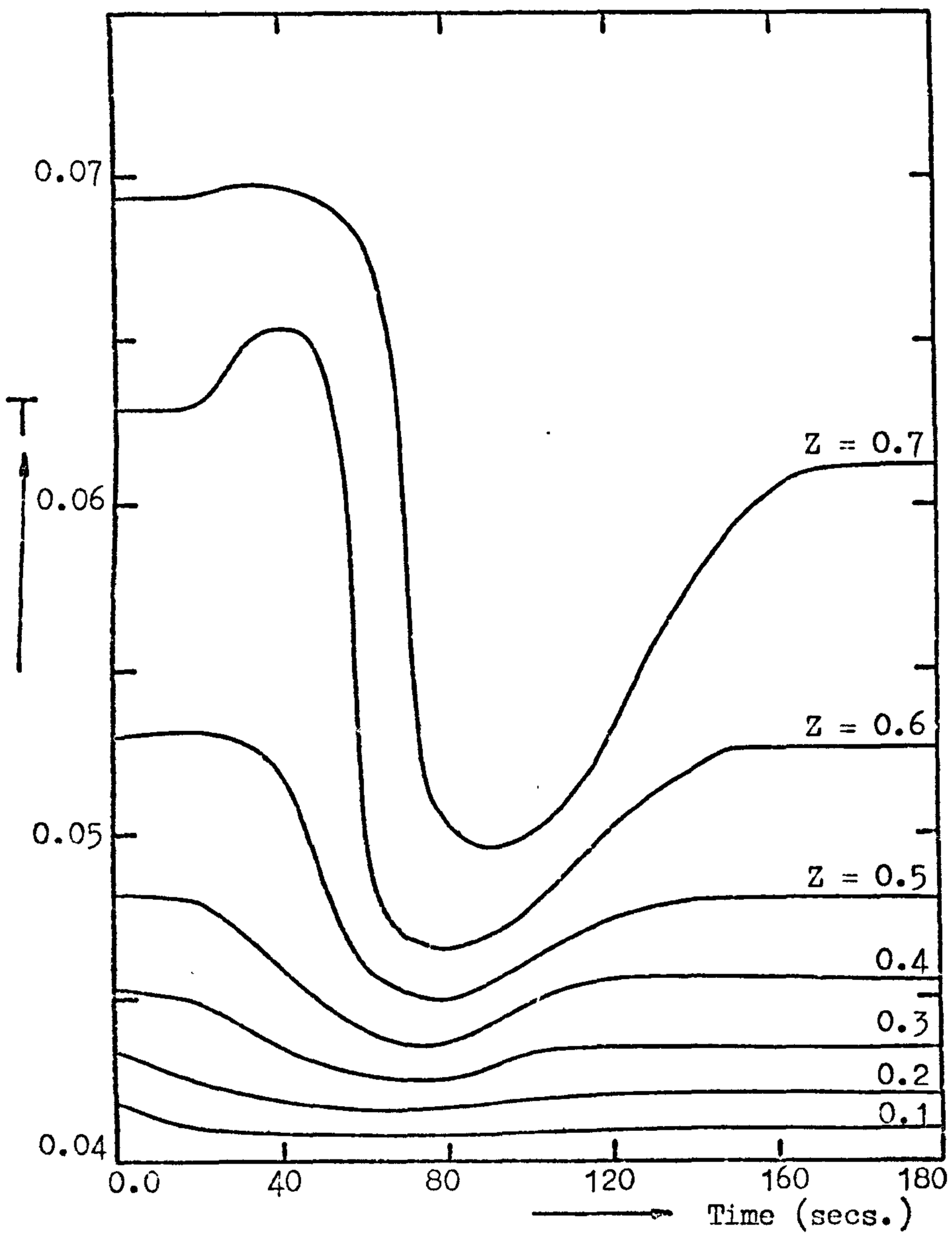

Figure 4.12: Centreline temperature profiles following a step decrease of 0.0008 in inlet temperature followed after 40 secs. by a step decrease of 0.2 in inlet concentration CA and for a period of 40 secs.

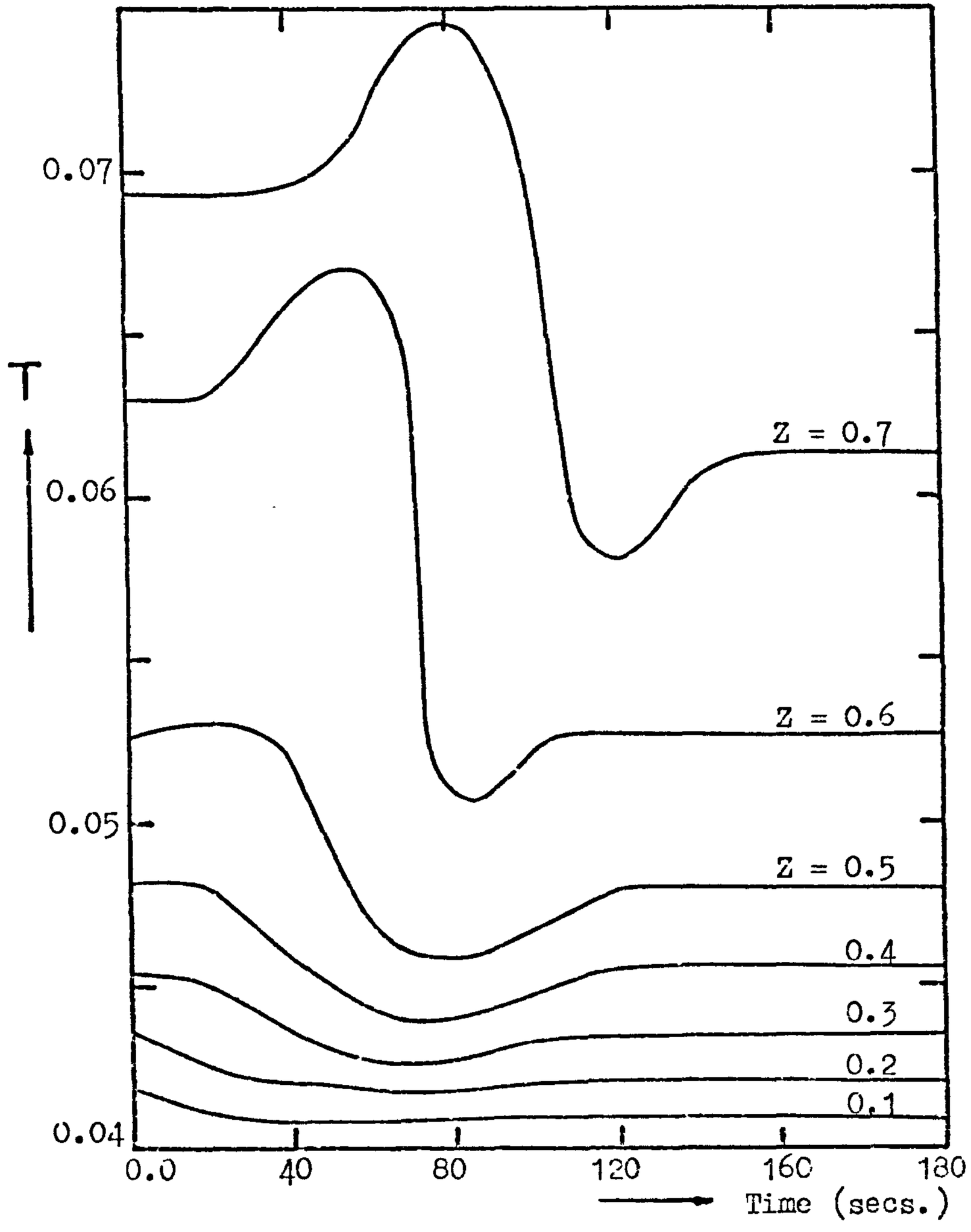

Figure 4.13: Centreline temperature profiles following a step decrease of 0.0008 in inlet temperature followed after 40 secs. by a step decrease of 0.1 in inlet concentration CA and for a period of 40 secs.

are used here for convenience and ease of interpretation. The dynamic behaviour for ramp changes has the general features produced by step changes. In this case, the gradients and duration of the ramp changes in temperature and concentration are adjusted to obtain the desired effect. In this case it might be necessary to use optimization or searching techniques to establish the best response.

It should be noted that while the system under study involves more than one concentration wave (i.e. for species CA and CB), the kinetic data used here is based on benzene oxidation, and indicates that CB does affect the dynamic response to a measurable extent. However, it may be always possible in such circumstances to consider the concentration CB as if it were a fraction of CA which is still in the reactor and interacting with the thermal wave. This point will be considered further in the next chapter.

4.6 Conclusions

The model reduction technique has been applied on the two dimensional dynamic model for the complex reaction scheme. The resulting one dimensional reduced model overcomes the limitations of the parabolic radial profile assumption, and the difficulties in estimating the radial mean values for the nonlinear reaction rates, by using a modified Nusselt number and suitably defined distribution factors.

The reduced model gives an estimate of the radial profiles with accuracy comparable with that of double collocation of the distributed system using 3 point collocation (N = 3) in the radial direction over a wide range of operating conditions. Computing time in relation to that of the collocation solution (N = 3) and the one dimensional using a parabolic radial temperature profile is of the order 3:4:1. The reduced model takes about the same computing time as the collocation solution with N = 2.

As the estimation of the distribution factors needs the solution of the pellet equations twice per axial step, further reduction in computing time has been achieved in two steps. A first approximation, where the distribution factors were evaluated by solving the pellet equations only once, which amounts to reduction of about 30% in computing time with maximum error of 1% in estimating the state variables at reactor axis (i.e. r = 0.0). A second approximation where the distribution factors are evaluated from purely algebraic expressions with maximum errors of 15% at r = 0.0. Computing time is comparable with the one dimensional model based on a parabolic radial profile.

The proposed dynamic reduced model with the first approximation can be used over a wide range of operating conditions. The computational load is not excessive and the solution time is reduced to the extent that it is suitable for control and design purposes.

The dynamic behaviour of the reactor is determined by a combination of chemical and thermal effects, the relative magnitudes of which may change considerably with time and position in the bed. This results in dynamic responses which are not easily predicted without extensive simulation. Perturbations in inlet temperature, concentration and fluid flow indicate that the major dynamic effect is the solid thermal capacity, and its ratio to that of the fluid, since this causes the temperature effects to be delayed. Such action causes disturbances in mass distribution which have faster dynamic responses, with the result of irregular behaviour of the temperature profiles which are surprising. Knowing the relative velocities of propagation of the thermal and concentration waves, it is possible, by manipulating the inlet conditions, to enhance the reaction rate or to lower it in certain parts of the bed, where the reaction rate is very sensitive to temperature, and thus control temperature fluctuations.

This type of multivariable approach can be used to control the reactor when working near the maximum allowable temperature, without the possibility of excessive hot spots forming, and thus avoids the undesirable effects such as temperature runaway, general instability, catalyst deactivation or poor selectivity.

CHAPTER 5

REACTOR RESPONSE TO INLET SINUSOIDAL DISTURBANCES

5.1 Introduction

Concentration and temperature disturbances propagate through fixed bed reactors in a wavelike manner. While knowledge of the interaction between these travelling waves is central to the design of reactor control systems, and indeed to the design of the reactors, there has been only limited exploration of the nature of such phenomena.

In the previous chapter the dynamic response to step and ramp changes in inlet conditions were treated. Although they showed some of the dynamic effects of the reactor, they do not really reveal typical responses of the reactor to the control actions which are basically damped oscillatory responses. Thus, a study based on sinusoidal perturbations in feed variables should highlight some of the dynamic characteristics which can occur in real control problems.

Reported studies on sinusoidal perturbations in inlet temperature and concentration has been given by Foss and co-workers for liquid[67] and gaseous systems.[77,167] In the liquid system, inert glass packing has been used which merely acted as heat sink. In heterogeneous gaseous reactors, attention was confined to the development of a suitable linearized model to fit their experimental results. Denis and Kabel[107,116] have studied the response of a heterogeneous reactor to inlet saw tooth and square like waves. However, they assumed that the rate of adsorption of the reactant on to the catalyst surface is a significant dynamic effect. Hansen[110] has considered oscillatory inlet conditions on an adiabatic fixed bed reactor and confined his attention to the applicability of the model without linearization.

The above reported work considered the simple reaction A⟶B and the studies were confined to the quasi-stationary state (i.e. after the reactor

had settled down to a sustained dynamic response). No attempt has been made to study the period before the quasi-stationary state develops. As will be shown, this initial dynamic period could be of importance in control studies. Attention in this chapter is directed to sinusoidal disturbances in inlet temperature, concentration and fluid velocity when these lead to a unique steady state but where there is a complex reaction scheme. The importance and effect of radial temperature variations is outlined where temperature runaway or hot spots may develop over parts of the radial profile. Another objective is to conduct preliminary studies of the response of the reactor to damped sinusoidal disturbances. While in sinusoidal perturbation studies an initial and a quasi-stationary state have been observed, in damped disturbances the latter state is not achieved.

5.2 Formulation and solution of equations

The reaction scheme considered is the complex irreversible first order reaction $A \longrightarrow B$, $A \longrightarrow C$. The reactor model used is two dimensional taking into account radial variations in temperature and concentration and neglecting the axial diffusion, as given in the last chapter (equations 4.1 to 4.5). This model is coupled with the isothermal pellet model given in Appendix (A1.2.2). For reasons outlined in the last chapter, the mass and heat capacitances of the fluid are neglected, and only the heat capacitance of the pellet is considered. The fluid equations are solved by the double collocation method, while the pellet model is integrated by the Runge-Kutta-Merson procedure. The initial steady state profiles used in the following study are shown on figures 3.1 to 3.3 in Chapter Three. The form of the inlet perturbations applied to the reactor inlet is:

$$w(\tilde{t}) = w(0) + A \sin(2\pi F \tilde{t}) \qquad (5.1)$$

where $w(\tau)$ = value of inlet variable at time τ

$w(0)$ = value of inlet variable at time zero

A = amplitude of oscillation

F = frequency of oscillation.

5.3 Sinuscidal wave propagation characteristics

While in homogeneous reactors, temperature and concentration waves travel at the fluid velocity, in packed beds, because of the thermal capacity of the packing, the temperature wave travels slower than the concentration wave. Thus, because of the propagation velocity differences, they may act so as to enhance the reaction rate. In other locations, they may have opposing effects on that rate, causing it to be damped down. The concentration waves travel at a velocity which depends on the adsorptive capacity of the packing for the components in the fluid. However, in the case under study, the adsorption is neglected and thus it propagates at a velocity equal to that of the fluid flow rate. On the other hand, the ratio of the temperature wave velocity to the fluid velocity is approximately equal to the fraction of the total heat capacitance of the system contributed by the fluid. For the data used here (see Table 3.3), the concentration wave residence time is about 0.75 second and has a velocity of 164 cm/sec, while those of the temperature wave are respectively about 100 seconds and 1.24 cm/sec.

Knowing the propagation velocities of temperature and concentration waves, it is possible to predict when they would interact constructively or destructively. Thus, if the steady state values are taken as a reference, it can be said that at a given frequency, a slow temperature wave will interact, say, constructively with the concentration waves. The number of times will be approximately equal to the number of half periods elapsed at the inlet before the temperature wave reaches the reactor outlet. For example, for the frequency of 0.025 hz (i.e. a

period of 40 seconds) shown in figures 5.1 and 5.2, the high temperature wave would interact with two high and three low concentration waves and similarly for the low temperature wave (i.e. troughs). In the case of a frequency of 0.0125 hz (i.e. a period of 80 seconds) shown in figure 5.4, a high temperature wave would interact with half the number of concentration waves stated above. This argument then leads to the conclusion that if the frequency is lowered so that the half period is larger than the temperature wave residence time, it is then possible to result in only destructive interaction, i.e. for an initially positive going sine wave. In this case, the response of the reactor closely resembles that which occurs for ramp changes discussed in the last chapter and the reasoning and conclusions arrived at also applies here. Nevertheless, this point will be clearly seen in the following sections when dealing with different frequencies.

Because of the complex nature of the phenomena which occur, some typical cases have been described in some detail to illustrate the general behaviour of the reactor when subjected to inlet variable sinusoidal disturbances.

5.4 Temperature forcing disturbances

5.4.1 The initial transient period

For an amplitude of 0.0012 (equivalent to 20K for the given data) and a frequency of 0.025 hz , figures 5.1 and 5.2 show the response of the reactor at different axial positions. The initial transient is indicated on the figures by the first temperature peak. The duration of the initial transient period is equal to the residence time of the first temperature wave. It can be observed that the temperature peaks during this period are higher than those found in the quasi-stationary state. Thus, at z = 0.6, the first peak is higher by 40K, while at z = 0.3, it

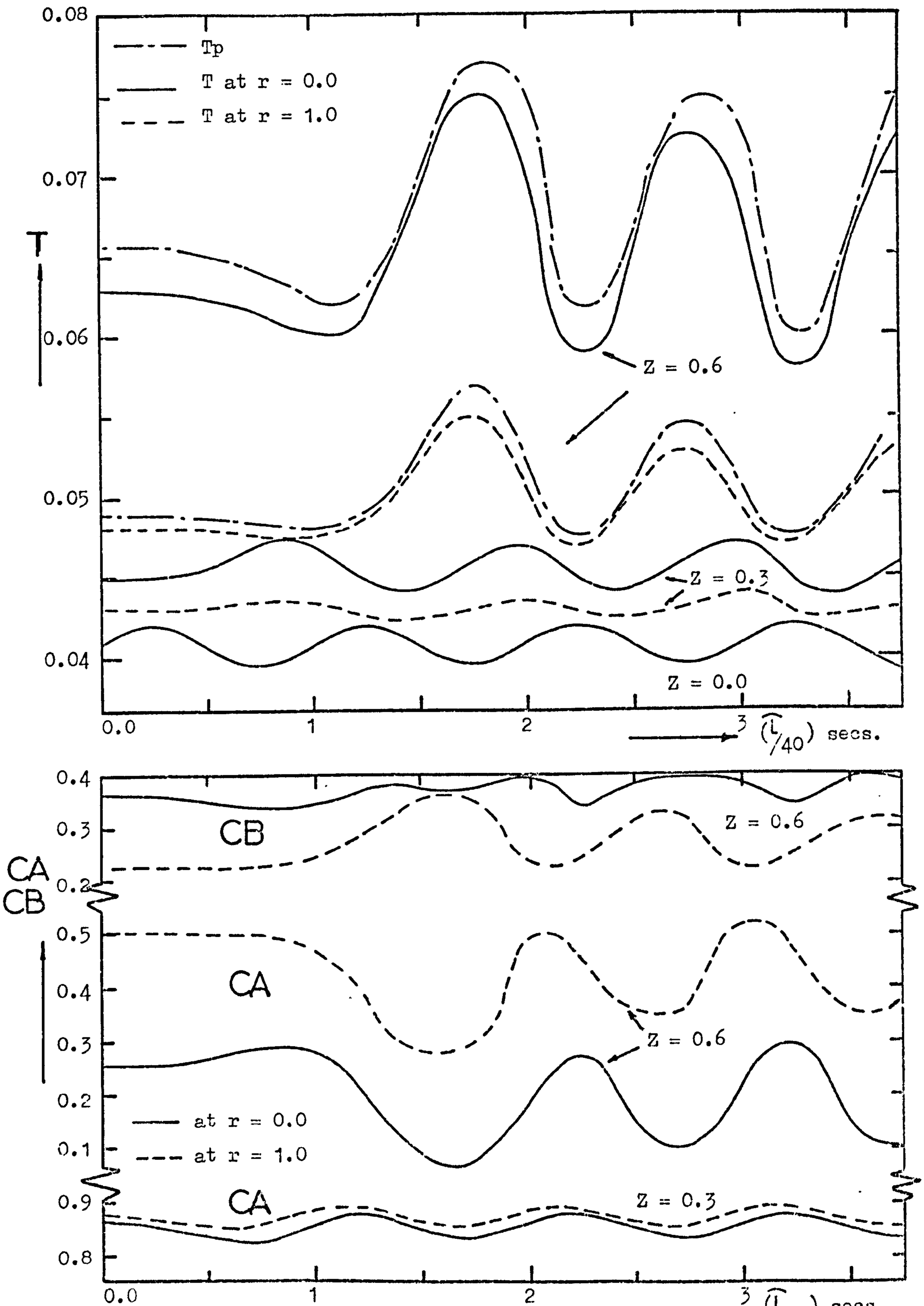

Figure 5.1: Temperature and concentration profiles at different axial positions during the response of the reactor to an inlet temperature perturbation of the form $T = 0.0408 + 0.0012 \sin(\frac{2\pi}{40} t)$

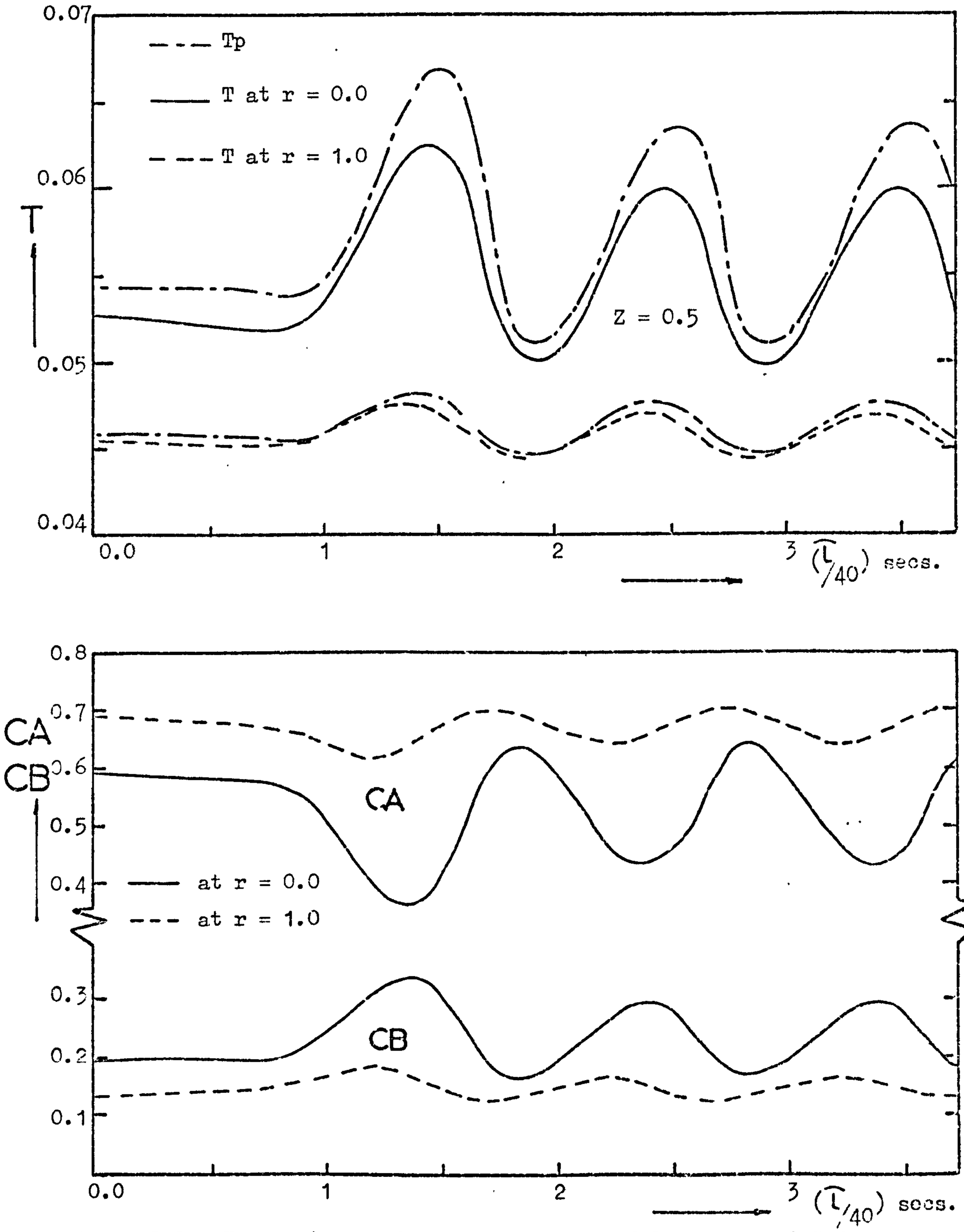

Figure 5.2: Temperature and concentration profiles at Z = 0.5 during the response of the reactor to an inlet temperature perturbation of the form $T = 0.0408 + 0.0012 \sin(\frac{2\pi}{40}\bar{t})$

is only 13K higher. Such temperature differences may lead to hot spots, or even temperature runaway, although those would not necessarily arise in the quasi-stationary state. At a frequency of 0.02 hz , a severe hot spot is formed at the initial transient only near the reactor axis where the temperature peak is higher than the subsequent ones by 62K. Decreasing the frequency further to 0.0125 h (see figure 5.4), temperature runaway takes place, at z = 0.6 near the reactor axis, both in the initial and quasi-stationary states. However, the temperature peak at the initial transient is still higher than the subsequent ones.

The reason for the higher temperature peaks observed in the initial transient period is that the temperature at the trough before the first peak is higher than the others. The solid is then heated up to temperature levels higher than those found in the quasi-stationary state.

The development and propagation of different waves may become more apparent by a closer examination of their interaction in the reactor. Thus, reference to figures 5.1 and 5.2, indicates that as the inlet temperature increases, a low concentration wave, resulting from the increase in temperature, moves down the bed. Because the concentration wave of A moves nearly at the fluid velocity, the temperature at axial positions z = 0.5 and 0.6 start to decrease slightly. However, little effect is apparent at z = 0.3 or at the wall (r = 1.0) of the reactor, where the temperature level is low. After about 30 seconds (i.e. 0.75 of the period), when the temperature wave arrives at z = 0.3, it causes the temperature to increase still further, resulting in a decrease further down the bed. At the same time, a large concentration wave, CA, is initiated at the inlet because of the fall in temperature in the second half of the first period. At z = 0.3 the high temperature peak occurs concurrently with that of CA, but with a slight phase lag. Consequently, they act constructively, increasing the rate of reaction. At z = 0.6 CA starts to increase at the

centre of reactor (i.e. at r = 0.0), until it reaches the temperature wave which has already arrived at that axial position. This results in a higher temperature peak than would be expected. However, because the temperature level at this axial position is high, it dominates the whole response. As a result of the coupling between the temperature and the concentration CA, the latter is forced to follow the temperature wave.

The importance of the temperature levels and their effects on the CA wave propagation can be observed from the difference in phase between the temperature and CA waves at the centre of reactor (r = 0.0) and at the wall (r = 1.0). At z = 0.6, the crests of fluid temperature wave and the troughs of the concentration CA wave differ in phase and increases at r = 1.0, where the temperature level is lower than that at the centre. This phase difference is observed in all cases where the temperature levels are not high enough to eliminate differential phase shifts between temperature and concentration across the radius.

The wave propagation of B is also shown on figures 5.1 and 5.2. With the values of the kinetic parameters used in this study, B is not produced in appreciable quantities until half-way down the reactor. Since CB production depends on CA consumption, it appears that the CB wave propagates at the same velocity as that of CA, with opposite trend as demanded by the kinetic rates. At z = 0.6 and r = 0.0, the CB wave is very flat compared with that at r = 1.0 or at the axial position z = 0.5 (figure 5.1). This suggests that part of the B produced is immediately consumed, thus contributing some heat to the temperature wave. Although the effect of CA wave starts to die out at the latter part of the bed, the CB wave can act constructively or destructively on the temperature wave. However, because the CB wave in the latter part of the bed is able to act independently of the CA, the phase shift between the CB and temperature waves can be changed, depending on the temperature levels.

5.4.2 Effect of sinusoidal perturbations on radial profiles

It is to be expected that as the radial temperature gradient increases, the rate of heat removal through the reactor wall also increases. However, due to the nonlinear nature of reaction rate it is possible to have a situation where the heat generation, arising from increase in reaction temperature, surpasses the rate of heat removal. This would lead to accumulation of heat over part of the reactor tube radius. As a consequence, a further increase in reaction rate occurs which in turn leads to severe hot spots or temperature runaway. The above situation manifests itself in the present study as can be seen from the plot of a frequency of 0.025 hz (figure 5.1), where the amplitudes of temperature oscillations are larger at r = 0.0 than at the wall at r = 1.0. Increasing the effective thermal conductivity and mass diffusivity, i.e. decreasing Peclet numbers, would decrease the amplitude differences of temperature and concentration across the radial direction. Figure 5.3 shows the reactor response for the same frequency as above (0.025 hz) but with the Peclet number equal 8. The result is a better temperature distribution across the tube radius. It can also be observed that the phase shift between temperature and concentration waves at r = 0.0 and r = 1.0 has decreased. For a Peclet number equal 6 or less the mean axial temperature computed by the one dimensional model closely follows the mean temperature based on the radial diffusion model used in this study, to frequencies as low as 0.0083 hz. It must be noted here that this low frequency has resulted in temperature runaway as will be discussed in the next paragraph. Nevertheless, the above observations may explain why Foss et al,[167] found agreement between their one and two dimensional models. This is because they were using a Peclet number equal 4.8, a value far below those usually found in industrial units.

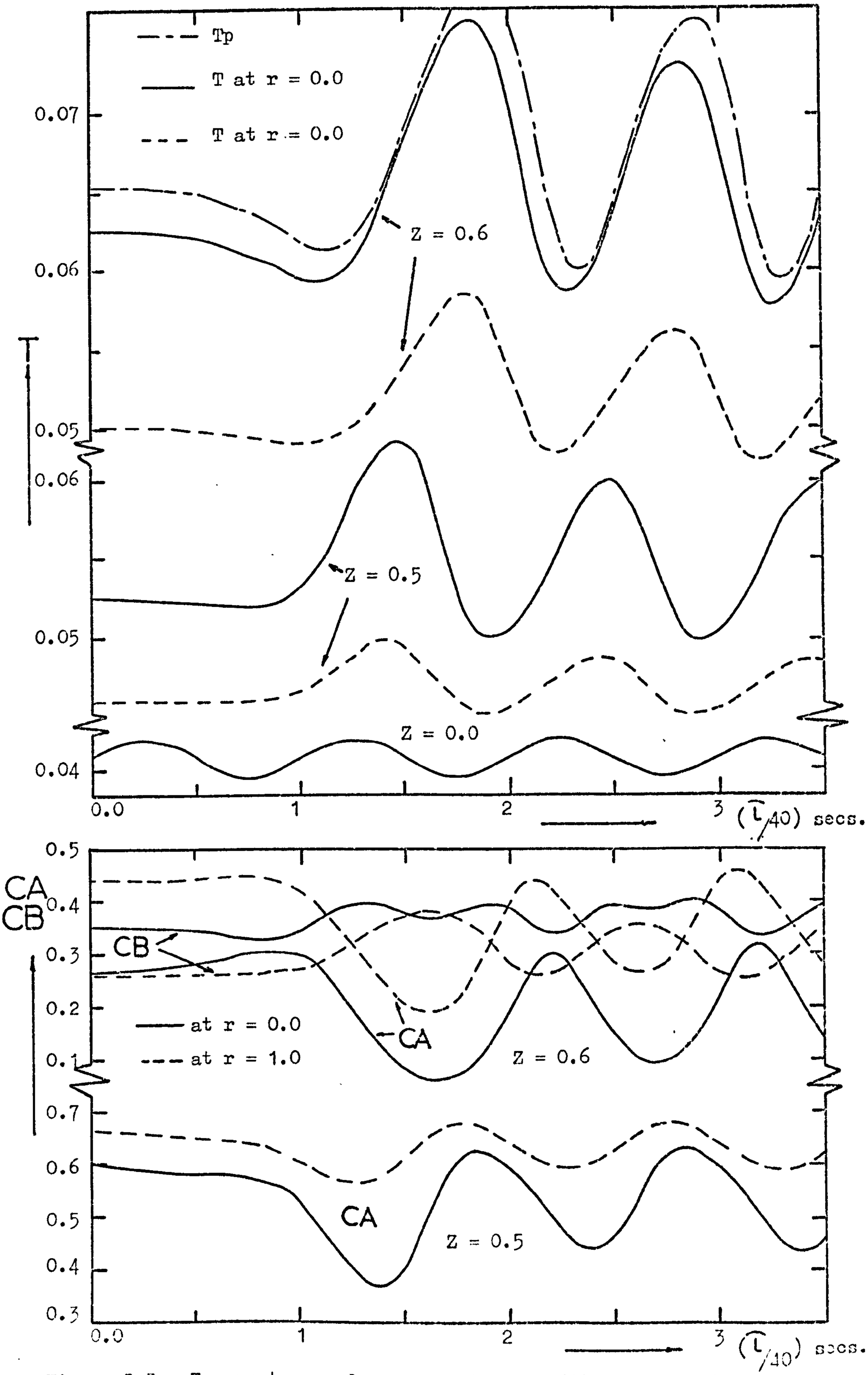

Figure 5.3: Temperature and concentration profiles during the response of the reactor to an inlet temperature perturbation of the form $T = 0.0408 + 0.0012 \sin(\frac{2\pi}{40}\hat{t})$
$Pe_M = Pe_H = 8.0$

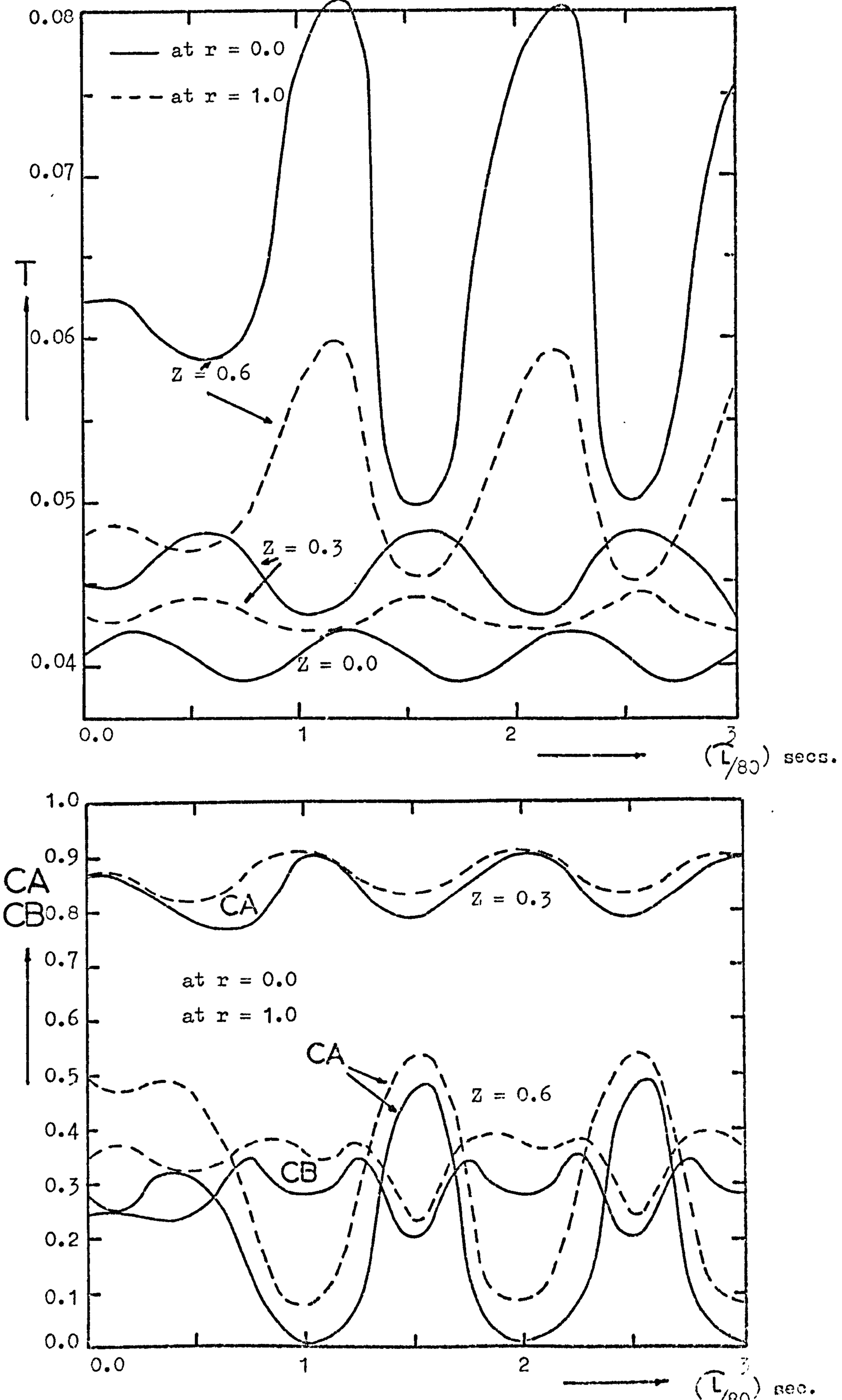

Figure 5.4: Temperature and concentration profiles during the response of the reactor to an inlet temperature perturbation of the form $T = 0.0408 + 0.0012 \sin(\frac{2\Pi}{80} t)$

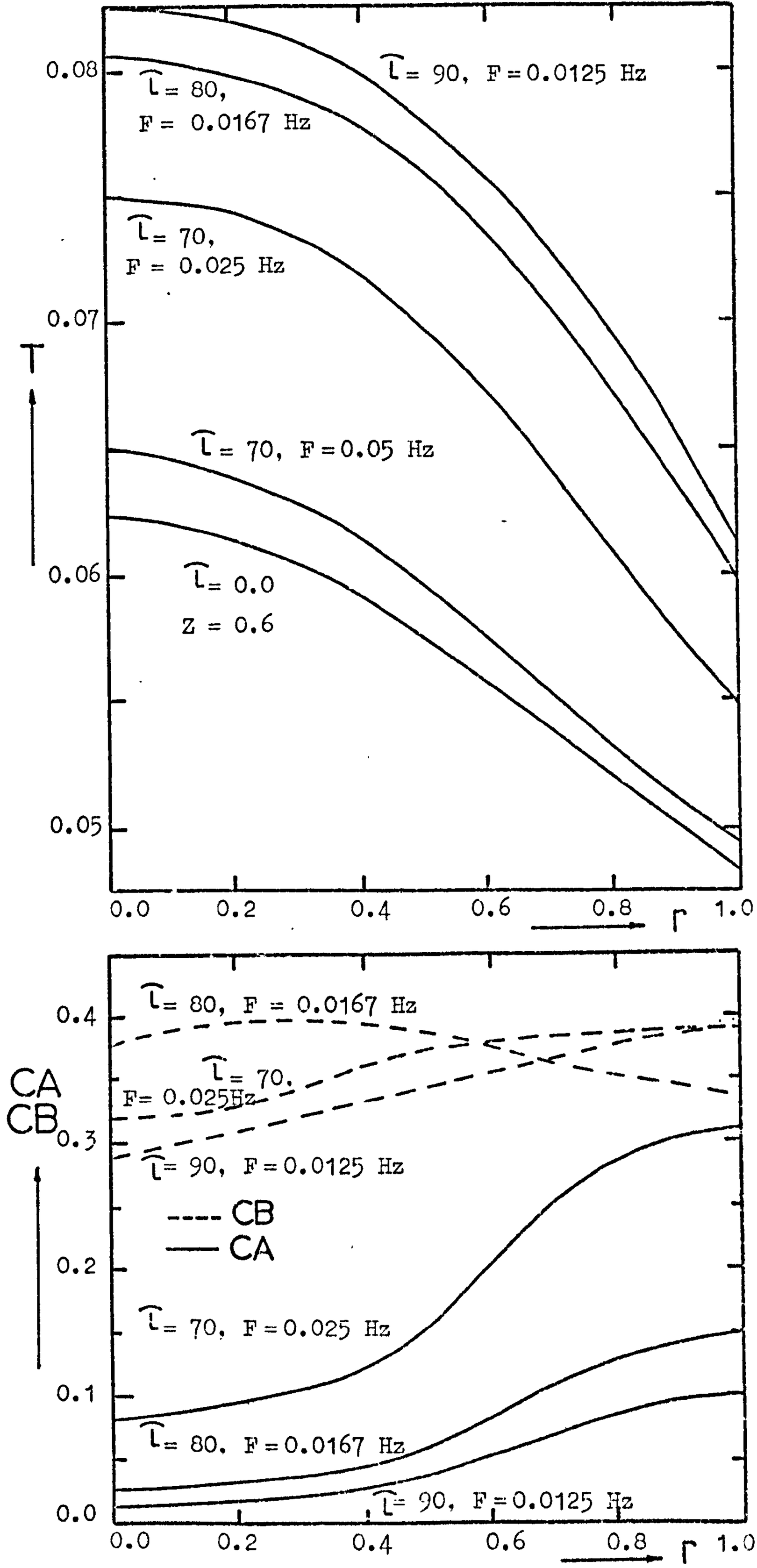

Figure 5.5: Radial temperature and concentration profiles at Z = 0.6 in response to various inlet temperature frequencies and during the initial transient maximum temperature rise.

In such exothermic reactions, where the radial temperature gradient is severe, as in the case under study, it is possible to have a temperature runaway over part of the radial profile because of the limited rate of heat removal. Over how much of the radial direction this could happen depends on the frequency of the perturbations. As has been reported, earlier, for frequencies larger than 0.02 hz, temperature runaway did not take place. However, decreasing the frequency of temperature waves merely allows more time for the solid to heat up or cool down. Thus, at a frequency of 0.0125 hz , figure 5.4 shows the temperature and concentration waves at different axial positions. While the initial transient can still be seen as a high temperature peak of the first wave, it seems that at z = 0.6 temperature runaway has occurred near the reactor axis (i.e. r = 0.0) but is not apparent at the wall (i.e. r = 1.0). The radial profiles at z = 0.6 and at the peak temperature occurred in the first wave as can be seen in figure 5.5 for the above frequency as well as other frequencies. It is clear that as the frequency decreases, the temperature gradient increases, but the steepest part of the radial profile is at the reactor wall. This illustrates how the temperature wave moves across the radial direction. It can also be observed from figure 5.5 that in the case of species CB at a frequency of 0.025 hz the peak in the profile arises at points other than the reactor axis. At a frequency of 0.0083 hz , the species CA was depleted completely, so a further decrease in frequency would result in the product CB reacting.

5.5 Concentration forcing disturbances

Since the reaction rate terms are structured to have an Arrhenius form, thus emphasizing the nonlinear dependency on temperature, it is to be expected that the rate terms will be more sensitive to temperature than to concentration perturbations. Moreover, in the case under study,

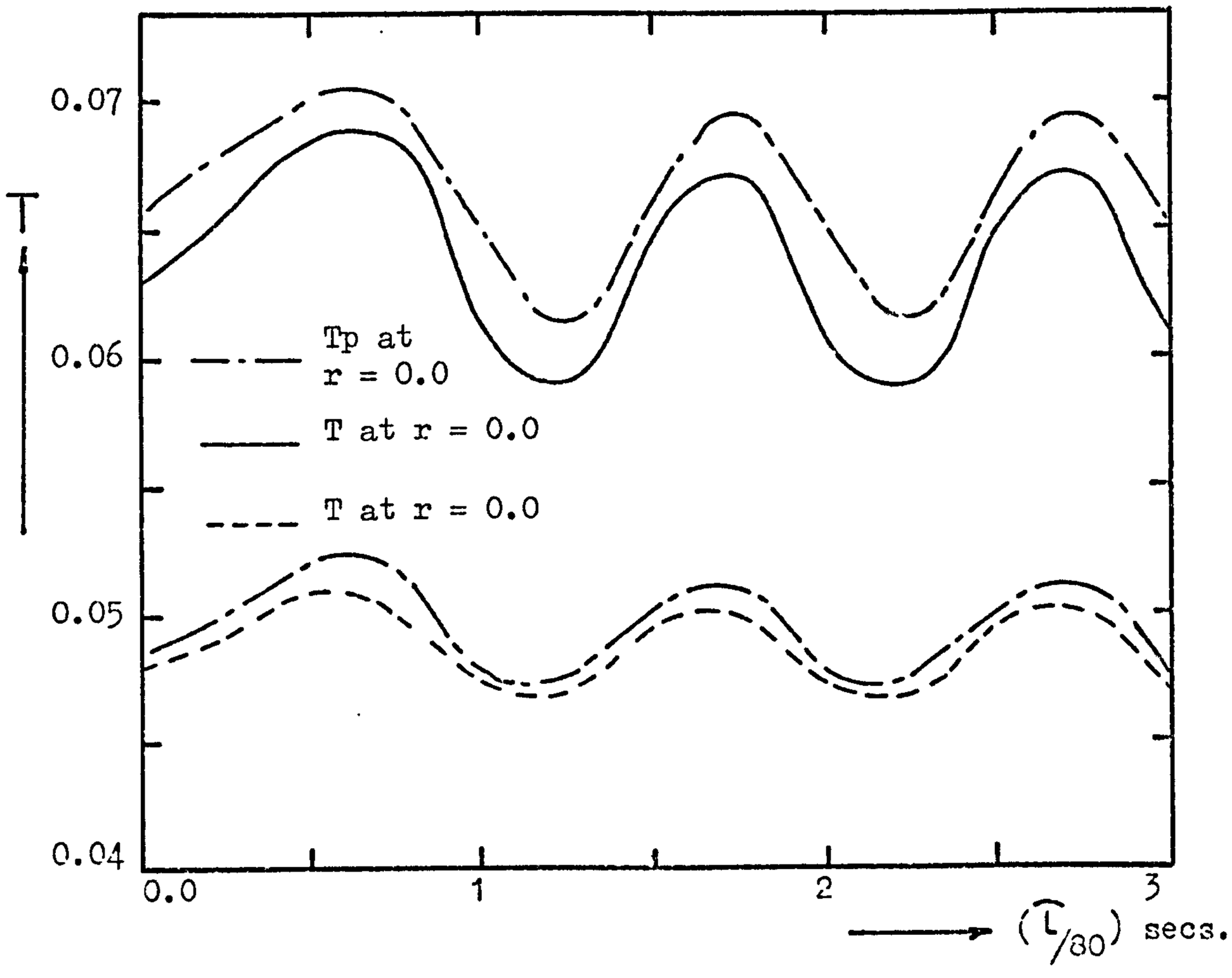

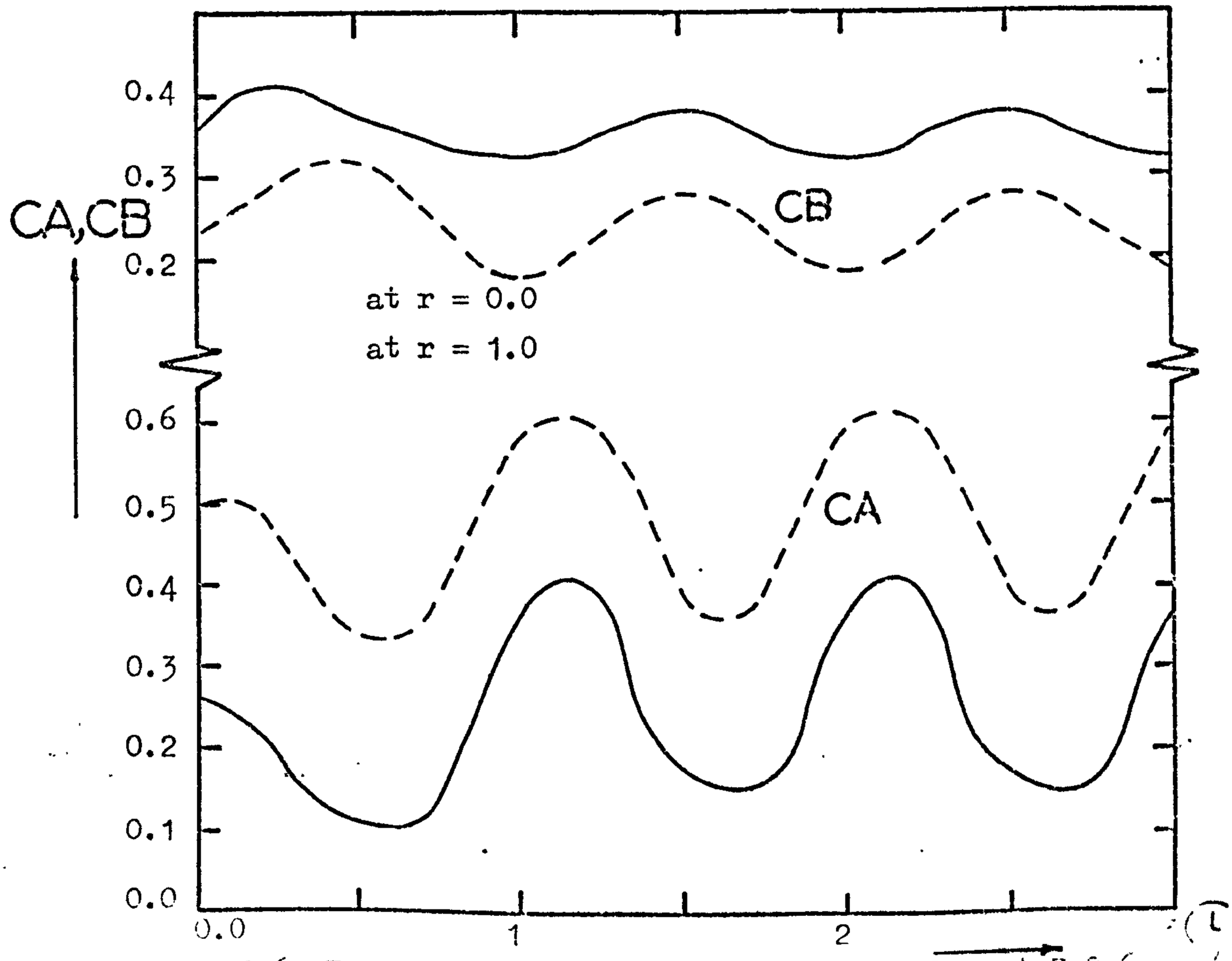

Figure 5.6: Temperature and concentration profiles at Z=0.6 during the response of the reactor to an inlet concentration perturbation of the form CA = 1.0 + 0.1Sin($\frac{2\Pi t}{80}$)

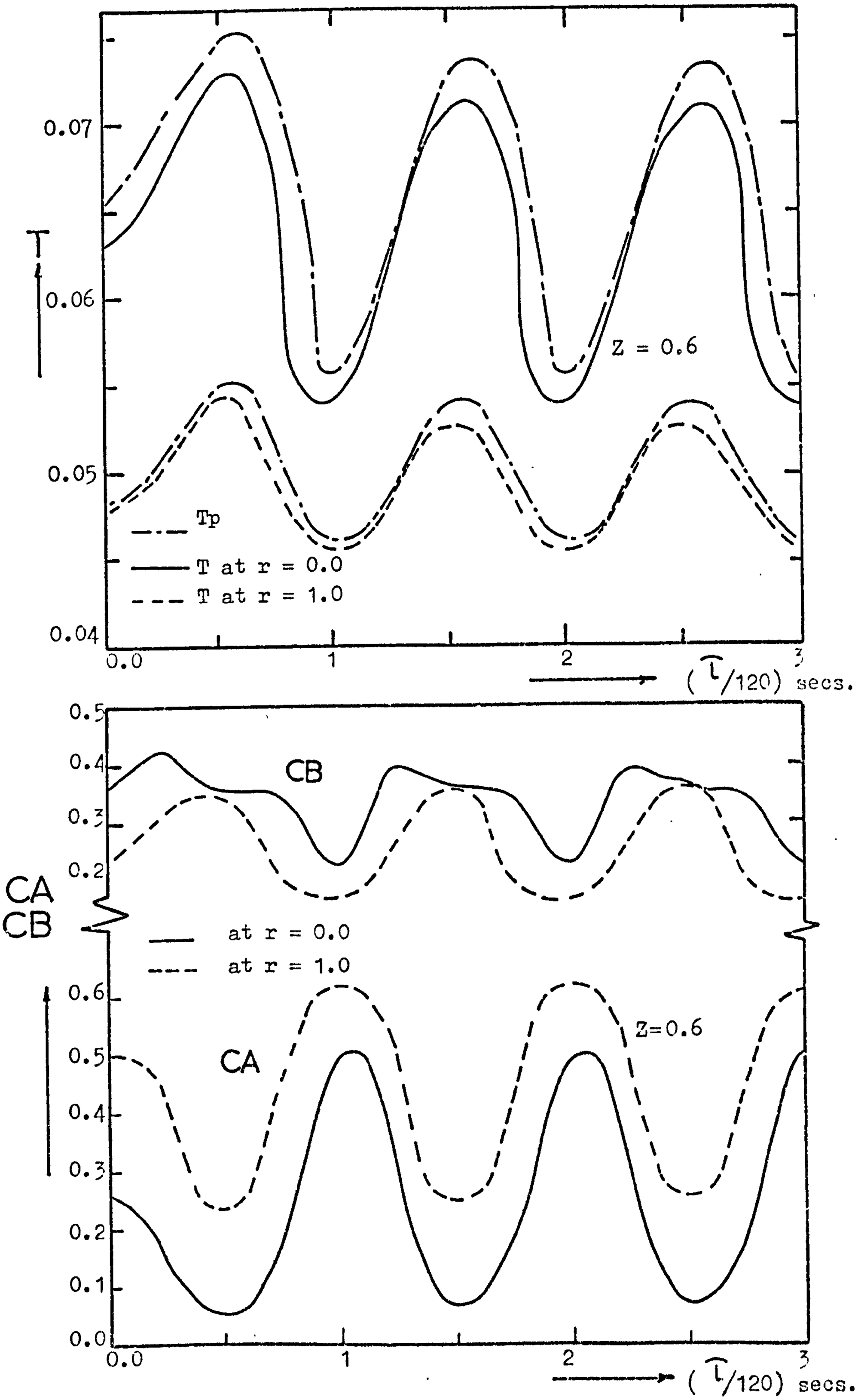

Figure 5.7: Temperature and concentration profiles during the response of the reactor to an inlet concentration perturbation of the form CA = 1.0 + 0.1 $\sin(\frac{2\pi}{120}\tau)$

the reaction orders for species A and B are taken as unity, making the response to CA disturbances smoother. This can be seen from figure 5.6 which shows the temperature and concentration waves at the axial position $z = 0.6$ at a frequency of 0.0125 hz and an amplitude equal to 10% of the inlet concentration value. The general features observed in the case of a temperature forcing function also apply to concentration variations. Thus, the higher temperature peak occurring in the initial transient can still be seen.

As would be expected, decreasing the frequency will increase the temperature wave amplitude. Figure 5.7 shows such effects for frequency of 0.00833 hz at the axial position $z = 0.6$.

Note that this frequency has caused temperature runaway in the case of temperature forcing with an amplitude of 2.9% of the inlet temperature value. In the case of concentration forcing and for an amplitude of 10% of the inlet concentration, temperature runaway occurs at a frequency of 0.0063 hz or less.

It should be noted that for equal amplitudes of 10% of inlet variable, a frequency five times smaller is needed for the concentration forcing to give approximately similar behaviour to that of temperature forcing. It is therefore expected that significantly less stringent constraints will be required for perturbations in concentration, than for temperature.

5.6 Velocity forcing disturbances

Figure 5.8 shows the temperature and propagation waves for CA and CB at different axial positions for a sinusoidal perturbation in the mean fluid feed velocity of 0.0125 hz and an amplitude of 10% of the steady state value. As the fluid velocity increases in the first half period, the effective thermal conductivity KF and the wall heat transfer coefficient U increase, making the radial dissipation of heat faster.

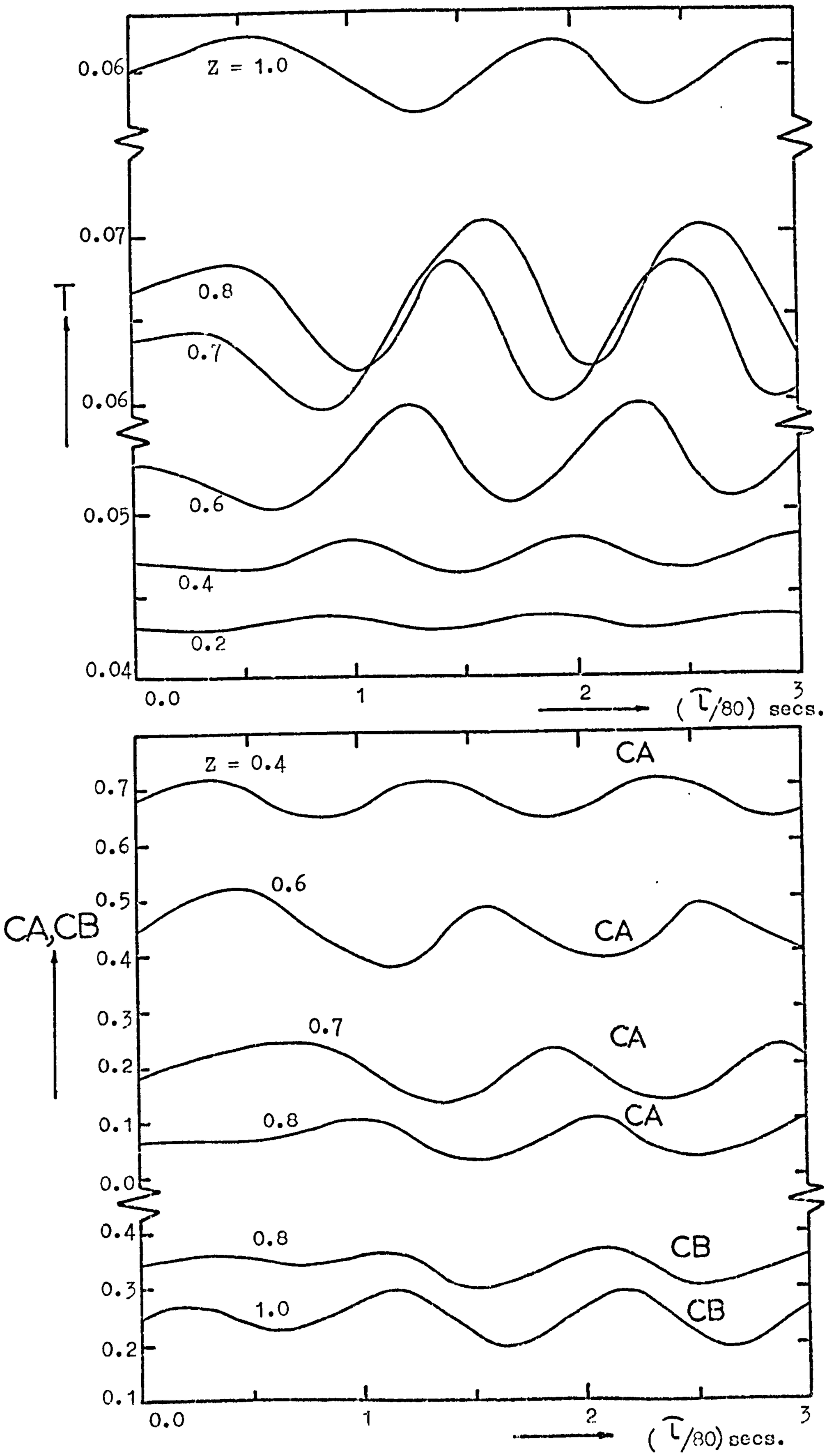

Figure 5.8: Centreline temperature and concentration profiles at various axial positions during the response of the reactor to an inlet velocity perturbation of the form $u = 164 + 10\ \mathrm{Sin}(\frac{2\pi}{80}\bar{t})$.

Also the heat transfer between the solid and the fluid increases. Thus the increase in rate of heat removal whether from the solid to the fluid and/or from the fluid through reactor wall would cause a drop in fluid temperature in the inlet region with the result of an increase in concentration. Although this high concentration wave should increase the temperature everywhere in the reactor, as in the case of concentration perturbations, a decrease in temperature is observed down the bed as far as $z = 0.6$. Unlike the previous cases of temperature and concentration forcing, three waves are interacting with each other, i.e. temperature, concentration and fluid velocity. It seems that because the temperature level is still low at $z = 0.6$, the effect of increasing the transfer coefficients, as a result of velocity increases, does not allow the solid to heat up sufficiently for the reaction rate to increase. In this case, the effect of the velocity is apparent. However at $z = 0.7$ and 0.8, the temperature level is already high making the reaction rate more sensitive to concentration changes. As a result the reaction rate increases, i.e. the heat generation increase is larger than can be dissipated by the increase in heat transfer and thus the temperature increases at these positions.

As the velocity passes through a minimum in the second half of the first period, the transfer coefficients decrease. The solid is then not able to dissipate the heat generated fast enough, and so becomes hotter. These conditions favour higher rates of reaction resulting in higher temperature and low concentration waves at the reaction inlet region. Their interaction with the fluid velocity wave follows a similar argument as discussed above.

Some observations are worth mentioning on the effect of sinusoidal fluid velocity perturbations compared with concentration disturbances. These are:

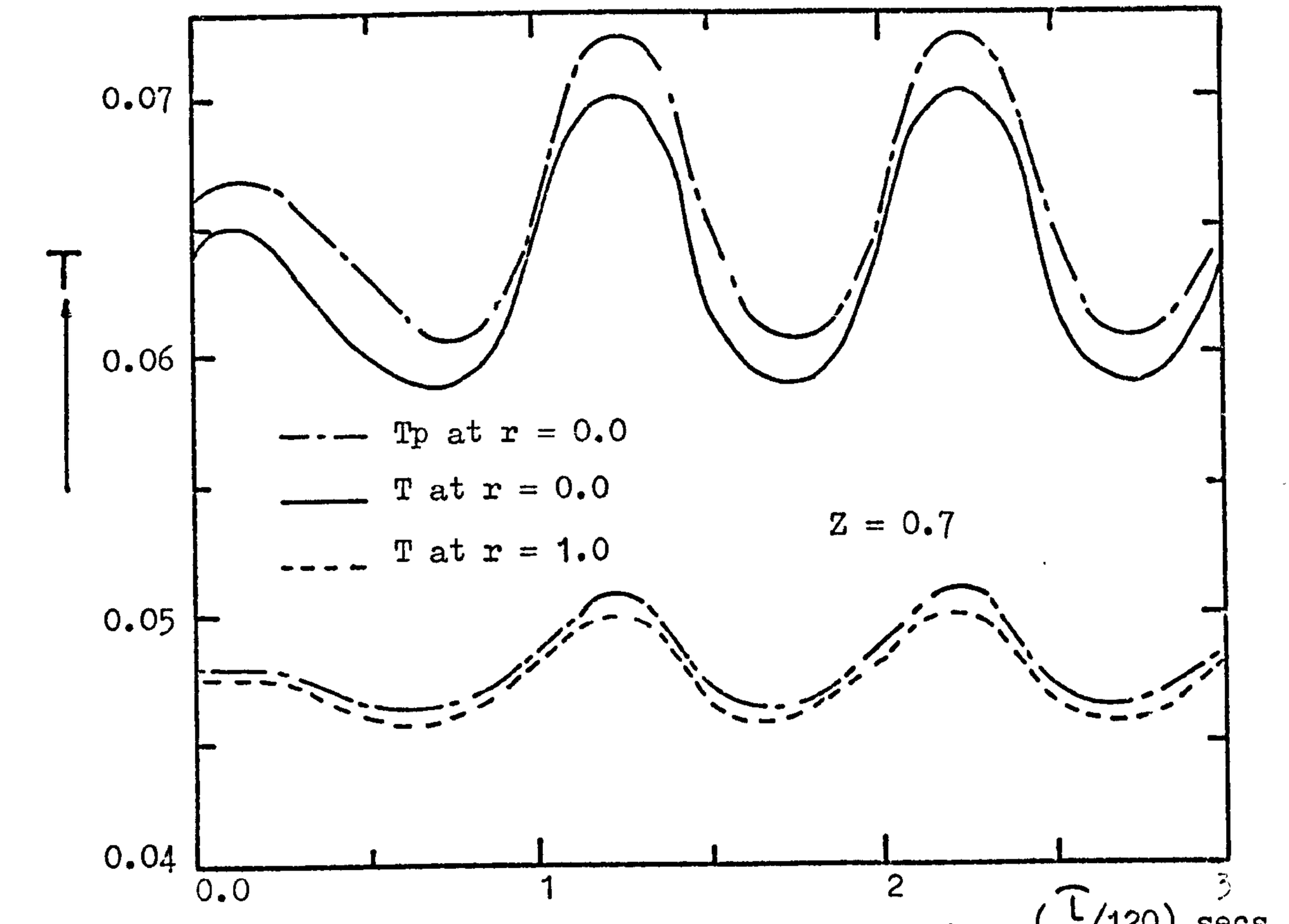

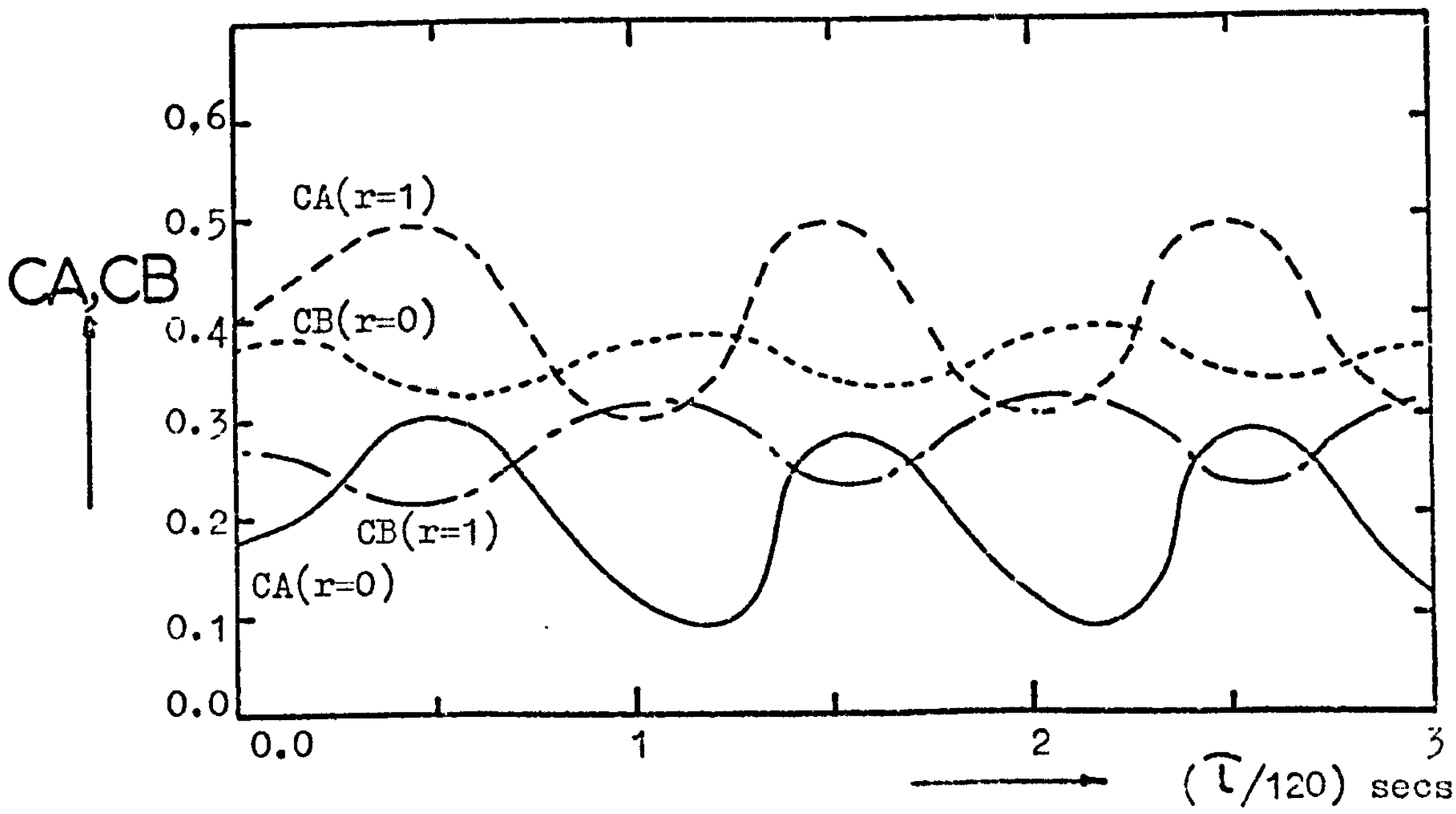

Figure 5.9: Temperature and concentration profiles at Z=0.7 during the response of the reactor to an inlet fluid velocity perturbation of the form u = $164 + 10\ \mathrm{Sin}(\frac{2\pi}{120}\bar{t})$.

1. Unlike the case of concentration disturbances, in fluid velocity perturbations, the temperature peaks found in the initial transient period have lower values than those of the quasi-stationary state. For example from figure 5.8 for a frequency of 0.0125 hz and at z = 0.7, the temperature peak at the initial transient is lower by about 56K. At a lower frequency of 0.0083 hz (figure 5.9) the temperature peak is lower by 80K at z = 0.7 compared with peaks in the quasi-stationary state.

Following the propagation mechanism of fluid velocity described earlier, it is reasonable to say that the different behaviour observed in the initial transient is due to the fact that the fluid velocity wave acts against the concentration wave, i.e. they always interact destructively with the temperature wave. This behaviour manifests itself in the initial transient period as seen above.

2. When the reaction is subjected to a sinusoidal perturbation in inlet concentration or fluid velocity for frequencies larger than 0.01 hz and amplitude of 10% of the inlet value, the temperature waves in the quasi-stationary state have about the same magnitude of oscillation. For frequencies lower than 0.01 hz the reactor is generally more sensitive to concentration changes than to fluid velocity. In this respect, for a frequency of 0.0063 hz temperature runaway did not take place in the case of velocity disturbances which is not the case in concentration perturbations. Note that the low temperature peaks found in the initial transient in the case of fluid velocity disturbances indicate that at certain frequencies temperature runaway or severe hot spots may develop after the quasi-stationary state is reached.

5.7 Temperature damped sinusoidal perturbations

Many industrial reactions are highly exothermic. Unavoidably, the temperature gradients in the reactor will vary, making the control problem more difficult. Trying to avoid high temperatures by operating the reactor at low but safe temperature levels, productivity and efficiency of the reactor itself may be affected. Thus, knowledge of the dynamic behaviour of the reactor under various conditions can widen the safe limits of operation. The control of feed temperature is but one important problem among many. The response of industrial control instruments in general is a damped oscillatory function. It is therefore useful to study a damped oscillation as a further step in investigating the reactor response to such idealized responses, but at the same time ensuring that it is sometimes near to a real control situation. The damping effect is represented as a decreasing function of time (i.e. $e^{-p\tilde{t}}$ in equation 5.2 below), where p is a damping factor. As p is increased, the oscillations decrease, thus taking less time to return to the original setting. Decreasing the damping factor has the reverse effect. Nevertheless, the following study is only intended to outline some of the differences, if any, which may exist if a damping effect is present. The equation describing the damped sinusoidal perturbation in inlet fluid temperature is of the following form:

$$T(\tilde{t}) = T(0) + Ae^{-p\tilde{t}}\sin(2\pi F\tilde{t}) \qquad (5.2)$$

where T(0) is the steady state inlet temperature. The term $Ae^{-p\tilde{t}}$ has been chosen such that its value gives a maximum rise in temperature in the first half of the first period, equal to that without damping, considered previously.

Figure 5.10 shows the response of the temperature at the reactor axis (r = 0.0) to a damped oscillation in feed temperature of a frequency

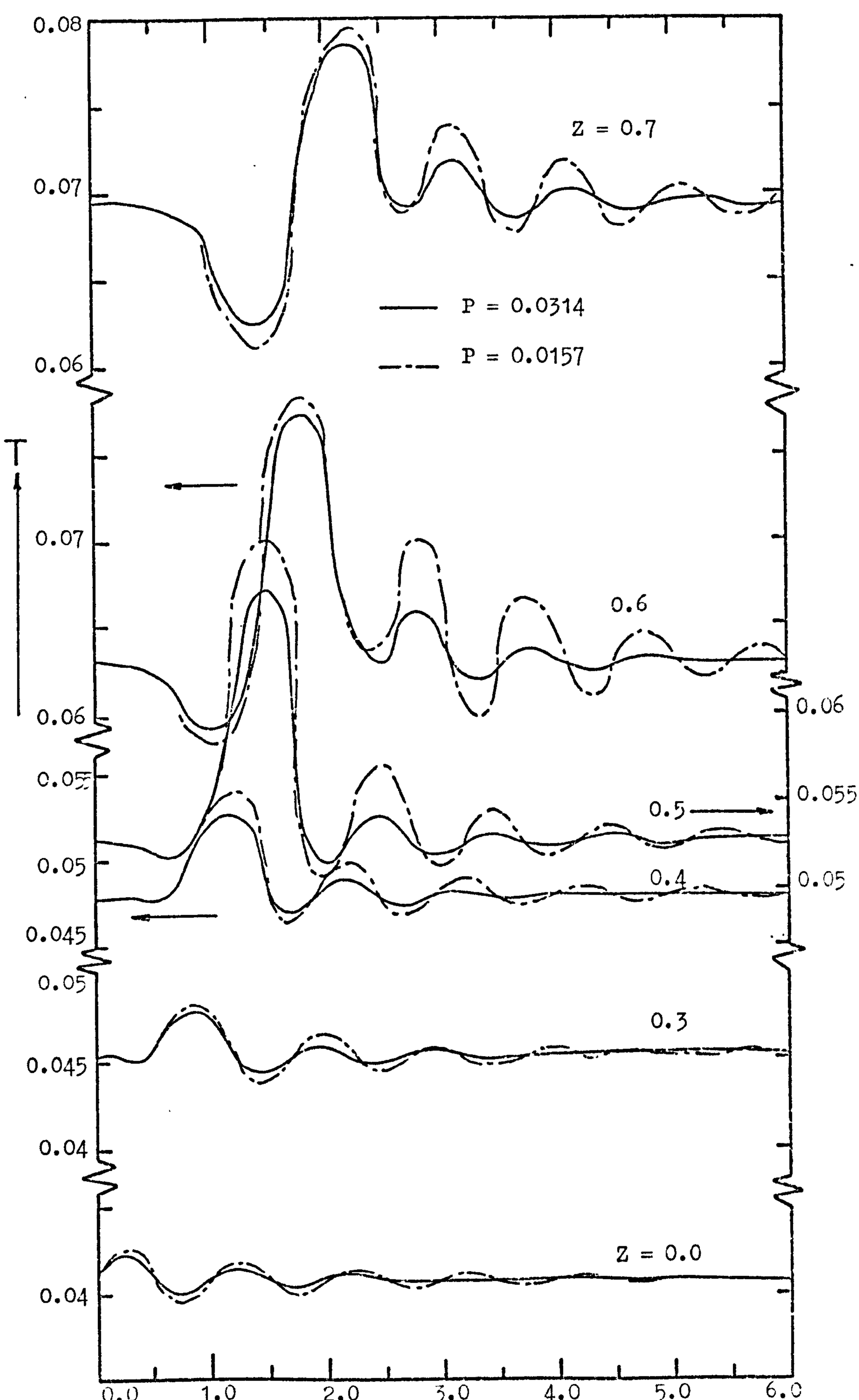

Figure 5.10: Centreline temperature profiles at various axial positions during the response of the reactor to damped oscillation in inlet temperature of the form $T = 0.0408 + 0.00659e^{-P\tilde{t}} \sin(\frac{2\pi}{40}\tilde{t})$.

of 0.025 hz and a damping factor p = 0.0157 and 0.0314. For an initially positive going sine wave, the feed temperature starts to increase, initiating a heat wave. At the same time a low concentration wave also moves down the bed. The effect of this wave can be seen as the temperature starts to decrease everywhere in the reactor. Meanwhile, the first temperature wave continues to move slowly down the bed. In the second half of the first period, the temperature starts to decrease which initiates another high concentration wave and in general the propagation follows the same features observed before. However, as these waves continue to propagate, the amplitude also continues to decrease exponentially. As a result they die down. On the same figure is shown the effect of decreasing the damping factor, and it can be seen that the amplitudes of the oscillations increase, and take more time to damp down.

By comparing the reactor response for sinusoidal perturbations with and without damping (see figures 5.10 and 5.1 respectively), it should be noted that the temperature peak in the initial transient period is higher in the case with damping. For example at z = 0.6 on both figures, the peak temperature is 0.077 for the case with damping while it is 0.075 for the case without damping. This is in spite of the fact that in the former case the successive concentration waves are weaker because of the damping effect. The reason for this is due to the propagating temperature waves, which are of higher intensity in the case without damping, so it reduces the possibility of mass accumulation from the early parts of the bed. This concentration accumulation also accounts for the higher hot spots formed in the latter parts of the bed. The initial transient period appears to be even more important in the case with damping. This is because the reactor actually does not reach the quasi-stationary state observed previously.

Although the sinusoidal perturbations analysis has given invaluable insight into the reactor behaviour, with damped disturbances more stringent conditions may be required regarding the allowable amplitudes and/or frequencies, to prevent temperature runaway or hot spot formation in the initial transient periods.

While damped oscillation with an initially positive going sine wave may lead to the formation of severe hot spots in the reactor, its response to an initially negative going sine wave is different. Thus, figure 5.11 shows such a response at different axial positions for a frequency of 0.025 h z. It can be seen that the initial decrease in temperature (as a result of the negative going sine wave) has led to the formation of a cold wave to propagate. Even the hot spots formed later are not so large as to endanger the activity of the catalyst or cause any other undesirable results. This behaviour is partly due to the fact that the catalyst bed is cooled down by the first temperature wave and that the successive waves are not of the same intensity. Thus, even their constructive interaction will always be weaker.

The initial transient in this case shows comparatively low temperature peaks. This observation has been reported on a similar system by Adderley[109] in his studies on sinusoidal oscillations without damping. Note that the behaviour shown above may be compared with that given in Chapter Four on the multivariable approach (i.e. manipulating both the inlet temperature and concentration) shown in figures 4.12 and 4.13. In that respect the damped negative going sine wave behaviour suggests that it may be possible to decrease the reactor inlet temperature without the dangers of hot spot formation in an oscillatory manner. In this way, it is in fact a multivariable approach but with the difference that the heat waves are used to manipulate the concentration propagation. This approach to the reactor control, however, needs further investigation.

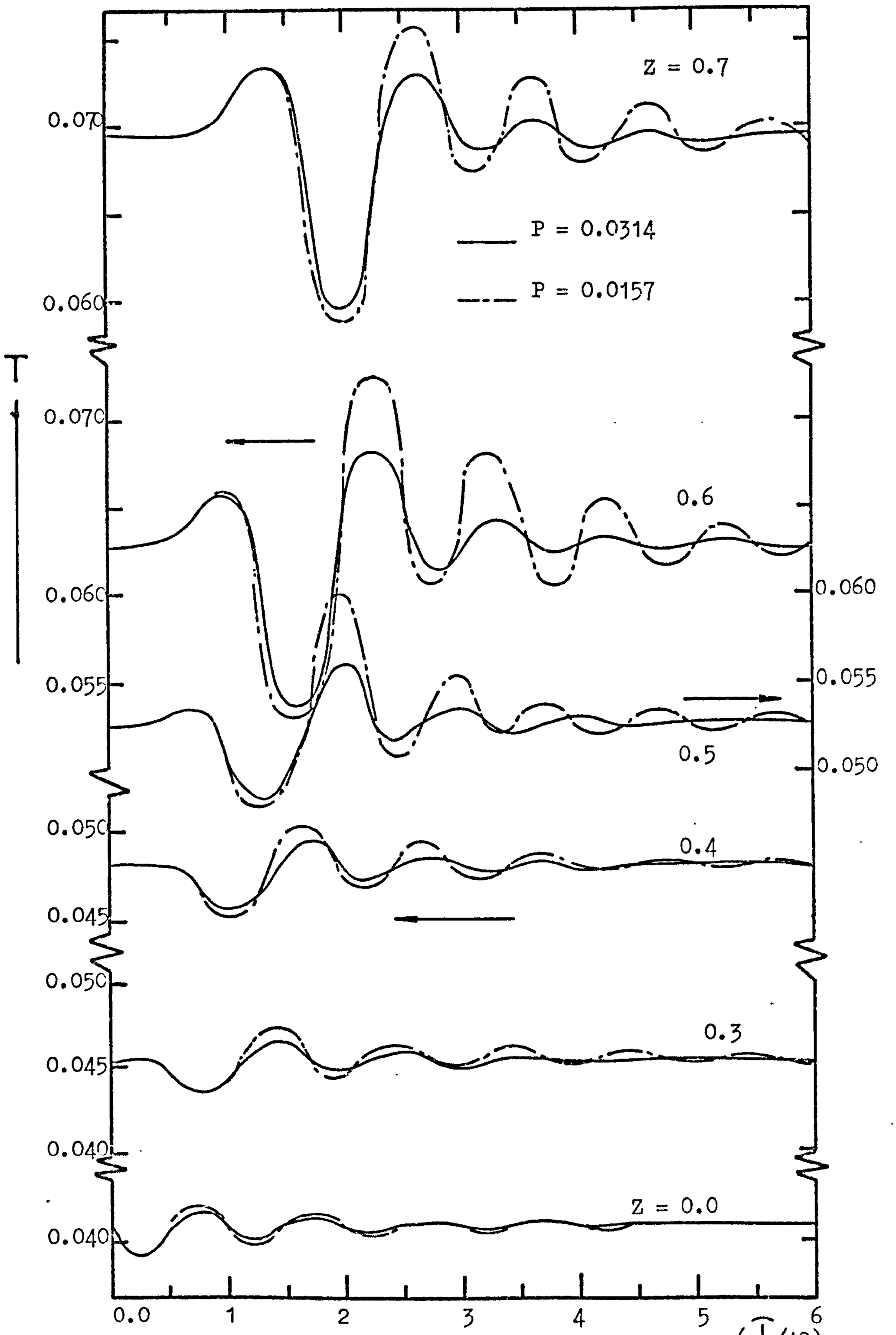

Figure 5.11: Centreline temperature profiles at various axial positions during the response of the reactor to a damped oscillation in inlet temperature of the form $T = 0.0408 - 0.00659e^{-P\hat{\tau}} \sin(\frac{2\pi}{40}\hat{\tau})$

5.8 Concluding Remarks

The dynamic response of the fixed bed reactor to sinusoidal perturbations in inlet temperature, concentration and fluid velocity indicates that two apparently distinct transient situations exist. There is an initial transient period followed by a quasi-stationary state. The time duration of the former is approximately equal to the residence time of the first temperature wave. While the concentration wave propagates at the fluid velocity, the ratio of the latter to the temperature wave velocity equal to the fraction of the total heat capacity of the system contributed by the fluid. Thus the concentration and temperature waves have residence times of 0.75 and 100 seconds respectively.

In the case of temperature and concentration disturbances with an initially positive going sine wave, the temperature peaks reached higher values in the initial transient than those in the quasi-stationary state. Thus, for certain frequencies, temperature runaway or hot spots may take place in the initial transient period only. In the case of fluid velocity disturbances the temperature peaks which occurred in the initial transient period have lower values than those in the quasi-stationary state, indicating that temperature runaway or severe hot spots may develop after the quasi-stationary state is reached.

For a Peclet number of 10, a hot spot may occur over some part of the radius near the axis and a two dimensional model should be used. However, for Peclet less than 6, the one dimensional axial mean temperature closely follows that based on the two dimensional model.

Preliminary study of damped sinusoidal perturbations with an initially positive going sine wave indicates that temperature peaks occur in the initial transient which may reach higher values when compared with cases without damping. This means that more stringent

controlling action is needed in such cases. For an initially negative going damped sine wave, comparatively low temperature peaks occur. This suggests that reactor inlet temperature may be changed in a sinusoidal damped manner without the danger of severe hot spot formation.

Finally the complex nature of the phenomena taking place in the reactor has been further demonstrated in this chapter and revealed some of the characteristics which might be of importance in control studies of fixed bed reactors. Further work on damped oscillations is required. This will be a necessary step before deciding on a control strategy.

CHAPTER 6

AXIAL DIFFUSION MODEL

6.1 Introduction

The complex nature of the events in fixed bed catalytic reactors has recently invoked an assessment of the importance of axial dispersion of heat and mass. Generally the significant mixing mechanism in axial direction is due to the turbulence arising from the presence of the packing and can be accounted for by superimposing an effective mechanism upon the overall transport by plug flow.[118,7] The flux due to this is described by an expression analogous to Fick's and Fourier's laws for mass and heat respectively. The respective proportionality constants are effective diffusivity and conductivity coefficient (see equations 6.1 to 6.5), and they implicitly take into account the effect of velocity and short circuiting due to packing.[131,132,133,134]

Considering axial mixing in adiabatic operation, Carberry and Wendel[118] and Hlavacek and Marek[119] indicated that axial dispersion effects may be neglected, provided the length of the reactor is long enough. It appears that the length should be of the order of 400 pellet diameters. This may be justified on physical grounds, since at that length the conversion due to reaction is nearly completed and thus the temperature in adiabatic operation reaches a constant magnitude at the reactor outlet regardless of what effect the axial diffusion might have on the profiles in the reactor.[120] In fact the axial dispersion may result in a redistribution of heat and mass inside the reactor and this has been shown by Liu and Amundson,[125] who reported that the axial dispersion can have a significant effect on axial profiles especially in the region of multiple states.

In non-isothermal operation, where account of radial variation of heat and mass must be taken into consideration, the resulting system would

be complex and difficult to solve.[126] Carberry and Wendel[118] developed a steady state model for a catalytic reactor which includes axial dispersion of heat and mass and radial variations in temperature were approximated by assuming a parabolic radial temperature profile. They reported that axial dispersion can be neglected if the bed depth is more than 50 particle diameters, which is a condition usually satisfied in industrial practice.[7] Although their conclusion has found acceptance by others,[7,9] more recently Young and Finlayson[120] analysed their results and argued that the Carberry and Wendel criterion is not general and that they, in fact, were studying the effect of varying the axial diffusivity and conductivity (i.e. variation in Pe_{Ha} and Pe_{Ma}) and not the reactor length. The former authors[120] showed that for a reactor length of 50 particle diameters the axial diffusion does have, in certain cases, a significant effect.

It seems, therefore, that the criterion put forward for non-isothermal reactors is open to question and it may be incorrect to extrapolate these conclusions to more general cases.

If an attempt is made to include axial and radial dispersion of heat and mass in the system, the resulting model is even more complex and takes a considerable amount of computing time to solve.[60,66,62] Such general models have been ignored, apparently for two reasons. Firstly, axial dispersion has generally been considered unimportant.[9,71,129] Secondly, the model has been considered too formidable to solve.[9,128] Nevertheless, for the simple reaction A ⟶ B, Dente, Biardi and Ranzi[130] did give a solution using an integral transformation technique. They included the particle transport limitations and indicated that for comparatively long reactors (200 pellet diameters) the axial dispersion has a significant effect on axial profiles. Similar conclusions have been reported[120] for reactor lengths of 50 particle diameters.

The generally acceptable methodsfor solving the above models are some forms of finite difference representation and even using quasi-linearization[127] to increase the efficiency of solution, the reported computing times are excessive. More recently the application of the collocation method on such problems has proved more efficient.[80,121,120]

In this chapter, a mathematical model with axial dispersion is developed for the complex reaction scheme in which the inter- and intraparticle transport resistances are included. The radial heat transport is lumped at the wall based on the assumption of parabolic radial profile. An assessment of this model and the applicability of the collocation method to such problems, particularly with reference to computing time and accuracy of approximation, is presented. In addition, the limitations imposed by the parabolic temperature profile assumption is treated with the lumping technique used in Chapter Four. This increases the accuracy of radial profile representation without increasing the computing time appreciably.

The effects of axial dispersion will be investigated and an attempt made to identify circumstances in which it may be significant.

6.2 Formulation of equations

The heat and mass balances are most conveniently expressed in dimensionless form as follows:

$$\frac{1}{Pe_{Ma}}\frac{d^2CA}{dZ^2} - \frac{dCA}{dZ} - G_2\gamma(\phi_1^2 + \phi_3^2)CA = 0 \qquad (6.1)$$

$$\frac{1}{Pe_{Ma}}\frac{d^2CB}{dZ^2} - \frac{dCB}{dZ} + G_2\gamma\psi(\phi_1^2 + \phi_3^2)CA = 0 \qquad (6.2)$$

$$\frac{1}{Pe_{Ha}}\frac{d^2T}{dZ^2} - \frac{dT}{dZ} - \frac{2N_{uw}}{G_3}(T - Tc) + G_4(Tp - T) = 0 \qquad (6.3)$$

Subject to the boundary conditions

$$\frac{1}{Pe_{Ma}} \frac{dCA}{dZ} = (CA - CA_0)$$

$$\frac{1}{Pe_{Ma}} \frac{dCA}{dZ} = (CB - CB_0) \qquad \text{at } Z = 0 \qquad (6.4)$$

$$\frac{1}{Pe_{Ha}} \frac{dT}{dZ} = (T - T_0)$$

$$\frac{dT}{dZ} = \frac{dCA}{dZ} = \frac{dCB}{dZ} = 0 \qquad \text{at } Z = 1 \qquad (6.5)$$

The additional dimensionless quantities which have been introduced are the Peclet numbers $Pe_{Ma} = \frac{uL}{DF_a}$ and $Pe_{Ha} = \frac{\rho CpuL}{KF_a}$. The axial peclet number Pe_{Ma} for mass and Pe_{Ha} for heat are usually linear functions of velocity, having values between 1 and 2 (based on the pellet diameter) for high fluid velocities.[133,134] It may also be assumed that the axial diffusivities are equal for each component in the fluid phase. This occurs because dispersion is caused mainly by mechanical disturbances of the stream lines under conditions of turbulent flow. The additional assumptions involved in the formulation of the above equations are given in appendix (A4). The state variables occurring in the above system of equations are all radial mean values and for an initial policy the rates of reaction may be evaluated by solving the catalyst pellet equations given in appendix (A1.2.1) at the radial mean conditions.

6.3 Solution of the equations

The solution of the system of equations given above can be obtained by applying the collocation method. The system of equations at the J^{th} collocation point can be written as follows:

$$\frac{1}{Pe_{Ma}} \sum_{i=1}^{M+2} BB_{J,i}\, CA_i - \sum_{i=1}^{M+2} AA_{J,i}\, CA_i - G_2 \eta (\phi_1^2 + \phi_3^2) CA\Big|_J = 0 \qquad (6.6)$$

$$\frac{1}{Pe_{Ma}}\sum_{i=1}^{M+2} BB_{J,i}\ CB_i - \sum_{i=1}^{M+2} AA_{J,i}\ CB_i + G_2\,\eta\psi(\phi_1^2 + \phi_3^2)CA\Big|_J = 0 \qquad (6.7)$$

$$\frac{1}{Pe_{Ha}}\sum_{i=1}^{M+2} BB_{J,i}\ T_i - \sum_{i=1}^{M+2} AA_{J,i}\ T_i - \frac{2N_{uw}^*}{G_3}(T - Tc)_J + G_4(Tp - T)\Big|_J = 0 \qquad (6.8)$$

The boundary conditions are transformed as

$$\sum_{i=1}^{M+2} AA_{1,i}\ CA_i = Pe_{Ma}(CA_1 - CA_0)$$

$$\sum_{i=1}^{M+2} AA_{1,i}\ CB_i = Pe_{Ma}(CB_1 - CB_0) \qquad \text{at } Z = 0 \qquad (6.9)$$

$$\sum_{i=1}^{M+2} AA_{1,i}\ T_i = Pe_{Ha}(T_1 - T_0)$$

$$\sum_{i=1}^{M+2} AA_{M+2,i},\ CA_i = \sum_{i=1}^{M+2} AA_{M+2,i},\ CB_i = \sum_{i=1}^{M+2} AA_{M+2,i},\ T_i = 0 \text{ at } Z = 1 \qquad (6.10)$$

Thus, the system of differential equations has been reduced to 3(M+2) algebraic nonlinear equations. By substituting the boundary conditionsto eliminate CA_1, CB_1 and T_1 and CA_{M+2}, CB_{M+2} and T_{M+2}, the number of algebraic equations may be reduced to 3M nonlinear equations to be solved simultaneously. A Newton Raphson method can be used to promote the convergence of the solution. The pellet equations are given in Appendix (A1.2.1) and are used to calculate T_p, η and ψ at the J^{th} collocation point. The steps in the solution are as follows:

1. Assume values for the inlet fluid temperature To and species concentration CAo and CBo.

2. Assume values for the state variables, T, CA and CB at the collocation points equal to the values of the previous iteration (or equal to the inlet conditions).

3. Solve the pellet equations at the collocation points to obtain values for T_p, γ and ψ for the current iteration.

4. Estimate the linearized reaction rate terms at the collocation points.

5. Evaluate the function values at each collocation point and for each state variable, i.e. F_m where m = 1,2,.....3M.

6. Evaluate the Newton Raphson iteration matrix Q_m.

7. Estimate the new values of the state variables by the general form $Y_{i+1} = Y_i - Q_m^{-1} F_m$.

8. Compare the new values at the $(i+1)^{st}$ iteration with those of the previous iteration i. If unsatisfactory, repeat from step 2, otherwise continue to step 9.

9. If satisfactory, the converged values at iteration number i+1 are the required values of the state variables at the interior collocation points.

10. To obtain values of state variables at the inlet and outlet (i.e. T_1, CA_1, CB_1 and T_{M+2}, CA_{M+2}, CB_{M+2}), use can be made of the boundary equations given by 6.9 and 6.10.

Since the axial dispersion problem given above is unsymmetrical, it is expected that the matrix of coefficients $AA_{J,i}$ and $BB_{J,i}$ are different from those used in the case of a symmetrical boundary value problem. However, they can be evaluated by a similar method as shown in appendix (A1.4.2). The solution at any point other than the collocation points can be approximated by an unsymmetrical expansion function of the following form: $$Y(z) = (1 - Z)Y(0) + ZY(1) + \sum_{i=1}^{M} a_i P_{i-1}(z)$$

where the Y's are the state variables, a_i are arbitrary coefficients which can be determined in a similar manner to that described in appendix (A1.4.1). $P_{i-1}(z)$ are the shifted orthogonal polynomials, of a kind which depend upon the weighting function used. Usually, from 11 to 19 interior collocation points are required for the problems considered in this study.

6.4 Evaluation of the collocation method

Apart from the collocation technique, the type of orthogonal polynomials used gives some idea of the power of the method itself. It might be possible in some cases to choose certain types of orthogonal polynomials to satisfy some conditions in the desired solution. In the problem considered here, shifted Legendre and Chebyschef polynomials have been used. A property of the Legendre polynomial is that it gives minimum end point errors,[121] although large errors may arise elsewhere in the integration interval. On the other hand, Chebyschef polynomials minimize the maximum errors over the whole interval. In reactor problems where high peaks in temperature or concentration may arise in the integration intervals, interest is primarily inobserving the magnitudes of these changes. In this respect Chebyschef polynomials may be more appropriate.

Figure 6.1 shows the axial radial mean temperature profiles for an axial peclet number Pe_a = 1200.0. (This value is equivalent to Pe_a = 4.0 when based on pellet diameter.) Both Legendre and Chebyschef shifted polynomials have been used. These temperature profiles have been compared with those of the one dimensional model without axial diffusion (i.e. $Pe_a = \infty$). By using such high value of Pe_a = 1200.0 the axial diffusion would have a negligible effect on the concentration and temperature profiles. This last comparison, with the case of $Pe_a = \infty$, is intended to show that the collocation method is quite adequate in approximating the temperature and concentration profiles.

6.4.1 Approximation accuracy

Table (6.1) compares different kinds of polynomials for estimating the axial mean temperature and concentration (for Pe_a = 1200.0). Also the case of $Pe_a = \infty$ is presented for comparison.

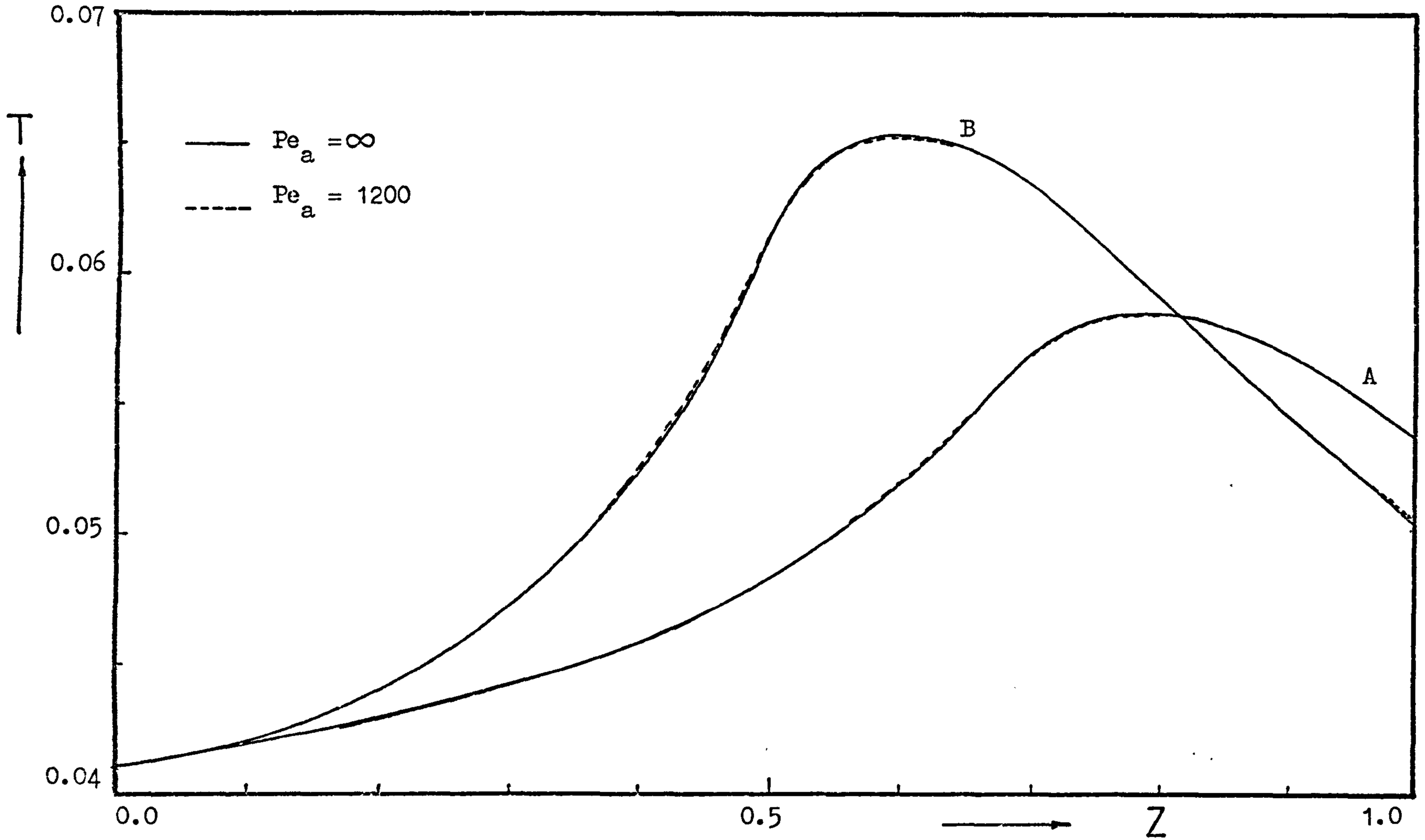

Figure 6.1: Comparison of radial mean temperature profiles predicted by the one dimensional axial diffusion model and the corresponding model neglecting it.
Data as given in Table 3.3.

Table 6.1

		Case A			Case B		
		Z = 0.0	Z = 0.7	Z = 1.0	Z = 0.0	Z = 0.6	Z = 1.0
Plug flow F.D. (1)	T	0.0408	0.05652	0.05367	0.04080	0.06592	0.0506
	CA	1.0	0.2620	0.01659	1.0	0.1042	0.0031
	CB	0.0	0.3394	0.25587	0.0	0.3412	0.2117
ADM	T	+0.00003	-0.00014	-0.0003	+0.00005	-0.0002	-0.00036
Cheb. (2)	CA	-0.0008	-0.005	-0.002	-0.0009	-0.01	+0.0002
	CB	+0.00005	+0.001	-0.0001	+0.00006	+0.002	+0.0001
Legdr. (3)	T	+0.00001	-0.00036	-0.0001	+0.00001	-0.00043	-0.00031
	CA	1.0	-0.01	+0.001	1.0	-0.012	-0.0001
	CB	+0.00002	+0.0039	0.0000	+0.00005	+0.0045	+0.0001

(1) Integrated by finite difference method (200 axial steps)

(2) Chebyschef polynomials, 15 points used

(3) Legendre polynomials, 15 points used

(+) Added values to those of plug flow

(-) Subtracted values from those of plug flow.

It can be seen that the discrepancies in values of the state variables at Z = 0.0 and 1.0 approximated by the different polynomials are comparatively small. However, the differences increase at the peak values (i.e. at Z = 0.6 and 0.7). For concentration profiles, the differences are greater than in the case of temperature, but follow the same pattern. In case B, the differences between this and the polynomial approximation using 15 points is about 1% at the hot spot. If these profiles are approximated by 14 collocation points, from 2 to 3 decimal places accuracy can be obtained in comparison with those profiles computed by 15 points and the difference between the two polynomials increases to about 2%.

It should be noted that the differences for the various polynomials are related to a great extent to the order of the polynomials employed, as well as to the function to be approximated. Generally for problems which can be approximated by low order polynomials (less than 7 points), the distribution of these collocation points in the integration interval becomes crucial,[121] and various polynomials of different distribution of zeros will be expected to give different accuracies as indicated in Chapter 3. As higher order of polynomials are used, the distribution of zeros becomes less important and so the differences in approximation between various polynomials decreases. In the problem under study, the minimum number of collocation points used was 11. This may explain why the different polynomials gave about the same accuracy. In this case, it is profitable to look to other advantages these polynomials may have.

6.4.2 Convergence properties

The convergence properties of the orthogonal polynomials has been demonstrated by the fact that starting from flat profiles at values equal to the inlet conditions, profiles such as those shown in figure 6.1 result. However, Legendre polynomials have been observed to converge faster than Chebyschef polynomials in several cases. For example, from figure 6.1, Case A, when approximated with 15 points needs 7 and 10 iterations to converge to about 4 figure accuracy, using Legendre and Chebyschef polynomials respectively. In Case B, shown in figure 6.1, using 15 to 19 Chebyschef points requires from 12 to 20 iterations, while using Legendre, from 8 to 15 iterations are sufficient. Not only do Legendre polynomials give faster rates of convergence, but in the case of changing the value of Pe_a from 1200 to 100 for case B, the rate of convergence remains essentially unchanged. In other words, for the same set of parameters used in case B, as Pe_a is decreased from 1200 to 100, the number of iterations increases from 8 to 10 for the solution to converge, using 15 Legendre points; on the other hand, an increase from 12 to 17 is necessary

in the case of Chebyschef polynomials. This may be explained on the basis that, in the case of Legendre, the number of zeros near the ends of the integration interval is greater than those of Chebyschef. This leads to a more accurate approximation for changes in inlet conditions, i.e. changes in Pe_a, and hence is consistent with rates of convergence.

6.4.3 Function behaviour

As seen above it is advantageous to use a small number of collocation points, as this will not only decrease the computing time and storage requirements considerably, but also the number of iterations. However, the number of points required is usually related to the behaviour of the function to be approximated, and whether it is well behaved or not inside the integration interval. For example a high order polynomial (17 points) has to be used to adequately approximate the temperature profile for the comparatively severe case shown in figure 6.5, with the corresponding CA and CB profiles being shown in figure 6.6. It is apparent why high order polynomials are required, not only because of the temperature and CA profiles, but also because of the variations in CB. This poses one of the major problems in solving a complex reaction scheme. If the reactor is terminated at Z = 0.5, the axial profiles can be represented by a much lower order polynomial. In fact 11 points are sufficient for comparable accuracy. A maximum of 11 points has been reported in the literature,[80] for the simple reaction A ⟶ B. No information has been given regarding the accuracy of the approximations, or the type of polynomials used. Only Young and Finlayson[120] reported an accuracy of 1% (equivalent to 2 figures accuracy here), using 6 points and this is reasonable for the case they reported.

It may also be observed that the computing time per iteration, using 15 and 17 collocation points, is of the order of 5 and 7 seconds respectively (using ICL-1906A computer). For cases A and B using 15 collocation

points, about 30% more computing time is required over the plug flow model (i.e. $Pe_a = \infty$) integrated by an implicit finite difference scheme with 200 axial steps.

In the above study the collocation method is shown to be feasible with respect to the accuracy of the approximation and small computational times for solving such complicated problems. The final decision concerning the number of collocation points required is related to the case being solved, and usually an initial check is required to estimate the minimum number of points to the demanded accuracy. This check is especially important in cases where a certain accuracy is necessary consistent with minimum computing time.

In the next section a model will be proposed which can estimate, in addition, the radial profiles with reasonable accuracy, so any discussion of results using the above model may therefore be more conveniently carried out and/or compared with the more detailed model.

6.5 The proposed lumped model

The axial diffusion model discussed above represents a moderately complex one, since it takes into account the back mixing of heat and mass. It also takes into consideration the radial transport of heat based on the parabolic radial temperature profile assumption. In the case of a highly exothermic reaction, it has been demonstrated that the parabolic temperature approximation does yield erroneous results. Attempting to include the radial and axial transport of heat and mass, the resulting model becomes very complex and takes very large amounts of computing time.[60,62] Most workers argue that only the transport mechanism which has an appreciable effect on the temperature and concentration profiles in the reactor should be included. In this respect, the radial transport is the most important, and the axial dispersion mechanicm can be neglected

for a high aspect ratio $^{L}/_{Dp}$ (i.e. reactor length to pellet diameter). However, as will be shown later, this is not always the case. Even for relatively large ratios of $^{L}/_{Dp}$, axial diffusion can affect the temperature and concentration levels in the reactor.

Therefore in the case of highly exothermic reactions, it is preferable to have a general model which includes the axial and radial transport. This is especially true if the aim is to use these models in optimizing such quantities as yield, maximum axial temperature, reactor length, etc.

It has been shown in Chapter Four that the radial diffusion can be lumped and accounted for by introducing a modified Nusselt number and distribution factors. The radial profiles are then regenerated from the algebraic expressions which depend on the axial radial mean state variables. The fully distributed model. which takes into account the radial and axial diffusion of mass and heat and which is represented by a system of coupled nonlinear partial differential equations, may thus be lumped in a similar way. For the steady state equations, lumping the system to eliminate the radial transport differential operators, a system of ordinary differential equations of the boundary value type may be obtained. In dimensionless form the lumped system of equations is as follows:

$$\frac{1}{Pe_{Ma}}\frac{d^2CAm}{dZ^2} - \frac{dCAm}{dZ} - \frac{D_{CA}}{G_1}\left(\gamma(\phi_1^{*2}k_1 + \phi_3^{*2}k_3)CA\right)\Big|_m = 0 \qquad (6.11)$$

$$\frac{1}{Pe_{Ma}}\frac{d^2CBm}{dZ^2} - \frac{dCBm}{dZ} + \frac{D_{CB}}{G_1}\left(\gamma\psi(\phi_1^{*2}k_1 + \phi_3^{*2}k_3)CA\right)\Big|_m = 0 \qquad (6.12)$$

$$\frac{1}{Pe_{Ha}}\frac{d^2Tm}{dZ^2} - \frac{dTm}{dZ} - \frac{2Nu'}{G_3}(T_m - 1) + D_T G_4(T_p - T)\Big|_m = 0 \qquad (6.13)$$

The boundary conditions are:

$$\frac{1}{Pe_{M_a}} \frac{dCAm}{dZ} = (CA_m - CAO_m)$$

$$\frac{1}{Pe_{Ma}} \frac{dCBm}{dZ} = (CB_m - CBO_m) \qquad \text{at } Z = 0 \qquad (6.14)$$

$$\frac{1}{Pe_{Ha}} \frac{dTm}{dZ} = (T - T_{om})$$

$$\frac{dCAm}{dZ} = \frac{dCBm}{dZ} = \frac{dTm}{dZ} = 0 \qquad \text{at } Z = 1.0 \qquad (6.15)$$

where all the quantities subscripted by m are mean values. The distribution factors D_{CA}, D_{CB} and D_T as well as the modified Nusselt number Nu' have the same general formsas stated in Chapter Four. The system of equations shown above is similar to those given by equations (6.1 to 6.5) and can be solved by the collocation method. Thus, the above set of differential equations can be reduced to an algebraic system of nonlinear equations similar to that given by equations (6.6 to 6.10), and may be solved similarly. The isothermal pellet equation given in Appendix (A1.2.1) is solved by Newton Raphson method at the collocation points permitting evaluation of Tp_m, η_m and ψ_m which are necessary for the solution of the fluid equations. The evaluation of the distribution factors necessitates the solution of the pellet equation at two other radial positions, namely r = 1.0 and r = 0.5. The fluid state variables at these positions which are required to solve the pellet equation can be obtained from the algebraic expression given in Chapter Four equations (4.10 to 4.12). Apart from the above mentioned modifications, the solution follows the same steps. At any axial collocation point the radial profiles may be obtained by making use of the algebraic expression given by equations (4.10 to 4.12). Having obtained the radial temperature and concentration profiles at the collocation points, the following expansion function can be used to obtain the values of the state variables at points other than that at the collocation points:

$$Y(r,Z) = (1 - Z)\,Y(r,0) + ZY(r,1) + \sum_{i=1}^{M} a_i(r)P_{i-1}(Z)$$

where $a_i(r)$ are arbitrary coefficients dependent of the radial co-ordinates, the value of which may be obtained as discussed before (see appendix A1.4.1).

6.5.1 Assessment of the proposed model

To assess the proposed lumped model given by equations (6.11 to 6.15) in terms of accuracy and computing times, it must first be compared with the previous model given by equations (6.1 to 6.5). In this comparison, the addition of the distribution factors and the modified Nusselt number in the proposed model can be looked at as correction factors which depend on the point values of the state variables. The axial mean temperature profiles computed by both models are shown in Figure 6.2. For a high axial peclet number Pe_a = 900.0, where the effect of axial mixing is small, the profiles are compared with those based on the radial diffusion model (i.e. Pe $=\infty$)solved in Chapter Three. It can be seen that the proposed model gives a more accurate representation. The large discrepancy of the profiles based on the parabolic representation is mainly because of the values of the parameters used here since rather large radial temperature gradients are formed. The axial temperature at r = 0 is about 30% more than that at the wall of the reactor at the hot spot. These steep gradients are usually poorly approximated by a parabola. When such large errors arise it makes the addition of the axial diffusion terms meaningless. On the other hand, for relatively small differences in the temperature between the reactor wall and axis, the lumped model based on the parabolic approximation may be used. In the case of a radial temperature difference of about 15%, it can be seen in Figure 6.3 that the discrepancy between the profiles of the different models are quite small.

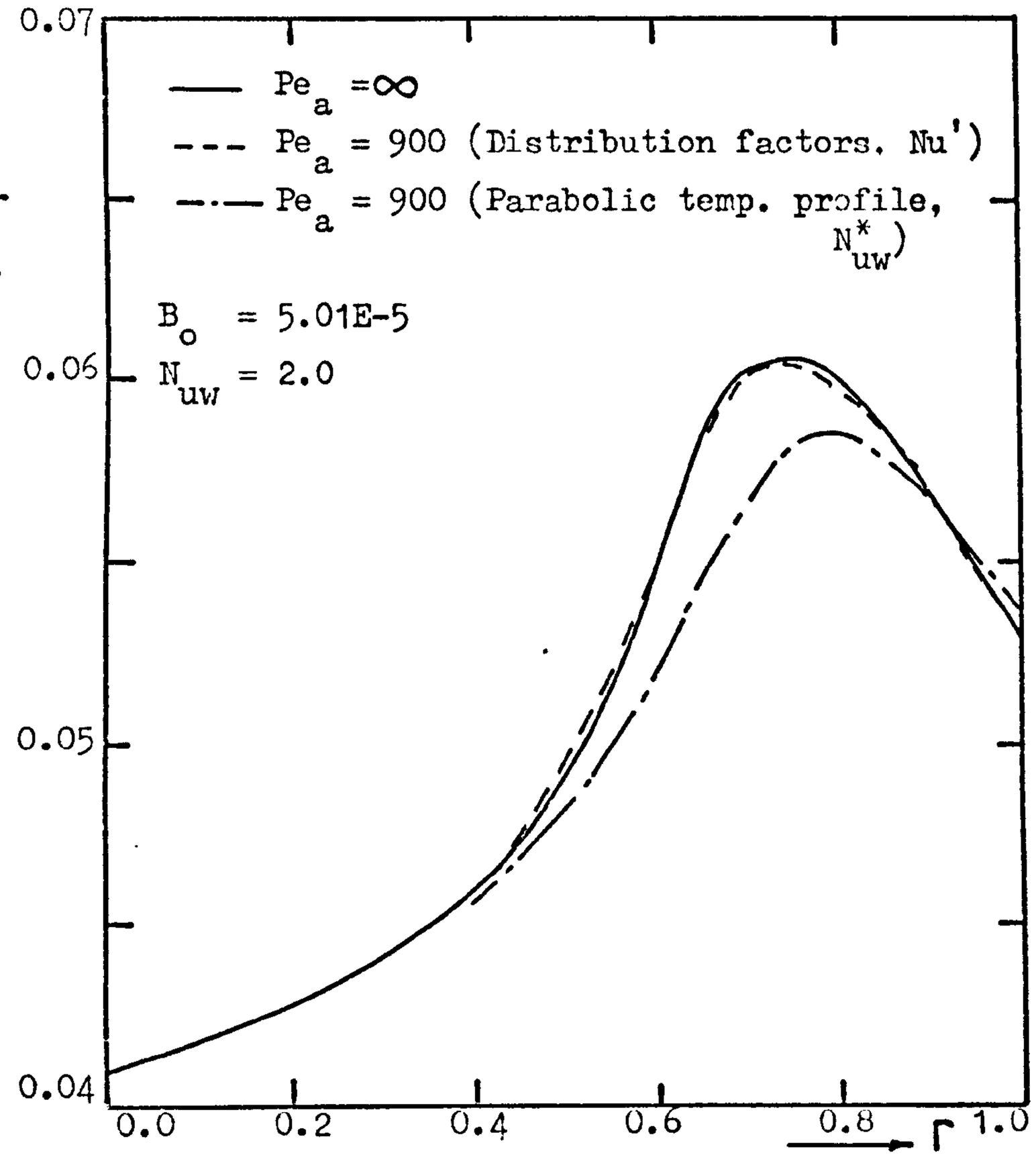

Figure 6.2: Comparison of radial mean temperature profiles predicted by the radial diffusion model and the axial diffusion model with various forms of radial mixing approximations. 30% maximum increase in temperature across tube radius.

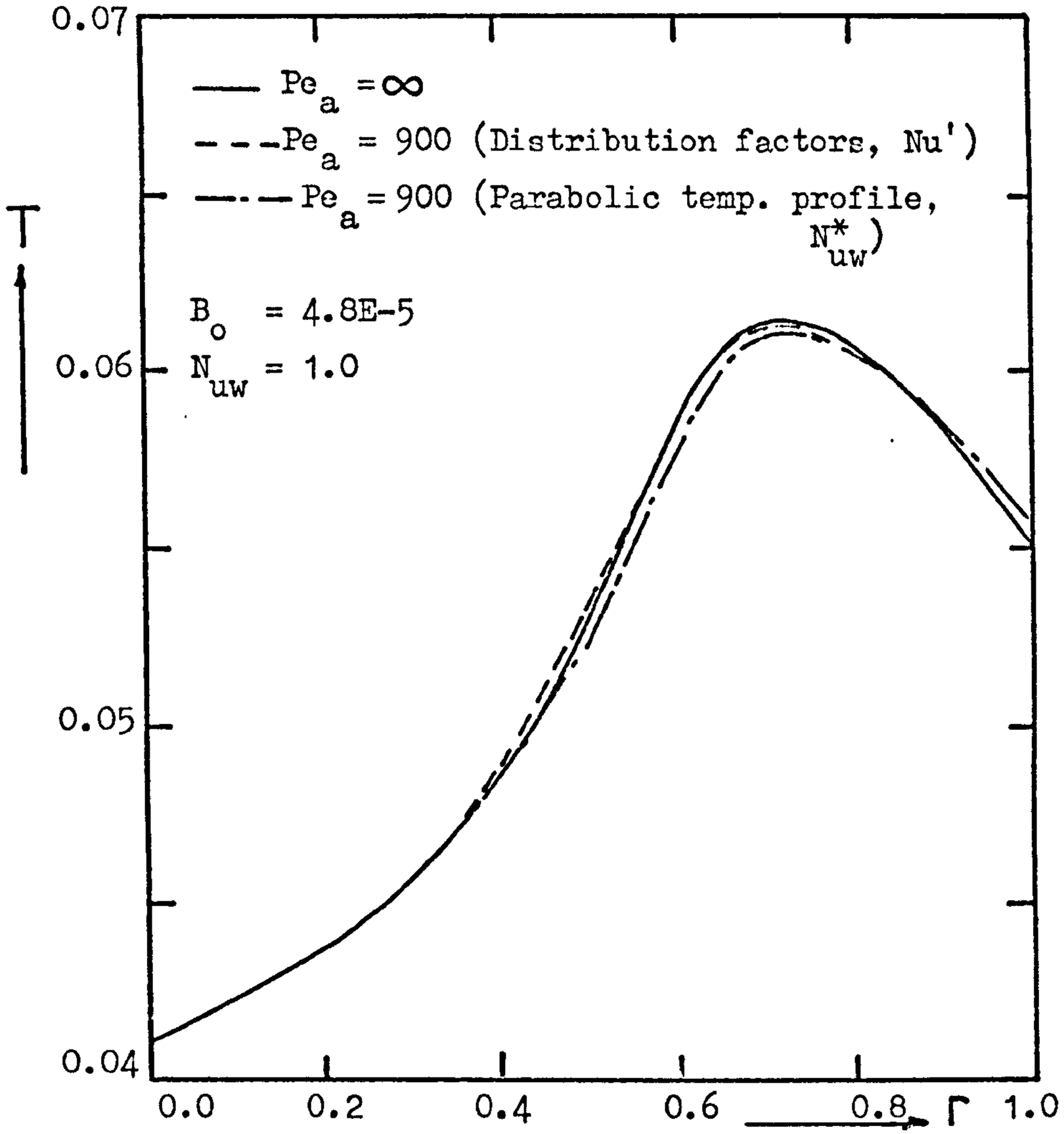

Figure 6.3: Comparison of radial mean temperature profiles predicted by the radial diffusion model and the axial diffusion model with various forms of radial mixing approximations. 15% maximum increase in temperature across tube radius.

Such bounds would restrict the practical advantage of lumped models, especially if used in dynamic simulation, where the radial temperature profiles may increase beyond such limits.

In the above discussion, although the proposed lumped model has been shown to approximate the mean temperature for radial differences of more than 50%, this advantage may be overridden by the increase in computing times, to more than twice the computing time over that based on the parabolic approximation. This is because at each collocation point, the pellet equations must be solved twice to evaluate the distribution factors. It has been shown (see Chapter Four) that the distribution factors may be evaluated by solving the pellet equations once (i.e. the first approximation denoted by D_1) or it may be evaluated from a purely algebraic expression (i.e. the second approximation D_2). While approximations for the distribution factors have proved adequate in the case of the dynamic model, it can also be shown to be valid in the case of the steady state model with axial diffusion. Figure 6.4 shows the axial fluid temperature at r = 0.0 and for Pe_a = 600 for the three cases using the distribution factors with D_1 and D_2. There is hardly any difference between using the distribution factors or their first approximation D_1. In the case of D_2, it is clear that the discrepancies increase as the peak temperature increases. The average computing time for the proposed model compared with that using the first approximation D_1, the second approximation D_2 and the one dimensional model with $Pe_a = \infty$ are of the order 3:2:1.5:1 respectively. In this comparison, 15 collocation points have been used in the axial diffusion model. At this stage, the axial diffusion model with the distribution factors being estimated by the first approximation D_1 is adequate and represents the radial and axial temperature and concentrations with reasonable accuracy over a wide range of parameter values.

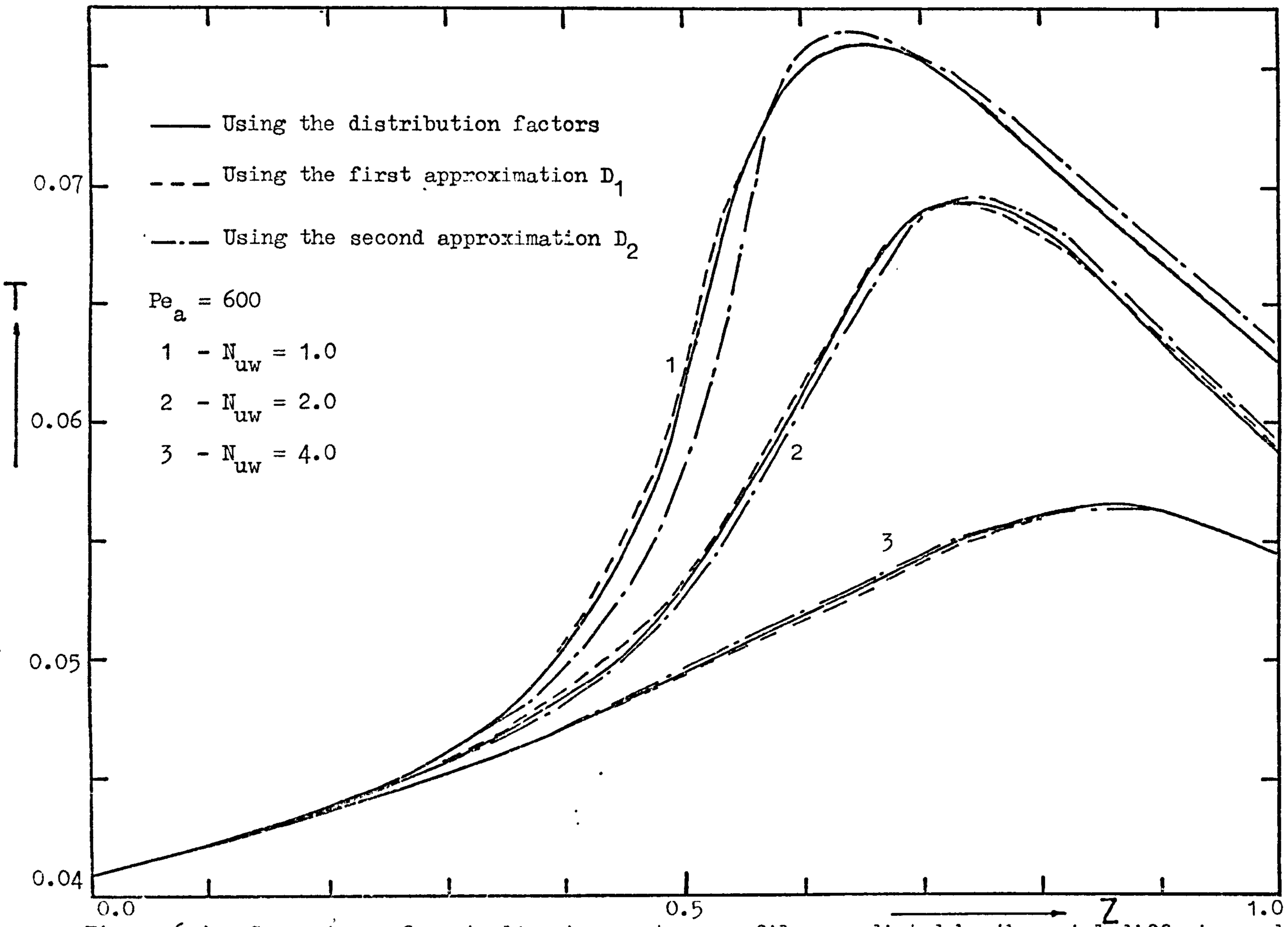

Figure 6.4: Comparison of centreline temperature profiles predicted by the axial diffusion model using various forms of distribution factors. Data as given in Table 3.3.

6.6 Discussion of results

The axial temperature profiles at r = 0.0 for different inlet concentration CA and for an axial peclet numbers Pe_a = 300, 600 and ∞, are shown in Figure 6.5. It is clear that for a given value of Pe_a, as the changes in temperature and concentration increase, the effect of the axial diffusion increases. In particular this is true at places where the axial temperature gradients become steep. When Pe_a = 300, as shown in Figure 6.5, when it is within the allowable practical range used in design, the effect of back diffusion is even more significant. These figures indicate that the magnitudes of temperature and/or concentration changes in the reactor, and particularly the steepness of such changes, has a significant bearing on the axial diffusion. In other words, as the temperature and concentration gradients increase, the effect of axial diffusion becomes more significant, as would be expected from physical considerations.

When axial diffusion is considered, it can affect the temperature and concentration distribution in the bed in two ways:

1. In the inlet region
2. Outside the inlet region.

This kind of classification is arbitrary and not entirely rigid, but is convenient as a basis for discussion of the main effects. Thus, from the boundary conditions at Z = 0.0, $\frac{1}{Pe_a}\frac{dT^*}{dZ} = T^* - T_0$ where T^* is the temperature at $Z = 0^+$ and T_0 is the temperature at $Z = 0^-$. Similar argument can be made for concentrations. It is apparent that for T^* to approach T_0, the temperature gradient at the inlet should approach zero. However if $\frac{1}{Pe_a}\frac{dT^*}{dZ}$ 0, then $T^* = T_0 + \frac{1}{Pe}\frac{dT^*}{dZ}$, and similarly for CA^* and CB^*. These values will be different from the inlet values T_0, CA_0 and CB_0 and thus may affect the heat and mass distribution inside the reactor.

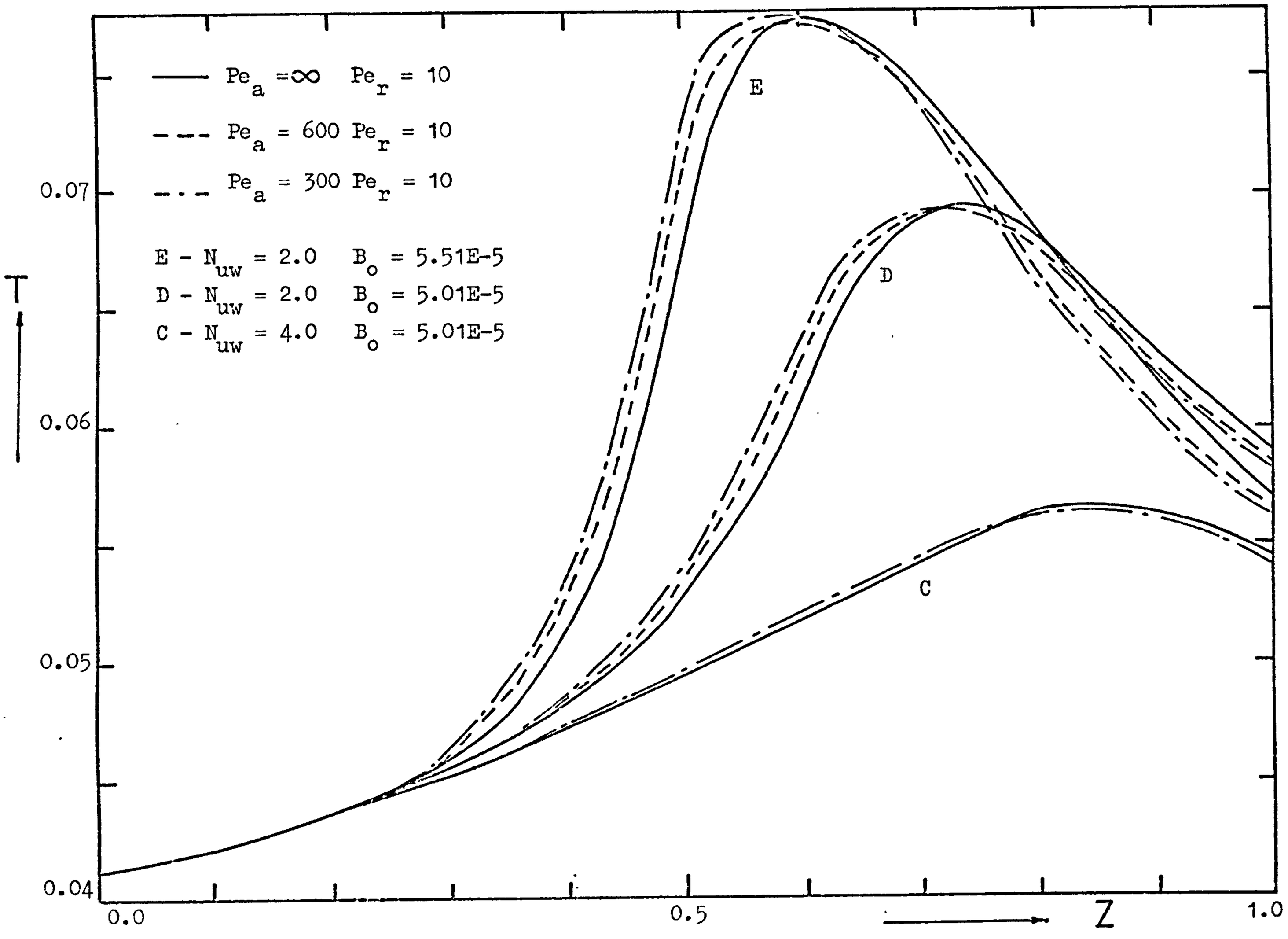

Figure 6.5: The effect of axial dispersion on centreline temperature profiles for different axial temperature gradients. Data as given in Table 3.3.

For non-isothermal reactors (and less than 50 particle diameter[118]), it is to be expected that the peak temperature would induce a gradient near the inlet and thus the effect of the inlet boundary conditions can be significant. Young and Finlayson[120] simulated experimental results for the oxidation of sulphur dioxide in a reactor ($\cong$50 particle diameter), where it would be expected that axial diffusion is negligible. However the peak in temperature occurred at Z = 0.3 and they reported an increase in T^*over T_0 of 15°C for Pe_a = 1.0. As a result, a 20°C decrease in peak temperature was predicted in a total temperature rise of 120°C. This difference is significant and in cases where higher magnitudes and/or gradients occur at the inlet, and could increase. In the case under study, where the reactor length is about 300 particle diameters, no steep gradients take place near the inlet, as shown in Figures 6.5 and 6.6, and T^* is higher than T_0 by only 1.6K. It is obvious that discrepancies in temperature and concentration occur at points other than the inlet region as a result of the axial diffusion. It is possible, based on the absolute values of the state variable gradients, to approximately indicate whether axial diffusion should be included or not. If the axial temperature gradient is approximated by finite differences, i.e. $\left|\frac{dT}{dZ}\right| \cong \left|\frac{\Delta T}{\Delta Z}\right|$, bounds can be established relating to the importance of axial diffusion. In the case under study, based on the $Pe_a = \infty$, if $\left|\frac{\Delta T}{\Delta Z}\right| > 0.08$ (this value is based on the dimensionless groups used), axial diffusion can be a significant effect. From Figure 6.5, the approximate gradients for cases C and D between Z = 0.5 and 0.6 are 0.025 and 0.08 respectively, and for case E between Z = 0.4 and 0.5, it is approximately 0.16. Of course, the above condition may vary according to the values of Pe_a used, but it has been found that for $1 \leqq Pe_a \leqq 2$ (based on pellet diameter), then $0.08 \leqq \left|\frac{\Delta T}{\Delta Z}\right| \leqq 0.09$. Thus, for example, in case D in Figure 6.5, if the reactor is to be terminated at Z = 0.65, which represents a reasonable length to give nearly complete

conversion of species CA, the outlet temperature would be higher in the case of axial diffusion (Pe_a = 1.0), by about 27°K. These discrepancies in temperature can mean longer reactor for the same conversion, if the axial diffusion has not been considered. In cases D and E shown in Figure 6.5, the maximum discrepancies in axial temperature for Pe_a = 300 is between 4 to 5% of that computed for $Pe_a = \infty$. This percentage represents from 25°K to 60°K respectively.

For the complex reaction considered and where the temperature gradients at some point in the reactor can exceed 0.08, it is therefore desirable to include axial diffusion terms in the reactor models, especially when used in optimization or design algorithms. Note that if the gradients occur in the inlet region, lower values than above may be used as a condition. Thus, in the case studied by Young and Finlayson,[120] $\left|\frac{\Delta T}{\Delta Z}\right| \cong 0.035$ for Z between 0.0 and 0.2 (figure 6 in their paper). Also Ranzi and co-workers[130] simulated experimental results for the catalytic oxidation of methyl alcohol in a tube length of 200 particle diameters and found that including the axial diffusion in their model fitted their results much more satisfactorily. Their peak temperature occurred at Z = 0.16 with $\left|\frac{\Delta T}{\Delta Z}\right| \cong 0.055$ (figure 2 in their paper) and it was lower by about 50°K than that calculated ignoring axial diffusion.

Although the condition put forward depends on the state variable gradients is not rigorous, it does give an indication as to whether the axial diffusion should be included. How much the magnitude of the resulting discrepancies will have any significance will obviously depend on the individual case under study, and in particular on the dependancy of the kinetic rates on temperature and concentration. Certainly the criterion put forward by Carberry and Wendel[118] is necessary but not a sufficient condition for ignoring the effects of axial diffusion.

From Figure 6.5 for case E, it can be observed that not only does the

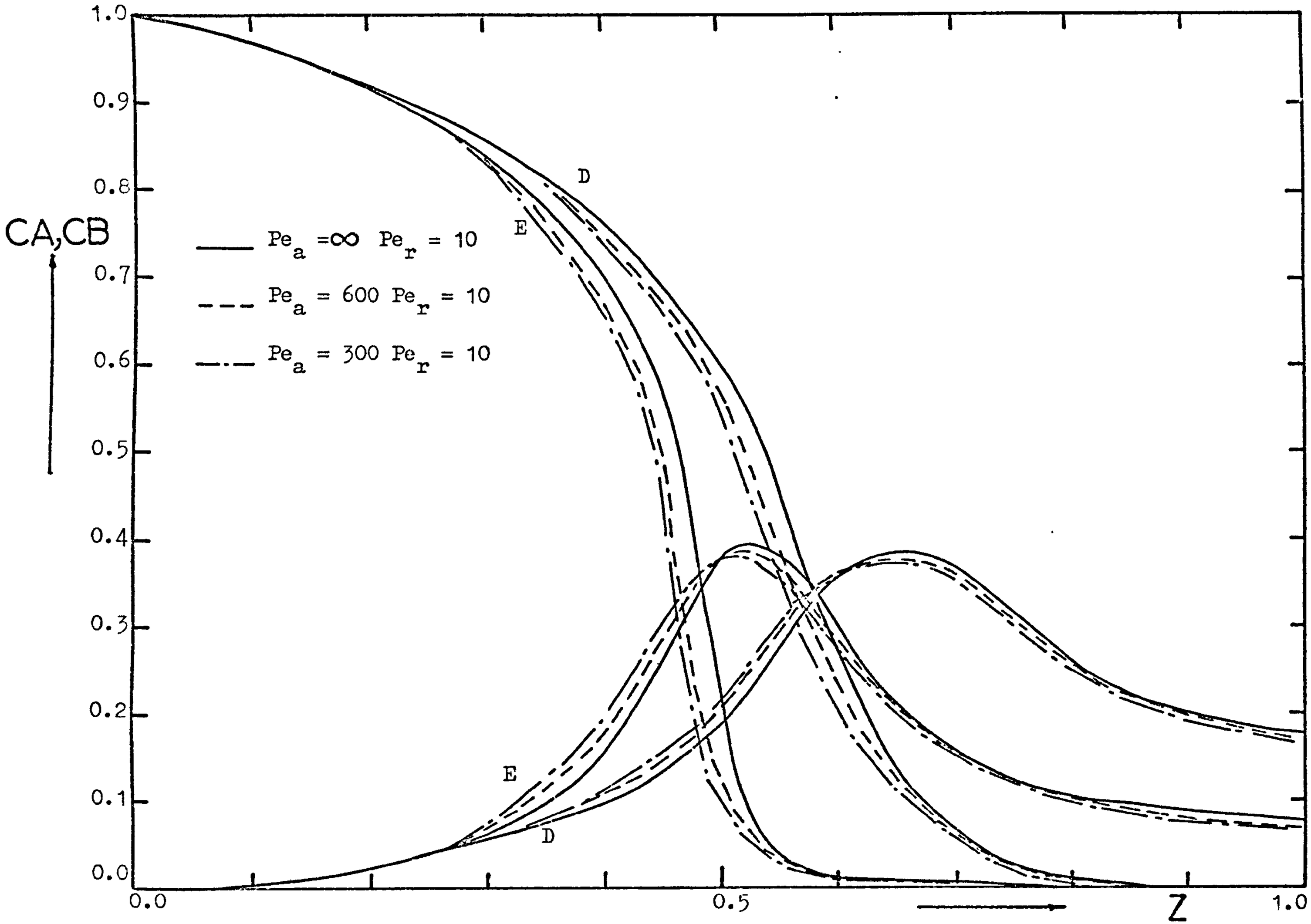

Figure 6.6: Axial concentration profiles corresponding to cases D and E in Figure 6.5.

peak in temperature move nearer to the reactor inlet, but it flattens and in the case of Pe_a = 300 the temperature peak is actually higher than for $Pe_a = \infty$ (see figure 8.7 also). This behaviour may be explained by the complex nature of the reaction. Examining Figure 6.6 shows the corresponding axial concentration profiles for species CA and CB for Pe_a = 300. Due to the axial diffusion, higher temperature levels may be encountered at higher concentrations in the earlier parts of the bed with a resulting increase in rate of reaction. For highly temperature sensitive reactions such small increases may have a considerable effect. In addition, the product CB diffuses to regions of still higher temperature and thus generates an additional amount of heat. Although such amounts of heat may be small, it promotes consumption of the more sensitive temperature species CA. This behaviour would result in not only flatter temperature peaks, but in certain cases higher peaks than expected are forced even for the case of the simple reaction A ⟶ B.

Therefore, in formulating any criteria for bounds of runaway or multiplicity, and where the axial gradients of temperature are usually large, the changes occurring in the axial profiles due to axial dispersion should be considered.

Since axial dispersion of heat increases as the temperature gradient in the reactor increases, it would be expected that in the case of a steep radial temperature profile, the axial diffusion should be maximum at the reactor axis and decrease to a minimum near the wall. In effect, the axial dispersion causes not only flatter axial profiles but also flatter radial profiles. Figure 6.7 shows the radial temperature profiles (corresponding to the case E in Figure 6.5), at different axial positions for Pe_a = 300 and ∞ . For both cases the radial peclet number, Pe_r = 10, for heat and mass. Although in some parts of the bed the axial temperature at r = 0.0 is higher than that at the case of $Pe_a = \infty$, e.g. Z = 0.5, the interaction of both axial and radial diffusion transport results

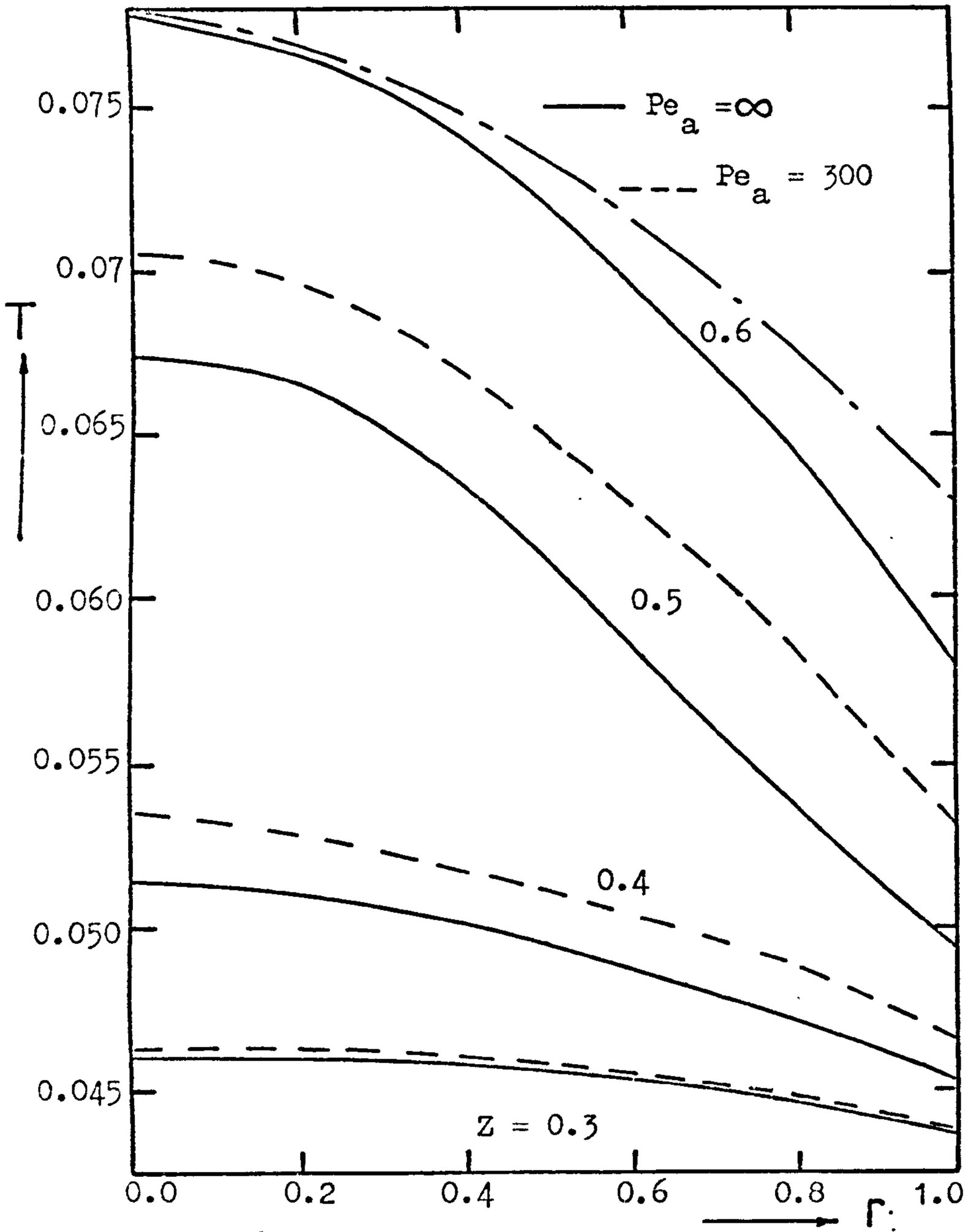

Figure 6.7: Radial temperature profiles corresponding to case E in Figure 6.5.

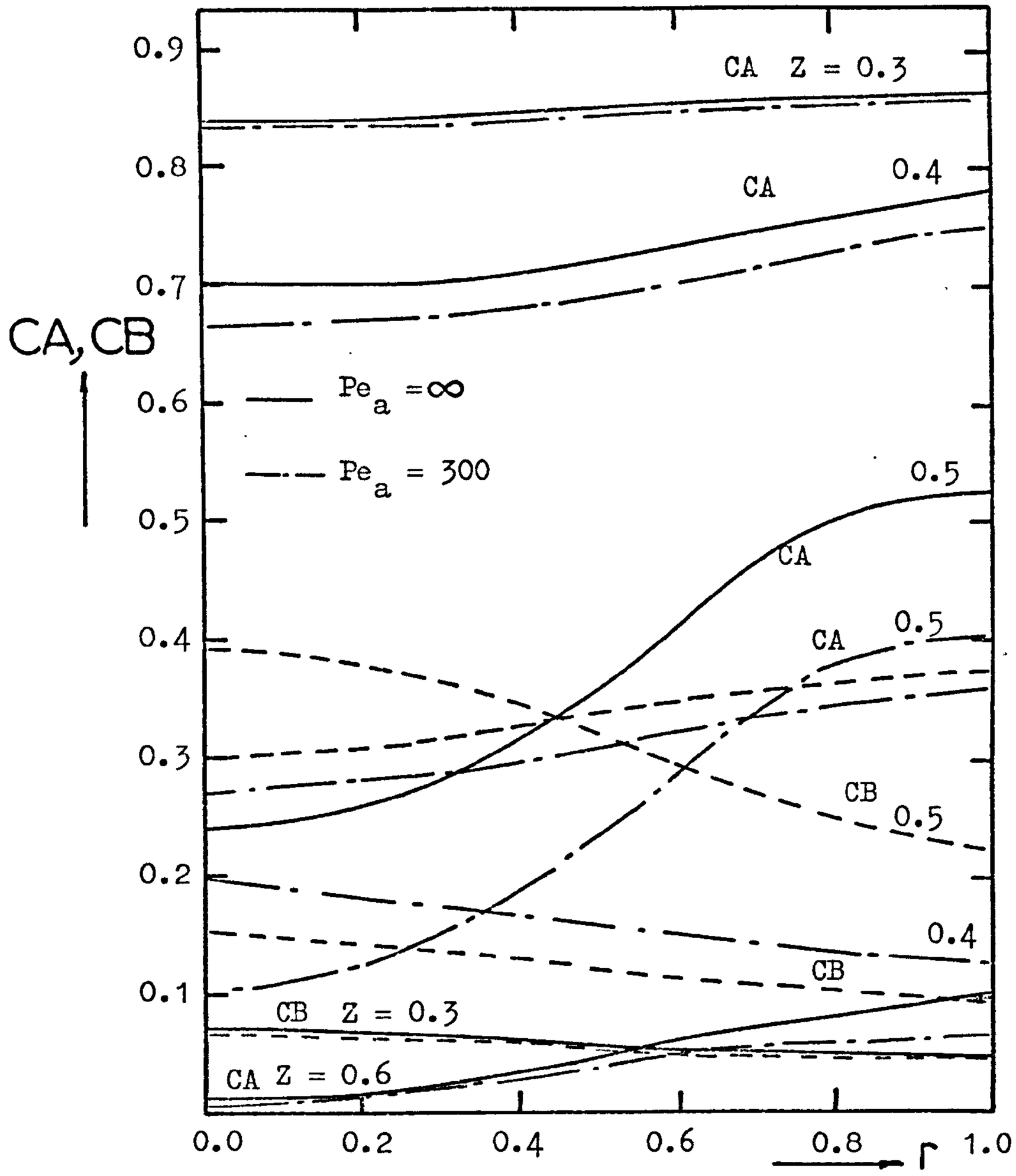

Figure 6.8: Radial concentration profiles corresponding to case E in Figure 6.5.

in higher temperature levels everywhere at that radial position. At Z = 0.6, where the radial temperature gradient in the case of $Pe_a = \infty$ is severe, the effect of both transport mechanisms is evident, resulting in flatter profiles than for Pe_a = 300. The corresponding radial profiles for the species CA and CB can be seen from Figure 6.8. The effect of axial diffusion of mass on the radial concentration profiles is not as apparent as in the case of radial temperature profiles. This is due to the fact that for the exothermic reaction discussed here, the axial diffusion of heat overshadows the effect of mass diffusion, with a resulting increase in the rate of reaction.

Although it is of importance to study the transport of heat and mass mechanisms in the reactor bed, such quantities as the axial peclet numbers for heat and mass, the argument as to whether these physical phenomena should be considered or not rests to a great extent on their interaction with the kinetic rates and their dependency on temperature and concentration. In other words, the importance of such physical quantities affecting the distribution of heat and mass in thereactor should be evaluated through their effect on the kinetic rates of the reaction under consideration. For reactants having high activation energies and heats of reaction, the reactions are usually sensitive to temperature and reaction order. This complex interaction between the physical and chemical parameters obviously renders any criterionput forward which does not take into consideration such interaction, unreliable.

The gradient of state variables can be computed by simpler models which give an indication as to whether the axial dispersion should be considered and if not what deviation from the true state variable values may be expected.

6.7 Conclusions

An axial diffusion model in which a parabolic radial temperature distribution is assumed has been solved by the collocation method. From 11 to 19 collocation points were used, depending on the case under study. It has been indicated that when using 15 points, about a 30% increase in computation time is required compared with that of the plug flow model without axial diffusion. Legendre polynomials are shown to converge faster than Chebyschef polynomials and is better suited to integrate these unsymmetrical boundary value problems.

For more than 15% increase in temperature across the reactor tube radius, the model may give inaccurate representation of axial profiles due to the deviation of the radial temperature profile from the assumed parabolic distribution.

A model has been proposed which treats the limitations imposed by the radial temperature parabolic assumption and represents the axial and radial profiles with reasonable accuracy. The solution of this model, using 15 collocation points, takes twice the computational time required by the corresponding plug flow model without axial diffusion.

It has been shown that the effect of the axial diffusion of heat and mass on the axial temperature and concentration profiles becomes increasingly significant as the gradients increase. If the axial temperature gradient, computed by the plug flow model without axial diffusion, increases beyond 0.08 (this value is based on the dimensionless quantities used in this study), the axial dispersion may have a significant effect and should be included in a reactor model. In some cases, the axial diffusion when included in a model may result in a flatter radial profile. This effect becomes significant for radial profiles of about 30% or more increase in temperature across the tube radius.

CHAPTER 7

DYNAMIC MODEL INCLUDING AXIAL AND RADIAL DIFFUSION

7.1 Introduction

It has been demonstrated that if the axial and radial diffusion of heat and mass are included in a reactor model, the resulting system of equations is very difficult to solve in the steady state. If the transient case is considered, the system becomes even more complex, and may become intractable. As a result this has encouraged the adoption of some simplifying assumptions for engineering design or verification purposes. Neglecting either radial or axial dispersion or both has been common practice in most of the work done in this field. The validity of some of these simplifications is justified by the satisfaction of some semi-quantitative criteria or sometimes merely on intuitive grounds. But when the discriminatory criteria are not satisfied, it is desirable to examine a more exhaustive description by treating the complete problem (i.e. including both radial and axial transport of heat and mass).

Most of the work reported has been concerned with quasi-homogeneous reactors with axial diffusion and arose from consideration of stability and parametric sensitivity.[92,93,161,163,166] Liu and Amundson[125] developed an adiabatic reactor with axial diffusion and concluded that in the multiple state region, the temperature and concentration profiles were more sensitive to axial diffusion than in the case of a single steady state. They solved it with an implicit finite difference representation and reported a computation time of about 2 hours for a transient run (using Control Data 1604 computer). Although linearization of the system reduces the computing time,[127] it is still too long for practical use and it has already been shown that orthogonal collocation is a feasible and

efficient method of solution for such problems.

Attempts to solve the comprehensive model (i.e. including axial and radial diffusion) have been made by Feick and Quon.[62] They employed a modified alternating direction explicit method. However, the computing time reported was excessive and no detailed studies were reported.

All the models discussed above are a continuum representation, where once the mathematical model is formulated, the equations no longer reflect the idea that there are discrete particles in the bed. In contrast Deans and Lapidus[66] and later McGaire and Lapidus[60] utilized a model which describes the bed by an array of two dimensional mixing cells. Again the computing time is quite long and no detailed studies have been reported.

It seems that very limited studies have been carried out for the transient nonisothermal case and this may be construed as acceptance of the criteria found in literature on the corresponding steady state studies. However, it was indicated in the last chapter that these criteria do not necessarily apply and that the importance of the axial diffusion increases as the state variable gradients increase, a situation frequently existing in transient studies where the gradients can vary appreciably in magnitude over a period of time.

In this chapter a comprehensive model will be proposed based on the conclusions of the last chapter which takes into consideration the axial and radial dispersion of heat and mass, as well as inter- and intra-particle transport limitations. It will be shown that in spite of the fact that the reactor model includes such detail, the computing time is reduced to a reasonable level, such that it can be used in detailed simulation studies. The importance of axial diffusion in dynamic operation will also be discussed.

7.2 Formulation of equations and solution

Based on the proposed model given by equations (6.11 to 6.15), the transient equations describing the heat and mass balances on a differential element of the reactor can be conveniently written in dimensionless form as follows:

$$G_5' \frac{\partial CA_m}{\partial \tilde{t}} = \frac{1}{Pe_{Ma}} \frac{\partial^2 CA_m}{\partial Z^2} - \frac{\partial CA_m}{\partial Z} - \frac{D_{CA}}{G_1} \left(\zeta (\phi_1^{*2} k_1(m) + \phi_3^{*2} k_3(m)) CA \right)_m \quad (7.1)$$

$$G_5' \frac{\partial CB_m}{\partial \tilde{t}} = \frac{1}{Pe_{Ma}} \frac{\partial^2 CB_m}{\partial Z^2} - \frac{\partial CB_m}{\partial Z} + \frac{D_{CB}}{G_1} \left(\zeta_4 (\phi_1^{*2} k_1(m) + \phi_3^{*2} k_3(m)) CA \right)_m \quad (7.2)$$

$$G_6' \frac{\partial T_m}{\partial \tilde{t}} = \frac{1}{Pe_{Ha}} \frac{\partial^2 T_m}{\partial Z^2} - \frac{\partial T_m}{\partial Z} - \frac{2Nu'}{G_3}(T_m - 1) + D_T G_4 (Tp - T)_m \quad (7.3)$$

The boundary conditions are:

$$\frac{1}{Pe_{Ma}} \frac{\partial CA_m}{\partial Z} = (CA_m - CA_{Om})$$

$$\frac{1}{Pe_{Ma}} \frac{\partial CB_m}{\partial Z} = (CB_m - CB_{Om}) \qquad \text{at } Z = 0 \text{ and } \tilde{t} \geqq 0 \quad (7.4)$$

$$\frac{1}{Pe_{Ha}} \frac{\partial T_m}{\partial Z} = (T_m - T_{Om})$$

$$\frac{\partial CA_m}{\partial Z} = \frac{\partial CB_m}{\partial Z} = \frac{\partial T_m}{\partial Z} = 0 \qquad \text{at } Z = 1.0 \text{ and } \tilde{t} \geqq 0 \quad (7.5)$$

The initial conditions being

$CA_{Om} = CA_{Om}(\tilde{t}, Z)$, $CB_{Om} = CB_{Om}(\tilde{t}, Z)$, $T_{Om} = T_{om}(\tilde{t}, Z)$ at $Z = 0.0$ and $\tilde{t} \geqq 0$

The additional dimensional groups introduced are

$$G_5' = \frac{L}{u} \text{ sec.} \qquad G_6' = \frac{L}{u} \text{ sec.}$$

All the quantities subscripted by m are mean values. The distribution factors (i.e. D_T, D_{CA} and D_{CB}) and the modified Nusselt number (Nu') have the same general form given in Chapter Four.

The above system can be further simplified if the fluid capacitance to absorb heat and mass is considered small compared with that of the solid. This simplification has been shown to be reasonable in Chapter Four and also in other cases reported.[46,109] In this case the fluid temperature and concentrations may be considered at a pseudo-steady state, i.e. the time derivatives in the above system may be neglected in comparison with the other terms. The dynamic response therefore comes from the equations describing the heat and mass transport in the catalyst pellet, given in Appendix (A1.2.2). They may be solved simultaneously with the above pseudo-steady state system. The collocation method may be used to solve the system as shown in Chapter Six and the pellet equations solved with Runge-Kutta-Merson to provide Tp, ζ and γ at the collocation points, necessary to evaluate the distribution factors and the mean state variables. For the purpose of the algorithm, it is necessary to be able to specify values of state variables at points other than the start and finish at any given time step. This is done by assuming that the changes in fluid conditions are linear over one time step and that the pellet is effectively subjected to a ramp change in fluid conditions. For solving the above system with reasonable accuracy, from 13 to 19 collocations points are needed, depending on the system parameters and initial conditions used. Time steps from 0.5 to 1 second are adequate for representing the changes taking place in the cases studied here, and from 1 to 2 iterations per time step are sufficient for the solution to converge.

7.2.1 Remarks on solution method

In the following computations, the distribution factors have been evaluated using the first approximation D_1, as discussed in Chapter Six. Preliminary computed results of the above model with Pe_a = 1200.0 ($\cong$ 4 when based on pellet diameter) have been compared with the radial diffusion model results shown in Chapter Four. This comparison is necessary to identify the limits of accuracy and polynomial order which are required to approximate the transient changes taking place at the inlet. The following observations may be drawn:-

1. Following a step decrease in dimensionless temperature of 0.0008 (equivalent to 13K), similar to that shown in Figure 4.2, 16 collocation points, using Legendre polynomials, are required to give an average of 3 to 4 decimal figures accuracy, for a time step of 1 second.

Generally a step change is a severe test and may require higher order polynomials to approximate such changes, especially near the inlet region to ensure that the cumulative errors from successive time steps may be kept to a minimum. These conditions are partially met by the properties of the Legendre polynomials.

2. Following a ramp increase in inlet concentration (0.2 in 20 seconds), similar to that shown in Figure 4.8, with a time step of 1 second, an accuracy similar to above can be obtained by 15 collocation points using Legendre polynomials. It may be expected that fewer collocation points may be required to approximate a ramp change.

3. For profiles such as those shown in Figure 7.1 where the state variable profiles are reasonably well-behaved, from 13 to 14 collocation points can be used to describe a ramp or step change of the above magnitudes.

It should be noted that in cases where the peak in temperature is at or near the inlet region, it may be necessary to use higher order polynomials than stated above or a smaller time step.

7.3 Discussion of Results

Since the comprehensive model proposed above includes axial diffusion, it is necessary to examine its effects on the reactor performance. Such a study should provide a basis for evaluating the significance of including the axial diffusion in the transient state. This information would be necessary when deciding on a model for implementing a control strategy, particularly when the states are near to the maximum limits of temperature allowed, to avoid problems of reactor stability or temperature runaway.

Table 3.3 gives the values of the parameters used in the simulation.

Figure 7.1 shows the axial temperature profiles at different times for a ramp increase in inlet concentration. Although the initial steady state profiles for Pe_a = 300 and ∞ indicate that axial diffusion has an insignificant effect, it can be seen that as the gradient of axial temperature increases, the discrepancies between the profiles increase. In the transient response, these differences would then vary according to the instantaneous value of gradients. For example, at τ = 0.0, 40, 60, and 140, the temperature at Z = 1.0 is lower in the case of Pe_a = 300 by about 0.5, 10, 11 and 25K respectively. These discrepancies are not the same in magnitude over the whole of the transient response. Closer examination indicates that for Pe_a = 300, the final steady state is essentially reached at τ = 136 seconds, while for $Pe_a = \infty$, it takes 140 seconds. Although this time difference is small in comparison to the total transient period, a decrease of 2.9% based on the case $Pe_a = \infty$, it shows that including the axial diffusion in the reactor model may alter the response time. This action may be explained by the nature of axial diffusion, since it is the movement of the fluid temperature upstream and thus would tend to dispense more heat to the catalyst with a resulting increase in reaction rate. Since the major dynamic factor affecting the reactor response is the solid heat capacity and its ratio to that of the fluid,

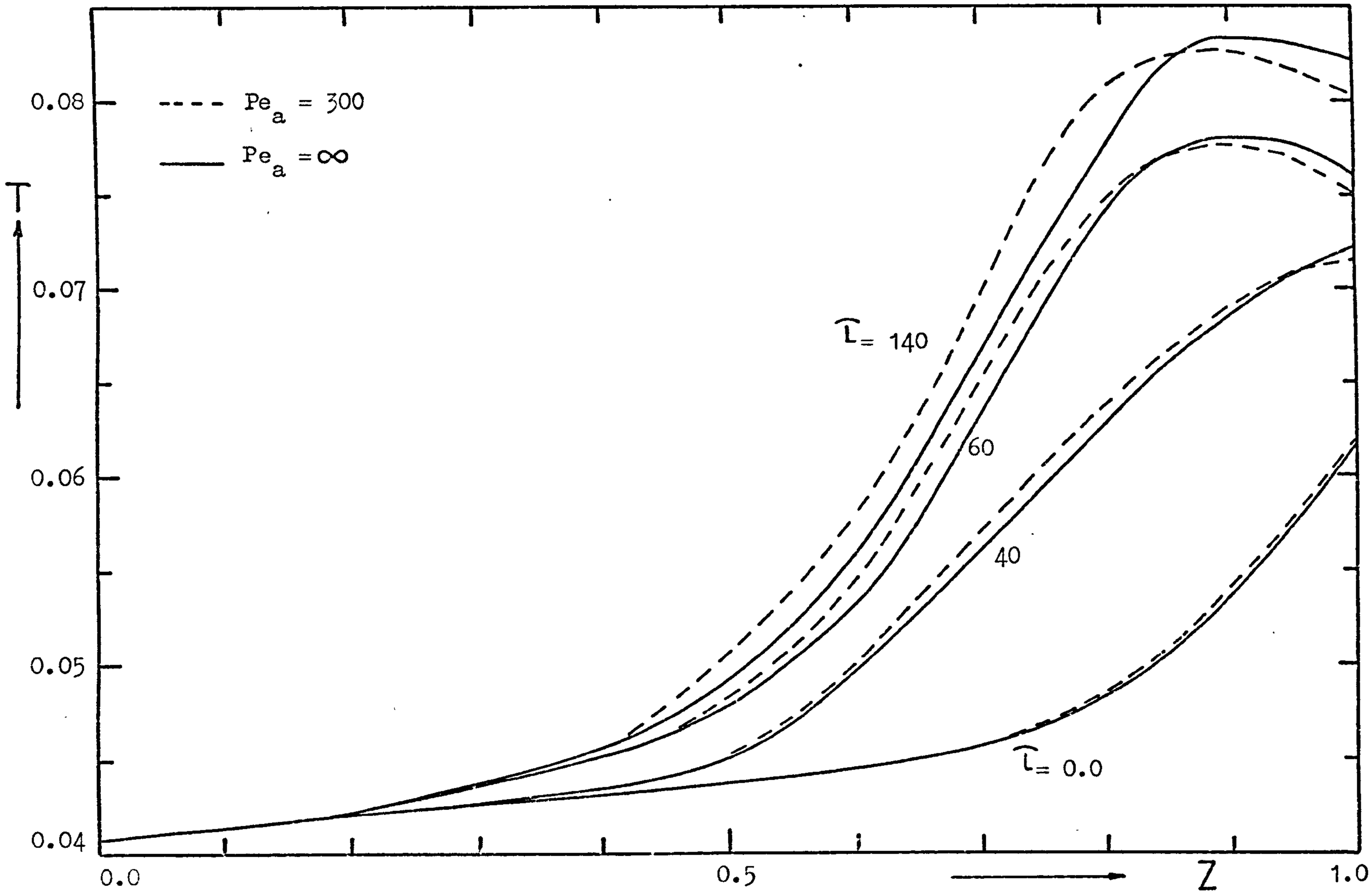

Figure 7.1: The effect of axial dispersion on centreline temperature profiles following a ramp increase in inlet concentration CA of 0.02 per second for a period of 10 seconds. Data as given in Table 3.3. (L = 74.4 cms ≃ 179 DP).

it may be expected that if this ratio increases, the effect of axial diffusion in the fluid would have less effect on the response time. Thus, increasing the solid heat capacity from 1.5 in the case studied above to 3, the final steady state is reached after 360 seconds for $Pe_a = \infty$, while for $Pe_a = 300$, $\tau = 351$ seconds, i.e. decrease of about 2.5%.

The above observations indicate that for the transient changes in inlet concentration where the final steady states have higher magnitudes of change, i.e. steeper gradients, including the axial diffusion would result in accelerating the dynamic response. This enhancement increases as the gradients increase. The fractional time difference depends on the ratio between solid to fluid heat capacities, and increases as the ratio decreases.

Similar observations would be expected for a ramp increase in inlet temperature. The redistribution of heat and mass in the reactor space as a result of the axial diffusion can be categorized into the form of discrepancies in response time and differences in axial temperature and concentration values for specific position and time in the bed.

In practical terms, however, these discrepancies stated above have no significant effects on the general response of the reactor. This is especially true if the uncertainties associated with reactor parameter estimation are taken into consideration. On the other hand, precisely because of these uncertainties, parametric sensitivity studies are carried out so that the discrepancies between the experimental and computed state variables can be considered in establishing a safe limit for reactor operation. This last point should become more apparent in the following paragraphs in reference to the following example. Figure 7.2 shows the axial temperature profiles at different times for a step decrease in inlet temperature with $Pe_a = 300$ and ∞.

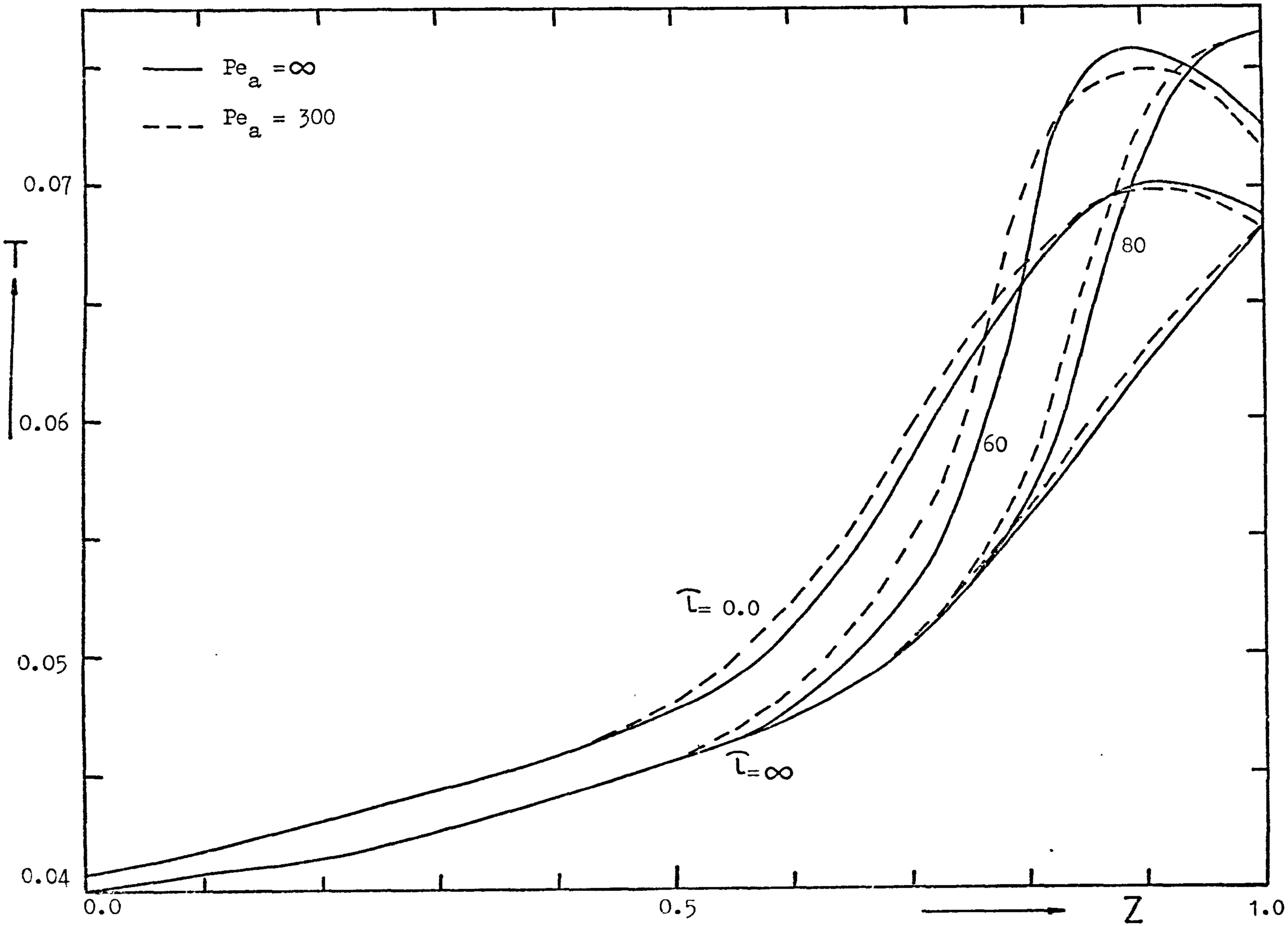

Figure 7.2: The effect of axial dispersion on centreline temperature profiles following a step decrease of 0.0008 in dimensionless inlet temperature. L = 99 cms. ≃ 232 DP, other data as given in Table 3.3.

It can be observed that, although the initial and final steady states the effect of the axial diffusion is small, it is more apparent at $\tilde{t}$ = 60 and 80 seconds. This is because the gradients of temperature and concentration are steeper in the latter cases. In contrast to the steady state problem, where the importance of the axial diffusion can be estimated from the state variable gradients alone, in the dynamic response the duration where the gradient condition is satisfied may be of importance. In the case shown in Figure 7.2, it can be seen that the gradients indicate that the axial diffusion is significant between $\tilde{t}$ = 40 and 90 seconds. This is about 33% in a total time for the transient of 150 seconds. The axial temperature values computed for the case $Pe_a = \infty$ during the above period are up to 6% different from those for case $Pe_a = 300$. Also the maximum gradient is approximately 0.14 (based on the dimensionless quantities used). This gradient is equivalent to about 220K temperature rise over a 10% of the reactor length of 99 cm.

As stated before, the effect of axial diffusion on the transient response of the reactor is, in general, insignificant. This is true if only certain factors are taken into consideration, in particular if the reactor response is studied in the safe limits of the allowed maximum temperature. In this case, the response of the reactor simulated with a model without axial diffusion will be in error by less than 6% (i.e. about 80K) of the computed axial temperature values provided that the maximum temperature gradients do not exceed a value of 0.14. Therefore, if this percentage difference in temperature can be considered to be inside the safe limits, then the effect of axial diffusion may be neglected.

However, the effects of the axial dispersion may become of significance if the interest is to study the maximum temperature at which the reactor

can operate without the dangers of temperature runaway, or other undesirable effects associated with parametric sensitivity. In this case, the axial diffusion should be taken into consideration, since a variation much smaller than the indicated percentage of uncertainty stated above may cause temperature runaway. This may be particularly important if the reactor is to be controlled by a feed back mechanism where the discrepancies observed may result in over- or under-estimation of the response and lead to unsuitable control action. For example in the schematic diagram shown in Figure 7.3, the temperature at C for the case $Pe_a = \infty$ is lower than that at D for $Pe_a = 300$. If a high concentration wave arrived at that position, temperature runaway may take place at D, but not at C if a suitable action is taken.

In a parallel research project, Adderley[109] has shown that for the simple reaction A⟶B without axial diffusion, it is possible to indicate regions where temperature runaway can take place. On a phase diagram as shown in Figure 7.4, the region of non-unique solutions in the catalyst pellet is drawn for a given system. It is then possible to plot the longitudinal trajectories of the reactor on the same chart, if any trajectory passes through the multiple solution region the reactor will tend to have multiple solutions at some point. Near the cusp of the non-unique region a high parametrically sensitive region exists at which temperature runaway may result. This region is represented on the phase diagram by the broken line. Reactor trajectories which cross this line are in the runaway region and therefore potentially unstable and those below it are in the safe region.

Cases C and D above can be represented on that diagram and it is clear that axial diffusion can result in temperature runaway. It is also possible, as a result of the axial diffusion, to have a temperature runaway or multiple states at an early stage of the transient response. For example

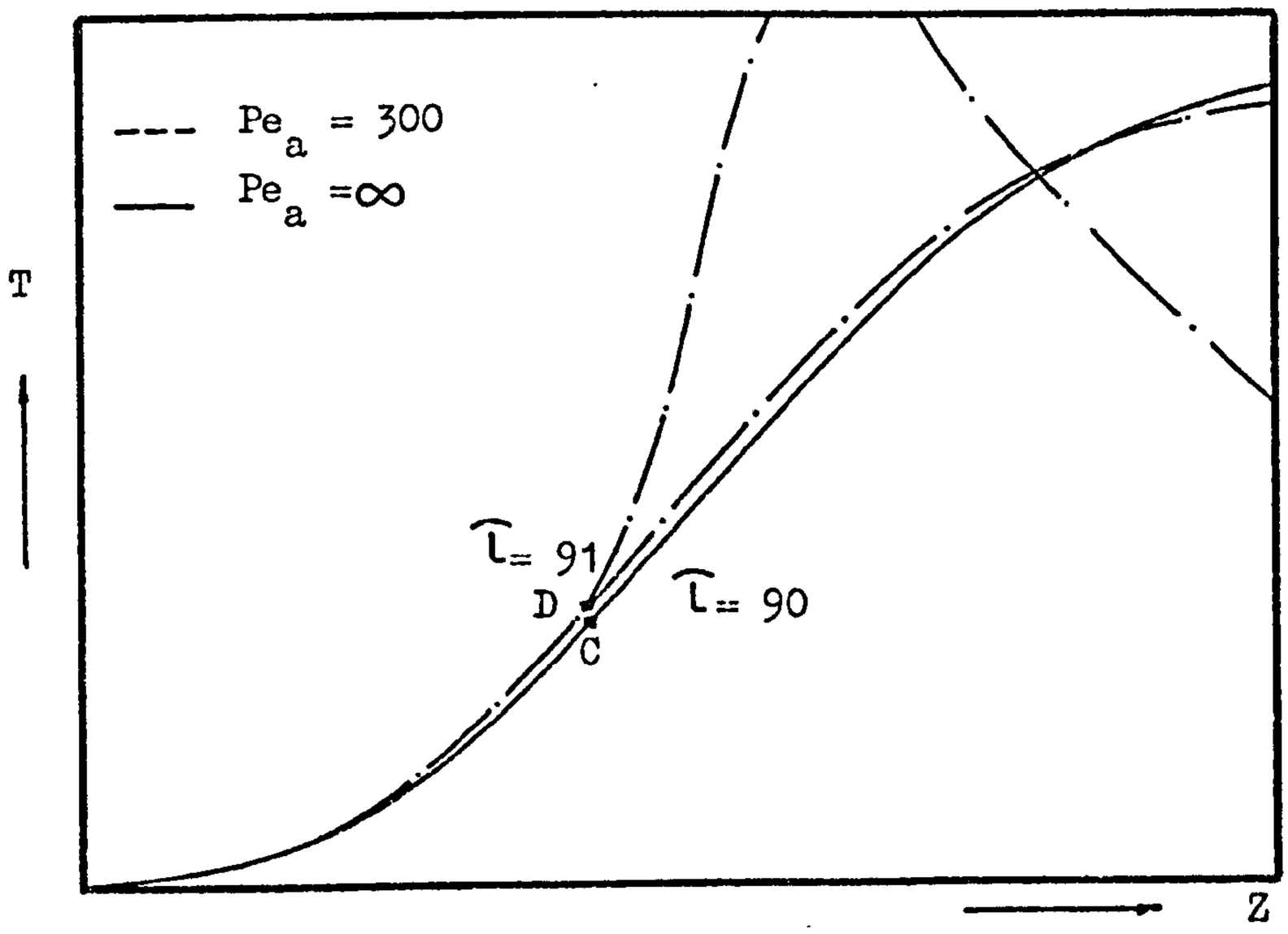

Figure 7.3: Schematic diagram showing effect of axial dispersion on temperature profiles in region of parametric sensitivity.

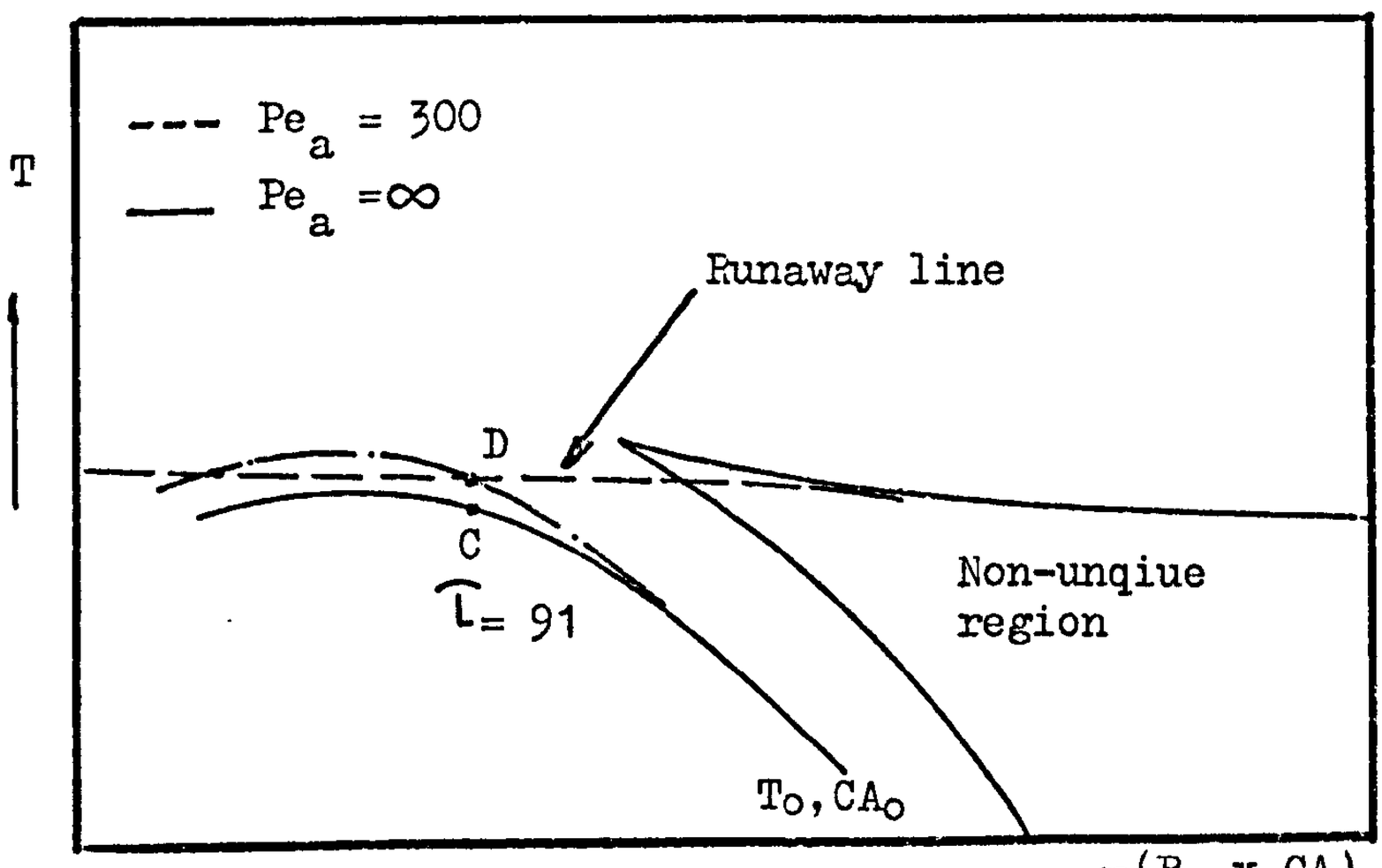

Figure 7.4: The reactor trajectories corresponding to figure 7.3 on T vs (B_o x CA) phase diagram.

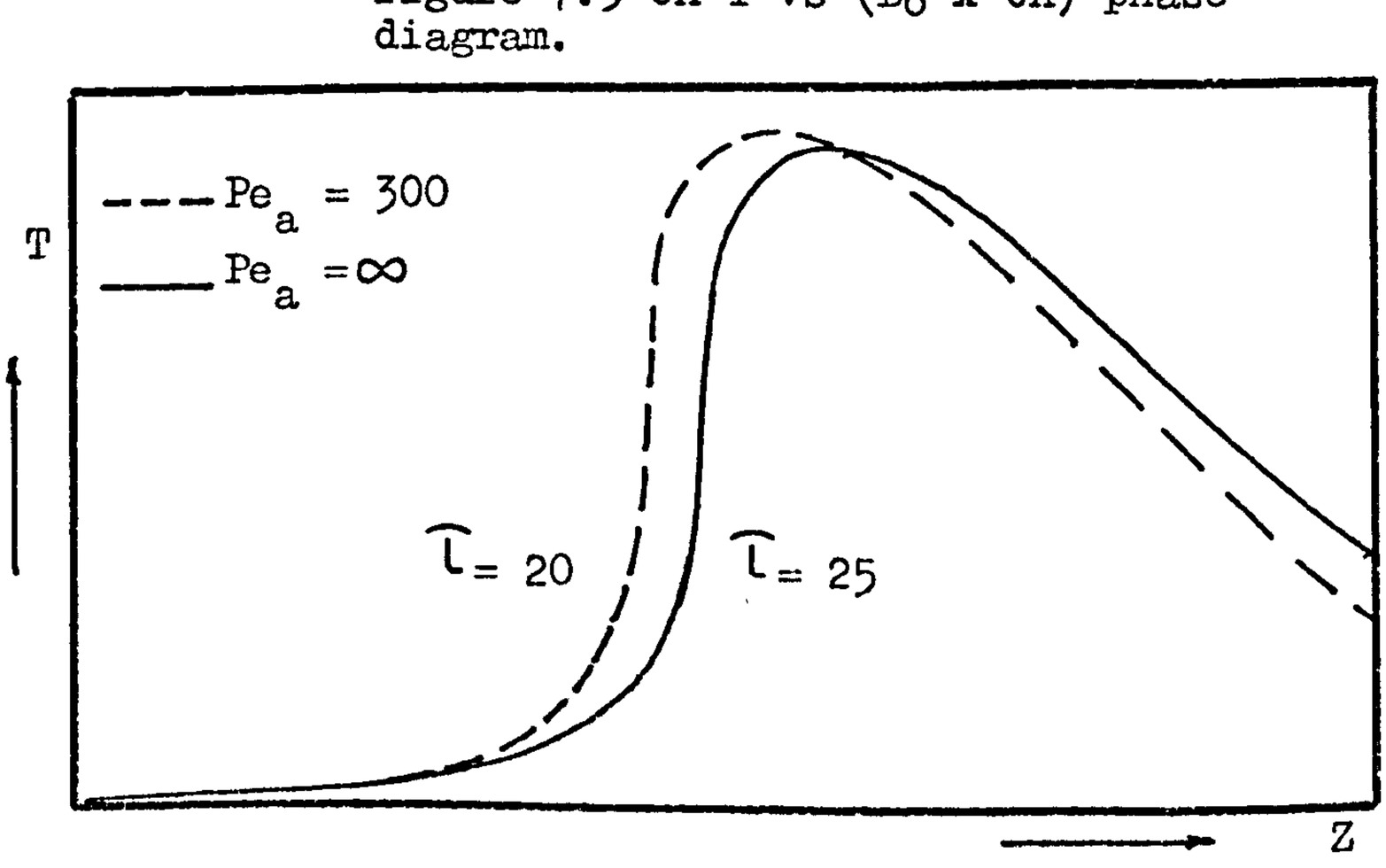

Figure 7.5: Schematic diagram showing the effect of axial dispersion in causing temperature runaway early in transient response.

as shown on Figure 7.5, in the case of $Pe_a = 300$, runaway can occur at $\tau = 20$ seconds, while in the case of $Pe_a = \infty$, it takes place at $\tau = 25$ seconds. Similar cases have been shown by Liu and Amundson[125], based on steady state studies of adiabatic reactors (for temperature gradients $\ggg 0.14$). They indicated that as Pe_a is decreased multiplicity occurs nearer the reactor inlet.

The conditions under which temperature runaway or multiplicity of states can take place is being studied in parallel research[109], and it is the intention here to show that axial diffusion warrants further consideration in these cases or in formulating general criteria for the onset of undesirable behaviour.

7.4 Conclusions

A comprehensive dynamic model, which takes into consideration the axial and radial dispersion mechanisms is proposed. Lumping the radial dispersion by applying the model reduction technique and solving the resulting system by the collocation method has been shown to be efficient in describing the transient response. The computing time for solving such a model has been reduced to acceptable levels, comparable with corresponding models without axial diffusion.

It has been demonstrated that, in general, the inclusion of axial dispersion mechanism in the reactor model does not alter the dynamic response significantly. But nevertheless, the axial state variables computed with models which do not include the axial dispersion may predict values up to 6% different for a transient, if the axial temperature gradient does not exceed 0.14 (this value is based on the dimensionless groups used). These differences decrease as the gradients decrease and reaches 4% for gradients of 0.08.

In studies related to parametric sensitivity, where deviations less than stated above can greatly alter the response, the axial diffusion should be included in the mathematical model. Such cases, where temperature runaway may occur and where the axial temperature gradients approach infinity, should include axial dispersion.

CHAPTER 8

REACTOR STABILITY

8.1 Introduction

If very small changes in the inlet conditions of a reactor can cause very large changes to take place in the bed, then the reactor may be described as unstable in operation. Such instability may be solely due to parametric sensitivity, in which case removal of the disturbances will generally restore the original state. On the other hand it may be due to parametric sensitivity, accompanied by multiple steady states. In the latter case, simply removing the disturbance will not always cause the reactor to return to its original state unless certain conditions are fulfilled.[46] In either case, the consequences of the instability are similar; rapid reaction, ignition or blow out may occur. Both of these phenomena are undesirable for fixed bed catalytic reactors; more especially ignition since temperature runaway develops and this causes catalyst deactivation, sintering and poor product selectivity. Obviously, then, a prior knowledge of the regions of potential instability is desirable so that satisfactory and safe operational procedures for the reactor may be specified.

Despite the fact that at an operational level instability is essentially a dynamic problem, steady state information can be used to indicate regions of potential instability. For example, if for given inlet conditions, a reactor may have two steady states, then it may be possible with small perturbations to cause it to switch rapidly from one state to another.[115] If the parameter regions over which the two simultaneous steady states occur (i.e. multiple states) can be identified, then this behaviour may be avoided. To design a stable system, it may be necessary to sacrifice some of the steady state performance in order to achieve desired transient behaviour which is both stable and predictable. With this argument in mind the question

of stability is therefore not simply the specification of 'hard' boundaries, but demands a broader view that can be expressed in terms of the intrinsic characteristics of the system.

The physical system can be described in quantitative terms by mathematical models. Such models have a common basis in that they are a statement of the mass and energy conservation laws. As a result, they take the form of ordinary or partial differential equations, the complexity depending on the physical mechanisms assumed to be operative. Nonetheless, implicitly in these models is the understanding that the equations are in some significant respect analogous to the physical system and that behaviour deduced from these models will closely parallel that of the physical system. For example, the model describing heat and mass balances on a catalyst particle indicates that a region of multiple steady states is characterized by an upper and lower bound fluid temperature for a given concentration. To attain the upper steady state the pellet must be perturbed across the upper bound and subsequent transition to the lower steady state is only possible by crossing the lower bound. In this way the catalyst particle exhibits hysteresis in the region of multiple states and does not actually attain the middle metastable state, as shown in Figure 8.1. This behaviour has been demonstrated experimentally with a single catalyst pellet in which the ethylene hydrogenation reactions occurred by Furusacua and Kunii[136] and Ray[10] reports that similar behaviour has been observed by Horak and Jiracek.[108] Also Luss et al.[115] have demonstrated the existence of multiple states experimentally using the oxidation reaction of butane gas on a heated electric wire. As shown in Figure 8.2 (corresponding to Figure 7 in reference 115), for 1.5% butane, two steady states exist for 80°C T_{gas} 264°C. They showed that the difference of surface temperature in the two steady states exceeds 600°C.

The numerical solution of such nonlinear models contributes greatly to the understanding of certain reactor behaviour. On the other hand the choice

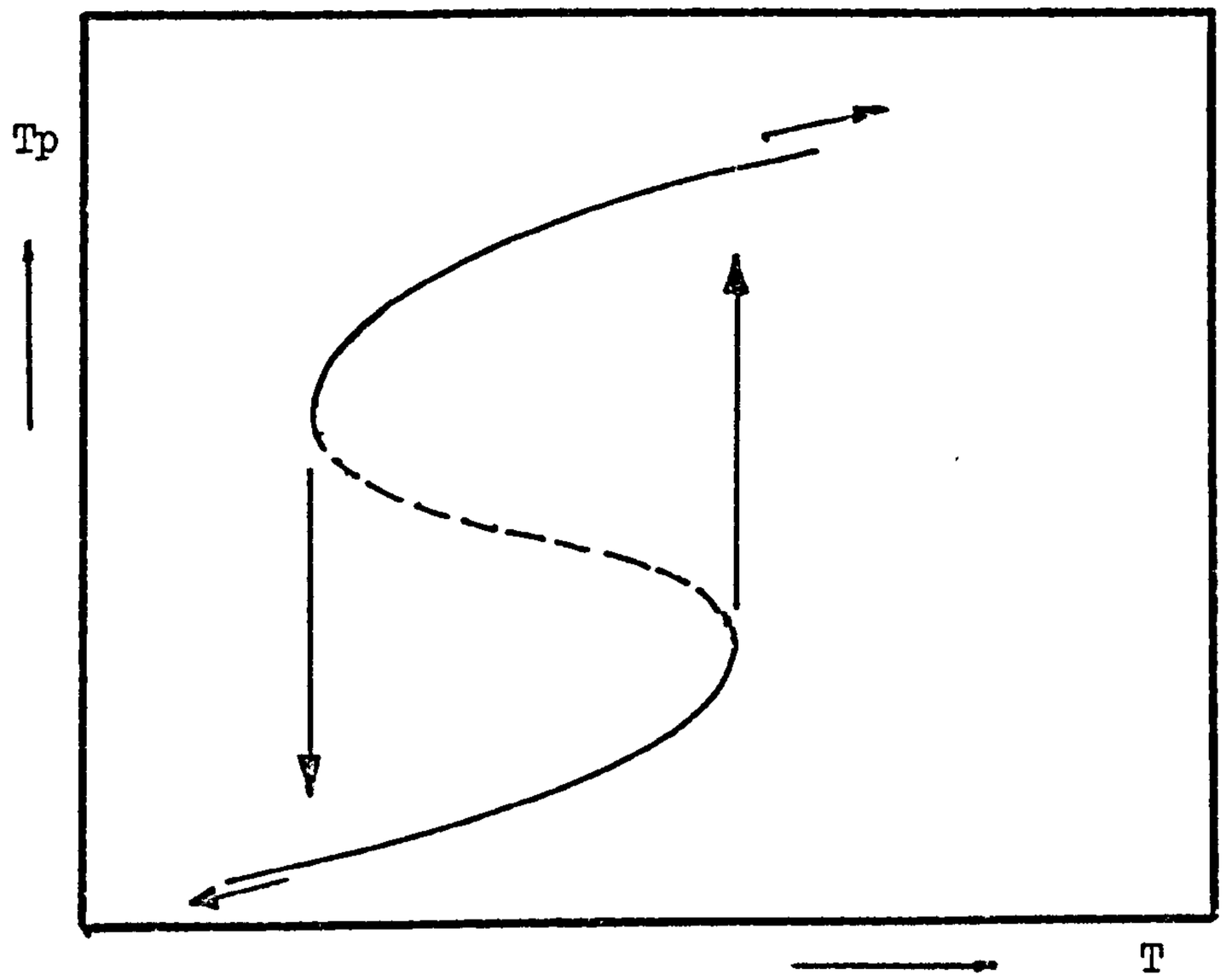

Figure 8.1: Schematic diagram showing hysteresis of the catalyst steady states predicted by mathematical models.

Figure 8.2: Experimental results of butane oxidation showing catalyst multiple steady states.

of a model for a given system may yield analytical results which can indicate qualitative behaviour and which may be used to describe the physical events taking place in a reactor.

Stability, as applied to a nonlinear reactor system, can be identified by looking at the phase trajectories of the system variables. A steady state may be called stable if the trajectories in a neighbourhood all approach it, and unstable if any one trajectory is directed away. Some trajectories may form limit cycles, which are characterized by periodic behaviour.[6] Thus, all trajectories starting within the enclosed area will spiral out until they merge with the limit cycle. Trajectories starting outside the cycle will also decay to the same periodic pattern. Such behaviour was obtained experimentally as a sustained oscillation by Bush[139] in his studies of gas phase chlorination of methyl chloride and by McGowin and Perlmutter[89] in their studies of a recycle system.

It may well be asked how small or large the region of study has to be before the definition of stability is to be considered satisfied. This requires a definition of local stability as applied to non-linear systems. As the mathematical tools to analyse such systems are well established for linear systems, it may be reasonable to linearize the nonlinear system so that it can be analysed more easily. Many important reactor models can be approximated more or less adequately by linearization, depending on the purposes to which the approximation is to be put. Whether or not any real systems are truly linear is questionable,[6] since although continuous systems remain linear in the small, no physical chemical system could be expected to be linear over a wide range of its variables. As a consequence, it is usually only possible to study the local stability of a nonlinear system. In cases where the nonlinear system can be analysed without linearization, such as by computational or graphical methods and the analysis indicates that the system is stable for all possible operating conditions, the system may be said to be globally stable.

In the heterogeneous system of interest here, instability may be caused by the catalyst packing, or by the fluid phase behaviour. It is convenient to note here some of the studies done in these areas in an attempt to try to relate them to local and global stability problems associated with heterogeneous systems.

For the catalyst particle, when all the interphase transport resistances are considered, the number of multiple steady states is usually three, with the middle state being unstable. Although Hutfield and Aris[43] have shown that five steady states are possible, the parameter values used are out of the practical range. Lumping the Laplacian operators of the distributed systems has also been used to simplify the problem. The disadvantages of lumping procedures are that not all the characteristics of the original system are carried over to the lumped system, the results and criteria obtained at least agree qualitatively with those of the real system in many cases.[140,141,142] Luss and Lee[143] lumped the space parameters of the transient pellet equations and obtained criteria they claimed superior to other lumping techniques. Their criteria indicate that it is possible to ensure uniqueness in the catalyst particle by reducing its size or diluting the reaction mixture. However, diluting the reaction mixture may reduce conversion and yield of a catalytic reactor and reducing the catalyst size may cause temperature runaway as reported by Thornton.[46] Kuo and Amundson[137] have directly treated the distributed parameter system and developed a necessary and sufficient conditions for particle stability. These conditions require the computation of eigenvalues of non self adjoint linear system by Galerkin's method. However some computational difficulties were experienced by Lee and Luss[138] for very small Lewis number. For a Lewis number equal to unity the system can be reduced to a single equation for which the maximum principle can give stronger

conditions.[144] Application of the Liapunov direct method on the distributed system to obtain the necessary condition for particle stability has been carried out.[145,146,147] Although these criteria are in the form of algebraic inequalities and need steady state information, they are usually conservative. On the other hand Amundson and Raymond[87] showed that the slope condition (i.e. the slope of heat removal line should be greater than that of heat generation), is a necessary and sufficient condition for particle steady states stability. Also McGreavy and co-workers[42] arrived at the same conclusion studying the transient sinusoidal perturbation on the isothermal pellet model.

It is recognised that for a one dimensional reactor model (i.e. neglecting both axial and radial dispersion), unique profiles[149] apart from that which may be accounted for from the pellet are possible. However instability in such a homogeneous reactor may arise from consideration of parametric sensitivity. Nonetheless, whenever heat or mass can move upstream there exists the possibility of multiple steady states.[150] The upstream movement can be the result of physical recycle or feedback control, but can also arise even more simply from axial dispersion,[6] and has in fact been demonstrated experimentally.[151,152] However, when effects such as back mixing allow the possibility of multiple states, their occurrence is not in general guaranteed, but will depend on the parameter values specific to the system under study. For a fixed degree of axial dispersion, as many as five steady states[6] may exist for a quasihomogeneous reactor over a wide range of heat transfer coefficients. Similar results were obtained by Hlavacek and Hofmann[92,93] in their studies on the effect of axial Peclet number. However, in the latter case Froment[7] indicated that the range of peclet number to cause such an effect may be considered to be outside the practical values found industrially.

Van Heerd en[150] in his studies on adiabatic reactors with axial mixing

suggested that the slope condition is a necessary and sufficient condition for stability. For an adiabatic reactor modelled by a surface reaction model with no concentration gradient in the interparticle region, Blodgett[153] and Orcutt and Lamb[154] found that the slope condition is a necessary and sufficient condition for stability and for small perturbations. For large perturbations Han and Mayer[155] indicate that, for the same system as above, the rate of heat removal should be greater than the greatest slope of the heat generation curve. Vanderveen et al.[156] obtained necessary and sufficient conditions for stability of an adiabatic reactor with surface reaction and for small perturbations. However, they treated the reactor as a series of stirred tank reactors, which is equivalent to approximating the axial derivatives by a finite difference scheme. A similar study has been made by Agnew and Narsimhan[157] for a non catalytic adiabatic reactor.

Following the criteria put forward earlier[118] which indicate that the effect of axial diffusion is usually negligible in long reactors and for the commonly used high flow rates, the interest has been mainly directed towards reactor models with radial diffusion. In exothermic reactions, appreciable radial temperature and mass gradients are usually encountered and they have to be taken into consideration. A review of the studies which have been made on quasihomogeneous models[129] has been mainly concerned with criteria for parametric sensitivity or temperature runaway. McGuire and Lapidus[60] studied the dynamics of a two dimensional model without axial diffusion with the view to examining the behaviour of the reactor when some of the catalyst particles lie in a region of multiple steady states. Their interests were concerned with whether the reactor would return to its original steady state after the removal of an imposed perturbation. A similar study had been made earlier by Liu and co-workers.[125,158]

Efforts have been made to relate instabilities arising from catalyst

particle to that due to the reactor. Thus, McGreavy and co-workers[46,109] plotted regions of multiplicity and highly parametric sensitive areas of the particle on a phase diagram as a function of fluid conditions for each reaction system of the simple form A——B. Reactor trajectories can be plotted on the same diagram, thereby giving an immediate indication of potential instability and operating conditions. Using this method Thornton[46] indicated that radial variations should be considered in constructing such criteria. He indicated that some of the pellets may enter the multiplicity region near the reactor axis which is not accounted for from radial mean conditions. Although the method described above is simple to apply and gives an immediate indication of the potential instability regions, in complex reactions the method may be difficult to apply.

Although the studies reviewed above cover a broad area in reactor stability, they involve such assumptions as neglecting the axial or radial dispersion or both. Also different pellet models have been used. No attempts have been made to analyse the complex reactions at present under study, either because some of the methods used above are not applicable, or because of the complexity involved in their analysis. In the following discussion, interest will be directed to two models, the first given by equations (4.1 to 4.5) neglecting axial dispersion and considering radial transport and particle transport limitations. The second model given by equations (6.1 to 6.5) takes into consideration the axial diffusion while radial variations of heat are assumed to follow a parabolic distribution. This division is thought to be reasonable, since it might be indicated that further consideration of any of three dispersion mechanisms may not necessarily be required in deriving a stability criteria for the complex system being studied. The assumption of pellet isothermality is used and the models employed are given in Appendices (A1.1) and (A1.2) for the steady and unsteady states, together with the additional assumptions involved.

8.2 Method of Analyses

In order to define the stability of a system consider a perturbation about the steady state profile. If the system is stable the resulting transient response will remain within a finite region of the steady state profile. If the transient profile approaches the steady state and the displacement can be made as small as desired, if given sufficient time, the system is said to be asymptotically stable. The above definition of stability is called Liapunov stability[6,146] and can be put in the following mathematical form:

A functional V(u) is sought for the system such that

$$V(u) > 0 \text{ for } u \neq 0$$

$$V(u) = 0 \text{ for } u = 0$$

and if $\frac{\partial V}{\partial \tilde{t}} \leqq 0$ for $u \neq 0$ and $\tilde{t} \geqq \tilde{t}_0$

then the system is stable and if

$$\frac{\partial V}{\partial \tilde{t}} < 0 \text{ for } u \neq 0 \text{ and } \tilde{t} \geqq \tilde{t}_0$$

the system is asymptotically stable.

The general form of V(u) can be looked at as an energy function of the perturbed state from the steady state and it is required therefore that its derivative with respect to time would decrease and thus approach the original steady state. A general form for V(u) used in the case of partial differential equations is:[6]

$$V(u) = \tfrac{1}{2} \int_{\Omega} u^T P u \, d\Omega \qquad \Omega \equiv (r,Z) \tag{8.1}$$

$$\text{therefore} \quad \frac{\partial V(u)}{\partial \tilde{t}} = \int_{\Omega} u^T P \frac{\partial u}{\partial \tilde{t}} \, d\Omega \tag{8.2}$$

where P is a positive definite symmetric matrix and u is the vector containing the values of the perturbed state variables, defined as $u(r,Z,\tilde{t}) = Y(r,Z,\tilde{t}) - Y(r,Z,0)$, where $Y(r,Z,0)$ are the steady state values of the state variables.

The general steps followed in applying equation (8.2) to the distributed systems to be analysed may be as follows.

1. Substitute the perturbed form u defined above in the original distributed system. This will involve linearization of the nonlinear reaction rate terms R(u) around the steady state, by making use of a Taylor series approximation:

$$R_i(u) = R_i(0) + \frac{R(0)}{Y(r,Z,0)}\Bigg|_{i,J} u_i \qquad i = 1,2,3,4 \qquad J = 1,2,3,4$$

Note that the derivative terms in the above equation (Jacobian matrix) are evaluated at the steady state values.

2. Substitute for $\frac{\partial u}{\partial \tau}$ in equation (8.2) by the linearized space derivatives of the distributed system.

3. Integrate the resulting equation and substitute the boundary condition of the linearized system.

4. After the necessary mathematical manipulation, conditions are sought that ensure that $\frac{\partial V(u)}{\partial \tau}$ will be less than zero over the entire integration interval, thus indicating that the system is stable.

Note that in step 4, sometimes the Liapunov functional can be divided into several integrals, some of which may be negative irrespective of the integral values. Those in which the integral values depend on the parameters to be integrated are computed and conditions under which they have negative values can be identified. This policy was adopted here, and the following discussion is related to the integrals which depend on the parameters. Further details of the application of Liapunov method to the distributed systemsunder study can be found in Appendix (A3).

8.3 Discussion of Results

Consider the application of the Liapunov direct method to the radial diffusion model. The elements of the weighting matrix P shown above in Liapunov functional can take any value. Some authors have used the identity matrix.[146] However others[6,153] have suggested that other forms may yield better results. In this study the weighting matrix has been chosen as diagonal, with elements of the form e^{-KZ}, where K is a constant to be determined later.

The steps taken in applying Liapunov method to the distributed system with radial diffusion can be seen in Appendix (A3.1). However by following the general steps stated in the last section the integrals which have to be computed to determine whether their values are larger or smaller than zero can be put in a determinant of the following form:

$$C_1 = e^{-KZ} \begin{vmatrix} 2(-K\frac{G_1}{G_5} + \frac{\partial RA}{\partial CA}) & b_{12} & b_{13} & b_{14} \\ b_{21} & 2(-K\frac{G_1}{G_5} + \frac{\partial RB}{\partial CB}) & b_{23} & b_{24} \\ b_{31} & b_{32} & 2(-K\frac{G_3}{G_6} + \frac{\partial RT}{\partial T}) & b_{34} \\ b_{41} & b_{42} & b_{43} & 2\frac{\partial RS}{\partial Tp} \end{vmatrix}$$

The elements of C_1 represent the partial derivatives of the reaction rate terms arising from the linearization procedure and having values evaluated at the steady state (see Appendix (A3.1) for further details).

A necessary condition for the distributed parameter system with radial diffusion to be stable for any small perturbation in system variables is that the determinant C_1 should have a value less than zero when evaluated at any point in the reactor. A simple criterion can be extracted by observing that the condition for C_1 to be negative definite is that the diagonal elements should be negative and larger than the off-

diagonal elements. By making the constant K large enough, the only condition to be satisfied is that $\frac{\partial RS}{\partial T_p}$ (see equation (A3.7) in Appendix (A3.1)), should be negative. This is, in fact, the slope condition applied to the complex reaction in the catalyst pellet.

$$Nu > Q_g$$

In other words the heat removal (i.e. Nu) should be greater than the heat generation (i.e. Qg) in the catalyst pellet (for details of Qg, see Appendix (A3.1)). Before examining this condition in relation to the reactor model, it is worthwhile illustrating the complex nature of the reaction under study, by confining attention to the catalyst pellet.

For the data given in Table 3.3, figure 8.3 shows the multiple state region for different concentrations of species CA and CB. It can be observed that merely increasing the product CB can push the pellet into a region of high parametric sensitivity or even to the non unique region. Thus, increasing the concentration of CB from zero to 0.4, while keeping CA constant (i.e. $B = 5 \times 10^{-4}$) results in driving the pellet into the non unique region, as can be seen from curves A_1 and A_3. Of course, the amount of CB which can cause such behaviour depends on the relative values of the parameters. Such physical and chemical parameters are the activation energies, heats of reaction, Sherwood numbers and the rate constants. Nevertheless this kind of behaviour means that under certain conditions in the reactor where the ratio of CA to CB is changing during transient changes, highly parametrically sensitive areas or even multiplicity may occur and cannot be observed from a steady state analysis.

The slope condition defined as (Qg - Nu) for the curves A_1, A_2 and A_3 is shown in Figure 8.4. For values of Qg - Nu < 0, the slope condition is satisfied and the pellet has a unique steady state, if Qg - Nu > 0, the pellet has multiple states. While the slope condition is satisfied in the case of a unique state represented by curves A_1 and A_2, in the case of curve A_3 it is obvious that the heat generation in the pellet is greater than the

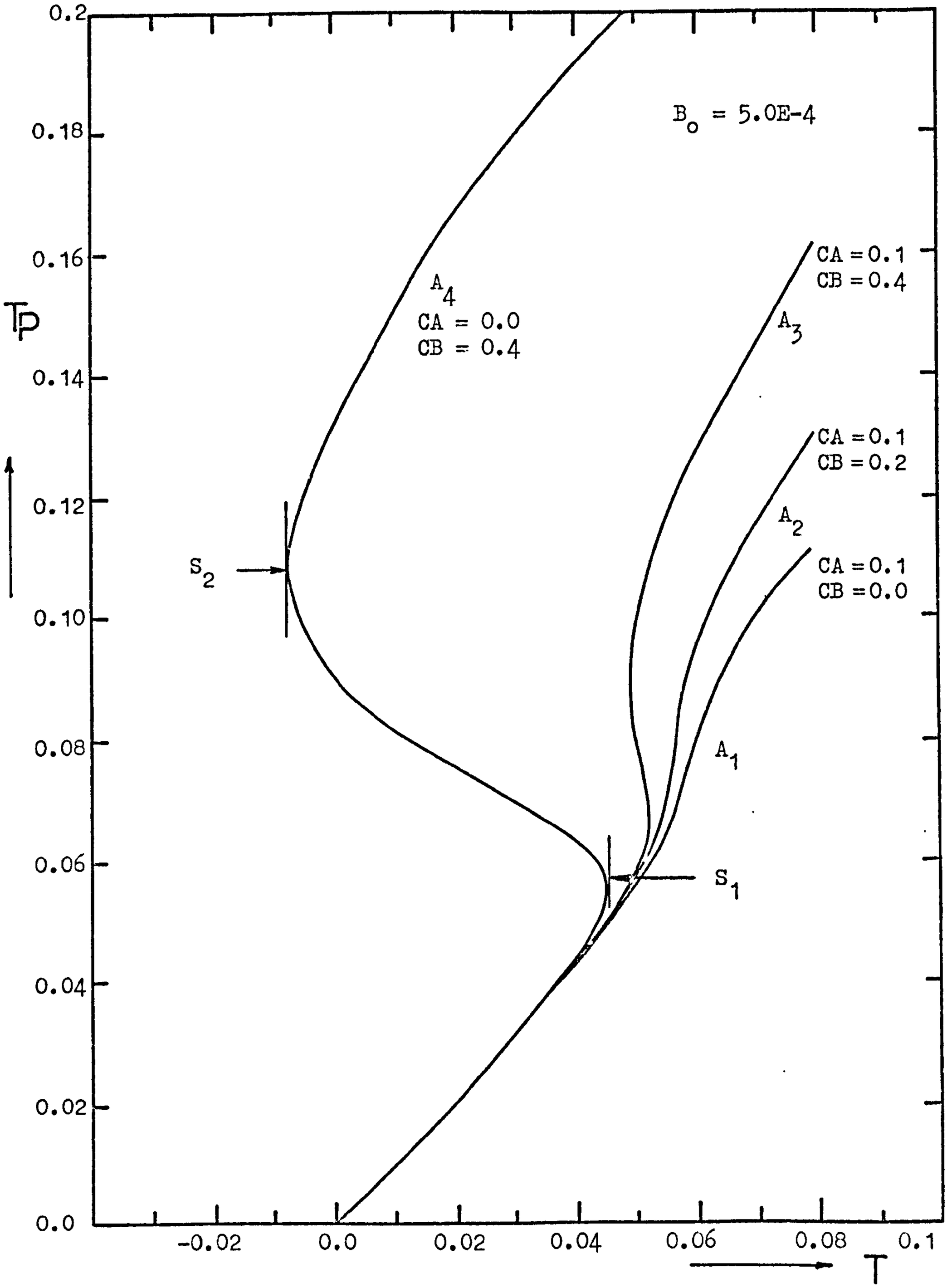

Figure 8.3: The relationship between T and Tp obtained by solving the catalyst pellet model for typical values of parameters.

heat removal in the region of multiplicity. It should be noted that in the case of high temperature sensitivity, as in the case of curve A_2, or at the positions S_1 (Figure 8.3), the heat generation is about equal to the heat removal. These situations, when they arise in the reactor, are points of parametric sensitivity and may be potentially unstable.

The values of the determinant C_1 is also shown in Figure 8.4 for different values of the constant K. The degree of conservation of the C_1 criterion can be examined in comparison to the slope condition in the pellet. It can be observed that in the case A_2 where the maximum value of $Qg - Nu = -0.07$ (indicating that the pellet is parametrically sensitive, as shown in Figure 8.3), the value of the determinant for $K = 600$ is $C_1 < 0$ while for $K = 50$, $C_1 > 0$. This latter value indicates that no conclusion can be inferred regarding this state stability. On the other hand in case A_3, and for $K = 600$ and 50, C_1 changes sign from negative to positive by crossing the broken line at a $Qg - Nu$ value of -0.05 and -0.11 respectively. In fact, for $K = 0.0$ C_1 changed sign according to the slope condition at $Qg - Nu = -0.15$. It seems that the sharpness of the value of C_1 as a stability criterion depends on the value of the constant K, as would be expected. This may be determined for every specific case, probably by making use of optimization. However the above observation suggests that for reasonable values of K the criterion C_1 indicates that the reactor cannot be unstable while the catalyst pellet is at a stable state. This is understandable on physical grounds since the reaction is assumed to take place only in the catalyst pellet and that the spatial distribution of mass and heat in the reactor depends on the rate of reaction in the solid. It would appear that in heterogeneous reactors, catalyst stability is a necessary condition for a stable reactor. This conclusion has been arrived at by various authors[153,148] for the simple reaction scheme $A \longrightarrow B$.

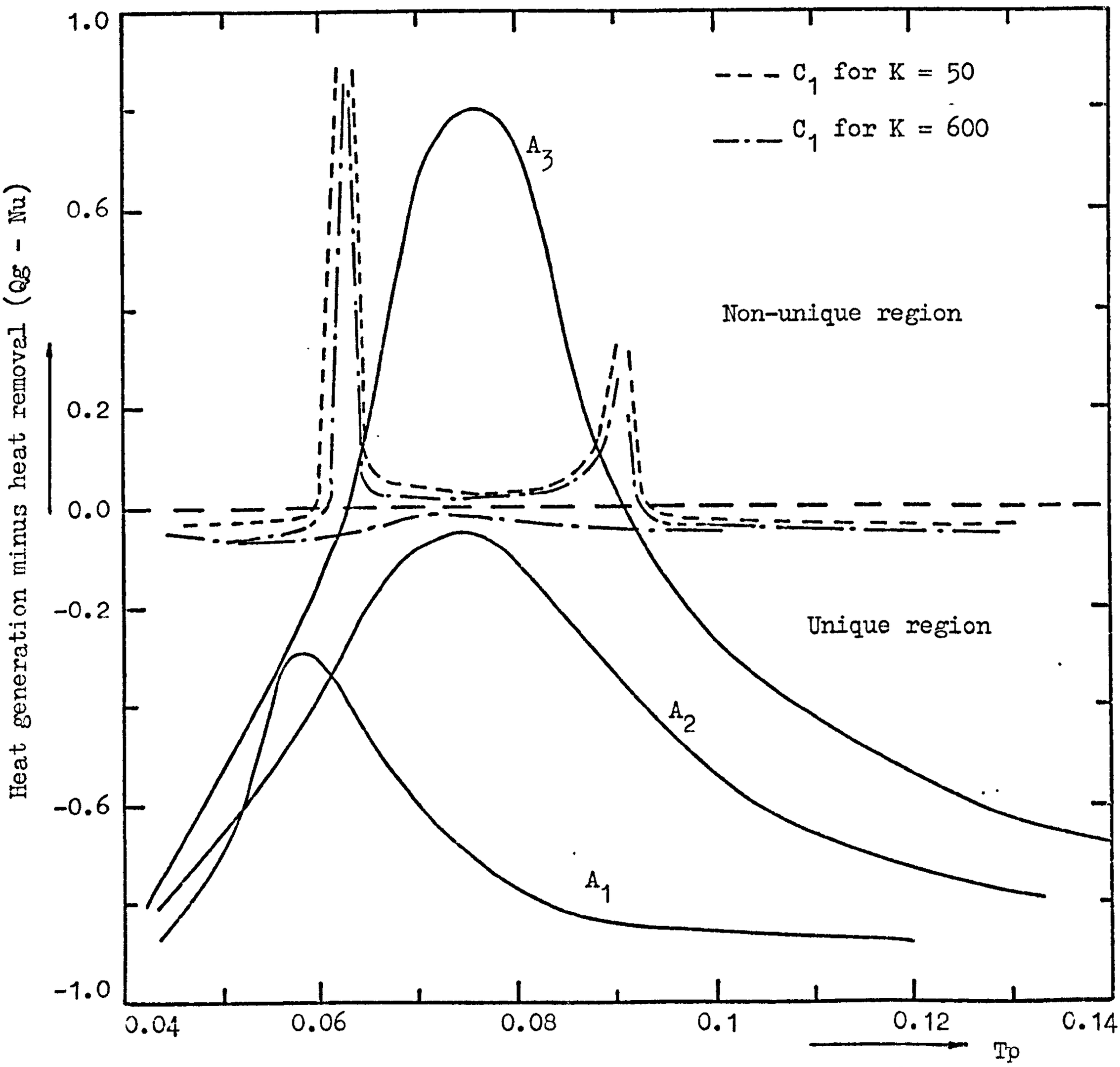

Figure 8.4: The relationship between pellet slope condition, reactor stability criterion C_1 and pellet temperature for typical values of parameters.

The pellet model used is the simplest which can describe the dynamics of a catalyst particle in regions of practical variations of the parameters. Studies of the pellet response to sinusoidal perturbation in temperature and concentration indicate[149] that the slope condition is a necessary and sufficient condition for particle stability for small perturbations. It is therefore required to apply the slope condition in the reactor and along the radial direction to determine how conservative this condition is. To establish this, the slope condition has been computed for different reactor parameters. Thus, Figure 8.5 shows the axial temperature profiles at r = 0.0 for lower and upper steady states. In both cases the slope condition is satisfied (i.e. $Qg - Nu < 0$). The maximum values estimated at r = 0.0 for the lower state is $Qg - Nu = -0.13$, and for the upper state is -0.096. These have been tested for small perturbations in temperature (10K) and concentration CA (0.05) and been found to be stable. Note that the slope condition is applied at r = 0.0. When applied along the radial direction the maximum mean value of $(Qg - Nu)_m$ for the lower and upper states are -0.188 and -0.12 respectively. In this respect, the mean value of the slope condition may be a less conservative criterion, as shown by the next example.

Figure 8.6 showed the axial temperature profiles at r = 0.0 when the reactor is in a parametrically sensitive region whereby increasing the inlet dimensionless concentration CA from 1.0 to 1.03, temperature runaway took place at Z = 0.35. For the profile denoted by 1, the maximum value of the slope condition is $Qg - Nu = -0.09$ at r = 0.0 and a radial mean value of 0.1, while for the profile 2, $Qg - Nu = -0.05$ at r = 0.0, (Z = 0.35), and a radial mean value of -0.08. This value indicates that the whole radial profile at this axial position is parametrically sensitive. The point which should be considered here is that although some pellets

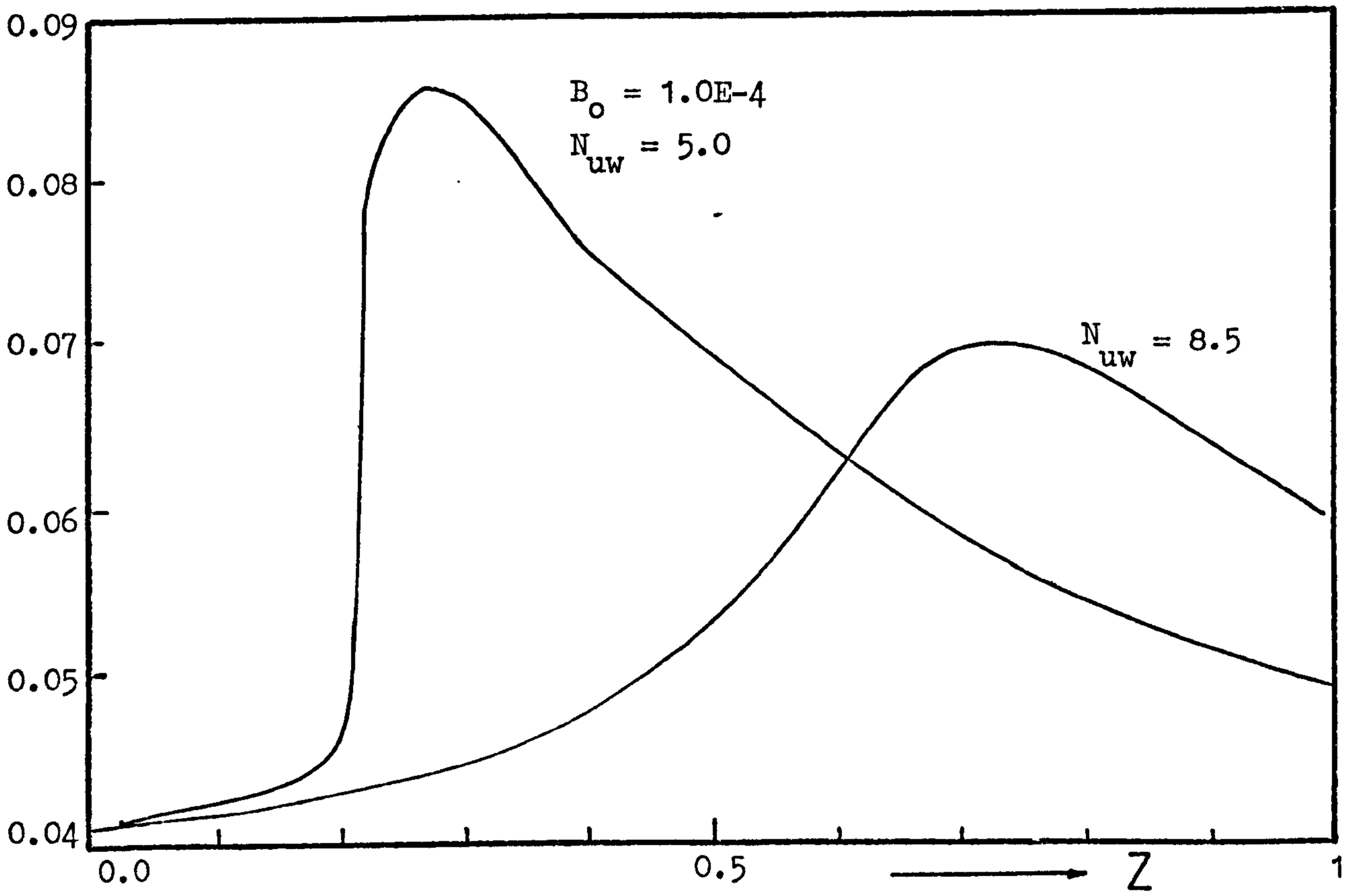

Figure 8.5: Axial temperature profiles at r = 0.0 showing the upper and lower steady states in the reactor predicted by the radial diffusion model. Data as given in Table 3.3.

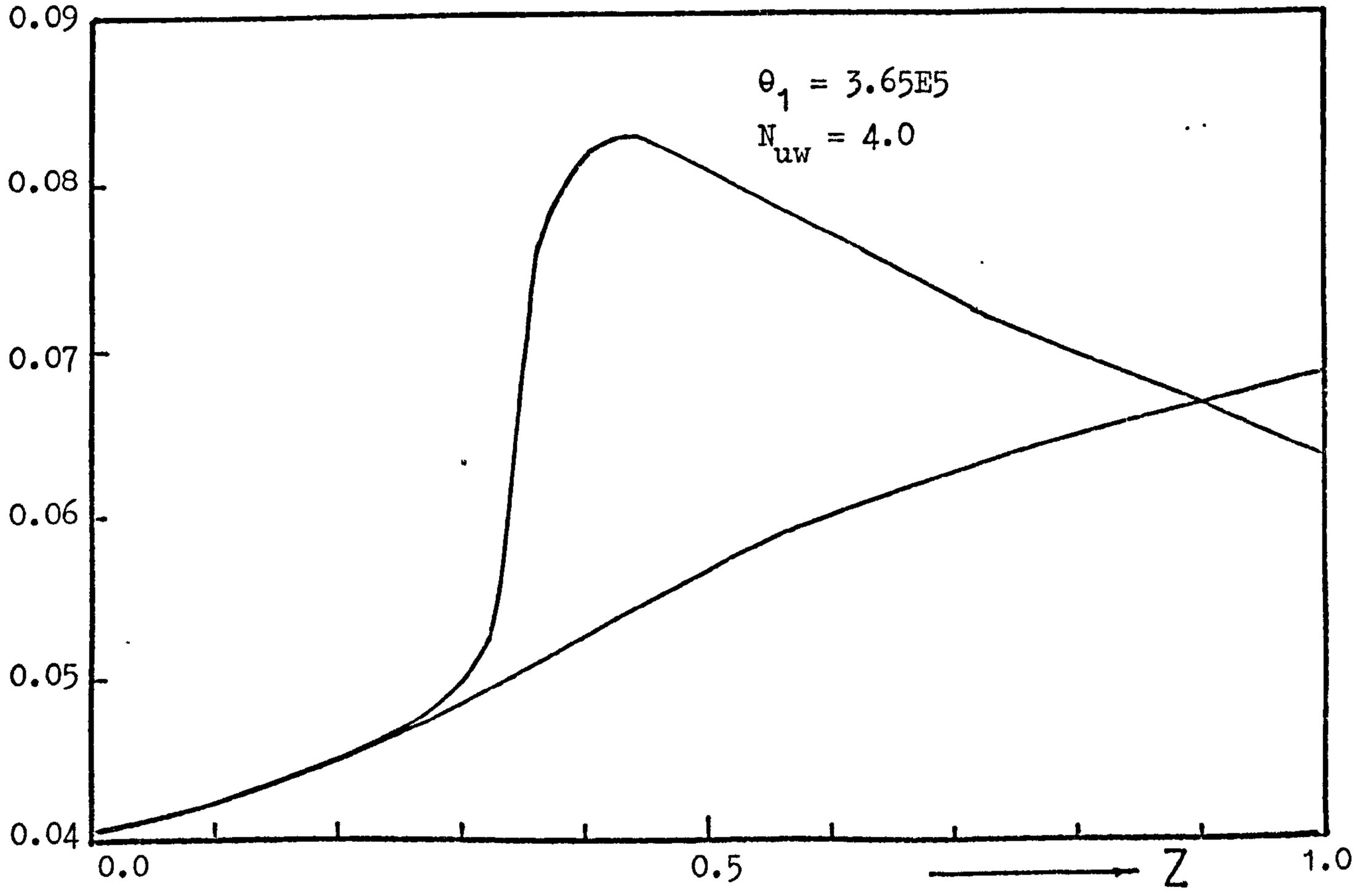

Figure 8.6: Axial temperature profiles at r = 0.0 for two values of inlet concentration CA of 1.0 and 1.03 in the region of parametric sensitivity. Data as given in Table 3.3.

near r = 0.0 may be parametrically sensitive, it is not necessary that the reactor should reflect such sensitivity unless sufficient section of the radial profile is in this region. Similar observations have been arrived at by Thornton,[46] using alternative approach for the simple reaction A⟶B. This suggests that the mean radial slope condition is a less conservative criterion for reactor stability.

It appears that as a result of several computed results, the radial mean slope condition is a necessary and sufficient condition for local stability, if $(Qg - Nu)_m \leqq -0.11$. This condition is easily computed and can be used as a first estimate, since it is simple and takes negligible computing times and requires only steady state information.

Applying Liapunov analysis to the axial diffusion model using the same general form of Liapunov functional given before. The weighting matrix P is a diagonal matrix with elements of the form $\cos a\pi(Z - \frac{1}{2})$, where a is a constant to be determined later. This form of P which has been suggested before[169] has been found satisfactory and yields a less conservative criterion than other forms. Following similar steps to those stated in the previous case the criterion shown below can be derived (for details see Appendix (A3.2)).

A necessary condition for the axial diffusion model to be stable is that the following determinant value should be negative definite at any point in the reactor

$$C_2 = \begin{vmatrix} \frac{-2\lambda^2}{G_5 Pe_a} - \frac{0.25}{G_5} Pe_a + \frac{\partial RA}{\partial CA} & 0.5\, b_{12} & 0.5\, b_{13} & 0.5\, b_{14} \\ 0.5\, b_{21} & \frac{-2\lambda^2}{G_5 Pe_a} - \frac{0.25}{G_5} Pe_a \frac{\partial RB}{\partial CB} & 0.5\, b_{23} & 0.5\, b_{24} \\ 0.5\, b_{31} & 0.5\, b_{32} & \frac{-2\lambda^2}{G_6 Pe_a} - \frac{0.25}{G_6} Pe_a \frac{\partial RT}{\partial T} & 0.5\, b_{34} \\ 0.5\, b_{41} & 0.5\, b_{42} & 0.5\, b_{43} & \frac{\partial RS}{\partial Tp} \end{vmatrix}$$

where the elements of C_2 represent the partial derivatives of the reaction rate terms with respect to the variables CA, CB, T and Tp, evaluated at

the steady state conditions.

An additional condition arises from the boundary conditions which have to be satisfied. This is

$$2\lambda \text{Tan } \lambda = Pe_a$$

where $\lambda = \frac{a\Pi}{2}$ and $0 < a < 1$

Pe_a = axial peclet number (assuming that the heat and mass peclet numbers are equal).

The value of should have the value of the smallest positive root of the above equation for any particular value of Pe_a. For the range of Pe_a numbers between 100 and 600 (with Pe_a based on the length of the reactor), the value of λ lies between 1.5 and 1.6 and starts to decrease rapidly for $Pe_a < 50$. This behaviour is apparent from the form of the above equation (i.e. tan λ).

It may be observed that in the case of the axial diffusion criterion, C_2, as Pe_a is increased the diagonal elements can be made a large negative values and again the slope condition is a criterion for stability. This point, which can be observed from the matrices C_1 and C_2, is reasonably sound on physical grounds. As the axial pellet number Pe_a increases, the effect of backmixing or diffusion, which is responsible for the instability or multiplicity solutions in homogeneous reactors, can be considered negligible. As $Pe_a \longrightarrow \infty$ (i.e. the one dimensional plug flow), the slope condition is a necessary and sufficient condition for reactor stability.

The effect of the boundary conditions, which is expressed as $2\lambda^2/Pe_a$, may be considered to be of negligible importance in relation to reactor stability compared with $0.25\ Pe_a$, which describes the effect of axial diffusion in the reactor. This is true in the case of large Pe_a. As it decreases, the effect of the boundary conditions on reactor stability increases.

Figure 8.7 shows the axial temperature profiles for the lower and upper steady states for Pe_a values of 100 and 600. The data used is given

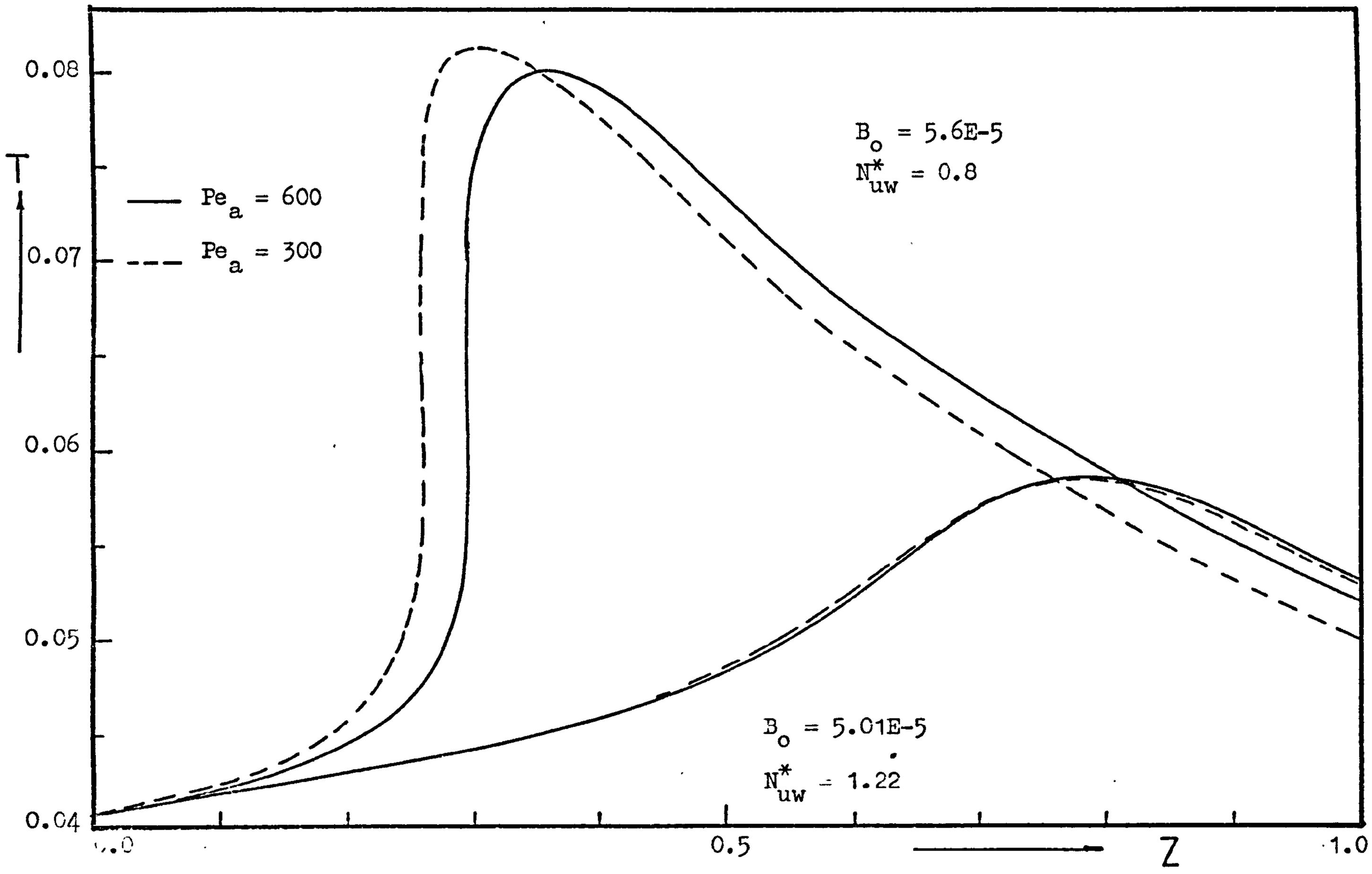

Figure 8.7: Axial temperature profiles at r = 0.0 showing upper and lower steady states in the reactor predicted by the axial diffusion model. Data as given in Table 3.3.

in Table 3.3. Applying the stability criterion developed above on the lower steady states, the C_2 value is found to be negative over the whole reactor length, with an average value of -9.8×10^9 at Z = 0.7. For the upper steady states, the stability criterion C_2 has a positive value and therefore is unable to supply any information regarding reactor stability. The slope condition is satisfied at both the upper and lower states and that the range of Pe_a used (i.e. between 100 and 600) above does not affect the sign of the matrix C_2.

Following the argument used in the case of the radial diffusion model, instability is primarily due to the possible potential instabilities arising in the solid state. In the case of the axial diffusion model and due to the similarity between C_1 and C_2, the same observation is applied here and the slope condition can be considered a necessary condition for the local stability of the reactor for the range of Pe_a used.

8.4 Concluding Remarks

A stability analysis using the Liapunov direct method has been carried out on a distributed system of partial differential equations describing the heat and mass transfer in fixed bed catalytic reactors. Two mathematical models have been used. The first takes into consideration the radial transport process (RDM) and the second the axial diffusion process (ADM). It has been shown that for the RDM, the slope condition (i.e. the heat removal should be greater than the heat generation in the pellet) is a necessary condition for reactor local stability. The slope condition is able, when applied at reactor axial position r = 0, to detect whether the lower and upper steady states are stable and it has been shown that the middle state is unstable. The mean radial slope condition can be

considered a less conservative stability criterion. In this case, some of the pellets near r = 0 may experience instability or parametric sensitivity, yet the whole radial profile may be considered stable.

In the case of the ADM model, a stability criterion in the form of a matrix has been developed. The criterion depends on the sign definiteness of the determinant value, and if it is negative the system is stable. Otherwise no conclusion can be drawn. For the lower steady state, the value of the determinant has been shown to be negative. No information concerning the stability of the upper steady state is available. The slope condition is satisfied for both states. It has been indicated that, as the axial peclet number increases, the slope criterion is a necessary condition for stability and in the limit, as $Pe_a \longrightarrow \infty$ (i.e. approaching plug flow) the slope condition is a necessary and sufficient condition.

CHAPTER 9

FINAL COMMENTS

9.1 Summary of the present work

Consideration has been given to the problems of characterizing the behaviour of highly exothermic reactions in fixed bed catalytic reactors where the kinetic scheme may be represented by A→B→C, with A→D. For this system, both steady state and dynamic models of the fixed bed catalytic reactor have been developed. Various aspects of the dynamic behaviour have been studied to identify some of the important features of the system and in particular those which are relevant to design or control problems. To establish the minimum requirements needed to adequately describe the physical and chemical events occurring in the reactor, models of various complexities have been considered. However, since the reactor model includes so much detail, the computation time taken to solve them is usually excessive. Thus, effort has been made to develop more rapid solution methods and also to simplify the models without sacrificing the detail necessary to satisfy the requirements of representation accuracy.

The collocation method has been employed to solve the steady state radial diffusion model. A comparison in terms of accuracy of solution and computing time has been carried out between the implicit finite difference representation (Crank-Nicholson), and single collocation procedure (collocating the radial direction and integrating the resulting system with Runge Kutta Merson), and the double collocation (using the collocation in radial and axial directions). It has been shown that single collocation is appreciably faster than the finite difference solution and a better approximation of the radial profiles has been obtained with fewer collocation points. This may be done if the distribution of the

location of the collocation points, not necessary at the orthogonal polynomials zeros, is such that they emphasize certain regions where the function value is needed with greater accuracy.

The comparison between the single collocation and double collocation procedures revealed that for nonlinear problems, where linearization methods are used, no appreciable reduction in computing time is possible, unlike linear problems. This is because the time taken in matrix inversion involved in iterative application to the linearized process. However, in transient cases where the change over the time steps is small, the double collocation can be used without employing a linearization procedure; it is faster than the single collocation and the solution converged in a small number of iterations.

Further reduction in computing time is necessarily coupled with a reduction in model dimensionality. However, this is usually accompanied by a loss of accuracy. Model reduction technique, in which the radial differential operators can be eliminated from the model and then reconstructed from simple algebraic expressions, have been applied to a dynamic radial diffusion model. The resulting one dimensional reduced model is treated by approximating radial temperature profiles by examining the deviation of temperature profiles from a parabolic distribution and relating this to the radial mean values, in the form of a modified wall Nusselt number and distribution factors. The estimation of the distribution factors require the solution of the pellet equations twice per axial step, so further reduction in computing time has been achieved in two steps, in which the distribution factors are estimated from algebraic expressions. In all cases, the reduced dynamic model evaluates the radial profile with an accuracy comparable with double collocation of the distributed system and over a wide range of operating conditions. The computational load is in fact reduced to reasonable levels making it suitable for control studies and design purposes.

Examination of the dynamic behaviour of the reactor has revealed that it is controlled by a combination of chemical and thermal effects, the relative magnitudes of which may change considerably with time and position in the bed. This results in dynamic responses which are not easily predicted without extensive simulation. Step and ramp perturbations in inlet temperature, concentration and fluid velocity indicate that the major dynamic effect derives from the solid thermal capacity, which causes the temperature effects to be delayed. Detailed examination has shown that it is possible to categorize the dynamic responses into a hot and cold wave propagation mechanism which are independent of the particular variable causing the disturbances at the inlet. Thus, the mass accumulation resulting from cooling effects on the solid are responsible for the high temperatures reached in front of the cold wave. Based on the velocities of propagation of heat and mass waves it is possible to enhance the reaction or to oppose it in certain parts of the bed by manipulating the inlet conditions. Thus, the objective to control the intensity of the heat wave and the mass accumulation where the reaction is very sensitive to temperature and concentration variations. It has been demonstrated that this type of multivariable approach can be used to control the reactor when working near the maximum allowable temperature, without the possibility of excessive hot spots forming.

When the reactor is controlled by manipulation of the inlet conditions, some oscillations of these variables are likely to occur as a result of control action. For this reason the behaviour of the reactor sinusoidally varying inlet temperature, concentration and fluid velocity has been considered. The response of the reactor to this type of perturbation may be divided into two distinct stages. There is an initial transient period, the duration of which is equal to the residence time of the first heat wave. The subsequent stage is a quasi-state in which regular oscillation of the whole bed is established. In the case of temperature and concentration

inlet perturbations, the greatest disturbances occur during the initial transient period. Thus, at certain frequencies severe hot spots or temperature runaway may take place. In the case of velocity inlet perturbations and at certain frequencies, the greatest disturbances occur in the quasi-stationary state only. As the frequencies of oscillation decrease further, temperature runaway or hot spot formation may take place in both the initial and quasi-stationary state. It has been indicated that the above behaviour is due to the differences in heat and mass wave propagation velocities and these hot spots which are formed may arise across the tube radius and near to the centre line. This is due to heat accumulation effects resulting from the increased reaction rates, and is not possible to dissipate fast enough across the tube radius and through the wall. As a result it may be necessary to limit on permissible inlet frequencies, or on the allowed variations in the radial temperature gradients.

The behaviour of the reactor in the initial transient period has important implications in relation to the control strategies which may be adopted, since control action is often basically a damped oscillatory input. Further examination of the reactor response to a damped sinusoidal perturbation in inlet temperature indicates that disturbances which occur in the initial period are even greater. This is because in damped oscillation, the quasi-stationary state does not occur. It would appear that the quasi-state causes temperature waves of greater emplitude, than with damping and thus reduces the mass accumulation in the latter parts of the bed and hence the disturbances during the initial transient period. Consequently the feed temperature can be used for control by employing a damped oscillation, where the inlet temperature variations can control the concentration waves.

The significance of dispersion of heat and mass on the reactor behaviour has been investigated and the areas where it is of importance

have been identified. To this end, steady and unsteady state models which take into consideration the effects of axial and radial diffusion have been developed. In these models, the reduction technique used above has been successfully employed to approximate the radial dispersion and the resulting system can then be solved by the collocation method. The computing time of such comprehensive models has been reduced to levels comparable to those neglecting axial dispersion.

Steady state simulation indicates that the effect of axial dispersion on the spatial distribution of heat and mass in the reactor becomes increasingly significant as the axial temperature and concentration gradients increase as would be expected. Based on the temperature gradients computed from models which do not consider axial diffusion, it has been shown that it is possible to decide whether or not axial diffusion should be included in a reactor model. If the axial temperature gradient is not very steep, the effect of axial dispersion can be looked at as a discrepancy in the computed state variables estimated from models neglecting it. Bounds on these discrepancies have been given for certain axial temperature gradients.

Examination of the dynamic response to inlet temperature and concentration disturbances has revealed that axial diffusion does not have a significant effect on the general behaviour of the reactor. For certain responses, however, the axial diffusion may become important during the transient, even if it has a negligible effect on the inlet and final steady states. Some bounds are provided for the discrepancies resulting from neglecting axial diffusion, particularly in relation to the maximum temperature gradients attained during the transient response. Axial diffusion effects can be considered unimportant, if suitable adjustments are made in determining a safe maximum temperature for operation. In studies related to parametric sensitivity, multiplicity of states or

stability of reactor, where small discrepancies in state variables may result in undesirable behaviour, axial diffusion should be considered in making a detailed examination of reactor behaviour.

Consideration has been given to the stability of fixed bed reactor. Liapunov-stability analysis has been carried out on two models. The first is the radial diffusion model neglecting axial dispersion. The second model takes it into consideration and assumes a parabolic radial temperature profile. The derived stability criteria for both models are in the form of determinants which can be computed from steady state information. If the sign of these determinants is negative they indicate stability, otherwise no information can be obtained regarding reactor stability. Based on computed results these criteria are able to indicate the stability of the lower steady states only, although the slope condition in the pellet (i.e. the heat removal should be greater than heat generation) is satisfied in both the lower and upper steady states and for both models. Although these criteria are conservative in their estimate, closer examination indicates that if instability arises, it must take place in the pellet irrespective of the mechanisms considered in the fluid phase. Therefore the slope condition in the catalyst pellet is a necessary condition for reactor local stability and may be used as a first estimate.

9.2 Suggestions for further work

The present work has produced reactor models which represent the transport phenomena with reasonable accuracy and only requires a modest computational time. Yet, still much can be done to furtherreduce the computing time. Thus it is desirable to continue with the development of model reduction techniques and efforts should be directed to minimize the number of pellet equation evaluations since they represented the greater part of the computing time. The accuracy of estimating the

distribution factors from algebraic expressions can still be improved and this may be achieved by considering the limiting factors governing the reaction. Attempts should be made to further reduce the steady state model by exploitation of the analogy between the reduction technique and the use of orthogonal splines.

In dynamic simulation attention has been directed to classify the transient response into identifiable categories based on the wave propagation velocities. This line of approach to reactor control needs further investigation to proceed with the multivariable design procedures probably by making use of optimization or optimal control algorithms. Also, the damped oscillation work suggests that the control of reactors in this manner is a possibility and certainly warrants further examination.

It is necessary to establish the relationship between amplitude and frequency of inlet perturbation which produce severe hot spots in the initial transient period. The nonlinearity of the problem, however, suggests a semi-empirical approach.(42)

Comprehensive study is needed to investigate the effects of axial diffusion in parametrically sensitive regions and also in relation to reactor stability. Although the effect of axial diffusion has been related to axial gradients of state variables using computed results, a rigorous criterion is required which involves the chemical and physical phenomena governing the reactor behaviour. But because of the highly nonlinear nature of the problem, a semi-empirical approach may be required.

The stability of the reactor requires further study to establish the degree of conservation of the derived criteria. They indicate that the major factor which determines the reactor stability arises from its heterogeneity, and manifests itself in the catalyst particle. The fluid

mechanisms seem to be of minor importance. Examination of the fluid and solid contributions to the stability of the reactor is required. This may be verified by comparison with the method now available[109] which is based on representing areas of potential instability of the particle, in relation to reactor trajectories, on a phase diagram.

Finally, although the present work has been theoretical it is clear that the reliability of the models can only be finally established by comparing the predictions of the models with the results obtained from real systems. There is some indication that they are basically correct. Clearly, it is not feasible to carry out experimental work on the stability problem. Nevertheless, there is ample scope for confirming the fundamental findings reported here and they can be used to identify areas where safe experiments can be conducted. The current experimental work of the Reactor Group on this problem will then be able to exploit the findings reported here.

APPENDIX 1

THE CATALYST PELLET MODELS

A1.1 The fully distributed catalyst pellet model

A1.1.1 The steady state

For a spherical catalyst pellet in which the n^{th} order complex reaction $A \xrightarrow{K_1} B \xrightarrow{K_2} C$, $A \xrightarrow{K_3} D$ with Arrhenius kinetics occurs, a mass balance on species A and B in dimensionless form gives:(46)

$$\frac{d^2C_{pA}}{dy^2} - \frac{2}{(1-y)}\frac{dC_{pA}}{dy} - (K_1 C_{pA}^{n_1} + K_3 C_{pA}^{n_3}) = 0.0 \qquad (A1.1)$$

$$\frac{d^2C_{pB}}{dy^2} - \frac{2}{(1-y)}\frac{dC_{pB}}{dy} + \delta K_1 C_{pA}^{n_1} - \delta K_2 C_{pB}^{n_2} = 0.0 \qquad (A1.2)$$

Similarly a heat balance gives:

$$\frac{d^2T_p}{dy^2} - \frac{2}{(1-y)}\frac{dT_p}{dy} + H(K_1 C_{pA}^{n_1} + H_2K_2 C_{pB}^{n_2} + H_3K_3 C_{pA}^{n_3}) = 0 \qquad (A1.3)$$

with boundary conditions

$$\frac{dC_{pA}}{dy} = \frac{dC_{pB}}{dy} = \frac{dT_p}{dy} = 0 \qquad \text{at } y = 1 \qquad (A1.4)$$

$$\frac{dC_{pA}}{dy} = 0.5\ Sh_A\ (C_{pA} - CA)$$

$$\frac{dC_{pB}}{dy} = 0.5\ Sh_B\ (C_{pB} - CB) \qquad \text{at } y = 0 \qquad (A1.5)$$

$$\frac{dT_p}{dy} = 0.5\ Nu\ (T_p - T)$$

where $C_{pA} = \frac{C^*_{pA}}{C_o}$, $CA = \frac{C_{FA}}{C_o}$, $C_{pB} = \frac{C^*_{pB}}{C_o}$, $CB = \frac{C_{FA}}{C_o}$,

$$Tp = \frac{R_g T_p^*}{E_1}, \quad T = \frac{R_g TF}{E_1}, \quad y = 1 - {}^{s}/_{b}$$

$$K_i = \theta_i^2 \exp(-\frac{E_i}{E_1 Tp}) \qquad i = 1,2,3$$

$$\theta_i^2 = \frac{b^2 A_{Oi}}{DP_A} \quad C_o^{n_i-1} \qquad H_2 = \frac{(-\Delta H_2)}{(-\Delta H_1)} \qquad H_3 = \frac{(-\Delta H_3)}{(-\Delta H_1)}$$

$$H = \frac{(-\Delta H_1)\ DP_A\ C_O R_g}{K_p E_1} \qquad Nu = \frac{2bh}{K_p}$$

$$Sh_A = \frac{2bK_{C_A}}{DP_A} \qquad Sh_B = \frac{2bK_{C_B}}{DP_B} \qquad \delta = \frac{D_{p_A}}{D_{p_B}}$$

Equations (A1.1) to (A1.5) may be solved numerically to give the temperature and concentration profiles in the pellet.

The effectiveness factor $$\eta = \frac{1.5\ Sh_A(CA - C_{pA\ y=0})}{(K_1 C_{pA}^{n_1} + K_3 C_{pA}^{n_3})} \qquad (A1.6)$$

and the selectivity $$\gamma = \frac{Sh_B(CB - C_{pB\ y=0})}{Sh_A(C_{pA\ y=0} - CA)} \qquad (A1.7)$$

A1.2 The lumped thermal resistance model of the catalyst particle

A1.2.1 The steady state

In this model the resistance to heat transfer within the catalyst particle is assumed to be negligible and the pellet is, therefore, isothermal. Thus, the temperature, Tp, is constant throughout the pellet. The mass balances on the pellet are identical with that for the fully distributed model given above. However, since Tp is not a function of y, equations (A1.1) and (A1.2) may be solved analytically for first order reactions (i.e. n = 1) to give the concentration profiles in the pellet.

For non-first order reactions a pseudo first order form of the rate expression may be used[46] and the parameter θ_i^2 is then redefined by

$$\theta_i^2 = \frac{b^2 A_{Oi}\ C_{pA}^{n_i-1}}{D_{p_A}}$$

A heat balance on the isothermal catalyst pellet gives, in dimensionless form:

$$B_0\left[\frac{Sh_A(CA - C_{pAS})(K_1(1 + H_2) + K_3H_3)}{(K_1 + K_3)} - Sh_B(C_{pBS} - CB)H_2\right] - Tp + T = 0 \qquad (A1.8)$$

where $C_{pAS} = C_{pA}\Big|_{y=0}$ and $C_{pBS} = C_{pB}\Big|_{y=0}$

$$B_0 = \frac{(-\Delta H_1)\ C_0 DP_A R_g}{2bhE_1}$$

The analytical solution of equations (A1.1 and A1.2) then gives the two concentration profiles within the pellet in terms of the unknown temperature Tp, which must be obtained by choosing a value to satisfy the heat balance on the pellet given by (A1.8).

The analytical solution of (A1.1) and (A1.2) takes the following form:

$$C_{pAS} = \frac{0.5\ Sh_A\ CA}{0.5\ Sh_A - 1 + \sqrt{K_1 + K_3}\ \mathrm{Coth}(\sqrt{K_1 + K_3})} \qquad (A1.9)$$

$$C_{pBS} = P_2 - P_1 \qquad (A1.10)$$

where $P_1 = \frac{K_1\ C_{pAS}}{K_1 + K_3 - \delta K_2}$

$$P_2 = \frac{0.5\ Sh_B CB + P_1((0.5\ Sh_B - 1) + \sqrt{K_1 + K_2}, \mathrm{Coth}(\sqrt{K_1 + K_3}))}{(0.5\ Sh_B - 1) + \sqrt{\delta K_2}\ \mathrm{Coth}\sqrt{\delta K_2}}$$

when $K_2 \neq K_1 + K_3$

and $C_{pBS} = P_4 - P_3 \qquad (A1.11)$

where $P_3 = \frac{K_1\ C_{pAS}}{2\sqrt{K_1 + K_3}\ \tanh(\sqrt{K_1 + K_3})}$

$$P_4 = \frac{0.5\ Sh_B\ CB + P_3(0.5\ Sh_B + \sqrt{K_1 + K_3}\ \tanh(\sqrt{K_1 + K_3}))}{(0.1\ Sh_B - 1) + \sqrt{K_1 + K_3}\ \mathrm{Coth}(\sqrt{K_1 + K_3})}$$

when $K_2 = K_1 + K_3$

These expressions for C_{pAS} and C_{pBS} may be substituted into equation (A1.8) which can then be solved for T_p by any of the usual root finding techniques, such as Newton Raphson.

A1.2.2 The unsteady state

In the case of the fully distributed model given by equations (A1.1) to (A1.5), a time derivative is added (46) in which the heat capacitance term $K_T = \frac{\rho^* Cp^* b^2}{K_p}$ is much larger than the mass capacitance $K_{C_A} = \frac{b^2 \rho^*}{Dp_A}$ or $K_{C_B} = \frac{b^2 \rho^*}{Dp_B}$ (see Chapter Two or reference 46), and usually the latter are neglected, thus the concentrations are considered at a pseudo-steady state.

In the case of the isothermal pellet formulation an unsteady state heat balance gives:(46)

$$\frac{2}{3}\frac{K_T}{Nu}\frac{dT_p}{d\tilde{t}} = T - T_p + B_0\left[\frac{Sh_A(CA-C_{pAS})(K_1(1+H_2)+K_3H_3)}{K_1+K_3}\right.$$

$$\left. - Sh_B H_2(C_{pBS} - CB)\right] \qquad (A1.12)$$

where C_{pAS} and C_{pBS} are given by equations (A1.9) and (A1.10) or (A1.11). Equation (A1.12) may be conveniently solved using the Runge Kutta Merson algorithm.

A1.3 Introduction to the collocation method

Almost all the numerical methods in current use for solving differential equations apply polynomial approximation, but by far the most widely used are based upon reformulation of Taylor Series expansions. Because of the difficulties encountered in derivative evaluations, formulations based on judicious combinations of function values have led to Runge Kutta methods to integrate initial value problems.

For boundary value problems, the partial derivatives are approximated by finite differences which is also really a representation based on Taylor Series. The implicit representation, which is an iterative method, is always preferred because of numerical stability considerations. This finite difference representation leads to a system of algebraic equations which, because it is slowly convergent, usually takes long computation times and sometimes cannot be justified. If a global equidistant approximation is employed, the problems of divergence arises,[121] but the global approximation methods based on orthogonal polynomials such as Galerkin, variational methods or orthogonal collocation always lead to a convergent solution. Approximate methods produce the solution in the form of functions which are close, in some sense, to the exact solution of the problem. Thus, they may be classified into the broad category[122] of asymptotic, weighted residual and iterative methods. Combination of more than one of these may be used in developing the approximate solution.

The weighted residual methods require the approximate solution to be close to the exact solution in the sense that the difference between them is minimized in some sense. The approximate solution can be represented in the following linear form:

$$Y(x) = \sum_{i=1}^{n} c_i Q_i + Q_0 \qquad \text{(A1.13)}$$

where the Q_i is a set of trial functions chosen beforehand. The Q_i may be chosen to satisfy either the boundary condition or the differential equation or perhaps neither of them. The Q_i are linearly independent and may be functions of all the independent variables. In which case the c_i are undetermined parameters. One or more of the variables may not be included in the choice of Q_i, and then the c_i are undetermined functions. In the weighted residual methods, the c_i are so chosen as to make a weighted average of the equation residuals vanish.

Some linear approximation operators used to represent the linear differential operators are:(121)

Taylor Series $$L_n(f,x) = \sum_{o}^{n-1} f^i(x_o) \frac{(x - x_o)^i}{i\,!} \qquad (A1.14)$$

Jacobi Series $$L_n(f,x) = \sum_{o}^{n-1} a_i^{(n)} P_i(x) \qquad (A1.15)$$

Fourier Series $$L_{n+1}(f,x) = \frac{a_o}{2} + \sum_{K=1}^{n} (a_K \cos Kx + b_K \sin Kx) \qquad (A1.16)$$

And associated with every approximation operator is a distance function

$$E_n(f,x) = f(x) - L_n(f,x) \qquad (A1.17)$$

where $E_n(f,x)$ represents a distance measure at any point x on the interval of approximation between the exact solution $f(x)$ and the approximate one $L_n(f,x)$. It follows that the best approximation operator is one that minimizes some functional derived from $E_n(f,x)$. A suitable functional form is the norm $L_p(f) = \left[\int_a^b (|E_n(f,x)|^p dx)\right]^{1/p}$

$$p \geqq 1 \qquad (A1.18)$$

Our purpose here is to use collocation, which is one of the class of weighted residual methods which capitalizes on the properties of orthogonal polynomials, where the parameters $a_i^{(n)}$ are given by (A1.15), or c_i which are given by (A1.13) and chosen such that the norm (A1.18) is a minimum. Now let $f(x)$ be the function to be approximated for which $\int_a^b w(x)\,(f(x))^2 dx$ exists and let $P_i(x)$ be a set of orthogonal functions for which $\int_a^b w(x) P_i(x) P_J(x) dx = c_i\, \delta_{iJ}$, $\delta_{iJ} = 0$ for $i \neq J$

$\delta_{ij} = 1$ for $i = J$ (A1.19)

Then the best set of parameters $a_i^{(n)}$ can be obtained as

$$a_i = \frac{1}{c_i} \int_a^b w(x)\, P_i(x)\, f(x) dx \qquad (A1.20)$$

for which the weighted norm

$$L_2(f) = \left(\int_a^b w(x)(f(x) - L_n(f,x))^2 dx\right)^{\frac{1}{2}} \qquad (A1.21)$$

is a minimum.

$w(x)$ is assumed to be integrable but not necessarily continuous over the interval a to b, where x (a,b).

Now let $w(x) = x^{\beta}(1-x)^{\alpha}$ for an orthogonality interval (0,1). Then the set of approximation orthogonal functions given in (A1.15) as $P_i(x)$, or $Q_i(x)$ as in (A1.13), are called Jacobi polynomials $P_n(x)^{(\alpha,\beta)}$ and they satisfy the condition

$$\int_0^1 w(x)\, P_n{}^{(\alpha,\beta)}(x)\, P_J{}^{(\alpha,\beta)}(x)\, dx = C_n\, \delta_{nJ} \qquad (A1.22)$$

where $\delta_{nJ} = 1$ for $n = J$

$\delta_{nJ} = 0$ for $n \neq J$

If $w(x) = 1$ i.e. $\alpha = 0$, $\beta = 0$, then the functions are Legendre polynomial.

$w(x) = (1-x)$ i.e. $\alpha = 1$, $\beta = 0$, then the functions are Jacobi polynomial.

$w(x) = (1-x)^{\frac{1}{2}}$ i.e. $\alpha = \frac{1}{2}$, $\beta = 0$, then the functions are Chebyschef polynomial.

These polynomials are given explicitly by[121]

$$P_n{}^{(\alpha,\beta)}x^{\beta}(1-x)^{\alpha} = \frac{(-1)^n \Gamma(\beta+1)}{\Gamma(n+\beta+1)} \frac{d^n}{dx^n}\left[x^{n+\beta}(1-x)^{n+\alpha}\right] = (-1)^n x^{\beta}(1-x)^{\alpha}$$

$$\sum_{K=0}^{n} h_K\, x^K (x-1)^{n-K} \qquad (A1.23)$$

where the coefficients h_K are functions of α, β, n and K.

If the first two members of these polynomials are known, i.e. P_n where n = 1 and 2, the following recurrence formula can be used to generate the members for $n > 2$.

$$P_n(x) = \frac{(2n+\alpha+\beta)(2n+\alpha+\beta-1)}{2(n+\beta)(n+\alpha+\beta)}\left(2x-1 + \frac{\alpha^2-\beta^2}{(2n+\alpha+\beta-2)(2n+\alpha+\beta)}\right)P_{n-1}(x)$$

$$- \frac{(n-1)(n+\alpha-1)(2n+\alpha+\beta)}{(n+\beta)(n+\alpha+\beta)(2n+\alpha+\beta-2)}\, P_{n-2}{}^{(x)} \qquad (A1.24)$$

and the coefficients defined in equation (A1.22) and used in (A1.20) are then given by[121]

$$C_n = \frac{\Gamma(\beta+1)^2\, n!\, \Gamma(n+\alpha+1)}{\Gamma(n+\beta+1)\,\Gamma(n+\alpha+\beta+1)(2n+\alpha+\beta+1)} \qquad (A1.25)$$

Putting $x = u^2$

$$\text{in}\int_0^1 (1-u^2)^{\alpha}\, u^{2\beta+1}\, P_i(u^2)P_J(u^2)du = \frac{C_i}{2}\,\delta_{iJ} \qquad (A1.26)$$

Defining $2\beta+1 = a$ we obtain, for $a = 0$, 1 and 2, plane, cylindrical and spherical symmetries respectively.

This even power series is suitable for symmetrical problems. The zeros of these orthogonal polynomials are well tabulated.[121,123]

A1.4 Orthogonal Collocation

In the solution of boundary value problems the solution can be represented in a similar form, to that used in other weighted residual methods where Y_n is expressed (the desired ordinate solution) as a perturbation to the boundary function.

$$Y_n(x) = Y(1) + (1-x^2)\sum_{0}^{n-1} a_i P_i(x^2) \qquad (A1.27)$$

This takes advantage of the symmetry of the problem to be solved to express Y_n as a sum of even polynomials.

The explicit representation of Y_n as a boundary function added to a weighted sum of trial functions $((1-x)^2 P_i(x^2))$ may in fact obscure the simplicity of the orthogonal collocation method, which does not make use of (A1.27) in the more satisfactory numerical schemes. Nevertheless, a solution of the form as presented in (A1.27) can be used to obtain the values of a_i, as will be illustrated later.

The assumption of a power series allows derivative terms in a system of differential equations to be expressed as a linear combination, and so can be carried forward to the trial solution represented by (A1.27),

or more simply $Y_n = \sum_{i=0}^{n-1} a_i^{(n)} P_i(x^2)$. Either of these forms can be represented as a series

$$Y_n(x) = \sum_{i=1}^{n} a_i x^{2i-2}$$

$$\text{i.e. } Y(x_1) = a_0 + a_1 x_1^2 + a_2 x_1^4 + \ldots\ldots\ldots + a_n x_1^{2n}$$

$$Y(x)_{n+1} = a_0 + a_1 x_{n+1}^2 + a_2 x_{n+1}^4 + \ldots\ldots\ldots + a_n x_{n+1}^{2n}$$

Now identify

$$Q_0 = \begin{bmatrix} 1 & x_1^2 & x_1^4 & & x_1^{2n} \\ 1 & x_2^2 & x_2^4 & & x_2^{2n} \\ & & & & \\ 1 & x_{n+1}^2 & x_{n+1}^4 & & x_{n+1}^{2n} \end{bmatrix}$$

where n = number of interior zeros of the orthogonal polynomial used $x_1, x_2, \ldots\ldots x_n$ and $x_{n+1} = 1$ to take account of the boundary condition at x = 1.

At any collocation point n, the first derivative can be represented by $\left.\frac{dY(x_i)}{dx}\right|_i = 2a_1 x_i + 4a_2 x_i^3 + \ldots\ldots\ldots 2na_n x_i^{2n-1}$

and for the Laplacial operator.

$$\left.\frac{1}{x^m}\frac{d}{dx}\left(x^m \frac{dY}{dx}\right)\right|_{x=x_i} = 4a_1 + 16a_2 x_i^2 + \ldots\ldots 4n^2 a_n x_i^{2n-2}$$

where i = 1,2,..... n+1, m = 1 for cylindrical co-ordinates. Therefore for the first and second derivatives Q_1 and Q_2 can be identified as follows:

$$Q_1 = \begin{bmatrix} 0 & 2x_1 & 4x_1^3 & & 2nx_1^{2n-1} \\ & & & & \\ 0 & 2x_{n+1} & 4x_{n+1}^3 & & 2nx_{n+1}^{2n-1} \end{bmatrix}$$

$$Q_2 = \begin{bmatrix} 0 & 4 & 16x_1^2 & 4n^2x_1^{2n-2} \\ \\ 0 & 4 & 16x_{n+1}^2 & 4n^2x_{n+1}^{2n-2} \end{bmatrix}$$

Therefore the linear differential operators can be approximated by the following expressions:

$$\left.\frac{dY}{dx}\right|_{x_J} = \hat{Q}_o^{-1} Q_1 \, Y(x_i) = \sum_{i=1}^{n+1} A_{J,i} \, Y(x_i) \qquad \text{(A1.28)}$$

$$\left.\frac{1}{x}\frac{d}{dx}\left(x\frac{dY}{dx}\right)\right|_{x_J} = Q_o^{-1} Q_2 \, Y(x_i) = \sum_{i=1}^{n+1} B_{J,i} \, Y(x_i) \qquad \text{(A1.29)}$$

where J = 1, 2, ...n+1.

A1.4.1 Determination of the parameters $a_i^{(n)}$

The parameters $a_i^{(n)}$ are determined by the solution at the collocation points, i.e. at $Y(x_1)$, $Y(x_2)$, ... $Y(x_{n+1})$; or from the interior ordinates when different quadrature formulae are used. Based on Gauss-Jacobi formulae, the trial solution given by (A1.27) can be put in the following form:

$$\frac{Y_n(x) - Y(1)}{1 - x^2} = \sum_{i=0}^{n-1} a_i^n \, P_i(x^2) \qquad \text{(A1.30)}$$

Multiply both sides by $w(x^2)$ and $P_J(x^2)$ and integrate from 0 to 1. Since $P_J(x^2)$ is at most a polynomial of degree n-1 in x^2 and $\dfrac{Y_n(x) - Y(1)}{1 - x^2} P_J(x^2)$ is at most a polynomial of degree 2n-2 in x^2, the following quadrature is exact.

$$\sum_{i=0}^{n-1} a_i \int_0^1 w(x^2) \, P_i(x^2) \, P_J(x^2) \, dx^2 = C_i a_i$$

$$= \sum_{K=1}^{n} w_K \frac{Y_n(x_K^2) - Y(1)}{1 - x_K^2} \cdot P_J(x_K^2)$$

where $C_i = \int_0^1 w(x^2) \, P_i(x^2) P_i(x^2) \, dx^2$

and $w(x)$ = the quadrature weights differ for different polynomials.

$$\text{Therefore } a_i^{(n)} = \sum_{I=0}^{n-1} \frac{1}{C_i} \sum_{K=1}^{n} w_K \frac{Y_n(x_K^2) - Y(1)}{1 - x_K^2} \cdot P_i(x_K^2) \qquad \text{(A1.31)}$$

The solution can therefore be generated at different positions between the collocation points from the trial solution (A1.27). In fact it is possible to generate such solutions without determining the parameters $a_i^{(n)}$ at all, by using a Lagrangian interpolation formula[121] based on

$$Y(x_J^2) \text{ and } Y(1)$$

$$Y(x) \sim Y_n(x) = \sum_{I=1}^{n+1} \frac{P_{n+1}(x^2)}{(x^2 - x_i^2) P_{n+1}^{(1)}(x_i^2)} Y(x_i^2)$$

where $P_{n+1}(x^2) = (x^2-1)\,(x^2-x_1^2)\,(x^2-x_2^2) \ldots\ldots (x^2-x_n^2)$

and $P_{n+1}^{(1)}(x_i^2) = \left.\frac{dP_{n+1}}{dx^2}\right|_{x^2 = x_i^2}$ $\qquad i = 1, 2, \ldots\ldots n+1$

A1.4.2 Unsymmetric collocation coefficients

If the problem is unsymmetric, the coefficients for the first and second order differential operator can still be obtained.[117,124]

In this case, the collocation points will be $x_1, x_2, x_3, \ldots\ldots x_m$, the interior zeros of the orthogonal polynomial and $x_{m+1} = 0$ and $x_{m+2} = 1$ to take account of the boundaries at both ends of the integration interval 0 and 1 respectively. Thus following the same argument as before:

$$\left.\frac{dY(x)}{dx}\right|_{x_J} = \begin{bmatrix} 1 & x_1 & x_1^2 & \cdots & x_1^{m+2} \\ \vdots & & & & \\ 1 & x_{m+2} & x_{m+2}^2 & \cdots & x_{m+2}^{m+2} \end{bmatrix}^{-1} \begin{bmatrix} 0 & 1 & 2x_1 & \cdots & (m+2)x_1^{m+1} \\ \vdots & & & & \\ 0 & 1 & 2x_{m+2} & \cdots & (m+2)x_{m+2}^{m+1} \end{bmatrix} \begin{bmatrix} Y(x_1) \\ \vdots \\ Y(x_{m+2}) \end{bmatrix}$$

$$= Q_0^{-1} Q_1 Y_n(x_J) = \sum_{I=1}^{m+2} AA_{J,i}\, Y(x_i) \qquad \text{(A1.32)}$$

where $J = 1, 2, \ldots\ldots m+2$

and for the Laplacial operator

$$\frac{1}{x^m}\frac{d}{dx}\left(x^m \frac{dY(x)}{dx}\right)\Big|_{x_J} = Q_0^{-1} Q_2 Y_m(x_J)$$

$$= \sum_{i=1}^{m+2} BB_{J,i}\, Y(x_i) \qquad \text{(A1.33)}$$

Note: In the case of an unsymmetrical problem, no use can be made of the even power representation. Accuracy of computing the coefficients AA_s and BB_s for large m is restricted by the process of matrix inversion. In this case the method described in reference (124) is recommended.

Tables (A1.1 to A1.3) give some of the coefficient values used in Chapter 3.

A1.5 Double Collocation

The process leading from the original partial differential equation to the discretized system of algebraic equations, as in the finite difference formulation, may be divided into two steps. The first is a discretization in one independent variable, say the r-direction. The second is a discretization in the other independent variable, say the z-direction. Thus, for a partial differential equation in two independent variables discretization of only one variable leads to a system of ordinary differential equations. These can be integrated explicitly e.g. by Runge Kutta methods, or implicitly e.g. by finite differences.

The second discretization is in reality a numerical method for integration. Collocation or a quadrature method can be used as well as an integration method. Thus by double collocation it is implied that the collocation method is used to discretize the two independent variables in the radial and axial directions.(117)

Method of solution

Consider the following scheme representing the location of the collocation points in the space co-ordinates of a tubular reactor. Taking three points in the radial direction (i.e. $N_{total} = 4$) and two points in the axial direction (i.e. $M_{total} = 4$).

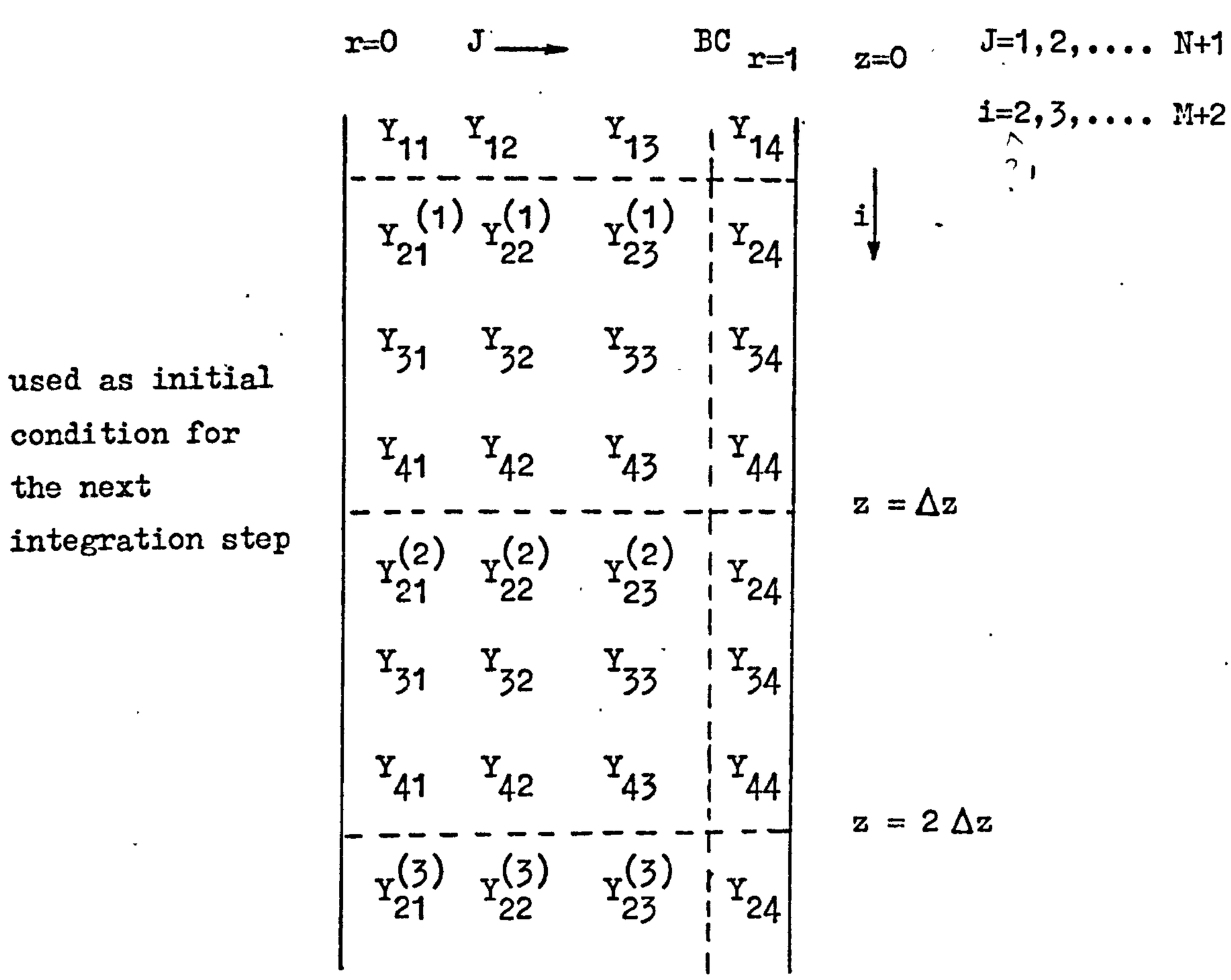

where $Y_{J,i}$ = A state variable, e.g. temperature or concentration.

N = number of interior zeros used in the r-direction, i.e.

$r_1^2, r_2^2, \ldots . r_N^2,$

and $r_{N+1}^2 = 1$ for the boundary condition (using an even polynomial because of the symmetry).

M = number of interior zeros used in the z-direction, i.e.

$z_1, z_2, \ldots . z_M$ and $z_{M+1} = 0$ and $z_{M+2} = 1$ to account for boundary condition at both ends of an integration step.

Δz = axial integration step.

The differential operator in the radial direction can be approximated

at the above collocation points as follows.

$$\frac{1}{r}\frac{\partial}{\partial r}\left(r\frac{\partial Y}{\partial r}\right)\Big|_{i,J} = B_{J,1}\,Y_{i,1} + B_{J,2}\,Y_{i,2} + B_{J,3}\,Y_{i,3} + B_{J,4}\,Y_{i,4} \qquad \text{(A1.34)}$$

in matrix form = $\left[Y_{i,1,2,3,4}\right]\left[B\right]$ $\qquad J = 1,2,3$

$\qquad\qquad\qquad\qquad\qquad\qquad\qquad\qquad\qquad\qquad\qquad\qquad\qquad\qquad i = 2,3 \text{ and } 4$

and the differential operator in the axial direction can be approximated at the collocation points as follows:

$$\left(\frac{\partial Y}{\partial z}\right)\Big|_{i,J} = AA_{i,1}\,Y_{1,J} + AA_{i,2}\,Y_{2,J} + AA_{i,3}\,Y_{3,J} + AA_{i,4}\,Y_{4,J} \qquad \text{(A1.35)}$$

$J = 1,2 \text{ and } 3$

$i = 2,3 \text{ and } 4$

in matrix form = $\left[AA\right]\left[Y_{1,2,3,4,J}\right]$

The partial differential equation without the non-linear term with an axial step Δz can be represented as follows:

$$\Delta z\,\frac{\partial Y}{\partial z} = \frac{1}{r}\frac{\partial}{\partial r}\left(r\frac{\partial Y}{\partial r}\right)$$

Substituting for the differential operators by these matrix approximations

$$\Delta z\left[Y\right]\left[B\right] = \left[AA\right]\left[Y\right]^{T} \qquad \text{(A1.36)}$$

The above matrix equation can be reformulated into a set of linear algebraic equations.

The boundary conditions in the radial direction at r = 1 can be approximated as follows:

$$\frac{\partial Y}{\partial r}\Big|_{i,J} = A_{J,1}\,Y_{i,1} + A_{J,2}\,Y_{i,2} + A_{J,3}\,Y_{i,3} + A_{J,4}\,Y_{i,4}$$
$$= N_{uw}\left(Y_c - Y_{i,4}\right) \qquad \text{(A1.37)}$$

in case of concentrations, this approximation will be equated to zero, i.e. $N_{uw} = 0$.

These equations resulting from boundary approximation at r = 1 can be substituted back into the system of equations obtained from (A1.34),

thus reducing the number of algebraic equations by one. The reformulation of the algebraic system (A1.36) in matrix form, the equation becomes:

$$\left[Q \right] \left[Y \right] = \left[V \right]$$

This matrix equation can be combined with the non-linear terms R to give the following form:

$$\left[Q \right] \left[Y \right] = \left[V \right] - \left[R \right] \qquad \text{(A1.38)}$$

which can be solved iteratively either by Newton Raphson or by simple matrix inversion.

$$
\left[\ Q\ \right] = \begin{bmatrix}
(AA_{22}-Q_{11}) & AA_{23} & AA_{24} & -Q_{12} & 0 & 0 & -Q_{13} & 0 & 0 \\
AA_{32} & (AA_{33}-Q_{11}) & AA_{34} & 0 & -Q_{12} & 0 & 0 & -Q_{13} & 0 \\
AA_{42} & AA_{43} & (AA_{44}-Q_{11}) & 0 & 0 & -Q_{12} & 0 & 0 & -Q_{13} \\
-Q_{21} & 0 & 0 & (AA_{22}-Q_{22}) & AA_{23} & AA_{24} & -Q_{23} & 0 & 0 \\
0 & -Q_{21} & 0 & AA_{32} & (AA_{33}-Q_{22}) & AA_{34} & 0 & -Q_{23} & 0 \\
0 & 0 & -Q_{21} & AA_{42} & AA_{43} & (AA_{44}-Q_{22}) & 0 & 0 & -Q_{23} \\
-Q_{31} & 0 & 0 & -Q_{32} & 0 & 0 & (AA_{22}-Q_{33}) & AA_{23} & AA_{24} \\
0 & -Q_{31} & 0 & 0 & -Q_{32} & 0 & AA_{32} & (AA_{33}-Q_{33}) & AA_{34} \\
0 & 0 & -Q_{31} & 0 & 0 & -Q_{32} & AA_{42} & AA_{43} & (AA_{44}-Q_{44})
\end{bmatrix}
$$

$$\left[\ Y\ \right] = \begin{bmatrix} Y_{21} \\ Y_{31} \\ Y_{41} \\ Y_{22} \\ Y_{32} \\ Y_{42} \\ Y_{23} \\ Y_{33} \\ Y_{43} \end{bmatrix}$$

and

$$\left[\ V\ \right] = \begin{bmatrix} \underbrace{\frac{B_{14}\ N_{uw}}{A_{14}+N_{uw}}\ Y_c}_{\text{B.C.}} - \underbrace{AA_{21}\ Y_{11}}_{\text{I.C.}} \\ \frac{B_{14}\ N_{uw}}{A_{14}+N_{uw}}\ Y_c - AA_{41}\ Y_{11} \\ \frac{B_{24}\ N_{uw}}{A_{24}+N_{uw}}\ Y_c - AA_{21}\ Y_{12} \\ \frac{B_{24}\ N_{uw}}{A_{24}+N_{uw}}\ Y_c - AA_{41}\ Y_{12} \\ \frac{B_{34}\ N_{uw}}{A_{34}+N_{uw}}\ Y_c - AA_{21}\ Y_{13} \\ \frac{B_{34}\ N_{uw}}{A_{34}+N_{uw}}\ Y_c - AA_{41}\ Y_{13} \end{bmatrix}$$

Note: In the case of using the above general matrix for concentration calculations, put Y_c, the coolant temperature, and N_{uw} (Nusselt number) equal to zero.

The reaction rate terms, together with the pellet equations given in the general matrix R , are evaluated at the following points:

$$\left[\ R\ \right] = \begin{bmatrix} R_{21}(T_{21}, CA_{21}, CB_{21}) \\ R_{31}(T_{31}, CA_{31}, CB_{31}) \\ R_{41}(T_{41}, CA_{41}, CB_{41}) \\ R_{22}(T_{22}, CA_{22}, CB_{22}) \\ R_{32}(T_{32}, CA_{32}, CB_{32}) \\ R_{42}(T_{42}, CA_{42}, CB_{42}) \\ R_{23}(T_{23}, CA_{23}, CB_{23}) \\ R_{33}(T_{33}, CA_{33}, CB_{33}) \\ R_{43}(T_{43}, CA_{43}, CB_{43}) \end{bmatrix}$$

The elements Q_{iJ} are given as follows:

$$Q_{i,J} = \Delta Z\, B_{i,J} - \frac{B_{i,M+1}\, A_{i,J}\, \Delta Z}{A_{i,M+1} + N_{uw}} \qquad \begin{matrix} i = 1,2,3 \\ J = 1,2,3 \end{matrix}$$

Note: In the case of concentration, put $N_{uw} = 0$.

A1.6 Computational procedure used to solve the system given by (3.13 to 3.17) in Chapter 3

1) Assume flat axial and radial profiles for T, CA and CB at the start of the integration, or use the previous profiles at the end of the previous integration step as the assumed values for the next integration step.

2) Fix the initial conditions of the state variables at the radial collocation nodes at values corresponding to those obtained at the end of the previous integration step.

3) Solve the pellet equations at each collocation point to obtain η, γ and T_p.

4) Use these values to evaluate the nonlinear terms in the system of equations at each collocation node.

5) Solve the matrix equation for new values of the state variables, as described in appendix (A1.5) (see equation A1.38).

6) Test for convergence by comparing the new values with those used in step 1. If unsatisfactory, repeat from step 3 using the new values of the state variables.

7) If satisfactory convergence is attained, repeat from step 1 while $Z < 1$.

Table (A1.1): Collocation constants for cylindrical symmetry using Jacobi zeros

N+1	i	x_i	w_i	A_{i1}	A_{i2}	A_{i3}	A_{i4}
3	1	0.393765	0.188202	-2.539584	3.825616	-1.286032	
3	2	0.803087	0.256243	-1.377677	-1.245195	2.622872	
3	3	1.0	0.055556	1.715476	-9.715476	8	
4	1	0.2976373	0.11023111	-3.359794	5.2924315	-3.1010284	1.1683903
4	2	0.63989598	0.19409673	-1.3980385	-1.5627540	4.3197367	-1.3589442
4	3	0.88750101	0.16442216	0.69721650	-3.6766754	-1.1267583	4.106272
4	4	1.0	0.03125	-1.2266754	5.4010626	-19.174387	15.0
5	1	0.2389648	0.0718567	-4.184716	6.700685	-4.2747907	2.877766
5	2	0.5261587	0.140677	-1.5544544	-19005672	5.2436245	-2.8313988
5	3	0.7639309	0.155913	0.61626762	-3.258648	-1.3090185	5.6716139
5	4	0.9274913	0.111551	-0.47760638	2.0256145	-6.5291519	-1.0781784
5	5	1.0	0.02	0.9607694	-3.8593337	10.244479	-31.345915

(continued from previous column)

N+1	i	A_{i5}	B_{i1}	B_{i2}	B_{i3}	B_{i4}	B_{i5}
3	1		-9.902381	12.299660	-2.397279		
3	2		9.033674	-32.76486	23.730612		
3	3		22.757482	-65.424149	42.66667		
4	1		-15.881426	19.636380	-5.2811862	1.5262327	
4	2		11.151861	-34.497415	29.235709	-5.8901550	
4	3		-3.5405872	34.512110	-99.621159	68.649637	
4	4		-33.869987	136.24969	-252.37970	150.0	
5	1	-1.1190446	-23.61752	29.147844	-7.7608926	3.4249987	-1.1344299
5	2	1.0427958	14.888399	-43.686084	35.977207	-10.214416	3.0348938
5	3	-1.7202151	-3.576814	32.461648	-78.907038	62.645594	-12.623393
5	4	6.0593207	2.2062306	-12.881386	87.558120	-237.72935	160.84638
5	5	24.0	43.962646	-171.61952	413.81625	-670.15936	384.0

Table (A1.2): Collocation constants for cylindrical symmetry using the squares of Legendre zeros

N+1	i	x_i^2	w_i	A_{i1}	A_{i2}	A_{i3}	A_{i4}
3	1	0.2113248	0.134168	-1.1744576	1.8501968	-0.6757392	
3	2	0.7886751	0.542754	-1.080966	-1.4409269	2.5218930	
3	3	1.0	0.323076	1.3706100	-8.7552254	7.3846153	
4	1	0.1227016	0.0192434	-1.4691708	1.8026562	-0.5965425	0.2630571
4	2	0.5000	0.283846	-2.220537	1.0196078	2.0104531	-0.8095238
4	3	0.8872983	0.476955	1.1175509	-3.0575581	-2.7493166	4.6893238
4	4	1.0	0.219954	-1.7580995	4.3921570	-16.729295	14.095238
5	1	0.06943184	0.0220204	-1.9476331	2.2136892	-0.35694403	0.1752583
5	2	0.3300094	0.0962283	-3.8216261	2.7872708	1.3354975	-0.57105127
5	3	0.6699905	0.311207	2.6435722	-5.7293136	1.3146075	3.059090
5	4	0.9305681	0.404049	-1.9885867	3.7532664	-4.6866995	-4.8025616
5	5	1.0	0.166493	3.3237324	-6.1591694	6.8508831	-26.819184

(continued from previous column)

N+1	i	A_{i5}	B_{i1}	B_{i2}	B_{i3}	B_{i4}	B_{i5}
3	1		-10.467457	15.873371	-5.4059136		
3	2		6.2804747	-26.455619	20.175144		
3	3		17.245355	-54.168432	36.923076		
4	1		-24.952452	30.117647	-9.1805593	4.0153650	
4	2		5.3048488	-17.882353	19.625123	-7.0476191	
4	3		-8.7466123	30.117647	-84.403290	63.032254	
4	4		-45.954990	109.17647	-190.45957	127.23809	
5	1	-0.08437034	-54.231907	61.049615	-9.1147009	4.4222004	-2.125071
5	2	0.26990897	4.0022945	-20.626417	20.723789	-7.6398847	3.5402183
5	3	-1.2879563	-1.1121886	12.996080	-35.221296	36.831517	-13.494115
5	4	7.7245804	23.422373	-46.438045	76.771487	-210.66803	156.91221
5	5		144.87523	-265.57488	276.42928	-476.47729	320.74765

Table (A1.3) Collocation constants for unsymmetrical systems using Legendre zeros

N+2	i	x_i	AA_{i1}	AA_{i2}	AA_{i3}	AA_{i4}	AA_{i5}	BB_{i1}	BB_{i2}	BB_{i3}	BB_{i4}	BB_{i5}
4	1	0.000	-7.000	8.196152	-2.196152	1.000		24.000	-37.176914	25.176914	-12.000	
4	2	0.211324	-2.732050	1.732050	1.732050	-0.732050		16.392304	-24.000	12.000	-4.392304	
4	3	0.788675	0.732050	-1.732050	-1.732050	2.732050		-4.392304	12.000	-24.000	16.392304	
4	4	1.00	-1.000	2.196152	-8.196152	7.000		-12.000	25.176914	-37.176914	24.000	
5	1	0.000	-13.000	14.788305	-2.666667	1.878361	-1.000	84.000	-122.063167	58.666667	-44.60350	24.000
5	2	0.112701	-5.323790	3.872983	2.065591	-1.290994	0.676209	53.237900	-73.33333	26.666667	-13.33333	6.762100
5	3	0.500	1.5000	-3.227468	0.000	3.227486	-1.5000	-6.000	16.666667	-21.33333	16.666667	-6.000
5	4	0.887298	-0.676210	1.290994	-2.065591	-3.872983	5.323789	6.762100	-13.333334	26.666667	-73.333334	53.237900
5	5	1.000	1.000	-1.878361	2.666667	-14.788305	13.000	24.000	-44.603501	58.66667	-122.063168	84.000

APPENDIX 2

A2.1 Computational procedure followed in solving the system given by 4.1 to 4.5

1. Assume values for CA, CB and T at the inlet conditions other than those of the steady state values at Z = 0 and $\tau > 0$.

2. Fix the initial conditions of the state variables at the radial collocation nodes at values corresponding to those obtained (at the inlet, i.e. Z = 0 or) at the end of the previous axial and present time step.

3. Let the state variables at the rest of the collocation points equal those values of the present axial step and previous time step.

4. Solve the transient pellet equations at each collocation point to obtain η, ψ and T_p at the present axial and time step.

5. Use these values to evaluate the nonlinear terms in the system of equations at each collocation node.

6. Solve the matrix equation for new values of the state variables, as described in Appendix (A1.3), equation (A1.38).

7. Test for convergence by comparing the new values with those used in step 3. If unsatisfactory, repeat from step 4 using the new values of the state variables.

8. If satisfactory convergence is attained, repeat from step 2 while $Z < 1$.

9. Repeat the whole computation for the next time step and continue as long as necessary.

For the purpose of this algorithm, it is necessary to be able to specify the values of the state variables at points other than the starting and finishing points at any time step. This is done by assuming that the change in fluid conditions are linear over one time step and that the pellet is effectively subject to a ramp change in fluid conditions. Time steps of

1.0 sec. and from 60 to 80 axial steps have been found satisfactory over the ranges of parameter values used here.

A2.2 Method of model reduction

The steps followed in lumping the distributed system given by equations (4.1 to 4.5) will be illustrated in general terms. Consider the following equation:

$$\frac{\partial T}{\partial \tau} = \frac{1}{r}\frac{\partial}{\partial r}\left(r\frac{\partial T}{\partial r}\right) - \frac{\partial T}{\partial z} + R(T) \qquad \text{(A2.1)}$$

with boundary conditions of the form

$$\frac{\partial T}{\partial r} = 0 \quad \text{at } r = 0 \qquad z \geqq 0 \qquad \text{(A2.2)}$$

$$\frac{\partial T}{\partial r} = -N_{uw}(T - 1) \quad \text{at } r = 1 \quad z \geqq 0 \qquad \text{(A2.3)}$$

The initial conditions being

$$T = T(r, \tau) \quad \text{at } \tau \geqq 0,\ Z = 0.0 \text{ and } 0 \leqq r \leqq 1$$

The radial mean value of T can be defined as

$$T(m) = \int_0^1 2T(r)\, r\, dr \qquad \text{(A2.4)}$$

Therefore by multiplying equation (A2.1) by 2rdr and integrating over the radius

$$\int_0^1 \frac{\partial T}{\partial \tau} 2rdr = 2r\frac{\partial T}{\partial r}\Big|_0^1 - \int_0^1 \frac{\partial T}{\partial z} 2rdr + \int_0^1 R(T)2rdr \qquad \text{(A2.5)}$$

Assuming that $\int_0^1 \frac{\partial T}{\partial z} 2rdr = \frac{\partial}{\partial z}\int_0^1 T\ 2rdr$ and similarly for the time derivative. Equation (A2.5), after substituting for the boundary conditions and considering equation (A2.4), can take the following form:

$$\frac{\partial Tm}{\partial \tau} = -\frac{\partial Tm}{\partial z} - 2N_{uw}(T(1) - 1) + R(Tm) \qquad \text{(A2.6)}$$

the initial conditions being $T = T(r, \hat{t})$ at $\hat{t} \geqq 0, Z$

To express equation (A2.6) in terms of mean conditions a pseudo parameter is defined as

$$Nu' = \frac{N_{uw}(T(1) - 1)}{(T(m) - 1)} \qquad (A2.7)$$

By substituting equation (A2.7) into equation (A2.6), the final form of the reduced equation is as follows:

$$\frac{\partial T_m}{\partial \hat{t}} = - \frac{\partial T_m}{\partial z} - 2Nu'(T_m - 1) + DR(T_m) \qquad (A2.8)$$

where D is a pseudo parameter defined as a distribution factor and it is the ratio of the radial mean reaction rate to the reaction rate at the radial mean conditions at any axial position.

Accuracy of this reduced model given by (A2.8) will therefore depend on adequate formulation of the two pseudo parameters Nu' and D.

A2.3 Method of Characteristics (17)

The general form of the hyperbolic system of equations given by (4.7) to (4.9) can be represented in the following general form:

$$A \frac{\partial w_i}{\partial z} + B \frac{\partial w_i}{\partial \hat{t}} = R(w_1, w_2, \ldots\ldots w_i) \qquad (A2.9)$$

where A and B are constants and $R(w_1, \ldots\ldots)$ represents the reaction term.

The transient pellet model given in appendix (A1.2.2) can be represented as follows:

$$\frac{\partial w_s}{\partial \hat{t}} = R(w_1, w_2, \ldots\ldots w_s, \ldots\ldots) \qquad (A2.10)$$

The initial conditions are

$$w(0, z) = w(z) \qquad \text{at } \hat{t} = 0 \text{ and } z \geqq 0$$

$$w(\hat{t}, 0) = w(\hat{t}) \qquad \text{at } z = 0 \text{ and } \hat{t} \geqq 0$$

Consider the $\hat{t}$-Z plane shown in Figure A2.1 and two families of lines I and II such that

$$\frac{d\tilde{\tau}}{dz} = \left(\frac{A}{B}\right)^{-1} \text{ for the line I} \qquad \text{(A2.11)}$$

$$\text{and } Z = \text{constant for the line II} \qquad \text{(A2.12)}$$

These curves are plotted in figure A2.1 and are known as the characteristics of the differential equations (A2.9) and (A2.10).

$$\text{Since } \frac{dw}{dz} = \frac{\partial w}{\partial z} + \frac{\partial w}{\partial \tilde{\tau}} \frac{d\tilde{\tau}}{dz}$$

along an arbitrary direction in the $\tilde{\tau}$-Z plane, then along any characteristic I

$$\left(\frac{dw}{dz}\right)_I = R(w_1, w_2, \ldots . w_i)/A \qquad \text{(A2.13)}$$

because of equations (A2.9) and (A2.11) the above notation denotes the derivative of w along the characteristic

$$\tilde{\tau} = Z + \text{constant}$$

On the other hand, along any characteristic II

$$\left(\frac{dw_s}{d\tilde{\tau}}\right)_{II} = R(w_1, w_2, \ldots . w_s, \ldots) \qquad \text{(A2.14)}$$

Finally the initial conditions can be transformed into

$$\left(\frac{dw_i}{dz}\right)_I = R(w_i(\tilde{\tau}, 0)) \text{ along the characteristic } \tilde{\tau} = Z \qquad \text{(A2.15)}$$

$$\left(\frac{dw_s}{d\tilde{\tau}}\right)_{II} = R(w_i(0, z), \ldots w_s) \text{ along the characteristic Z}$$

$$= \text{constant} \qquad \text{(A2.16)}$$

These two equations are now two independent ordinary differential equations which have to be solved numerically along I and II with

$$\tilde{\tau} = Z + K\Delta\tilde{\tau}$$

$$\text{and } Z = L\Delta Z$$

where $\Delta\tilde{\tau}$ and ΔZ are arbitrary steps and K and L are integers depending on the accuracy of integration required.

The initial conditions enable the values of w_i and w_s at points

(0,J) and (J,0) to be calculated a priori for all integers J > 0

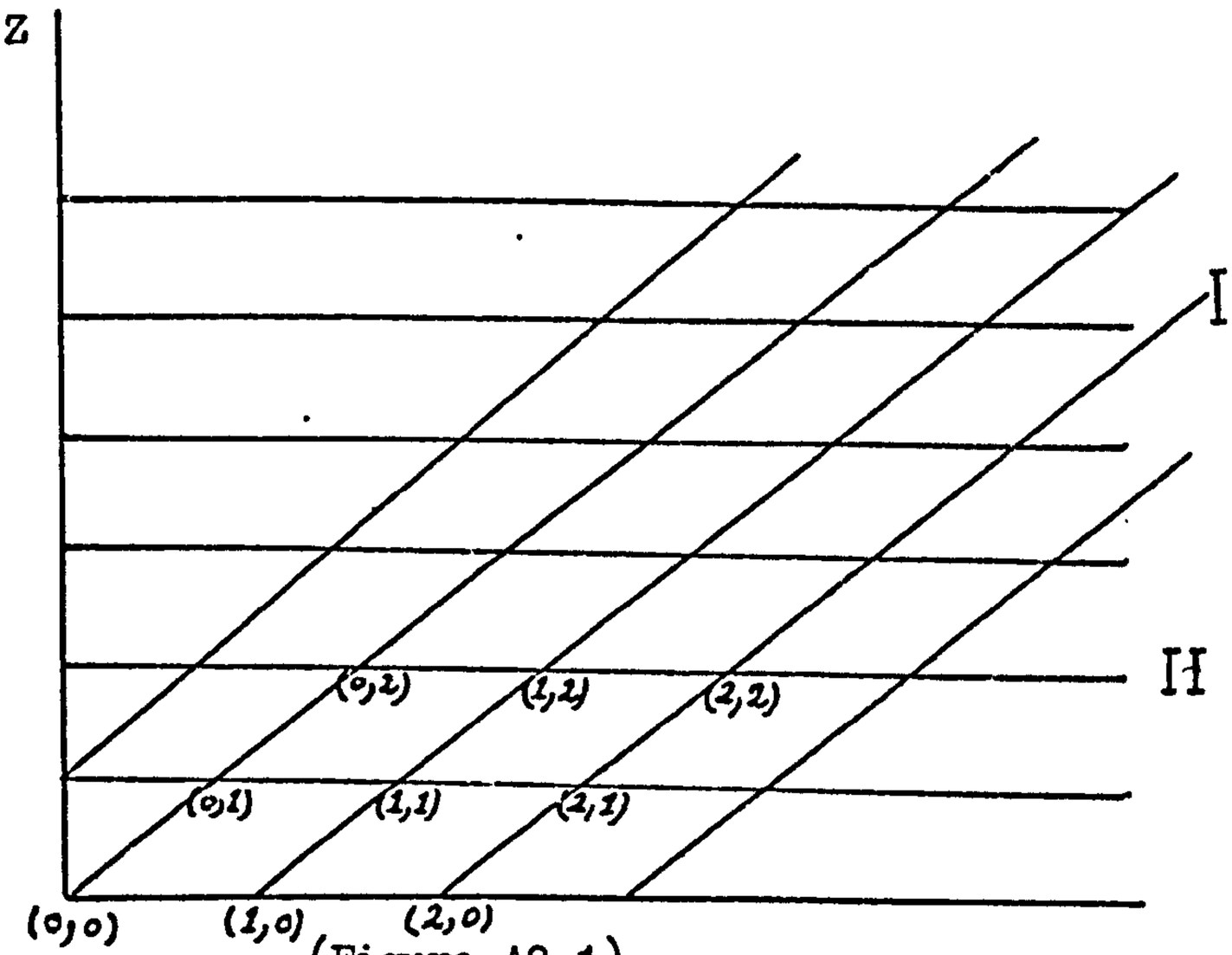

(Figure A2.1)

The significance of equation (A2.16) is self evident, since at $Z = 0.0$, $w_i = w_{i0}$ for all times. On the other hand, equation (A2.15) may be justified by the following physical reasoning. If the continuity equations are written down in the Lagrangian form, then it can easily be shown that the characteristic I describes the trajectories in the $\tilde{t}$-Z plane of individual elements of fluid which enter the bed at $Z = 0$ and move through it with a velocity $\frac{dz}{d\tilde{t}} = \frac{A}{B}$ (this velocity is represented as the slope of line I). It follows that the element of fluid which enters the bed at $\tilde{t} = 0$ will move along the characteristic $\tilde{t} = Z$ (i.e. along lines I) and the solid would move along the characteristic $Z =$ constant (i.e. along lines II).

Note: If the constant B in equation (A2.9) is equal to zero, i.e. the fluid equations are considered at a speudo-steady state, then $\frac{dz}{d\tilde{t}} = \infty$ and the characteristic lines I would be vertical.

APPENDIX 3

A3.1 Derivation of the stability criterion for the radial diffusion model

The heat and mass balances given by equations (4.1 to 4.5) together with the dynamic pellet model given by equation (A1.12) are used to derive the stability criterion for small perturbations around the steady state values CA^*, CB^*, T^* and T_p^*.

Define the perturbation variables as

$$u(\tilde{t},r,Z) = CA(r,z,\tilde{t}) - CA^*(r,z)$$

$$v(\tilde{t},r,z) = CB(r,z,\tilde{t}) - CB^*(r,z)$$

$$U(\tilde{t},r,z) = T(r,z,\tilde{t}) - T^*(r,z)$$

$$V(\tilde{t},r,z) = T_p(r,z,\tilde{t}) - T_p^*(r,z)$$

By substituting these perturbed variables in the system of equations mentioned above, the following linearized set of equations may be obtained.

$$\frac{\partial u}{\partial \tilde{t}} = \frac{1}{G_5}\frac{1}{r}\frac{\partial}{\partial r}\left(r\frac{\partial u}{\partial r}\right) - \frac{G_1}{G_5}\frac{\partial u}{\partial z} + RA_a u + RA_b v + RA_t U + RA_s V \qquad (A3.1)$$

$$\frac{\partial v}{\partial \tilde{t}} = \frac{1}{G_5}\frac{1}{r}\frac{\partial}{\partial r}\left(r\frac{\partial v}{\partial r}\right) - \frac{G_1}{G_5}\frac{\partial v}{\partial z} + RB_a u + RB_b v + RB_t U + RB_s V \qquad (A3.2)$$

$$\frac{\partial U}{\partial \tilde{t}} = \frac{1}{G_6}\frac{1}{r}\frac{\partial}{\partial r}\left(r\frac{\partial U}{\partial r}\right) - \frac{G_3}{G_6}\frac{\partial U}{\partial z} + RT_a u + RT_b v + RT_t U + RT_s V \qquad (A3.3)$$

$$\frac{\partial V}{\partial \tilde{t}} = (RS_s V + RS_a u + RS_b v + RS_t U) \qquad (A3.4)$$

The boundary conditions are

$$\frac{\partial u}{\partial r} = \frac{\partial v}{\partial r} = \frac{\partial U}{\partial r} = 0 \qquad \text{at } r = 0 \qquad (A3.5)$$

$$\left.\begin{aligned} \frac{\partial u}{\partial r} &= \frac{\partial v}{\partial r} = 0 \\ \frac{\partial U}{\partial r} &= -N_{uw}\,U \end{aligned}\right\} \qquad \text{at } r = 1 \qquad (A3.6)$$

The initial conditions are

$$u = v = U = 0 \qquad \text{at } Z = 0.0 \text{ and } \tilde{t} \geqq 0$$

The reaction rate expressions appear in the fluid equations and are defined as follows:

$$RA = -D(CA^* - C^*_{pAS})$$

$$RB = D(CB_s^* - C^*_{pBS})$$

$$RT = D(Tp^* - T^*) - \frac{N_{uw}}{G_3 G_6}(T^* - T_c)$$

where $D = \frac{G_1 G_2}{G_5} = \frac{G_3 G_4}{G_6}$ in the case of the radial diffusion model

$$N_{uw} = 0.0$$

and $D = \frac{G_2}{G_5} = \frac{G_4}{G_6}$ in the case of the axial diffusion model

Therefore the partial derivatives of the above rates which appear in the linearized system (A3.1) to (A3.3) are as follows:

$$RA_a = \frac{\partial RA}{\partial CA} = -D\left(1 - \frac{\partial C_{pAS}}{\partial CA} - \frac{\partial C_{pAS}}{\partial T_p}\frac{\partial T_p}{\partial CA}\right)$$

$$RA_b = \frac{\partial RA}{\partial CB} = D\left(\frac{\partial C_{pAS}}{\partial T_p}\frac{\partial T_p}{\partial CB}\right)$$

$$RA_t = \frac{\partial RA}{\partial T} = D\left(\frac{\partial C_{pAS}}{\partial T_p}\frac{\partial T_p}{\partial T}\right)$$

$$RB_a = \frac{\partial RB}{\partial CA} = D\left(\frac{\partial C_{pBS}}{\partial T_p}\frac{\partial T_p}{\partial CA} + \frac{\partial C_{pBS}}{\partial CA}\right)$$

$$RB_b = \frac{\partial RB}{\partial CB} = D\left(\frac{\partial C_{pBS}}{\partial CB} + \frac{\partial C_{pBS}}{\partial T_p}\frac{\partial T_p}{\partial CB} - 1\right)$$

$$RB_t = \frac{\partial RB}{\partial T} = D\left(\frac{\partial C_{pBS}}{\partial T_p}\frac{\partial T_p}{\partial T}\right)$$

$$RT_a = \frac{\partial RT}{\partial CA} = D\frac{\partial T_p}{\partial CA}$$

$$RT_b = \frac{\partial RT}{\partial CB} = D \frac{\partial T_p}{\partial CB}$$

$$RT_t = \frac{\partial RT}{\partial T} = D(\frac{\partial T_p}{\partial T} - 1) - N_{uw}$$

The reaction expression of the solid, i.e. RS, is given by equation (A3.7a) in Appendix (A3) and the partial derivatives of RS with respect to CA, CB, T and T_p can be found in reference (46). The additional partial derivatives required are

$$\frac{\partial T_p}{\partial T} = \frac{1}{E} \quad -$$

$$\frac{\partial T_p}{\partial CA} = B_0(Sh_A(1 - \frac{\partial C_{pAS}}{\partial CA})(\frac{K_1(1 + H_2) + K_3H_3}{K_1 + K_3}) - H_z \frac{\partial C_{pBS}}{\partial CA})/E$$

$$\frac{\partial T_p}{\partial CB} = B_0 Sh_B H_z (1 - \frac{C_{pBS}}{CB})/E$$

where $E = 1 + B_0(Sh_A \frac{\partial C_{pAS}}{\partial T_p}(\frac{K_1(1 + H_2) + K_3H_3}{K_1 + K_3}) - Sh_A(CA - C_{pAS})$

$$\frac{\partial}{\partial T_p}(\frac{K_1(1 + H_2) + K_3H_3}{K_1 + K_3}) + Sh_B H_2 \frac{\partial C_{pBS}}{\partial T_p})$$

Note that all the above partial derivatives are evaluated at the steady state.

Now define a Liapunov functional of the following form:

$$I = \tfrac{1}{2} \int_0^1 \int_0^1 [u\ v\ U\ V] \begin{bmatrix} P_1(x) & & & \\ & P_2(x) & & \\ & & P_3(x) & \\ & & & P_4(x) \end{bmatrix} \begin{bmatrix} u \\ v \\ U \\ V \end{bmatrix} r\,dr\,dz$$

where the parameters P_1, P_2, P_3 and P_4 will be chosen later.

By differentiating I with respect to time we obtain

$$\frac{dI}{d} = \int_0^1 \int_0^1 (P_1 u \frac{\partial u}{\partial t} + P_2 v \frac{\partial v}{\partial t} + P_3 U \frac{\partial U}{\partial t} + P_4 V \frac{\partial V}{\partial t})\, r\,dr\,dz$$

Then substituting for the time derivatives of the perturbed states by their linearized equations (A3.1 to (A3.6), we obtain:

$$\frac{\partial I}{\partial t} = \frac{1}{G_5}\int_0^1\int_0^1 (\frac{P_1}{r}\frac{\partial}{\partial r}(r\frac{\partial u}{\partial r})\,u + \frac{P_2}{r}\frac{\partial}{\partial r}(r\frac{\partial v}{\partial r})\,v + \frac{P_3}{r}\frac{\partial}{\partial r}(r\frac{\partial U}{\partial r})U)\,r\,dr\,dz$$

$$- \frac{G_1}{G_5}\int_0^1\int_0^1 (P_1\frac{\partial u}{\partial z}u + P_2\frac{\partial v}{\partial z}v + P_3\frac{\partial U}{\partial z}U)\,r\,dr\,dz$$

$$+ \int_0^1\int_0^1 (P_1\,RA_a\,u^2 + P_2\,RB_b\,v^2 + P_3\,RT_t\,U^2)\,r\,dr\,dz$$

$$+ \int_0^1\int_0^1 (P_1(RA_b\,uv + RB_t\,Uu + RA_s\,Vu) + P_2(RB_a\,uv + RB_t\,Uv + RB_s\,Vv)$$

$$+ P_3(RT_a\,Uu + RT_b\,Uv + RT_s\,UV) + P_4(RS_a\,Vu + RS_b\,vV + RS_t\,UV + RS_s V^2))$$

$$r\,dr\,dz$$

Integrating the first and second integrals by parts and substituting for the boundary conditions given by (A3.5) and (A3.6) we obtain:

$$I_1 = -\int_0^1 \frac{P_3}{G_5}\,N_{uw}\,U^2\Big|_{r=1}\,dz - \frac{1}{G_5}\int_0^1\int_0^1 (P_1(\frac{\partial u}{\partial r})^2 + P_2(\frac{\partial v}{\partial r})^2 + P_3(\frac{\partial U}{\partial r})^2)\,r\,dr\,dz$$

$$I_2 = -\tfrac{1}{2}\frac{G_1}{G_5}\int_0^1 (P_1u^2 + P_2v^2 + P_3U^2)\Big|_{Z=1}\,r\,dr + \tfrac{1}{2}\frac{G_1}{G_5}\int_0^1\int_0^1 (\frac{\partial P_1}{\partial z}\,u^2 + \frac{\partial P_2}{\partial z}\,v^2 + \frac{\partial P_3}{\partial z}\,U^2)\,r\,dr\,dz$$

Add the second integral of I_2 to the rest of the integrals in Liapunov functional to form I_3. This integral has a positive sign and it is necessary to look for conditions for which I_3 can be negative definite.

By choosing $P_1 = P_2 = P_3 = P_4 = e^{-Kz}$ (where $K > 0$) and putting I_3 in matrix form after transforming it to symmetrical form (i.e. $I_3 = \frac{1}{2}(I_3 + I_3^T)$, the following may be obtained:

$$\begin{bmatrix} uvUV \end{bmatrix} \begin{bmatrix} 2(\frac{G_1}{G_5}K + \frac{\partial RA}{\partial CA}) & b_{12} & b_{13} & b_{14} \\ b_{21} & 2(-\frac{G_1}{G_5}K + \frac{\partial RB}{\partial CB}) & b_{23} & b_{24} \\ b_{31} & b_{32} & 2(-\frac{G_3}{G_6}K + \frac{\partial RT}{\partial T}) & b_{34} \\ b_{41} & b_{42} & b_{43} & 2\frac{\partial RS}{\partial Tp} \end{bmatrix} \begin{bmatrix} u \\ v \\ U \\ V \end{bmatrix} e^{-Kz}$$

where $b_{12} = \frac{\partial RB}{\partial CA} + \frac{\partial RA}{\partial CB}$, $b_{13} = \frac{\partial RA}{\partial T} + \frac{\partial RT}{\partial CA}$, $b_{14} = \frac{\partial RA}{\partial Tp} + \frac{\partial RS}{\partial CA}$

$b_{21} = b_{12}$, $b_{23} = \frac{\partial RB}{\partial T} + \frac{\partial RT}{\partial CB}$, $b_{24} = \frac{\partial RB}{\partial Tp} + \frac{\partial RS}{\partial CB}$

$b_{31} = b_{13}$, $b_{32} = b_{23}$, $b_{34} = \frac{\partial RT}{\partial Tp} + \frac{\partial RS}{\partial T}$

$b_{41} = b_{14}$, $b_{42} = b_{24}$, $b_{43} = b_{34}$

For the Liapunov functional to be negative, the above matrix should be negative definite. A condition for this matrix to be negative is that the diagonal elements must be negative. In the first three diagonal elements, K can be made large enough to ensure their negativity. For the fourth diagonal element to be negative, $\frac{\partial RS}{\partial Tp}$ must be negative,

where $RS = \frac{3Nu}{2K_T}(T - Tp) + \frac{3H}{2K_T}\left[\frac{Sh_A(CA - C_{pAS})(K_1(1 + H_2) + K_3H_3)}{K_1 + K_3} - Sh_B(C_{pBS} - CB)H_2\right]$ (A3.7a)

$$\frac{\partial RS}{\partial Tp} = -\frac{3Nu}{2K_T} + \frac{3H}{2K_T}\left[(Sh_A(CA - C_{pAS})\frac{\partial}{\partial Tp}\frac{(K_1(1 + H_2) + K_3H_3)}{K_1 + K_3} - \frac{K_1(1 + H_2) + K_3H_3}{K_1 + K_3}\right.$$

$$\left.\frac{\partial C_{pAS}}{\partial Tp} - Sh_BH_2\frac{\partial C_{pBS}}{\partial Tp}\right] \qquad (A3.7)$$

Therefore, for the above equation to be negative

$$Nu > Qg$$

where Nu represents the heat removal and Qg is the heat generation in the pellet.

A3.2 Derivation of the stability criterion for the axial diffusion model

The heat and mass balance to be considered are represented by the system of equations (6.1 to 6.5)* together with the dynamic pellet model given in appendix (A1) by equation (A1.12).

Consider the stability of the reactor around the steady state values CA^*, CB^*, T^* and T_p^* and define perturbed variables

$$A(\tilde{t},z) = CA(\tilde{t},z) - CA^*(z)$$

$$B(\tilde{t},z) = CB(\tilde{t},z) - CB^*(z)$$

$$C(\tilde{t},z) = T(\tilde{t},z) - T^*(z)$$

$$D(\tilde{t},z) = T_p(\tilde{t},z) - T_p^*(z)$$

Substituting these perturbed variables into the system of equations mentioned above and linearizing around the steady state solution, the following simplifications can be made:

$$u = A\exp(0.5\ Pe\ Z) \qquad v = B\exp(0.5\ Pe\ Z)$$

$$U = C\exp(0.5\ Pe\ Z)$$

where $Pe_{Ma} = Pe_{Ha} = Pe$, and $f = G_5' = G_6'$.

After carrying out the necessary mathematical steps, the linearized set of equations is reduced to the following form:

$$\frac{\partial u}{\partial \tilde{t}} = \frac{1}{fPe}\frac{\partial^2 u}{\partial z^2} + D_1 u + RA_b v + RA_t U + RA_s V \qquad (A3.8)$$

$$\frac{\partial v}{\partial \tilde{t}} = \frac{1}{fPe}\frac{\partial^2 v}{\partial z^2} + RB_a u + D_2 v + RB_t U + RB_s V \qquad (A3.9)$$

$$\frac{\partial U}{\partial \tilde{t}} = \frac{1}{fPe}\frac{\partial^2 U}{\partial z^2} + RT_a u + RT_b v + D_3 U + RT_s V \qquad (A3.10)$$

$$\frac{\partial V}{\partial \tilde{t}} = (RS_s V + RS_a u + RS_b v + RS_t U) \qquad (A3.11)$$

with boundary conditions:

*Add time differential operators for heat and mass similar to those in equations (7.1 to 7.3).

$$\frac{\partial u}{\partial z} = 0.5\ Pe\ u$$

$$\frac{\partial v}{\partial z} = 0.5\ Pe\ v \qquad \text{at } Z = 0 \qquad \text{(A3.12)}$$

$$\frac{\partial U}{\partial z} = 0.5\ Pe\ U$$

$$\frac{\partial u}{\partial z} = -0.5\ Pe\ u$$

$$\frac{\partial v}{\partial z} = -0.5\ Pe\ v \qquad \text{at } Z = 1 \qquad \text{(A3.13)}$$

$$\frac{\partial U}{\partial z} = -0.5\ Pe\ U$$

where $D_1 = RA_a - 0.25\ Pe/f$ $\qquad D_2 = RB_b - 0.25\ Pe/f$

and $D_3 = RT_t - 0.25\ Pe/f$

Define a Liapunov functional of the following form:

$$I = \tfrac{1}{2}\int_0^1 \begin{bmatrix} u & v & U & V \end{bmatrix} \begin{bmatrix} P_1(x) & & & \\ & P_2(x) & & \\ & & P_3(x) & \\ & & & P_4(x) \end{bmatrix} \begin{bmatrix} u \\ v \\ U \\ V \end{bmatrix} dz$$

where the parameters P_1 to P_4 are to be determined later.

Therefore $\frac{\partial I}{\partial t} = \int_0^1 (P_1 \frac{\partial u}{\partial t} u + P_2 \frac{\partial v}{\partial t} v + P_3 \frac{\partial U}{\partial t} U + P_4 \frac{\partial V}{\partial t} V)dz$

Substituting for the time derivatives of the perturbed variables from equations (A3.8 to A3.11), we obtain:

$$\dot{I} = \frac{1}{f}\int_0^1 (\frac{P_1}{Pe} u \frac{\partial^2 u}{\partial z^2} + \frac{P_2}{Pe} v \frac{\partial^2 v}{\partial z^2} + \frac{P_3}{Pe} \frac{\partial^2 U}{\partial z^2})dz + \int_0^1 (P_1 D_1 u^2 + P_2 RB_b v^2$$

$$+ P_3 RT_t U^2)dz + \int_0^1 (P_1(RA_b uv + RA_t uU + RA_s uV) + P_2(RB_a vu + RB_t vU +$$

$$RB_s vV) + P_3(RT_a Uu + RT_b Uv + RT_s UV) + P_4(RS_a Vu + RS_b Vv + RS_t VU))dz \qquad \text{(A.14)}$$

Integrating the first integral by parts and substituting for the boundary conditions:

$$I_1 = \left(\frac{P_1}{fPe} u \frac{\partial u}{\partial z} + \frac{P_2}{fPe} \frac{\partial v}{\partial z} + \frac{P_3}{fPe} U \frac{\partial U}{\partial z}\right)\Bigg|_0^1 - \frac{1}{f}\int_0^1 \left(\frac{P_1}{Pe}\left(\frac{\partial u}{\partial z}\right)^2 + \frac{P_2}{Pe}\left(\frac{\partial v}{\partial z}\right)^2 + \right.$$

$$\left. \frac{P_3}{Pe}\left(\frac{\partial U}{\partial z}\right)^2\right)dz \quad -\frac{1}{f}\int_0^1 \left(\frac{u}{Pe} \frac{\partial^{P_1}}{\partial z} \frac{\partial u}{\partial z} + \frac{v}{Pe} \frac{\partial^{P_2}}{\partial z} \frac{\partial v}{\partial z} + \frac{U}{Pe} \frac{\partial^{P_3}}{\partial z} \frac{\partial U}{\partial z}\right)dz$$

Further integration by parts of the last integral above gives:

$$I_2 = -\frac{1}{f}\left(\frac{u}{Pe} \frac{\partial^{P_1}}{\partial z} u + \frac{v}{Pe} \frac{\partial^{P_2}}{\partial z} v + \frac{U}{Pe} \frac{\partial^{P_3}}{\partial z} U\right)\Bigg|_0^1 + \frac{1}{f}\int_0^1 \left(\frac{u^2}{Pe} \frac{\partial^{2P_1}}{\partial z^2} + \frac{v^2}{Pe} \frac{\partial^{2P_2}}{\partial z^2}\right.$$

$$\left. + \frac{U^2}{Pe} \frac{\partial^{2P_3}}{\partial z^2}\right)dz + \frac{1}{f}\int_0^1 \left(\frac{u}{Pe} \frac{\partial^{P_1}}{\partial z}\frac{\partial u}{\partial z} + \frac{v}{Pe} \frac{\partial^{P_2}}{\partial z} \frac{\partial v}{\partial z} + \frac{U}{Pe} \frac{\partial^{P_3}}{\partial z} \frac{\partial U}{\partial z}\right) dz$$

The last integral in I_2 is similar to the last integral in I_1. If they are added together, it is obvious that they equal half the rest of I_2. Therefore the Liapunov functional of the system is

$$\frac{\partial I}{\partial \tau} = \frac{1}{f}\left(\frac{P_1 u}{Pe} \frac{\partial u}{\partial z} + \frac{P_2 v}{Pe} \frac{\partial v}{\partial z} + \frac{P_3 U}{Pe} \frac{\partial U}{\partial z}\right)\Bigg|_0^1 - \frac{0.5}{f}\left(\frac{u^2}{Pe} \frac{\partial^{P_1}}{\partial z} + \frac{v^2}{Pe} \frac{\partial^{P_2}}{\partial z} + \frac{U^2}{Pe} \frac{\partial^{P_3}}{\partial z}\right)\Bigg|_0^1$$

$$-\frac{1}{f}\int_0^1 \left(\frac{P_1}{Pe}\left(\frac{\partial u}{\partial z}\right)^2 + \frac{P_2}{Pe}\left(\frac{\partial v}{\partial z}\right)^2 + \frac{P_3}{Pe}\left(\frac{\partial U}{\partial z}\right)^2\right)dz + \frac{0.5}{f}\int_0^1 \left(\frac{u^2}{Pe} \frac{\partial^2 P_1}{\partial z^2} + \right.$$

$$\left. \frac{v^2}{Pe} \frac{\partial^2 P_2}{\partial z^2} + \frac{U^2}{Pe} \frac{\partial^2 P_3}{\partial z^2}\right)dz$$

+ the last two integrals in equation (A3.14).

Now all the positive integrals in the above functional may be represented as matrices and transformed to a symmetrical form. Furthermore, by defining the elements of the weighting matrix to be $P_1 = P_2 = P_3 = P_4 = \cos a\pi(z - \frac{1}{2})$, the following may be obtained:

$$[uvUW]\begin{bmatrix} -\frac{(a\Pi)^2}{2Pef}-\frac{0.25Pe}{f}+\frac{\partial RA}{\partial CA} & 0.5\,b_{12} & 0.5\,b_{13} & 0.5\,b_{14} \\ 0.5\,b_{21} & \frac{(a\Pi)^2}{2Pef}-\frac{0.25Pe}{f}+\frac{\partial RB}{\partial CB} & 0.5\,b_{23} & 0.5\,b_{24} \\ 0.5\,b_{31} & 0.5\,b_{32} & -\frac{(a\Pi)^2}{2Pef}-\frac{0.25Pe}{f}+\frac{\partial RT}{\partial T} & 0.5\,b_{34} \\ 0.5\,b_{41} & 0.5\,b_{42} & 0.5\,b_{43} & \frac{\partial RS}{\partial T_p} \end{bmatrix}\begin{bmatrix} u \\ v \\ U \\ V \end{bmatrix}\cos a\Pi\ (2-\tfrac{1}{2})$$

For the system to be stable the above matrix should be negative definite. However another condition must also be satisfied for the Liapunov functional to be negative. By substituting the boundary conditions in the first part of the functional, the following conditions apply:

$$\frac{a\Pi}{2Pe}\,\mathrm{Tan}\,\frac{a\Pi}{2} < 1$$

Letting $\lambda = \frac{a\Pi}{2}$ for $0 < a < 1$,

then $2\lambda \mathrm{Tan}\,\lambda = Pe$

where λ is the smallest positive root of the above equation.

APPENDIX 4

ASSUMPTIONS ON WHICH THE PROPOSED MODELS ARE BASED

The general assumptions stated and discussed in Chapter Two are involved in the formulation of the models used in this thesis. In addition, the following assumptions also apply to all models used, unless stated otherwise:

1. The inlet radial temperature profile is assumed to be flat, and the coolant temperature value is taken as the inlet fluid temperature.
2. The axial diffusion mechanism in the fluid is considered negligible. This simplifying assumption is used in Chapters 3, 4 and 5. Its effect is discussed in detail in Chapters 6 and 7.
3. The reactions are irreversible and obey rate expressions of the Arrhenius type.
4. The rate of reaction along any path depends on the concentration of one reactant only, i.e. the reactant being consumed in that step, and the reaction scheme may then be represented by 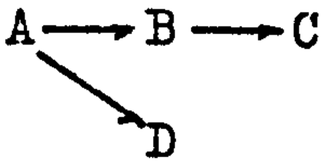

where species A and B are limiting reactants for the reaction steps in which they are consumed.
5. The reaction order along any path is considered first order (i.e. n = 1). For non first order reactions the same models can be used without any difficulty. This is done by redefining n for the fluid concentrations CA and CB appearing in the rate expressions. In this case a pseudo-first order form of the rate expression may be used in case of the catalyst pellet as shown in appendix (A1.2.1).

NOMENCLATURE

a_i Parameter defined in the trial function given by equations (3.7 to 3.9).

A Amplitude of oscillation used in Chapter 5.

$A_{i,J}$ Matrix representing the first order radial differential operator for cylindrical geometry.

$AA_{i,J}$ Matrix representing the first order axial differential operator for planner unsymmetrical geometry.

A_{oi} Arrhenius pre-exponential factor for reaction i.

b Pellet radius.

$b_{i,J}$ Parameter defined in appendix (A3).

B_o Dimensionless exothermicity factor $\dfrac{(-\Delta H_1)\ DP_A C_o Rg}{2bhE_1}$

$B_{i,J}$ Matrix representing the radial Laplacian operator for cylindrical geometry.

$BB_{i,J}$ Matrix representing the axial Laplacian operator for planner unsymmetrical geometry.

C_1, C_2 Determinants defined in Chapter 8.

C_i Parameter defined under equation (A1.13)

C_n Parameter defined in equation (A1.25)

CA, CB Dimensionless concentrations in the fluid $\dfrac{C_{FA}}{C_o}$, $\dfrac{C_{FB}}{C_o}$

CA_o, CB_o Inlet values of CA and CB.

CA_{om}, CB_{om} Radial mean values of CA_o and CB_o

CA_m, CB_m Radial mean values of CA and CB

C_{FA}, C_{FB} Concentrations in the fluid

C_{PA}, C_{PB} Dimensionless concentrations within the catalyst pellet $\dfrac{C^*_{PA}}{C_o}$, $\dfrac{C^*_{PB}}{C_o}$

C_{PAS}, C_{PBS} Surface values of C_{PA} and C_{PB}

C^*_{PA}, C^*_{PB} Concentrations within the catalyst pellet.

C_o Reference concentration of reactant A.

$C_p, C_p{}^*$ Specific heats of fluid and pellet respectively.

D_{CA}, D_{CB}, D_T Distribution factors defined in Chapter 4.

DF_a, DF_b Effective interstitial axial diffusivities in the fluid.

DF_A, DF_B Effective interstitial radial diffusivities in the fluid.

D_p Pellet diameter.

DP_A, DP_B Effective radial diffusivities within the catalyst pellet.

D_s Surface diffusion coefficient.

e, e^* Porosity of the fixed bed and pellet respectively.

E_i Activation energy for reaction i.

F Frequency of oscillation defined in Chapter 5.

G_1 to G_6 are parameters (dimensionless unless otherwise stated) used in the models of the reactor, and are defined as follows:

G_1 $\frac{R^2}{2bL} Pe_M$

G_2 $\frac{(1-e)LDP_A}{b^2 u e}$

G_3 $\frac{R^2}{2bL} Pe_H$

G_4 $\frac{(1-e)\ 3hL}{eb\ \ u\, cp}$

G_5, G_6 $\frac{L}{u}G_1$, $\frac{L}{u}G_3$ respectively. $G_5' = G_6' = \frac{L}{u}$ sec.

h Pellet to fluid heat transfer coefficient.

H Dimensionless exothermicity factor $\frac{(-\Delta H_1)DP_A\ C_o\ Rg}{K_p\ E_1}$

H_2, H_3 Ratios of heats of reaction $\left(\frac{-\Delta H_2}{-\Delta H_1}\right)$, $\left(\frac{-\Delta H_3}{-\Delta H_1}\right)$ respectively.

i Reaction number (1, 2 or 3)

i Number of a node in the collocation procedure.

J Number of a node in the collocation procedure.

k_i Reduced rate constant.

K' Adsorption equilibrium constant.

K Constant in Chapter 8.

K_1 Dimensionless first order (or pseudo-first order) rate constant evaluated at the pellet temperature = $\theta_i^2 \exp\left(\frac{-E_i}{E_1 T_p}\right)$ (for a first order reaction i.e. $n_i = 1$)

K_i^* Dimensionless rate constant defined as $\eta(m) \exp(\gamma_i)\exp\left(-\frac{\gamma_i}{Tm}\right)$ used in Chapter 4.

K_c 'Capacitance' of the catalyst pellet to absorb mass $\frac{b^2 e^*}{DP_A}$ seconds

K_T 'Capacitance' of the catalyst pellet to absorb heat $\frac{\rho^* b^2 C_p^*}{K_p}$ seconds

K_{CA}, K_{CB} Fluid to pellet mass transfer coefficients.

KF Effective interstitial radial conductivity in the fluid phase.

KF_a Effective interstitial axial conductivity in the fluid phase.

K_p Effective radial conductivity within the catalyst pellet.

l Distance from the reactor inlet.

L Reactor length.

m Denote mean condition.

m,M Number of interior collocation points in the axial direction.

n_i Order of reaction i.

n,N Number of interior collocation points in the radial direction.

Nu Modified Nusselt number for heat transfer between pellet and fluid = $\frac{2bh}{K_p}$

Nu' Effective Nusselt number = $N_{uw}\left(\frac{T(r)-1}{T(m)-1}\right)$

N_{uw} Nusselt number for heat transfer between fluid and tube wall = $\frac{RU}{eKF}$

N_{uw}^* Effective overall Nusselt number for heat transfer between fluid and tube wall. Used in the one-dimensional model = $\frac{4N_{uw}}{4+N_{uw}}$

P_i Weight factor, element of matrix P.

P Matrix in Liapunov functional, Chapter 8.

P Damping factor used in Chapter 5.

$P_i(x^2)$, $P_i(v^2)$ Orthogonal polynomial of even degree.

$P_i(z)$ Orthogonal polynomial of even degree.

Pe_a Axial Peclet number $Pe_a = Pe_{Ma} = Pe_{Ha}$

Pe_r Radial Peclet number $Pe_r = Pe_M = Pe_H$

Pe_{Ma} Axial Peclet number for mass $= \frac{uL}{DF_a}$

Pe_{Ha} Axial Peclet number for heat $= \frac{\ell uc_pL}{KF_a}$

Pe_M Radial Peclet number for mass $= \frac{uL}{DF}$

Pe_H Radial Peclet number for heat $= \frac{\ell uc_pL}{KF}$

$P(N_{uw})$, $Q(w_5, N_{uw})$ Correction functions to approximate effective Nusselt number.

Q_o, Q_i Trial functions defined under equation (A1.13).

Q Square matrix, defined under equation (A1.37).

Q_0, Q_1, Q_2 Matrices defined under appendix (A1.4). Used to represent $\frac{d}{dr}$ and Laplacial operators.

$Q_{i,J}$ Matrix defined under equation (3.12).

Q_g Heat removal in the pellet, defined under equation (A3.7).

r Dimensionless radial position in the reactor $\frac{x}{R}$.

R Reactor radius.

$RA_{,k,J'}$

$RB_{k,J}$, $RT_{k,J}$ Reaction rate terms, as defined under equation (3.17).

RA, RB, RT Reaction rate terms as defined under equation (A3.6).

RS The heat balance on the isothermal catalyst pellet defined by

Rg	The gas constant.
S	Distance from the centre of the catalyst pellet.
Sh_A, Sh_B	Modified Sherwood numbers $\frac{2bK_{CA}}{DP_A}$, $\frac{2bK_{CB}}{DP_B}$
T	Dimensionless fluid temperature $\frac{TF\ R_g}{E_1}$
T_o	Inlet value of T.
T_c	Dimensionless coolant temperature $\frac{TC\ R_g}{E_1}$
TC	Coolant temperature.
TF	Fluid temperature.
Tm	Radial mean value of T.
T_{om}	Inlet value of T_m.
T_p	Dimensionless pellet temperature $\frac{TP\ R_g}{E_1}$
TP	Pellet temperature.
u	Interstitial fluid velocity.
u,v,U,V	Perturbed state variables used in Chapter 8, and defined in appendix (A3.1).
U	Fluid to coolant overall heat transfer coefficient.
V	Liapunov functional defined by equation (8.1).
w_5	Temperature profile coefficient defined under equation (4.12).
W	Weighting function.
x	Distance from the reactor axis.
y	Dimensionless pellet co-ordinate = $1 - {}^{s}/_{b}$
y	A state variable.
Y	Vector defined under equation (A1.38).
z	Dimensionless axial position in the reactor $\frac{l}{L}$.

GREEK SYMBOLS

γ_i Activation factor = $\frac{E_i}{R_g\ TC}$

α, β Coefficients in orthogonal polynomials defined under equation (A1.22).

β_i Exothermicity group = $\frac{(-\Delta H_i)C_o\ DF_A}{KF\ TC}$

δ Ratio of diffusivities in the fluid = $\frac{DF_A}{DF_B}$

ΔCA_i Radial concentration difference for reactant i.

ΔCA_{ai} Asymptotic value of ΔCA_i.

ΔCA_T, CB Overall radial concentration differences for the reactant and product.

ΔZ Axial step.

ξ Axially dependent coefficient.

η Effectiveness factor.

θ_i Reaction-Diffusion modulus $b\sqrt{\frac{A_{oi}}{DP_A}}\ \ C_o^{n_i-1}$

ρ, ρ^* Densities of fluid and catalyst pellet respectively.

τ Time (seconds).

ϕ_i Thiele modulus evaluated at fluid conditions = $\theta_i\ \exp(\frac{-E_i}{2E_1\ T})$

ϕ_i^* Effective reactor reaction modulus = $\frac{(1-e)R^2A_{oi}\ \exp(-\gamma_i)}{eDF_A}$

ψ Selectivity for species B.

REFERENCES

1. Thomas, J.M. and Thomas, W.J., Introduction to the principles of heterogeneous catalysis, Academic Press, London (1967).

2. Setterfield, C.N. and Sherwood, T.K., The role of diffusion in catalysis, Addison-Wesley, Mass. (1963).

3. Aris, R., Introduction to the analysis of chemical reactors, Prentice-Hall Inc., N.J. (1965).

4. Petersen, E.E., Chemical Reaction Analysis, Prentice-Hall, N.J., (1965).

5. Denbigh, K. and Turner, J., Chemical Reactor Theory, C.U.P. (1971).

6. Perlmutter, D.D., Stability of Chemical Reactors, Prentice-Hall, N.J. (1972).

7. Froment, G.F., Symposium on Reactor Engineering, University of Leeds, England (1971).

8. Froment, G.F., Second International/Fifth European Symposium on Chemical Reaction Engineering, Amsterdam (1972).

9. Hlavacek, V., Ind. Eng. Chem., 62, 8 (1970).

10. Ray, W.H., Fifth European/Second International Symposium on Chemical Reaction Engineering, Amsterdam (1972).

11. Hougen, O.A., Ind. Eng. Chem., 53, 509 (1961).

12. Carberry, J.J., A.I.Ch.E.Jl., 7, 350 (1961).

13. Paris, J.R. and Stevens, W.F., Can. J. Chem. Eng., 48, 100 (1970).

14. Cresswell, D.L., Ph.D. Dissertation, University of Leeds (1969).

15. Finlayson, B.A., Chem. Eng. Sci., 26, 1081 (1971).

16. Ferguson, N.B. and Finlayson, B.A., Chem. Eng. Jl., 1, 327 (1970).

17. Acrivas, A., Ind. Eng. Chem., vol. 48, No. 4, 703 (1956).

18. McGreavy, C., Adderley, C.I. and Soliman, M.A., to be published.

19. Thiele, E.W. Ind. Eng. Chem., 31, 916 (1939).

20. Zeldowitsch, J.B., Acta Physicochim (U.S.S.R.), 10, 583 (1939).

21. Wheeler, A., Adv. in Catalysis, 3, 249 (1951).

22. Prater, C.D. and Weisz, P.B., Adv. in Catalysis, 6, 144 (1954).

23. Weisz, P.B., Z. Physik. Chem., 11, 1 (1957).

24. Weisz, P.B., Chem. Eng. Progr. Symp. Ser., 55 (25), 29 (1959).

25. Schneider, P. and Mitschka, P., Chem. Eng. Sci., 21, 455 (1966).

26. Hudgins, R.R., Chem. Eng. Sci., 23, 93 (1968).

27. Mingle, J.O. and Smith, J.M., A.I.Ch.E.Jl., 7, 243 (1962).

28. Carberry, J.J., Chem. Eng. Sci., 17, 675 (1962).

29. Carberry, J.J., A.I.Ch.E.Jl., 8, 557 (1962).

30. Weisz, P.B. and Hicks, J.S., Chem. Eng. Sci., 17, 265 (1962).

31. McGreavy, C. and Cresswell, D.L., Can. J. Chem. Eng., 47, 583 (1969).

32. Wheeler, A., in 'Catalysis', Vol. 2, Reinhold, N.Y. (1955).

33. Prater, C.D., Chem. Eng. Sci., 8, 284 (1958).

34. Tinkler, J.D. and Metzner, A., Ind. Eng. Chem., 53, 663 (1961).

35. Østergaard, K., Chem. Eng. Sci., 18, 259 (1963).

36. Hutchings, J. and Carberry, J.J., A.I.Ch.E.Jl., 12, 20 (1966).

37. Schilson, R.E. and Amundson, N.R., Chem. Eng. Sci., 13, 226 (1961).

38. Schilson, R.E. and Amundson, N.R., Chem. Eng. Sci., 13, 237 (1961).

39. Beek, J., A.I.Ch.E.Jl., 7, 337 (1961).

40. Petersen, E.E., Chem. Eng. Sci., 17, 987 (1962).

41. Petersen, E.E., Chem. Eng. Sci., 20, 587 (1965).

42. McGreavy, C. and Soliman, M.A., Chem. Eng. Jl., 6, 99 (1973).

43. Hatfield, B. and Aris, R., Chem. Eng. Sci., 24, 1913 (1969).

44. Gunn, D.J., Chem. Eng. Sci., 21, 383 (1966).

45. Tinkler, J.D. and Pigford, R.L., Chem. Eng. Sci., 15, 326 (1961).

46. Thornton, J.M., Ph.D. Thesis, University of Leeds (1970).

47. Hlavacek, V. and Kubicek, M., Chem. Eng. Sci., 25, 1537 (1970).

48. Hlavacek, V. and Kubicek, M., Chem. Eng. Sci., 25, 1761 (1970).

49. Aris, R., Chem. Eng. Sci., 6, 262 (1957).

50. Gunn, J., Chem. Eng. Sci., 22, 1439 (1967).

51. Luss, D. and Amundson, N.R., A.I.Ch.E.Jl., 13, 759 (1967).

52. Rester, S. and Aris, R., Chem. Eng. Sci., 24, 793 (1969).

53. Rester, S. et al., Chem. Eng. Sci., 24, 1019 (1969).

54. Copelowitz, I. and Aris, R., Chem. Eng. Sci., 25, 885 (1970).

55. Cunningham, R.A. et al., A.I.Ch.E.Jl., 11, 636 (1965).

56. Miller, F.W. and Deans, H.A., A.I.Ch.E.Jl., 13, 45 (1967).

57. Irving, J.P. and Butt, J.B., Chem. Eng. Sci., 22, 1859 (1967).

58. Fulton, J.W. and Crosser, O.K., A.I.Ch.E.Jl., 11, 513 (1965).

59. Ramaswami, D., Ph.D. Thesis, University of Wisconsin (1961).

60. McGuire, M.L. and Lapidus, L., A.I.Ch.E.Jl., 11, 85 (1965).

61. Wei, J., Chem. Eng. Sci., 21, 1171 (1966).

62. Feick, J. and Quon, D., Can. Jl. Chem. Eng., 48, 205 (1970).

63. Hansen, K.W., Chem. Eng. Sci., 26, 1555 (1971).

64. Kehoe, J.P.G. and Butt, J.B., Fifth European/Second International Symposium on Chemical Reaction Engineering, Amsterdam (1972).

65. Hughes, R. and Koh, H.P., Chem. Eng. Jl., 1, 186 (1970).

66. Deans, H.A. and Lapidus, L., A.I.Ch.E.Jl., 6, 656 (1960).

67. Crider, J.E. and Foss, A.S., A.I.Ch.E.Jl., 14, 77 (1968).

68. Feick, J., Ph.D. Dissertation, University of Alberta, Edmonton, Alberta (1968).

69. Froment, G.F., Chem. Eng. Sci., 17, 849 (1962).

70. Von Rosenberg, D.V. et al., Brit. Chem. Eng., 7, 186 (1962).

71. Beek, J., Adv. in Chem. Eng., 3, 203 (1962).

72. Mickley, H.S. and Letts, R.W.M., Can. Jl. Chem. Eng., 42, 21 (1964).

73. Amundson, N.R., Ind. Eng. Chem., 48, 26 (1956).

74. McGreavy, C. and Cresswell, D.L., 4th European Symposium on 'Chemical Reaction Engineering', Brussels, Sept. 1968.

75. Fan, L.T., Chen, K.C. and Erickson, L.E., Chem. Eng. Sci., 26, 379 (1971).

76. Stewart, W.E. and Sorensen, J.P., Fifth European/Second International Symposium on Chemical Reaction Engineering, Amsterdam (1972).

77. Hoiberg, J.A., Lyche, B.C. and Foss, A.S., A.I.Ch.E.Jl., 17, 1434 (1971).

78. Turner, K., Ph.D. Thesis, University of Leeds (1970).

79. Carberry, J.J. and Wendel, M.M., A.I.Ch.E.Jl., 9, 29 (1963).

80. Karenth, N.G. and Hughes, R., Paper presented at Symposium on Heterogeneous Reactors, University of Salford, England (1972).

81. Thierney, J.W. et al., A.I.Ch.E.Jl., 4, 460 (1958).

82. Valstar, J.M., A study of the fixed bed reactor with reference to the synthesis of vinyl acetate, Delftsche Uitgevas Maatschappij N.V., Delft (1969).

83. Ervin, M.A. and Luss, D., A.I.Ch.E.Jl., 16, 979 (1970).

84. Cardoso, M.A.A. and Luss, D., Chem. Eng. Sci., 25, 1527 (1970).

85. Hatfield, B. and Aris, R., Chem. Eng. Sci., 24, 1220 (1969).

86. Hlavacek, V. et al., Chem. Eng. Sci., 23, 1083 (1968).

87. Raymond, L.R. and Amundson, N.R., Can. Jl. Chem. Eng., 42, 173 (1964).

88. Kao, Y.K. and Bankoff, S.G., Chem. Eng. Sci., 26, 189 (1971).

89. McGowin, C. and Perlmutter, D.D., A.I.Ch.E.Jl., 17, 831 (1971).

90. Matsuyama, H., Chem. Eng. Jl. Japan., 5, 427 (1972).

91. Luss, D. and Medellin, P., Fifth European/Second International Symposium on Chemical Reaction Engineering, Amsterdam (1972).

92. Hlavacek, V. and Hofmann, H., Chem. Eng. Sci., 25, 173 (1970).

93. Hlavacek, V. and Hofmann, H., Chem. Eng. Sci., 25, 187 (1970).

94. McGreavy, C. and Thornton, J.M., Can. Jl. Chem. Eng., 48, 187 (1970).

95. Horn, F.J.M. et al., Chem. Eng. Jl., 1, 79 (1970).

96. Yang, R.Y.K. et al., Chem. Eng. Jl., 2, 218 (1971).

97. Jackson, R. and Horn, F.J.M., Chem. Eng. Jl., 3, 82 (1972).

98. Hlavacek, V. and Kubicek, M., Chem. Eng. Sci., 25, 1527 (1970).

99. Bischoff, K.B., Chem. Eng. Sci., 23, 251 (1968).

100. Copelowitz, I. and Aris, R., Chem. Eng. Sci., 25, 885 (1970).

101. Paris, J.R. and Stevens, W.F., 4th European Symposium on 'Chemical Reaction Engineering', Brussels, Sept. 1968.

102. Calderbank, P.H. et al., 4th European Symposium on 'Chemical Reaction Engineering', Brussels, Sept. 1968.

103. Shadman-Yazdi, F. and Petersen, E.E., Chem. Eng. Sci., 27, 227 (1972).

104. Brusset, H. et al., Chem. Eng. Sci., 27, 1475 (1972).

105. Nussey, C., Ph.D. Dissertation, University of Leeds (1968).

106. Elnashaie, S.S.E.H. and Cresswell, D.L., Can. Jl. Chem. Eng., 51, 201 (1973).

107. Denis, G.H. and Kabel, R.L., Chem. Eng. Sci., 25, 1057 (1970).

108. Horak, J. and Jiracek, F., Proceedings of 3rd CHISA Conference, Czechoslovakia (1969).

109. Adderley, C.I., Ph.D. Dissertation, University of Leeds (1973).

110. Hansen, K.W., Chem. Eng. Sci., 28, 723 (1973).

111. Jones, D.A., Ph.D. Dissertation, University of Leeds (1971).

112. Stanek, V. and Szekely, J., Can. Jl. Chem Eng., 51, 22 (1973).

113. Villadsen, J.V. and Stewart, W.E., Chem. Eng. Sci., 22, 1483 (1967).

114. McGowin, C.R. and Perlmutter, D.D., Chem. Eng. Sci., 3,275 (1971).

115. Cardoso, M.A.A. and Luss, D,, Chem. Eng. Sci., 24, 1699 (1969).

116. Denis, G.H. and Kabel, R.L., A.I.Ch.E.Jl., 16, 972 (1970).

117. Villadsen, J.V. and Sorensen, J.P., Chem. Eng. Sci., 24, 1337 (1969).

118. Carberry, J.J. and Wendel, M.M., A.I.Ch.E.Jl., 9, 129 (1963).

119. Hlavacek, V. and Marek, M., Chem. Eng. Sci., 21, 501 (1966).

120. Young, L.C. and Finlayson, B.A., Ind. Eng. Chem. Fundl., Vol. 12, No. 3, 412 (1973).

121. Villadsen, J.V., "Selected Approximation Methods for Chemical Engineering Problems".

122. Ames, W.F., "Nonlinear Partial Differential Equations in Engineering", Academic Press Inc., (1965).

123. Stroud, A.H. and Secrest, D., "Gaussian Quadrature Formulae", Prentice-Hall Inc. (1966).

124. Michelsen, M.L. and Villadsen, J.V., Chem. Eng. Jl., 4, 64 (1972).

125. Lui, S. and Amundson, N.R., Ind. Eng. Chem. Fundl., Vol. 2, No. 3, 183 (1963).

126. Coste, Rudd, J.D. and Amundson, N.R., Can. Jl. Chem. Eng., 39, 149 (1961).

127. Lee, E.S., Chem. Eng. Sci., 21, 143 (1966).

128. Lapidus, L., Chem. Eng. Progr. Symposium Ser. No. 36, 57, 35 (1961).

129. Froment, G.F., Ind. Eng. Chem., 59, 18 (1967).

130. Dente, M., Biardi, G. and Ranzi, E., Symp. on Chem. Reaction Engineering, 5th European, Second International, Amsterdam, May 1972.

131. Cairns, E.J. and Prausnitz, J.M., Ind. Eng. Chem., 51, 1441 (1959).

132. Yagi, S., Kunii, D. and Wakao, N., A.I.Ch.E.Jl., 6, 543 (1960).

133. Bischoff, K.B., Can. Jl. Chem. Eng., 40, 161 (1962).

134. Hiby, J.W., Symposium "Interaction between fluids and particles", Inst. Chem. Engr., London (1962).

135. McGreavy, C. and Turner, K., Symposium on Chemical Reaction Engineering, Leeds University, England (1971).

136. Furusawa, T. and Kunii, D., Chem. Eng. Jl. Japan, 4, 274 (1971).

137. Kuo, J.C.W. and Amundson, N.R., Chem. Eng. Sci., 22, 443 (1967).

138. Lee, J.C.M. and Luss, D., A.I.Ch.E.Jl., 16, 620 (1970).

139. Bush, S.F., Proc. Roy. Soc. A309, 1 (1969).

140. Hlavacek, V., Kubicek, M. and Marek, M., Jl. of Catalysis, 15, 31 (1969).

141. Hlavacek, V., Kubicek, M. and Marek, M., Jl. of Catalysis, 15, 17 (1969).

142. Hlavacek, V. and Kubicek, M., Jl. of Catalysis, 22, 364 (1971).

143. Luss, D. and Lee, J.C.M., Chem. Eng. Sci., 26, 1433 (1971).

144. Luss, D. and Lee, J.C.M., Chem. Eng. Sci., 23, 1237 (1968).

145. Wei, J., Chem. Eng. Sci., 20, 729 (1965).

146. Berger, A.J. and Lapidus, L., A.I.Ch.E.Jl., 14, 558 (1968).

147. Padmanabhan, L., Yang, R.Y.K. and Lapidus, L., Chem. Eng. Sci., 26, 1857 (1971).

148. McGreavy, C. and Soliman, M.A., Chem. Eng. Sci., 28, 1401 (1973).

149. Liu, S. and Amundson, N.R., Ind. Eng. Chem. Fundl., Vol. 1, No. 3, 200 (1962).

150. Van Heerden, C., Chem. Eng. Sci., 8, 133 (1958).

151. Padberg, G. and Wicke, E., Chem. Eng. Sci., 22, 1035 (1967).

152. Wicke, E., Padberg, G. and Arens, H., Fourth European Symp. on Chemical Reaction Engineering, Brussels (1968).

153. Blodget, R.E., Jl. Basic Eng., 475 (1966).

154. Lamb, D.E. and Orcutt, J.C., "Stability of a fixed bed cat. reactor system with feed effluent heat exchange", First International Congress, International Federation of Automatic Control, Butterworths, Vol. 4, pp. 274-279 (1961).

155. Han, C.D. and Meyer, A.V., Int. Jl. Control, 11, 509 (1970).

156. Vanderveen, J.W., Luss, D. and Amundson, N.R., A.I.Ch.E.Jl., 14, 636 (1968).

157. Agnew, J.B. and Narsimhan, G., Chem. Eng. Sci., 25, 685 (1970).

158. Liu, S.L., Aris, R. and Amundson, N.R., Ind. Eng. Chem. Fundl., 2, 12 (1963).

159. McHenry, K.W. and Wilhelm, R.H., A.I.Ch.E.Jl., 3, 83 (1957).

160. Carberry, J.J. and Bretton, R.H., A.I.Ch.E.Jl., 4, 367 (1958).

161. Luss, D. and Amundson, N.R., Chem. Eng. Sci., 22, 253 (1967).

162. Bernard, R.A. and Wilhelm, R.H., Chem. Eng. Prog., 46, 233 (1950).

163. Luss, D., Chem. Eng. Sci., 23, 1249 (1968).

164. Carberry, J.J., Can. Jl. Chem. Eng., 36, 207 (1958).

165. Epstein, N., Can. Jl. Chem. Eng., 36, 210 (1958).

166. Levenspiel, O. and Bischoff, K.B., Adv. Chem. Eng., 4, 95 (1963).

167. Sinai, J. and Foss, A.S., A.I.Ch.E.Jl., 16, 4, 658 (1970).

168. Beek, J. and Miller, R.S., Chem. Eng. Progr. Symp. Ser., 55 (25), 23 (1959).

169. Murphy, E.N. and Crandall, E.D., Trans. ASME, Series D, Jl. of Basic Eng., 92, 265 (1970).